LATVIJAS UNIVERSITĀTE

ULDIS BĒRZIŅŠ

AUTOLOGU MEZENHIMĀLO CILMES ŠŪNU DROŠUMA PĀRBAUDE

PROMOCIJAS DARBS
Doktora grāda iegūšanai bioloģijas nozarē
Apakšnozare: molekulārā bioloģija

Rīga, 2018

Latvijas Universitāte
Bioloģijas fakultāte

Uldis Bērziņš

Autologu mezenhimālo cilmes šūnu drošuma pārbaude

Promocijas darbs

Doktora grāda iegūšanai bioloģijas nozarē
Apakšnozare: molekulārā bioloģija

Rīga, 2018

Promocijas darbs izstrādāts Latvijas Universitātes Bioloģijas fakultātē, Molekulārās bioloģijas katedrā un Latvijas Biomedicīnas pētījumu un studiju centrā laika posmā no 2008. gada līdz 2017. gadam.

Promocijas darbs izstrādāts ar Latvijas Republikas Izglītības un zinātnes ministrijas projekta TOP 07-27, Latvijas Zinātnes padomes projektu Nr.09.1283 un Nr.10.0014, Eiropas Reģionālās attīstības fonda projekta 2010/0230/2DP/2.1.1.1.0/10/APIA/VIAA/075 un SIA Cilmes Šūnu Tehnoloģijas atbalstu.

Darbs sastāv no ievada, 6 nodaļām un literatūras saraksta.
Darba forma: publikāciju kopa bioloģijas nozarē, molekulārās bioloģijas apakšnozarē
Darba zinātniskā vadītāja: Dr. habil. biol. Tatjana Kozlovska

Darba recenzenti:

1. Dr.biol. Una Riekstiņa

2. Dr.biol. Dace Pjanova

3. Dr.biol. Dennis Khnikin

Promocijas darba aizstāvēšana notiks 2018. gada 9.martā plkst. 12:30 Latvijas Universitātes Dabas zinātņu Akadēmiskajā centrā, Jelgavas ielā 1, 217. aud.
Latvijas Universitātes bioloģijas nozares promocijas padomes atklātā sēdē.
Ar promocijas darbu un tā kopsavilkumu var iepazīties Latvijas Universitātes Bibliotēkā Rīgā, Kalpaka bulvārī 4.

LU bioloģijas zinātņu nozares promocijas
padomes priekšsēdētājs _____/ Dr. biol. Kaspars Tārs/
(paraksts)

promocijas padomes sekretāre _____/ Daina Eze/
(paraksts)

Anotācija

Pieaugošā reģeneratīvās medicīnas popularitāte ir sekmējusi no taukaudiem izdalīto cilmes šūnu (ASC) izmantošanu šūnu bāzēto terapiju izstrādē. Lai veicinātu šādu terapiju attīstību, Eiropas Savienības likumdošana pieļauj personalizēta, ārpus rutīnas apstākļiem sagatavota šūnu produkta izmantošanu klīnisko izņēmumu gadījumos. Šī darba mērķis bija raksturot cilvēka un suņa ASC, kas sagatavotas, izmantojot specifisku metodoloģiju, un pārbaudīt to drošumu *in vitro*, kā arī *in vivo* suņa modelī pēc divkāršas intravenozas ievadīšanas.

Iegūtie rezultāti parādīja, ka ASC var viegli izdalīt gan no cilvēka (hASC), gan suņa (cASC) taukaudiem un abu veidu ASC ir plastmasas adherentas šūnas ar tām raksturīgu vārpstveida morfoloģiju. Šīs īpašības neietekmē ne šūnu kultivēšana barotnē ar autologo serumu (AS), ne audzēšana pie 5% skābekļa koncentrācijas, ne divkārša sasaldēšana un atkausēšana. Daudzkrāsu plūsmas citometrijas analīze atklāja, ka pārbaudītās ASC populācijas ir fenotipiski homogēnas. hASC ekspresē tādus tipiskos ASC marķierus kā CD29, CD44, CD73, CD90 un CD105, bet cASC - CD44, CD73, CD90. Abu veidu ASC ir negatīvas pēc CD14, CD34, CD45 un HLA-DR, un hASC papildus neuzrāda CD19 ekspresiju. Šīs šūnas diferencējās adipogēnajā, osteogēnajā un hondrogēnajā virzienā, taču cASC diferenciācija par adipocītiem bija vāja. Blasttransformācijas reakcija atklāja, ka ASC no abiem avotiem būtiski samazina T šūnu proliferāciju un šī spēja ir atkarīga no šūnu devas.

Lai noteiktu ASC *in vitro* drošumu, tika pārbaudīta astoņu donoru hASC kultūru bioloģiskā novecošanās ilgstošas šūnu pavairošanas laikā. Tika novērotas izmaiņas šūnu morfoloģijā, kā arī samazinājās šūnu kultūru proliferatīvais ātrums un klonogenitāte. Arī hASC adipogēnās un osteogēnās diferenciācijas potenciāls vēlā pasāžā bija būtiski zemāks nekā agrā pasāžā. Ar senescenci saistītā β-galaktozidāzes ekspresija pieauga ilgstošas šūnu kultivēšanas laikā. Relatīvā telomēru garuma (RTL) noteikšanas analīze parādīja, ka trīs no pārbaudītajām hASC kultūrām sasniedza replikatīvo senescenci, bet pārējās - priekšlaicīgo senescenci. Visu donoru paraugos tika atklātas divas šūnu subpopulācijas ar būtiski atšķirīgu RTL un šūnu lielumu. Kopumā novērotais hASC *in vitro* novecošanās process bija nevienmērīgs un katram šūnu donoram izteikti specifisks.

ASC *in vivo* drošums tika noteikts, izmantojot tikko atkausētas cASC, kuras audzētas hipoksiskos apstākļos AS klātbūtnē un pakļautas diviem sasaldēšanas un atkausēšanas cikliem. Intravenoza šūnu iesaldēšanas barotnes, terapeitiskās cASC devas ($2x10^6$ dzīvas šūnas/kg) un piecas reizes lielākas šūnu devas ievadīšana diviem bīglu šķirnes suņiem neradīja būtiskas blaknes. Plaušu "barjeras" efekta pārbaude ļāva izslēgt plaušu trombembolisma risku. Dzīvnieku audu un orgānu histomorfoloģiskā analīze vairāk nekā divus gadus vēlāk atklāja tikai nelielas un relatīvi nespecifiskas izmaiņas, un nekādas ļaundabīgu audzēju veidošanās pazīmes netika novērotas.

Iegūtie rezultāti liecina, ka cASC ir līdzīgas hASC un drošas terapeitiskam pielietojumam. Darba gaitā izstrādātā metodoloģija ASC sagatavošanai ārpus rutīnas apstākļiem, kas iekļauj individuāli optimizētus šūnu audzēšanas apstākļus un piedāvā riskam piemērotu ārstēšanu, var tikt izmantota personalizētai, nekavējoties pieejamai terapijai nākotnē, piemēram, miokarda infarkta vai insulta gadījumā.

Darbā lietotie saīsinājumi

ASC	no taukaudiem izdalītas cilmes šūnas
AS	autologais serums
ATMP	jaunievestās terapijas zāles
cASC	no suņa taukaudiem izdalītas cilmes šūnas
CFU	koloniju veidojošā vienība
DMSO	dimetilsulfoksīds
EDTA	etilēndiamīn-tetraetiķskābe
FBS	fetālais liellopa serums
hASC	no cilvēka taukaudiem izdalītas cilmes šūnas
HE	klīniskais izņēmums
MSC	mezenhimālās cilmes šūnas
PBMNC	perifēro asiņu mononukleārās šūnas
P1, P2...	1. šūnu pasāža, 2. šūnu pasāža
SA-β-Gal	ar senescenci saistītā beta-galaktozidāze
PBS	fosfātu fizioloģiskais buferšķīdums
PDT	populācijas dubultošanās laiks
PD	populācijas dubultošanās
Flow FISH	fluorescences *in situ* hibridizācijas plūsmas citometrija
PHA	fitohemaglutinīns
p	p-vērtība
rmp	apgriezieni minūtē
RTL	relatīvais telomēru garums
SD	standartnovirze
SVF	stromas vaskulārā frakcija

Satura rādītājs

Ievads

Reģeneratīvā medicīna ir strauji augoša nozare ar plašām iespējām ārstēt smagas slimības, kas nepakļaujas tradicionālajām terapijām. Sagaidāms, ka reģeneratīvās medicīnas nozīme nākotnē tikai pieaugs, jo tā var kļūt par vienu no galvenajām jomām personalizētajā medicīnā, kas ir katra pacienta īpašībām, vajadzībām un izvēlei pielāgota ārstēšana visās tā aprūpes stadijās (www.fda.gov). Jau tagad reģeneratīvās medicīnas personalizācija ir sekmējusi modernizētu terapiju rašanos un attīstījusi tādu principiāli jaunu pieeju zāļu ražošanā kā jaunievieštās terapijas zāles (ATMP).

Viens no reģeneratīvās medicīnas perspektīvajiem virzieniem ir mezenhimālo cilmes šūnu (MSC) kā ATMP izmantošana. Kopš P. Zuk ziņojuma 2001. gadā par to, ka no taukaudiem var izdalīt multipotentas MSC (Zuk et al. 2001), taukaudi ir kļuvuši par vērtīgu avotu šo šūnu iegūšanai. No taukaudiem izdalītas MSC (ASC) ir lieliski piemērotas šūnu bāzēto terapiju izstrādei, jo tās spēj diferencēties dažādos šūnu veidos (Desiderio et al., 2013; Zuk et al., 2002), migrēt uz bojājuma vietu (Liu et al., 2012; Li et al., 2013; Karagiannis et al., 2017; Kim et al., 2017), atjaunot bojātos audus (Lim et al., 2013; Tsuji et al., 2014) un nodrošināt imunoloģisko līdzsvaru (Tyndall and Uccelli, 2009; Ghannam et al., 2010; Lo Sicco et al., 2017).

Pieaugošā cilmes šūnu terapiju popularitāte ir veicinājusi tādu šūnu kultivēšanas barotņu izmantošanu, kas nesatur dzīvnieku materiālu, jo tas varētu izraisīt autoimūnu reakciju pret paša pacienta cilmes šūnām (Spees et al., 2004). Viens no veidiem, kā to novērst, ir autologā seruma (AS) izmantošana, aizstājot ierasto fetālo liellopa serumu (FBS) visā terapijai paredzēto šūnu sagatavošanas procesā. Tāpat lielākajā daļā pētījumu šūnas tiek audzētas pie atmosfēras skābekļa koncentrācijas (21%), taču skābekļa koncentrācija organismā svārstās no 0–14% (Ivanovic, 2009). Pēc ievadīšanas pacientam, šūnām nākas piedzīvot būtisku hipoksisko stresu, kas noved pie apoptozes un ievērojami samazina šūnu terapijas efektivitāti. Lai palielinātu *in vitro* pavairotu ASC izdzīvošanas iespēju pēc to ievadīšanas, šūnas ir iespējams kultivēt hipoksiskos apstākļos. Tas nodrošina vidi, kas vairāk līdzinās *in vivo* situācijai, un palīdz saglabāt to multipotento stāvokli (Basciano et al., 2011), samazina novecošanās procesus (Tsai et al., 2011) un paaugstina audu atjaunošanas potenciālu (Leroux et al., 2010; Rosova et al., 2008).

Terapijai paredzētā šūnu apjoma iegūšana iekļauj ASC *in vitro* pavairošanu, taču šis process izraisa šūnu novecošanos jeb sensecenci (Dulic 2013; Baker&Sedivy, 2013). Novecojušas šūnas nespēj uzturēt pareizu audu homeostāzi (Rossi et al., 2007) un ir uzskatāmas par nedrošām, tādēļ ir nepieciešams izpētīt ASC senescences gaitu kultivēšanas laikā, lai pārliecinātos par šo šūnu *in vitro* drošumu. Tāpat klīniskajam pielietojumam domātām ASC ir jāveic drošuma pārbaude *in vivo*, kas balstās uz risku un ieguvumu attiecības novērtējumu (Veriter et al., 2015). Tam tiek izmantoti dzīvnieku modeļi. Tā kā suņi ir pietuvināti cilvēkam pēc anatomiskajām un funkcionālajām īpašībām, tiem dabiski piemīt līdzīgas saslimšanas (de Bakker et al., 2013; Hoffman and Dow, 2016) un to taukaudi arī satur MSC (Neupane et al., 2008; Vieira et al., 2010), tad tie var kalpot kā vieni no piemērotākajiem dzīvnieku modeļiem ASC drošuma pārbaudei.

Lai veicinātu šūnu terapijas attīstību Eiropas Savienībā, Eiropas Parlaments un Padome ir pieņēmuši Regulu (EK) Nr. 1394/2007 par ATMP, kuras 28. panta 2. punkts paredz īpašas (personalizētas) terapijas iespējas visās dalībvalstīs. Šādas terapijas pielietošana pieļaujama bez klīniskiem pētījumiem, taču nosakot stingras prasības šūnu produkta pagatavošanai ārpus rutīnas apstākļiem, uzraudzībai un tiesības ārstam uzņemties ekskluzīvu, profesionālu atbildību ārstniecībā (Regulation, 2007). Šādu personalizētu šūnu terapiju kopš 2011. gada ir atļauts realizēt arī Latvijā, un šis darbs sniedz ieskatu ASC kā ATMP sagatavošanas metodoloģijas izstrādē un attiecīgi sagatavotā produkta drošuma pārbaudē.

Šī doktora darba mērķis bija raksturot no cilvēka un suņa zemādas taukaudiem izdalītas ASC, kas sagatavotas, izmantojot specifisku metodoloģiju, un pārbaudīt to drošumu *in vitro*, kā arī *in vivo* suņa modelī pēc divkāršas intravenozas ievadīšanas. Šī mērķa sasniegšanai tika izvirzīti sekojoši uzdevumi:

- izstrādāt metodoloģiju ASC sagatavošanai ārpus rutīnas apstākļiem, kas iekļauj šūnu izdalīšanas, audzēšanas, pavairošanas, raksturošanas un iesaldēšanas metodes;
- izdalīt ASC no cilvēka un suņa taukaudiem un pavairot šīs šūnas atbilstoši izstrādātajai metodoloģijai, izmantojot barotni ar AS un hipoksiskus šūnu kultivēšanas apstākļus;
- raksturot iegūtās cilvēka un suņa ASC pēc to morfoloģijas, virsmas marķieru ekspresijas, diferenciācijas spējas adipocītos, osteocītos un hondrocītos un imunomodulatīvā potenciāla;
- noteikt ASC *in vitro* drošumu, analizējot cilvēka ASC novecošanos, balstoties uz šūnu morfoloģisko analīzi, proliferatīvajām spējām, ar senescenci saistītās β-galaktozidāzes aktivitātes pieaugumu, relatīvā telomēru garuma saīsināšanos un diferenciācijas potenciālu;
- pārbaudīt ASC *in vivo* drošumu, novērtējot to ietekmi uz plaušām un analizējot asins un urīna paraugus, elektrokardiogrammu, ehokardiogrammu un uzvedību pēc divkāršas tikko atkausētu suņa ASC intravenozas ievadīšanas dzīvnieka asinsritē;
- apstiprināt ASC *in vivo* drošumu, vairāk kā divus gadus pēc ASC ievadīšanas veicot dzīvnieka audu un orgānu histomorfoloģisko analīzi, lai noteiktu vēlīnas izmaiņas audos un izslēgtu ļaundabīgu audzēju veidošanās risku.

Promocijas darba aprobācija

Daļa no darba rezultātiem ir izmantoti šī promocijas darba autora vadītajā Latvijas Universitātes Bioloģijas fakultātes studentes Anetes Romanauskas bakalaura darbā "No cilvēka taukaudiem izdalītu mezenhimālo cilmes šūnu *in vitro* senescences raksturojums".

Zinātniskās publikācijas

1. Berzins, U., Matise-VanHoutana, I., Petersone, I., Duritis, I., Nikulshin, S., Bogdanova-Jatniece, A., Kalis, M., Svirskis, S., Skrastina, D., Ezerta, A., Kozlovska, T. (2018). Characterization and *In Vivo* Safety of Canine Adipose-Derived Stem Cells. Proceedings of the Latvian Academy of Sciences, Section B, iespiešanā.
2. Legzdina, D., Romanauska, A., Nikulshin, S., Kozlovska, T., Berzins, U. (2016). Characterization of Senescence of Culture-expanded Human Adipose-derived Mesenchymal Stem Cells. International Journal of Stem Cells, 9(1): 124-136.
3. Bogdanova, A., Berzins, U., Nikulshin, S., Skrastina, D., Ezerta, A., Legzdina, D., Kozlovska T. (2014). Characterization of Human Adipose-Derived Stem Cells Cultured in Autologous Serum After Subsequent Passaging and Long Term Cryopreservation. Journal of Stem Cells, 9(3): 135-148.

Zinātniskās konferences

1. Berzins U., Legzdina D. Biosafety aspects for clinical applications of adult human mesenchymal stem cells. Eiropas Biotehnoloģijas konference, Rīga, Latvija, 2016. Journal of Biotechnology, 231, lpp. S10, 2016.
2. Bogdanova A., Berzins U., Matise-Van Houtana I., Petersone I., Duritis I., Skrastina D., Muizniece Z., Kozlovska T. Safety test of canine adipose-derived stem cells. 22. IUBMB un 37. FEBS kongress, Seviļa, Spānija, 2012. FEBS JOURNAL, 279, Supplement 1, lpp. 541, 2012.
3. Bogdanova A., Berzins U., Matise-Van Houtana I., Petersone I., Duritis I., Skrastina D., Muizniece Z.,Kozlovska T. Characterization and safety test of canine adipose-derived stem cells. 10. ikgadējā ISSCR sanāksme, Jokohama, Japāna, 2012.
4. Berzins U., Bogdanova A., Matise-Van Houtana I., Petersone I., Duritis I., Skrastina D., Muizniece Z., Joffe R., Auzans A., Pumpens P., Kozlovska T. Autologu cilmes šūnu kā jaunieviesto terapijas zāļu drošuma pārbaude. Apvienotais Pasaules latviešu zinātnieku III

kongress un Letonikas IV kongress "Zinātne, sabiedrība un nacionālā identitāte", Rīga, Latvija, 2011.

5. Berzins U., Bogdanova A., Skrastina D., Matise-Van Houtana I., Petersone I., Duritis I., Kozlovska T. Implementation of Adult Stem Cell Bank for the Development of Advanced Therapy Product for Hospital Exemption. Pasaules biobanku samits, Hamburga, Vācija, 2011.
6. Bogdanova A., Berzins U., Skrastina D., Bruvere R., Eivazova G., Zvaigzne A., Kozlovska T. Properties of Adipose-derived Stem Cells Cultured in Autologous Serum. 1. Starptautiskā veselības zinātņu konference, Kauņa, Lietuva, 2011.
7. Bogdanova A., Berzins U., Matise-Van Houtana I., Petersone I., Duritis I., Ranka R., Pliss R., Skrastina D., Bruvere R., Timofejeva I., Kozlovska T. No suņa taukaudiem iegūtu mezenhimālo cilmes šūnu raksturojums. Latvijas Universitātes 69. konference, molekulārās bioloģijas sekcija, Rīga, Latvija, 2011.
8. Eivazova G., Berzins U., Zvaigzne A., Skrastina D., Bogdanova A., Kozlovska T., Lejnieks A. Immunomodulatory properties of adipose-derived stem cells cultured in autologous serum. 3. ikgadējā konference "Stem Cells Europe", Edinburga, Apvienotā Karaliste, 2010.
9. Berzins U., Bogdanova A., Skrastina D., Djackova I., Eivazova G., Zvaigzne A., Lejnieks A., Kozlovska T., Pumpens P. Mezenhimālo cilmes šūnu imunomodulatīvais potenciāls *in vitro*. Latvijas Universitātes 68. konference, molekulārās bioloģijas sekcija, Rīga, Latvija, 2010.

1. Literatūras apskats

1.1. No taukaudiem izdalītu MSC īpašības

MSC no taukaudiem pirmo reizi tika izdalītas 2001. gadā (Zuk et al., 2001), un kopš tā laika taukaudi ir kļuvuši par ļoti vērtīgu avotu MSC iegūšanai, kuras plaši pielieto šūnu bāzēto terapiju izstrādē. *In vitro* pavairotām ASC piemīt multilīniju diferenciācijas potenciāls (Desiderio et al., 2013; Zuk et al., 2002), spēja migrēt uz bojājuma vietu (Liu et al., 2012; Li et al., 2013; Karagiannis et al., 2017; Kim et al., 2017) un bojāto audu atjaunošanas spēja (Lim et al., 2013; Tsuji et al., 2014), kuras viens no galvenajiem mehānismiem ir ASC imunomodulatīvais potenciāls (Ghannam et al., 2010; Lo Sicco et al., 2017; Tyndall and Uccelli, 2009). Šis potenciāls parasti tiek noteikts blasttransformācijas testā, kurā tiek izmantotas nespecifiski aktivētas perifēro asiņu mononukleārās šūnas (PBMNC) un tiek vērtēta ASC spēja nomākt aktivētās PBMNC dažādās koncentrācijās.

Spējai nomākt aktivētus limfocītus ir nozīmīga loma ASC klīniskajam pielietojumam. Zināmi vairāki mehānismi, kā ASC var nomākt limfocītu proliferāciju, piemēram, ar citokīnu transformējošā augšanas faktora beta un hepatocītu augšanas faktora (Di Nicola et al., 2002), prostagalndīna E2 (Aggarwal et al., 2005; Cui et al., 2007), indolamīna 2,3-dioksigenāzes (Meisel et al., 2004), hēma oksigenāzes 1 (Chabannes et al., 2007), slāpekļa monoksīda (Sato et al., 2007), interleikīnu 6 un 10, cilvēka leikocitārā antigēna G5 un matriksa metaloptroteināžu (Abumaree et al., 2012; De Miguel et al., 2012) starpniecību. Turklāt ASC ir potenciāls aktivēt regulatoros T limfocītus (Djouad et al., 2003) un regulatorās antigēnus prezentējošās šūnas (Beyth et al., 2005). Tāpat ASC spēj nomākt komplementa reakciju, sekretējot H faktoru (Tu et al., 2010), un trombozi/agregāciju, sekretējot plazminogēna aktivatora inhibitoru-1 (Kaji et al., 2016; Zvonic et al., 2007). Šīm ASC īpašībām ir svarīga nozīme, lai pēc to ievadīšanas asinsritē samazinātu plaušu asinsvadu trombozes risku un nomāktu iekaisuma procesus.

Morfoloģiski ASC ir fibroblastiem līdzīgas vārpstveida šūnas, kurām ir normāls kariotips un kuras var viegli pavairot *in vitro* (Zuk et al., 2001). Turklāt šo šūnu sasaldēšana un atkausēšana neietekmē to diferenciācijas potenciālu (Rodriguez et al., 2005; Goh at al., 2007; Liu at al., 2008; De Rosa at al., 2009).

Starptautiskā šūnu terapijas biedrība ir noteikusi minimālos MSC raksturošanas kritērijus (Dominici et al., 2006), saskaņā ar kuriem tiek pierādīta iegūtās cilmes šūnu populācijas atbilstība MSC. Šie minimālie kritēriji attiecas arī uz ASC raksturošanu un rekomendējoši nosaka, ka 1) šīm šūnām jāspēj piestiprināties pie plastmasas, kad tās tiek audzētas un pavairotas standarta šūnu kultivēšanas apstākļos, 2) tām jābūt ar izteiktu CD90, CD105, CD73, CD44 un CD29 šūnu virsmas marķieru ekspresiju un nav jāuzrāda tādu hemopoētisko šūnu marķieru kā CD45, CD14, HLA-DR un CD34 ekspresija, 3) tām jāpiemīt potenciālam diferencēties adipogēnā, hondrogēnā un osteogēnā virzienā *in vitro*.

1.2. ASC drošums *in vitro*

ASC drošumu *in vitro* pavairošanas laikā raksturo šūnu morfofunkcionālais stāvoklis novecošanās procesā (ASC *in vitro* novecošanās). ASC pašatjaunošanās spēja ir limitēta ar dalīšanās reižu skaitu (Wagner et al., 2008). *In vitro* pavairošanas procesā šūnas noveco, un to raksturo neatgriezenisks šūnu dalīšanās kapacitātes zudums un dramatiskas izmaiņas šūnu morfoloģijā, metabolismā, gēnu ekspresijā un sekrēcijas fenotipā (Dulic 2013; Baker&Sedivy, 2013). Turklāt šūnu novecošanās spēja tiek uzskatīta par nozīmīgu audzēju supresijas mehānismu (Kuilman et al., 2010).

ASC novecošanos raksturo replikatīvā un priekšlaicīgā novecošanās. Kā viena no galvenajām replikatīvās novecošanas pazīmēm ir telomēru DNS saīsināšanās katrā šūnas cikla S fāzē, kuras iemesls ir DNS polimerāzes nespēja pilnībā replicēt atpaliekošo DNS pavedienu (Ohki et al., 2001). Telomēru saīsināšanās procesu dēvē par "mitotisko pulksteni", kurš regulē replikatīvo novecošanos un ir būtisks rādītājs tās noteikšanā (Shay&Wright, 2000). Priekšlaicīgās novecošanās iemesls var būt gan iekšēji, gan ārēji faktori, piemēram, barības

vielu nepietiekamība vai fizikāli vai ķīmiski stresori, uzkrāti DNS bojājumi un onkogēni (Kuilman et al., 2010; Naylor et al., 2013; Raggi&Berardi, 2012). Tādējādi ASC, kuras zaudējušas spēju dalīties un kuru funkcijas ir traucētas, nespēj uzturēt audu homeostāzi (Rossi et al., 2007) un ir uzskatāmas par nedrošām. Tāpēc, lai novērtētu, vai ASC ir drošas pēc *in vitro* pavairošanas, ir nepieciešams izpētīt to novecošanos kultivēšanas laikā (Estrada et al., 2013).

Par ASC novecošanos var spriest pēc:

Morfoloģiskām izmaiņām (Cristofalo&Pignolo, 1993). Novecojošām šūnām raksturīgs lielāks izmērs, tās ir plakanākas, ar lielāku kodolu un vairāk filopodiju un mikrofilamentu. Citoplazma ir ar ieslēgumiem un lielāku skaitu granulu un vakuolu (Mauney et al., 2004; Wagner et al., 2008; Zhao&Darzynkiewicz, 2013).

Proliferatīvās mazspējas. Vēlākās pasāžās samazinās populācijas dubultošanās ātrums (Izadpanah et al., 2006), kā arī koloniju veidojošo vienību (CFU) skaits (Sethe et al., 2006; Schellenberg et al., 2013).

Ar novecošanos saistītās β-galaktozidāzes (SA-β-Gal) aktivitātes pieauguma. SA-β-Gal ekspresijas pieaugums raksturīgs novecojošām šūnām, bet ne proliferatīvi aktīvām šūnām (Dimri et al., 1995; Lee et al., 2006). Tas novērojams arī kontaktinhibīcijas gadījumos, parasti, kad šūnu skaita blīvums ir pārāk liels (Dimri et al., 1995).

Relatīvā telomēru garuma saīsināšanās. Pavairojot šūnas, telomēru garums saīsinās (Harley et al., 1990), un, tam saīsinoties, mazinās šūnu dalīšanās potenciāls (von Zglinicki et al., 2005). Par kritisko telomēru garumu, kad šūnas pārstāj dalīties, tiek uzskatīts 10 kb (Baxter et al., 2004). Bet jāņem vērā, ka relatīvi homogēnā šūnu populācijā šūnas dažādām hromosomām telomēru garumi ir atšķirīgi un individuāli īsa telomēra ierosinās funkciju zuduma mehānismu (Hemann et al., 2001). Turklāt telomēru garums ir heterogēns gan vienas šūnas ietvarā starp dažādām hromosomām, gan starp dažādām šūnām kopējā populācijā, salīdzinot vienu hromosomu šajā populācijā (Lansdorp et al., 1996).

Diferenciācijas potenciāla mazināšanās. Ar pasāžām samazinās osteogēnas un adipogēnas diferenciācijas spēja (Baxter et al., 2004; Bonab et al., 2006; Geisler et al., 2012).

1.3. ASC drošums *in vivo*

ASC *in vivo* drošumu var aplūkot divos aspektos. Vispirms ir jānovērtē ASC ietekme/reakcija uz plaušām, kur šīs šūnas deponējas pēc ievadīšanas asinsritē (Eggenhofer et al., 2012; Fischer et al., 2009; Prologo et al., 2016). Intravenoza ASC ievadīšana ir droša (Kang&Park, 2014; Ra et al., 2011a; Ra et al., 2011b), bet tikko atsaldētu ASC ievadīšana asinsritē var izraisīt potenciālu plaušu embolijas, tūskas vai pat nāves risku (Cyranoski, 2010; Furlani et al., 2009; Jung et al., 2013; Lysaght et al., 2017; Tatsumi et al., 2013). Tam par cēloni var būt agregātu veidošanās plaušu asinsvados vai arī komplementa un imūnās sistēmas reakcija uz ievadītajām ASC (Eggenhofer et al., 2014; Moll&Le Blanc, 2015). Par sekundāru, hipotētisku aspektu uzskatāma atipisku audu vai ļaundabīgu audzēju veidošanās. Ņemot vērā, ka ASC pēc deponēšanās plaušās var migrēt uz iekaisumiem/bojājumiem, kas laika gaitā var rasties jebkur organismā (Anjos-Afonso et al., 2004; Bentzon et al., 2005; Kraitchman et al., 2005), atipisku audu veidošanās teorētiski var būt vērojama dažādās organisma vietās. Tomēr zinātniskajā literatūrā nav informācijas par to, ka autologas ASC pēc ievadīšanas asinsritē veidotu atipiskus audus vai ļaundabīgus audzējus.

1.4. Dzīvnieku modeļi ASC drošuma pārbaudei

Kā viens no piemērotākajiem dzīvnieku modeļiem ASC *in vivo* drošuma pārbaudei ir suņi. Tiem ir salīdzinoši liela dzīvildze, un tie ir tuvi cilvēkam gan pēc anatomiskajām, gan funkcionālajām īpašībām. Tāpat suņiem dabīgi piemīt cilvēkam līdzīgas autoimūnas saslimšanas, piemēram, atopiskais dermatīts (Hall et al., 2010), pemfigus (Han et al., 2015) un autoimūnas izcelsmes 1. tipa cukura diabēts (Abdi et al., 2008; Kim et al., 2017; O'Kell et al., 2017), kas padara pētījumus ar šiem dzīvniekiem daudz pietuvinātākus cilvēkam. Arī suņa taukaudi ir bagāti ar MSC, kuras ir viegli iegūstamas (Neupane et al., 2008; Vieira et al., 2010).

To izmērs, augšanas ātrums, virsmas marķieru ekspresija, diferenciācijas potenciāls ir tuvs cilvēka ASC (hASC), un suņa ASC (cASC) saglabā savu potenciālu pēc ilgstošas kriouzglabāšanas (Martinello et al., 2011; Reich et al., 2012). Tehniskie procesi, kas saistīti ar cASC izolēšanu no taukaudiem, pavairošanu un raksturošanu, ir ļoti līdzīgi darbam ar cilvēka materiālu. Tādējādi suņi var tikt veiksmīgi izmantoti ASC drošības pārbaudei kā pirmais solis šīs tehnikas pārnesei uz klīniku.

1.5. ASC kā jaunieviestās terapijas zāles

Reģeneratīvās medicīnas nozare ir sekmējusi modernizētu terapiju rašanos un attīstījusi tādu principiāli jaunu pieeju zāļu ražošanā kā ATMP, kas iekļauj gan gēnu, gan šūnu terapijas, kā arī audu inženieriju (European, 2014; General, 2015; Vives&Carmona, 2015). ASC var tikt izmantotas kā ATMP personalizētajā ārstniecībā smagu un parastajai ārstēšanai rezistentu slimību gadījumos, piemēram, transplantāta atgrūšanās reakcija, kas saistīta ar steroīdu terapijas rezistenci (Fang et al., 2009; Fang et al., 2007), psoriāzes gadījumi, kad uz parastās terapijas fona attīstās locītavu vai orgānu bojājumii (De Jesus et al., 2016), un multiplā skleroze (Stepien et al., 2016). Autologas ASC, kas sagatavotas konkrētai personai ārpus rutīnas apstākļiem, kā ATMP personalizētai ārstniecībai var izmantot īpašā klīniskā izņēmuma gadījumā (HE) saskaņā ar Eiropas Parlamenta un Padomes Regulas (EK) Nr. 1394/2007 28. pantu (Regulation, 2007). Šajā gadījumā tradicionālie klīniskie pētījumi netiek veikti, bet tāpat ir nepieciešams izvērtēt ASC drošumu, tajā skaitā, veicot šūnu drošuma pārbaudi uz dzīvniekiem.

2. Materiāli un metodes

2.1. ASC drošuma pētījuma tiesiskums un izpilde

Pētījumā iekļautie dzīvnieki izmantoti saskaņā ar Pārtikas un veterinārā dienesta atļauju Nr. 23. hASC pētījumā iegūtas un izmantotas pēc donoru rakstiskas piekrišanas un saskaņā ar Latvijas Centrālās medicīnas ētikas komitejas atļauju Nr. 12. Darbs ar dzīvniekiem un dzīvnieku materiālu izmeklējumi veikti Latvijas Lauksaimniecības Universitātes Veterinārās klīnikas institūtā (Jelgava). ASC no cilvēku un suņu taukaudiem tika iegūtas, pavairotas, iesaldētas un glabātas SIA "Cilmes šūnu tehnoloģijas" (Rīga). ASC raksturošana veikta Latvijas Biomedicīnas pētījumu un studiju centrā (Rīga).

2.2. ASC iegūšana, pavairošana un raksturošana

2.2.1. Autologā seruma sagatavošana

Asins paraugs pēc paņemšanas 1 h tika turēts istabas temperatūrā, lai tas sarecētu. Atdalījušais serums tika savākts, centrfugēts pie 2000 rmp 30 min, izfiltrēts caur 0,2 μm sietu, safasēts un uzglabāts pie -20°C. Asins paņemšana no dzīvniekiem aprakstīta 2.4.4. apakšnodaļā.

2.2.2. Taukaudu paņemšana

Cilvēka vēdera zemādas taukaudi tika iegūti plānveida kosmētiskās operācijas laikā sadarbībā ar SIA "Cilmes šūnu tehnoloģijas", un to veica ķirurgs.

Suņu taukaudu paņemšanu veica veterinārārsts sekojošā veidā. Lai sagatavotu ādu operācijai, vēdera sienas labajā kaudoventrālajā kvadrantā tika noskūts apmatojums 15x15 cm platībā. Tam sekoja ādas mazgāšana ar ziepēm, dezinfekcija ar 70% spirtu trīs reizes un joda šķīdumu vēl trīs reizes. Ādā tika izdarīts 5 cm garš griezums paralēli ķermeņa garengriezuma asij (mediālā plaknē), 5–7 cm laterāli no baltās līnijas (*linea alba*). Zemādas tauki tika iegūti, ar šķērēm izgriežot ~5 ml lielu taukaudu gabalu. Pēc tam tika veikta secīga zemādas (Safil, Aesculap, USA) un ādas aizšūšana (Supramid, S. Jackson, Inc., USA). Dzīvnieku pēcoperācijas aprūpe sastāvēja no nepārtrauktas fizioloģisko parametru uzraudzības operācijas laikā un 2 h pēc anestēzijas efekta beigām, kā arī brūces ikdienas apkopšanas līdz tās pilnīgai sadzīšanai.

Taukadu paraugi tika aptrādāti 3–5 h laikā pēc to iegūšanas.

2.2.3. ASC iegūšana un pavairošana

5 ml iegūto taukaudu tika sagriezti un apstrādāti ar 0,3% pronāzes šķīdumu (EMD Millipore, ASV) 1 h +37°C, viegli rotējot, un pēc tam centrifugēti pie 1000 rmp 7 min. Izveidojušās šūnu nogulsnes tika suspendētas, filtrētas caur 40 μm sietu un atkārtoti centrifugētas 5 min. Eritrocītu līze tika veikta 3 min +37°C, izmantojot eritrocītu līzes buferi Hybri-Max (Sigma-Aldrich, Vācija). Šūnu nogulsnes tika suspendētas svaigā kultivēšanas barotnē DMEM/F12 (Life Technologies, Lielbritānija), kuras sastāvā bija 10% AS, 2 mM L-glutamīns (Life Technologies, Lielbritānija), 20 ng/ml pamata fibroblastu augšanas faktors (BD, ASV), 100 U/ml : 100 g/ml penicilīns–streptomicīns (Life Technologies, Lielbritānija), un uzsētas uz 75 cm^2 šūnu kultivēšanas flakona (uzskatīta kā pasāža 0 (P0)). Visas manipulācijas ar ASC tika izpildītas speciālā šūnu darba stacijā (Xvivo System, Biospherix, ASV), kur šūnas tika audzētas pie +37°C automātiski kontrolētā darba atmosfērā - slāpekli saturošā vidē ar 5% CO_2 un 5% O_2.

Nākošajā dienā nepiestiprinājušās šūnas tika aizvāktas, kārtīgi skalojot ar fosfātu fizioloģisko buferšķīdumu (PBS) (Life Technologies, Lielbritānija). Piestiprinājušās šūnas pirmās 10 dienas tika audzētas barotnē ar 10% AS un pēc tam - 5% AS. P1 (cASC gadījumā) vai P2 (hASC gadījumā) beigās šūnas tika iesaldētas DMEM/F12 barotnē, kuras sastāvā bija

20% AS un 10% dimetil sulfoksīds (DMSO) (Sigma-Aldrich, Vācija), un uzglabātas šķidrajā slāpeklī

Pēc vismaz trīs mēnešu uzglabāšanas ASC tika atkausētas un audzētas kā iepriekš. hASC tika kultivētas no P3 līdz P8, iesaldējot nelielu šūnu daudzumu pirms katras nākamās pasāžas turpmākai analīzei (atkārtota iesaldēšana). Pēc 1,5 līdz 4 gadu uzglabāšanas, hASC tika atkausētas un izmantotas eksperimentiem. cASC tika kultivētas no P2 līdz P5, otro reizi iesaldējot pavairotās šūnas P5 beigās. Pēc vismaz trīs mēnešu uzglabāšanas, P5 cASC tika atkausētas un izmantotas raksturošanai.

2.2.4. Daudzkrāsu plūsmas citometrija

Plūsmas citometrija tika veikta, izmantojot svaigi atsaldētas hASC no P2, P3, P4, P5 un P8 un cASC no P5 saskaņā ar vispārpieņemtu protokolu (Shapiro & Shapiro, 2003). Īsumā, ASC tika strauji atkausētas, skalotas ar PBS un resuspendētas koncentrācijā $5x10^6$ šūnas/ml priekš 8 krāsu plūsmas citometrijas analīzes. Fenotipēšanai tika izmantoti divi savstarpēji saistīti paraugi. Pirmajam paraugam tika izmantotas sekojošas ar fluorohromiem iezīmētas monoklonālās antivielas priekš hASC: HLA-DR-V450, CD14/CD19/CD45 maisījums-V500, CD29-PerCP-Cy5.5, CD44-APC-H7 (BD, ASV), CD34-FITC, CD105-PE, CD73-PE-Cy7, CD90-APC (eBioscience, ASV). Priekš cASC: CD44-PerC-Cy5.5, CD34-PE (Exbio, Čehijas Republika) un CD45/CD14/HLA-DR maisījums-FITC (eBioscience, ASV). Vienas un tās pašas anti-CD90 un anti-CD73 antivielas tika izmantotas tika izmantotas gan hASC, gan cASC paraugiem. Otrais paraugs tika krāsots ar atbilstošajām izotipa kontrolēm. Šūnas tika inkubētas 30 min tumsā, skalotas, resuspendētas PBS un analizētas 2 h laikā. Analīze tika veikta, izmantojot BD FACSCanto II plūsmas citometru (BD, ASV) ar standarta trīs lāzeru konfigurāciju; vismaz 10000 mērījumi tika iegūti no katra parauga. Rezultātu apstrādei un attēlu iegūšanai tika izmantota Infinicyt v1.5.0 programmatūra (Cytognos S.L., Spānija).

Papildus tam, tika noteikta ASC dzīvspēja katrā paraugā, izmantojot 0,5 µM šūnu membrānu šķērsojošo Syto16 fluorescento nukleīnskābju krāsvielu (Life Technologies, Lielbritānija) FITC kanālā (Sparrow & Tippet, 2005). Plūsmas citometrijas analīze tika pielietota arī aneiploīdijas un ASC mitotiskā indeksa noteikšanai, izmantojot FACSCanto II PE kanālu, uz propīdija jodīda bāzēto BD Cycletest Plus DNA komplektu (BD, ASV) un ModFit LT v3.3 programmatūru (BD, ASV).

2.2.5. Diferenciācija trīs šūnu līnijās

Viena un tā pati metode *in vitro* diferenciācijai tika izmantota gan hASC, gan cASC. hASC diferenciācija tika veikta P3, P6 un P9, bet cASC diferenciācijas spēja tika pārbaudīta P6. Lai izraisītu ASC diferenciāciju, šūnas tika audzētas attiecīgajā diferenciācijas barotnē +37°C, 5% CO_2. Paralēli daļa ASC tika audzētas kontroles barotnē. Barotnes tika mainītas katru trešo dienu.

Adipogēnu diferenciācijas potenciālu noteica, audzējot šūnas DMEM barotnē ar augstu glikozes saturu (Life Technologies, Lielbritānija), kam pievienots 10% fetālais govs serums (FBS) (Life Technologies, Lielbritānija), 2 mM L-glutamīns, 10 µg/ml cilvēka insulīns (Life Technologies, Lielbritānija), 1 µM deksametazons (Sigma-Aldrich, Vācija), 100 µM indometacīns (Sigma-Aldrich, Vācija), 0,5 mM 3-izobutil-1-metilksantīns (Sigma-Aldrich, Vācija) un 5 µg/ml gentamicīns (Life Technologies, Lielbritānija). Kontroles barotni veidoja DMEM ar augstu glikozes saturu un 10% FBS. Pēc 16 dienām lipīdu ieslēgumi tika noteikti, izmantojot Oil Red O (Sigma-Aldrich, Vācija) krāsošanu pēc iepriekš aprakstītas metodes (Bogdanova et al., 2010).

ASC osteocītu diferenciācijas potenciāls tika noteikts, audzējot šūnas DMEM barotnē ar zemu glikozes saturu, bez L-glutamīna un fenola sarkanā (Life Technologies, Lielbritānija), kas saturēja 10% FBS, 2 mM L-glutamīnu, 10 mM glicerola-2 fosfātu (Sigma-Aldrich, Vācija), 50 µM L-askorbīnskābi (Sigma-Aldrich, Vācija), 0,1 µM deksametazonu, 5 µg/ml gentamicīnu (Life Technologies, Lielbritānija). Kontroles šūnas tika kultivētas DMEM barotnē ar zemu glikozes saturu un 10% FBS. Pēc 30 dienām ekstracelulārā kalcija uzkrāšanās tika noteikta ar

Alizarin Red S (Sigma-Aldrich, Vācija) krāsošanu (Bogdanova et al., 2010), un sārmainās fosfatāzes aktivitāte tika detektēta, kā substrātu izmantojot BCIP/NBT (Sigma-Aldrich, Vācija).

Lai noteiktu ondrocītu diferenciācijas potenciālu, 10µl ASC suspensijas (koncentrācija $8x10^6$ šūnas/ml) tika uznesti uz plastmasa plates un inkubēti 30 min +37°C, 5% CO_2. Pēc tam šūnām tika pievienota kontroles vai diferenciācijas barotne, kas sastāvēja no DMEM (ar zemu glikozes saturu, bez L-glutamīna un fenola sarkanā), kam pievienoti 10% FBS, 2 mM L-glutamīns, 1x insulīns-transferrīns-selēns-plus (BD, ASV), 40 µg/ml L-prolīns (Sigma-Aldrich, Vācija), 50 µM L-askorbīnskābes, 0,1 µM deksametazons, 10 ng/ml rekombinantais cilvēka transformējošais augšanas faktoru β3 (Life Technologies, Lielbritānija) un 5 µg/ml gentamicīns. Kontroles barotnes sastāvs bija identisks osteogēnajā diferenciācijā izmantotajai. Pēc 29 izveidojušies šūnu agregāti tika ieslēgti parafīnā, sagriezti un krāsoti ar 1% Alcian Blue (Sigma-Aldrich, Vācija) krāsvielas šķīdumu 0,1 N HCl (pH~1) 30 min, kam sekoja mazgāšana ar 0,1 N HCl.

2.2.6. Blasttransformācijas tests

Autologas PBMNC tika iegūtas no svaigām perifērajām asinīm ar Ficoll-Paque Premium blīvuma gradientu (GE Healthcare, Zviedrija). Izdalītās PBMNC tika kultivētas RPMI-1640 barotnē (Life Technologies, Lielbritānija), kas saturēja 10% AS, 2 mM L-glutamīnu un 100 U/ml : 100 g/ml penicilīnu–streptomicīnu, kopā ar ASC dažādās attiecībās (ASC:PBMNC - $5x10^4$: $5x10^4$ (1:1), $5x10^3$: $5x10^4$ (1:10), $2.5x10^3$: $5x10^4$ (1:20), $1.25x10^3$: $5x10^4$ (1:40), $5x10^2$: $5x10^4$ (1:100)) un fitohemaglutinīnu (Sigma-Aldrich, Vācija) koncentrācijā 2 vai 4 µg/ml 96 h +37°C, 5% CO_2. Blasttransformācijas reakcija tika veikta, izmantojot hASC no P3, P6 un P9 un cASC no P6. Uz pēdējām 18 h katram paraugam tika pievienots 1 µCi [3H]-deoksitimidīna (GE, Lielbritānija). Radioaktīvā timidīna ieslēgšanās analīze tika veikta, izmantojot šķidrās scintilācijas beta skaitītāju (Beckman Coulter, ASV).

2.3. hASC *in vitro* senescences noteikšana

2.3.1. Ilgtermiņa in vitro šūnu kultivēšana

Tika pārbaudītas astoņu donoru hASC kultūras (1. tabula). Visas šūnu kultūras tika iegūtas no šūnu bankas, kur tās tika glabātas P2 (izņemot donora CS-5 šūnas, kuras bija glabātas P3). Pēc atkausēšanas šūnas tika saskaitītas, izmantojot Burkera kameru, uzsētas uz 75 cm^2 šūnu kultivēšanas flakona ($2x10^5$ šūnas uz flakonu) DMEM/F12 barotnē, kas saturēja 10% FBS, 20 ng/ml pamata fibroblastu augšanas faktoru, 2 mM L-glutamīnu un 100 µ/ml:100 µg/ml penicilīnu-streptomicīnu, un audzētas mitrā gaisā +37°C, 5% CO_2. Barotne tika mainīta katru trešo dienu. Kad šūnas sasniedza 80–90% konfluenci, tās tika atdalītas no flakona, izmantojot šūnu disociācijas reaģentu TrypLE Express Enzyme (Life Technologies, Lielbritānija). Daļa šūnu tika sadalīta attiecībā 1:5 tālākai pārsēšanai. Atlikušās šūnas tika iesaldētas DMEM/F12 barotnē, kas saturēja 10% DMSO un 20% FBS, un uzglabātas šķidrajā slāpeklī turpmākai analīzei. hASC pārsēšana tika turpināta, saglabājot sadalīšanas attiecību 1:5, kamēr šūnu konfluence netika sasniegta četru nedēļu laikā.

Lai noteiktu hASC dalīšanās kinētiku, šūnas tika skaitītas Burkera kamerā katras pasāžas beigās. Populācijas dubultošanās laiks (PDT) un populācijas dubultošanās (PD) skaits tika noteikts pēc sekojošām formulām:

$$PDT=\ln 2*T/\ln(N_T/N_0) \text{ un } PD=T/PDT$$

kur T – kultivēšanas ilgums, N_T – šūnu skaits pasāžas beigās, N_0 – šūnu skaits pasāžas sākumā.

2.3.2. Koloniju veidojošo vienību pārbaude

10^3 hASC tika uzsētas uz sešu aiļu plastmasas plates divos atkārtojumos, izmantojot to pašu barotni, ko šūnu audzēšanai, un kultivētas divas nedēļas +37°C, 5% CO_2. Barotne tika mainīta katru ceturto dienu. Pēc tam plates tika novietotas uz ledus un divas reizes mazgātas ar aukstu PBS. Šūnas tika fiksētas ar ledusaukstu metanolu 10 min, pārvietotas istabas temperatūrā un krāsotas ar 0,5% kristālvioletā krāsas (Sigma-Aldrich, Vācija) šķīdumu metanolā. Krāsojums tika izšķīdināts ar 0,5% nātrija dodecilsulfātu, un absorbcija tika mērīta pie 539 nm viļņu garuma.

2.3.3. SA- β -galaktozidāzes noteikšana

$2{,}5x10^4$ hASC tika uzsētas uz 96 aiļu plastmasas plates trīs atkārtojumos. Pēc 48 h tika noteikta β-galaktozidāzes ekspresija, izmantojot Senescence Cells histoķīmiskās krāsošanas komplektu (Sigma-Aldrich, Vācija) pēc ražotāja instrukcijām. Lai iegūtu kvantificējamus rezultātus, ar PowerShot S80 digitālo fotokameru (Canon, ASV) tika iegūti krāsoto šūnu fotoattēli, kurus novērtēja divi neatkarīgi vērtētāji. Vērtēšana tika veikta pēc diviem parametriem: krāsas intensitāte un nokrāsoto šūnu daudzums procentos redzes laukā. Krāsojuma intensitātes noteikšanai tika izveidota piecu punktu intensitātes skala, kur 0 nozīmēja "nav krāsojuma" un 5 – "ļoti tumšs krāsojums".

2.3.4. Telomēru Flow FISH

Kultivētu hASC relatīvais telomēru garums tika noteikts, izmantojot Telomere PNA Kit/FITC priekš plūsmas citometrijas (Dako, Dānija) pēc ražotāja instrukcijām un FACSCanto II plūsmas citometru ar FACSDiva v7.0 programmatūru (BD, ASV). Jurkat šūnu līnija (ATCC/LGC Standards, Zviedrija) kalpoja kā iekšējā kontrole. Katrs paraugs tika pārbaudīts divreiz, un 20000 mērījumu tika iegūti no katra parauga. Plūsmas citometra kalibrācija tika veikta, izmantojot kalibrācijas lodītes (BD Cytometer Setup and Tracking Beads, BD, ASV). Rezultāti tika analizēti ar Infinicyt v1.5.0 programmatūru.

2.4. cASC *in vivo* drošums

2.4.1. Eksperimentālie dzīvnieki un to aprūpe

Divi bīglu šķirnes suņi - viens sieviešu un otrs vīriešu kārtas pārstāvis - tika izmantoti pētījumā. Neviens no dzīvniekiem nebija sterilizēts/kastrēts. Abi suņi tika iegūti no sertificētas laboratorijas dzīvnieku iestādes CEDS (Francija). cASC ievadīšanas laikā dzīvnieki bija 2,5 gadus veci un eitanāzijas laikā - 5 gadus veci. Suņu svars cASC ievadīšanas laikā bija 14,5 kg (sieviešu kārtas suns) un 18,5 kg (vīriešu kārtas suns). Pēc eitanāzijas dzīvnieku svars bija attiecīgi 17 kg un 18,4 kg, un ķermeņa stāvoklis bija labs (3,5 punkti sieviešu kārtas sunim un 3 punkti vīriešu kārtas sunim pēc 5 punktu skalas).

Dzīvnieki tika turēti apsildītos un norobežotos 2x1,5 m krātiņos ar ventilāciju. Dzīvnieku uzturēšanas telpās bija atsevišķa telpa ēdiena pagatavošanai, personāla ģērbtuve, duša un labierīcības. Visas telpas bija viegli dezinficējamas, un tām bija atsevišķa noteksistēma. Kompleksā sausā suņu barība dzīvniekiem tika dota divas reizes dienā, svaigs ūdens bija pieejams nepārtraukti. Pastaigas tika nodrošinātas trīs reizes dienā. Fizioloģiskie parametri (rektālā temperatūra, elpošanas un sirdsdarbības ātrums) tika kontrolēti divas reizes dienā, bet gļotādu un zemādas limfmezglu pārbaude tika veikta reizi dienā.

2.4.2. Autologu cASC ievadīšana

Pirms katetra ievietošanas cefāliskajā vēnā dzīvniekam tika veikta nomierinoša līdzekļa acepromazīna malāta (0,5 mg/kg) intramuskulāra injekcija. Dūriena vieta tika sagatavota

sekojoši: cefāliskajā iedobē tika noskūts apmatojums 5x5 cm platībā, un āda tika dezinficēta ar 70% spirtu (3x) un joda šķīdumu (1x). Ārējā cefāliskajā vēnā tika veikts aseptisks dūriens ar G18 adatu, un katetrs tika piestiprināts, izmantojot leikoplastu un marles saiti.

Vispirms, lai novērtētu iespējamos DMSO (kontroles barotne) blakusefektus un aprakstītu tā izvadīšanu no organisma, 100 ml fizioloģiskā šķīduma, kas saturēja 10% DMSO, tika intravenozi injicēti dzīvniekiem. Pēc tam sekoja terapeitiskās devas ievadīšana, ko veidoja $2x10^6$ dzīvas, tikko atkausētas, neskalotas, autologas cASC (P5) uz kg ķermeņa svara 100 ml kopējā tilpumā (pielāgots ar fizioloģisko šķīdumu). Vienu mēnesi vēlāk eksperimentālajiem suņiem tika intravenozi injicēta piecas reizes lielākā cASC deva ($1x10^7$ dzīvas šūnas/kg).

2.4.3. Suņu uzvedības novērtējums

Suņu uzvedības noteikšanai pirms un pēc DMSO barotnes un cASC intravenozas ievadīšanas tika veikti daļēji uzvedības novērtēšanas testi. Sabiedriskuma tests ļāva noteikt suņa uzvedību telpā, un tas iekļāva ķermeņa pozas, ostīšanas, telpas izpētes, acu un sociālā kontakta veidošanas ar cilvēkiem novērtējumu. Zobu pārbaude tika izmantota, lai testētu suņa atbildes reakciju uz zobu un mutes apskati 5 sec. Pieskaršanās tests tika pielietots, lai novērtēt dzīvnieka reakciju uz aiztikšanu un dažādu ķermeņa daļu glaudīšanu 5 sec, ieskaitot asti un ausis.

2.4.4. Asins un urīna paraugu paņemšana

Lai savāktu asins paraugus, dzīvnieku nomierināšana un dūriena vietas sagatavošana tika veikta tāpat, kā aprakstīts 3.4.1. apakšnodaļā. Tika izmantota G16 adata, un tika paņemti 50 ml (bet ne vairāk kā 0,5% no ķermeņa svara) asiņu.

Urīna un asins paraugi tika savākti 24 h pirms un 12, 24, 72 h pēc DMSO barotnes ievadīšanas, kā arī 24 h pirms un 24 h, 72 h, 7 dienas, 14 dienas pēc cASCs ievadīšanas. Asins paraugi tika paņemti no *v. jugularis* vai *v. saphena* un sapildīti asins ņemšanas stobriņos ar seruma stabilizatoru (priekš bioķīmiskajiem testiem), EDTA (priekš hematoloģiskās un morfoloģiskās raksturošanas) vai nātrija citrātu (priekš koagulācijas faktoru noteikšanas) (BD, ASV). Rīta urīna paraugi no urīna strūklas vidusposma tika paņemti, uzglabāti +4°C un pārbaudīti 3 h laikā pēc savākšanas.

2.4.5. Bioķīmisko, hematoloģisko un koagulācijas faktoru noteikšana

Bioķīmiskie testi tika veikti ar Ortho Vitros DT60/DTEII/DTSC analizatoru (Ortho Clinical Diagnostics, ASV), izmantojot vienreizlietojamo slaidu kalorimetrisko pārbaudi. Tāpat bioķīmiskie asins testi tika veikti sertificētas firmas (akreditācijas sertifikāts Nr. LATAK-M-43400-2011) SIA "Centrālā laboratorija" laboratorijā (reģistrācijas Nr. 215/L 430-C) pēc standarta laboratorijas protokoliem un saskaņā ar LVS NE ISO 15189:2008 standartu.

Asins hematoloģiskās pārbaudes tika izpildītas automātiski, izmantojot Nihon Kohden MEK 6318 K analizatoru (Nihon Kohden, Japāna), un morfoloģiskās pārbaudes tika veiktas, novērtējot asins uztriepes ar binokulārā mikroskopa Omax (Omax, Dienvidkoreja) palīdzību pie 40–2000x liela palielinājuma.

Koagulācijas faktori tika noteikti vienu dienu pirms un dienu pēc 10% DMSO ievadīšanas, kā arī pirms abām cASC ievadīšanām dzīvniekiem. Asins paraugi koagulācijas faktoru noteikšanai tika savākti stobriņos ar 3,8% nātrija citrātu; asins plazma tika centrifugēta, iesaldēta −20°C un nosūtīta uz IDEXX Vet Med laboratoriju (IDDEXX GmbH, Vācija) analīzēm. Tika pārbaudīti šādi koagulācijas faktori: protrombīna laiks, aktivētā parciālā tromboplastīna laiks (aPTT) un fibrinogēns. To normālās vērtības ir: aPTT <13,5 sec; fibrinogēns 1,2–2,9 g/l; protrombīna laiks <18 sec.

Urīna paraugi tika analizēti ar Combi-Screen Vet 11 Plus testa strēmelēm (Analyticon, Vācija), nolasot rezultātu 60 sec pēc parauga uzlikšanas. urīna blīvums tika noteikts, izmantojot refraktometru. Urīna paraugi tika centrifugēti pie 3500 rpm 10 min, un urīna nogulsnēs tika pārbaudīta leikocītu, eritrocītu, epiteliālo šūnu, baktēriju (skaits/HPF), kristālu un cilindru (skaits/LPF) klātbūtne ar binokulāro mikroskopu Omax pie 40–2000x liela palielinājuma.

2.4.6. Sirdsdarbības monitorings

Elektrokardiogrāfiskie izmeklējumi tika veikti 24 h pirms un 3, 7, 14 dienas pēc, bet ehokardiogrāfija - 24 h pirms un 3 dienas pēc abām cASC ievadīšanām. Papildus tam, nepārtraukts Holtera monitorings tika veikts 24 h pirms, kā arī pirmo 24 h laikā pēc abām cASC ievadīšanām.

Elektrokardiogrāfija tika veikta, izmantojot BTL-08 aparātu (BTL Industries, Inc., ASV), kamēr dzīvnieki gulēja uz labā sāna. Tika iegūti seši novadījumi (I, II, III, aVR, aVL, aVF). Dati tika saglabāti un apstrādāti ar BTL programmatūru (BTL Industries, Inc., ASV). Elektrokardiogramma tika izmantota, lai analizētu sirds ritmu: raidītāja norādīto primāro ritmu (sinoatriālais mezgls, sinusa ritms) un sirdsdarbības ātrumu. II novadījums tika pielietots P-QRS-T analīzei.

Ehokardiogrāfija tika veikta ar ultraskaņas skeneri Philips HD-11 (Philips, Nīderlande), kamēr dzīvnieki gulēja uz labā sāna, lai iegūtu labās puses parasternālo proksimālo un transverso sirds projekciju, un uz kreisā sāna, lai iegūtu kreisās puses parasternālo apikālo projekciju. Tika veikti sirds kreisā kambara standarta mērījumi sistolē un diastolē (M režīms), labā kambara un priekškambara vizuālais novērtējums, kreisā priekškambara un aortas mērījumi (2D režīmā) un doplerogrāfiskais izmeklējums transmitrālās un transtrikupsīdās asins plūsmas (pulsa viļņa doplerogrāfija), kā arī aortas un plaušu arteriālās asins plūsmas (nepārtrauktā viļņa doplerogrāfija) noteikšanai.

Holtera monitoringam tika pielietota Televet 100 sistēma (Televet, Vācija), piestiprinot elektrodus dzīvnieka krūšukurvim. Tika iegūti standarta novadījumi I, II un III. Iegūtie dati tika analizēti, izmantojot Televet 100 programmatūru. Sirds ritms tika analizēts pēc elektrokardiogrammas. Tika noteikts primārais ritma nodrošinātājs (sinoatriālais mezgls), vidējais sirdsdarbības ātrums katrā monitoringa stundā, kā arī maksimālais un minimālais sirdsdarbības ātrums.

2.4.7. Eitanāzija, nekropsija un histoloģiskā pārbaude

Dzīvnieki tika iemidzināti, izmantojot eitanāzijai paredzēto šķīdumu T-61 (0,3 ml/kg), kas saturēja 200 mg embutramīda, 50 mg mebezonija jodīda un 5 mg tetrakaīna hidrohlorīda 1 ml šķīduma. Eitanāzijas šķīdums tika ievadīts intravenozi pēc intramuskulāras nomierinoša līdzekļa injekcijas (acepromazīna malāts 0,02 mg/kg) un intravenozas narkozes līdzekļu ketamīna (4 mg/kg) un diazepāma (0,4 mg/kg) injekcijas.

Nekropsija tika veikta 30 min pēc eitanāzijas; suņu ķermeņi bija ļoti labā pēcnāves stāvoklī. Muskuļu stīvums vai autolīze netika novēroti. Apmatojums, āda un nagi bija tīri. Sieviešu kārtas sunim ārējās ķermeņa atveres bija tīras un bez ekskrēcijas. Vīriešu kārtas sunim anālā atvere bija atvērta un notraipīta ar sausiem izkārnījumiem; pārējās ārējās ķermeņa atveres bija tīras un bez ekskrēcijas. Sieviešu kārtas sunim bija novērojama neliela hipostāze uz labā sāna.

Dzīvnieku audus un orgānus raksturojoši paraugi tika savākti un fiksēti 10% formalīnā (Sigma-Aldrich, Vācija) vismaz 24 h. Ieslēgšanai parafīnā tika nogriezti mazāki audu un orgānu gabali. Pēc audu dehidratācijas pieaugošas koncentrācijas etanolā paraugi tika ieslēgti parafīna blokos un sagriezti 4 μm biezumā. Iegūtie audu griezumi tika krāsoti ar hematoksilīnu un eozīnu un analizēti, izmantojot Olympus BX51 (Olympus, Japan) mikroskopus.

2.5. Statistiskā analīze

Blasttransformācijas eksperimentu dati ir parādīti kā vidējais ± standartnovirze (SD) no trīs atkārtojumiem. hASC statistiskajai analīzei tika pielietots nesapārotais Stjūdenta t-tests. Vidējo lielumu salīdzināšana starp atšķirīgām grupām tika veikta, izmantojot vienfaktora dispersijas analīzi (ANOVA). Iegūto datu normālsadalījums tika analizēts ar Brauna-Forsaita un Bārtleta testiem. Atšķirības subjektu starpā un subjektu iekšējās atšķirības starp dažādām

grupām tika noteiktas ar divfaktoru ANOVA, kam sekoja *post-hoc* tests. Visos gadījumos divpakāpju Bendžamini, Krīgera un Jekutili metode tika izmantota kā *post-hoc* analīze. Lai noteiktu cASC imunosupresīvo efektu, tika veikta korelācijas un regresijas analīze. *p* vērtības, kas bija mazākas par 0,05, tika uzskatītas par statistiski nozīmīgām. Blasttransformācijas datu statistiskajai analīzei, aprēķiniem un grafiku iegūšanai tika izmantota GraphPad Prism v7.0 MacOS programmatūra (GraphPad Software, ASV).

Statistiskā analīze hASC *in vitro* senescences eksperimentiem tika veikta, izmantojot R v3.0.2 programmatūru. Divu datu kopu salīdzināšanai tika pielietots t-tests vai Vilkoksona tests, balstoties uz izkliedes viendabību, kas tika noteikta ar F-testu. Saistība starp rezultātiem, kas iegūti ar diviem dažādiem testiem, tika noteikta, izmantojot korelācijas vai regresijas analīzi. Korelācijas analīzei tika pielietots Šapiro-Vilka normalitātes tests, lai noskaidrotu, vai dati atbilst normālsadalījumam. Atkarībā no normalitātes, tika izmantota Pīrsona vai Spīrmena korelācijas analīze. Regresijas analīze tika veikta, izmantojot lm() funkciju. Regresijas pieņēmumi tika testēti ar grafiskās analīzes palīdzību. Katra datu punkta ietekme uz regresijas modeli tika noteikta, pielietojot Kuka distanci. Būtiskuma līmenis visiem testiem bija $\alpha = 0,05$.

3. Rezultāti un diskusija

3.1. hASC un cASC raksturojums

3.1.1. ASC kultivēšanas aspekti

ASC var viegli izdalīt gan no cilvēka, gan suņa taukaudiem. Iegūtās ASC no abiem avotiem bija plastmasas adherentas šūnas ar tipisku vārpstveida morfoloģiju, kas ir raksturīga hASC (Zuk et al., 2001) un jau iepriekš aprakstīta arī cASC (Martinello et al., 2011; Neupane et al., 2008; Vieira et al., 2010). Lai pavairotu ASC ar potenciālu terapeitisko vērtību, mēs izmantojām barotni ar AS, nevis FBS, lai izslēgtu kontaminācijas risku ar svešiem proteīniem, kas varētu novest pie iespējamas autoimūnas reakcijas pret paša pacienta cilmes šūnām (Spees et al., 2004). Pirmās desmit dienas ASC tika kultivētas barotnē, kas saturēja 10% AS, bet pēc tam serumam daudzums tika samazināts līdz 5%. Mēs esam izvērtējuši, ka tas ir pietiekami efektīvai ASC proliferācijai, kā arī tas ir mazāk invazīvi pacientam, jo nepieciešamais asins apjoms seruma iegūšanai ir mazāks nekā tas būtu gadījumā, ja visu laiku tiktu izmantots 10% AS. Mēs esam noteikuši, ka šādos kultivēšanas apstākļos no sākotnējiem 5 ml taukaudu var iegūt aptuveni 10^9 ASC P5 beigās. Tas ir pietiekami 3–4 atkārtotām ASC ievadīšanām 90–100 kg smagam pacientam, izmantojot terapeitisko devu 3x106 šūnas uz kg ķermeņa svara. Tāpat ir parādīts, ka MSC no dažādiem avotiem dalās ātrāk (Im at al., 2011; Mizuno at al., 2006; Nimura at al., 2008; Shahdadfar at al., 2005;) un saglabā augstāku nemetilētu stāvokli ilgtermiņa kultūrā (Dahl at al., 2008), ja tās tiek audzētas barotnē ar AS, nevis FBS.

Papildus tam, lai palielinātu izdzīvošanas iespējas *in vitro* pavairotām ASC pēc to ievadīšanas pacientam, ir svarīgi samazināt atšķirības starp apstākļiem šūnu kultūrā un ievadīšanas vietā. Tā kā praktiski visas šūnu kultūras tiek audzētas pie atmosfēras skābekļa koncentrācijas (21%), bet skābekļa koncentrācija audos var svārstīties no 4–14% labi apasiņotos orgānos līdz 0–4% kaula smadzenēs (Ivanovic, 2009), tad ievadītās ASC var saskarties ar ievērojamu hipoksisko stresu, kas noved pie apoptozes. Tāpēc mēs pielietojām 5% skābekļa koncentrāciju ASC pavairošanai, lai šūnām nodrošinātu vidi, kas ir līdzīgāka *in vivo* apstākļiem, un samazinātu šūnu stresu. Agrākie pētījumi ir parādījuši, ka MSC, kas kultivētas hipoksiskos apstākļos, uzrāda paaugstinātu spēju atjaunot miokardu pēc infarkta pazemināta šūnu nāves un paaugstinātas angioģenēzes dēļ (Hu et al., 2008). Tāpat tām piemīt straujāks audu atjaunošanas potenciāls (Leroux et al., 2010; Rosova et al., 2008), pastiprināta brūču dziedēšanas funkcija (Lee et al., 2009) un palielināta iedzīvošanās spēja *in vivo* (Hung et al., 2007), salīdzinot ar šūnām, kuras kultivētas normoksiskos apstākļos. Ir pierādīts, ka audzēšana pie samazinātas skābekļa koncentrācijas palīdz saglabāt MSC multipotento un nediferencēto stāvokli (Basciano et al., 2011) un var novērst proliferatīvo senescenci un palielināt šūnu dzīves ilgumu (Tsai et al., 2011).

Iegūtie rezultāti liecina, ka ne šūnu kultivēšanas barotne, kuras sastāvā FBS vietā bija AS, ne šūnu audzēšana pie 5% skābekļa koncentrācijas neietekmēja hASC un cASC raksturīgo fibroblastiem līdzīgo morfoloģiju, un tā saglabājās līdz vēlākām pasāžām un pēc divkāršas sasaldēšanas un atkausēšanas. Tas parāda, ka ASC var tikt efektīvi pavairotas, izmantojot šādu metodoloģiju.

3.1.2. Šūnas virsmas marķieru ekspresija

Daudzi pētījumi ir veltīti plašai hASC raksturošanai pēc to fenotipiskajām un funkcionālajām īpašībām, sākot ar šūnām stromas vaskulārajā frakcijā (SVF) un beidzot ar vēlām šūnu pasāžām (Astori at al., 2007; Gronthos at al., 2001; Katz at al., 2005; Mitchell at al., 2006; Park at al., 2010; Varma at al., 2007; Yang at al., 2011; Zhu at al., 2008). Nesen ir publicēta vispusīga kultivētu hASC fenotipa analīze (Baer at al., 2013), un tādu jaunu zinātnisko metožu kā daudzkrāsu plūsmas citometrija iespējas tiek izmantotas, lai raksturotu dažādas MSC populācijas (Astori at al., 2007; Baer at al., 2013; Lin at al., 2008; Martins at al., 2009).

Šajā darbā tika izmantota astoņu krāsu plūsmas citometrijas analīze, lai noteiktu izmaiņas šūnas virsmas marķieru ekspresijā dažādās hASC pasāžās pēc vairāk nekā četru gadu ilgas glabāšanas iesaldētā stāvoklī un divkāršas sasaldēšanas. Šūnas tika testētas uzreiz pēc to atkausēšanas, kā tas būtu tieši pirms ASC terapijas. Desmit dažādi virsmas marķieri tika vienlaicīgi pārbaudīti uz katras hASC. Plūsmas citometrijas analīzei tika izmantotas hASC (donora kods CS-5), kuras bija iesaldētas pēc pasāžām 2, 3, 4, 5 un 8. Šūnu dzīvotspējas tests (Syto16 krāsošana), kas tika veikts katram atkausētajam paraugam, uzrādīja, ka dzīvo šūnu koncentrācija visos paraugos ir vismaz 95%. Iegūtie rezultāti parādīja, ka visas hASC ir pozitīvas pēc tādiem MSC marķieriem kā CD29, CD44, CD73, CD90, CD105 un negatīvas pēc HLA-DR, CD34 un CD14/CD19/CD45 apvienojuma. Salīdzinot individuālo marķieru vidējo fluorescences intensitāti visās pārbaudītajās pasāžās, varēja novērot marķieru fluorescences intensitātes pieaugumu ar katru nākamo šūnu pasāžu, izņemot CD44, kam tika detektēts straujš kritums P5 (1. attēls). Tā kā hASC populācija saglabājās fenotipiski homogēna, ekspresējot CD29, CD44, CD73, CD90 un CD105 visās pārbaudītajās pasāžās, tad fluorescences intensitātes pieaugums var norādīt uz proteīna ekspresijas uzkrāšanos ar katru nākamo pasāžu. Salīdzinot fluorescences intensitāti starp marķieriem, varēja redzēt, ka vislielākajā daudzumā uz hASC virsmas ir atrodams CD90, kam seko CD29 un CD73, bet CD105 uzrāda viszemāko ekspresijas līmeni visās pasāžās. Iegūtie dati norāda, ka maksimālo proteīna ekspresiju CD73 un CD44 marķieriem var novērot attiecīgi P5 un P4, bet CD29, CD90 un CD105 gadījumā var detektēt proteīna pieaugumu līdz pat P8.

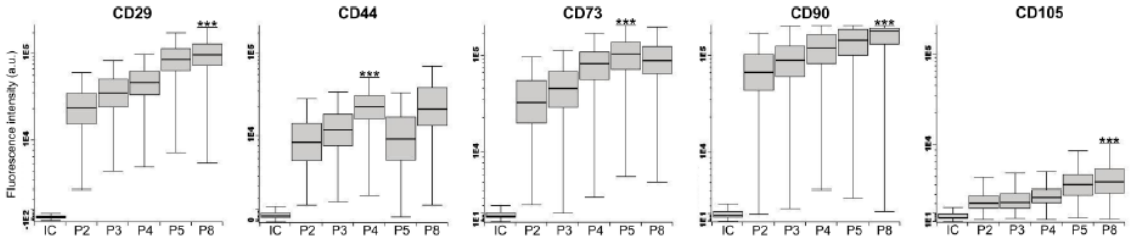

1. attēls. Šūnas virsmas marķieru ekspresijas fluorescences intensitātes analīze no cilvēka taukaudiem izdalītās dažādu pasāžu cilmes šūnās. Rezultāti ir parādīti kā kastīšu diagramma, kur mediānas vērtība atainota kā līnija, 25. un 75. procentīle - kā kastīte un 10. un 90. procentīle - kā slotiņas. Datu analīze veikta ar Infinicyt programmatūru (v1.5.0). Zvaigznītes pie šūnu pasāžas ar visaugstāko fluorescences intensitāti norāda uz statistiski nozīmīgu pieaugumu, salīdzinot ar P2. *** $p < 0{,}001$. IC – izotipa kontrole; P – pasāža; a.u. - arbitrārās vienības.

Daži autori ir demonstrējuši pozitīvo MSC virsmas marķieru ekspresijas pieaugumu ar pasāžām (Mitchell at al., 2006; Park at al., 2010; Varma at al., 2007), taču citi nav novērojuši atšķirību no P3 līdz P12 (Yang at al., 2011). Vislielākās domstarpības pastāv par CD34 ekspresiju hASC. Atsevišķos pētījumos CD34 nav detektēts (Zuk at al., 2002; Zhu at al.,2008), bet citi ziņo par augstu CD34 ekspresijas līmeni (Gronthos at al., 2001; Park at al.,2010). Kā iespējamos nesakritību iemeslus zinātnieki min atšķirīgus šūnu kultivēšanas apstākļus, donoru specifiskās atšķirības, antivielu iezīmju izvēli (Baer at al., 2013) un individuālas robežu izvēles stratēģijas, ko pielieto plūsmas citometrijā (Astori at al., 2007).

cASC no P5 arī tika pārbaudītas pēc septiņu dažādu šūnas virsmas marķieru vienlaicīgas ekspresijas, izmantojot daudzkrāsu plūsmas citometriju. Syto16 krāsošana parādīja apoptotisko šūnu daudzumu zem 5% abos cASC paraugos (2. F, L attēls), demonstrējot augstu šūnu dzīvotspēju. Abu suņu cASC kultūras uzrādīja fenotipiski homogēnu šūnu populāciju, kas ir izteikti pozitīva pēc MSC marķieriem CD44 un CD73, vidēji pozitīva pēc CD90 un negatīva pēc hemopoētisko cilmes šūnu marķiera CD34 un leikocītu līnijas antigēnu CD45, CD14 un HLA-DR apvienojuma (2. attēls).

Līdzīga cASC virsmas marķieru ekspresija ir aprakstīta iepriekš (Kisiel et al., 2012; Martinello et al., 2011; Reich et al., 2012; Russell et al., 2016; Takemitsu et al., 2012; Vieira et al., 2010). Lielākā daļa no šiem pētījumiem ir noteikusi konstantu CD90 un CD44 ekspresiju kopā ar citiem pozitīvajiem virsmas marķieriem, taču ziņas par CD73 ekspresiju atšķiras dažādu

autoru darbos. Daži ir parādījuši vidēju CD73 ekspresiju (Russell et al., 2016), bet citi to nav detektējuši vispār (Takemitsu et al., 2012; Vieira et al., 2010). Tāpat lielākajā daļā no pētījumiem cASC nav atrasta CD45 ekspresija, tomēr vāja CD14 un CD34 ekspresija ir detektēta (Russell et al., 2016; Vieira et al., 2010). Šīs atšķirības varētu izskaidrot ar dažādām taukaudu paņemšanas vietām (Sullivan et al., 2016) vai antivielu variācijām, kas izmantotas analīzei.

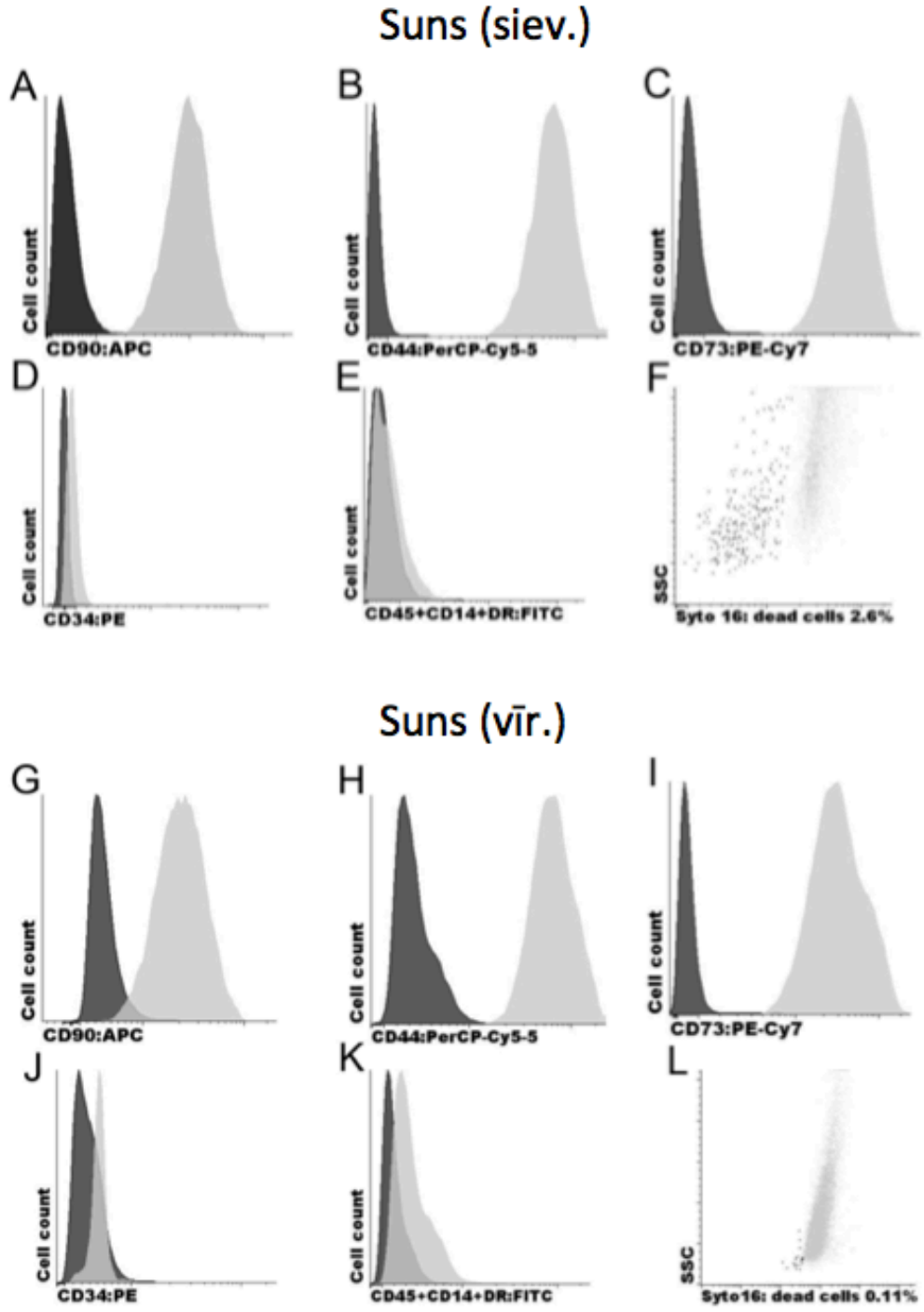

2. attēls. Tikko atkausētu no suņa taukaudiem izdalītu 5. pasāžas cilmes šūnu fenotipiskā analīze, izmantojot daudzkrāsu plūsmas citometriju. (A–E, G–K) Šūnas virsmas marķieru CD90, CD44, CD73, CD34, CD45, CD14 un HLA-DR ekspresija (tumšie pīķi – izotipa kontrole, gaišie pīķi – specifisks krāsojums). (F, L) Syto 16 šūnu dzīvotspējas krāsojums (tumšie punkti – apoptotiskas šūnas, gaišie punkti – dzīvas šūnas).

Kopumā daudzkrāsu plūsmas citometrijas analīze parādīja, ka gan cilvēka, gan suņa ASC, kuras audzētas barotnē ar AS un pie 5% skābekļa koncentrācijas, ekspresē tipiskus MSC marķierus vienlaicīgi, neatkarīgi no pasāžas, demonstrē ļoti homogēnu šūnu populāciju un uzrāda augstu šūnu dzīvotspēju pēc ilgtermiņa glabāšanas iesaldētā stāvoklī.

Papildus šūnas cikla analīze parādīja, ka hASC, kuras atrodas S un G2/M fāzēs, kopā sastāda aptuveni 2,8% P2 un P3, 3,4% P4 un P5, kā arī 6,6% P8, demonstrējot mitotiskās aktivitātes pieaugumu pa pasāžām. Šādu proliferējošu šūnu frakcija veidoja apmēram 3% vīriešu kārtas cASC un 6,9% sieviešu kārtas cASC no P5. Ne hASC, ne cASC netika detektēta aneiploīdija.

3.1.3. ASC diferenciācijas spēja

ASC spēja diferencēties citos mezodermālas izcelsmes šūnu veidos ir galvenais stūrakmens to identitātes apstiprināšanai. Lai noteiktu, vai ASC, kuras kultivētas barotnē ar AS, saglabā savu potenciālu diferencēties par adipocītiem, osteocītiem un hondrocītiem, hASC (donora kods CS-5) no P3 tika pakļautas *in vitro* diferenciācijai. Tāds pats eksperiments tika atkārtots pēc šo šūnu uzglabāšanas iesaldētā stāvoklī vairāk nekā četrus gadus, lai pārbaudītu to spēju saglabāt diferencēšanās potenciālu pēc ilgtermiņa glabāšanas un vēlākās pasāžās, piemēram, P6. Iegūtie rezultāti parādīja, ka hASC no P3 (Bogdanova et al., 2010) un P6 (Bogdanova et al., 2014) var efektīvi diferencēties par adipocītiem un hondrocītiem, bet kalciju saturoša ekstracelulārā matriksa veidošanās, kas apstiprinātu osteogēno diferenciāciju, ir vāja P3 un samazinās vēl vairāk P6. Tā kā, visticamāk, tas ataino hASC donora īpatnību, jo šis pats diferenciācijas protokols ir devis labus rezultātus ar citu donoru hASC, tad nav iespējams apgalvot, ka barotnē ar AS audzētu hASC spēja diferencēties par osteocītiem vēlākās pasāžās samazinās. Citi autori ir parādījuši, ka hASC, kuras kultivētas standarta barotnē, saglabā savu diferenciācijas potenciālu līdz P10 vai P13 (Wall et al. 2007, Gruber et al. 2012), bet tā kritums novērojams P25 (Zhu et al., 2008).

Lai pārbaudītu cASC *in vitro* diferenciācijas potenciālu, P6 šūnas arī tika diferencētas adipogēnajā, hondrogēnajā un osteogēnajā virzienā. hASC no P6 paralēli tika pakļautas tādiem pašiem diferenciācijas protokoliem, kalpojot kā pozitīvā kontrole. Iegūtie rezultāti parādīja, ka gan cASC, gan hASC piemīt līdzīgs hondrogēnais un osteogēnais diferenciācijas potenciāls. Hondrogēnās diferenciācijas Alcian Blue krāsojums (3. C, H, K attēls) apstiprināja sulfātus saturošu glikozaminoglikānu klātbūtni, kas raksturīgi hondrocītu ekstracelulārajam matriksam, un skrimslim līdzīgas lakūnu struktūras. Kalcija nogulsnes mineralizētā ekstracelulārajā matriksā, ko ražo diferencēti osteoblasti, tika detektētas, izmantojot Alizarin Red S krāsošanu osteogēnās diferenciācijas paraugiem (3. E, I, L attēls). Diferenciācija par adipocītiem tika pārbaudīta ar Oil Red O krāsvielu (3. A, G, J attēls). Lai gan cASC demonstrēja spēju diferencēties par adipocītiem, tā bija būtiski samazināta, salīdzinot ar hASC. Tikai dažas cASC uzrādīja iekššūnas lipīdu granulu uzkrāšanos, neskatoties uz to izmainīto morfoloģiju. Tāda pati tendence ir novērota jau iepriekš (Vieira et al., 2010), taču indukcijas protokola optimizācija spēj uzlabot adipogēno diferenciāciju (Neupane et al., 2008). Arī mēs esam mēģinājuši attiecīgi izmainīt pielietoto diferenciācijas protokolu, taču tas nesekmēja cASC diferenciāciju par adipocītiem (dati nav parādīti). Tas, ka cASC diferenciācija vairākās šūnu līnijās tika veikta P6, arī varētu izskaidrot vājo adipogēno diferenciāciju. Tā kā mēs novērojām osteogēnās diferenciācijas potenciāla samazināšanos vēlākās hASC pasāžās, pastāv iespēja, ka tas pats attiecas uz cASC. Ne cASC, ne hASC uzrādīja adipogēnās vai osteogēnās diferenciācijas pazīmes kontroles barotnēs, izņemot gaiši zilu krāsojumu, kas tika detektēts hondrogēnajā kontrolē. Rezultāti ar sieviešu kārtas cASC kontroles barotnēs ir parādīti šeit kā piemērs (3. B, D, F attēls).

Kopumā rezultāti no novērotās šūnu morfoloģijas, virsmas marķieru ekspresijas un diferenciācijas par adipocītiem, osteocītiem un hondrocītiem apstiprināja gan hASC, gan cASC atbilstību izvirzītajiem MSC kritērijiem (Dominici et al., 2006) un parādīja to savstarpējo līdzību.

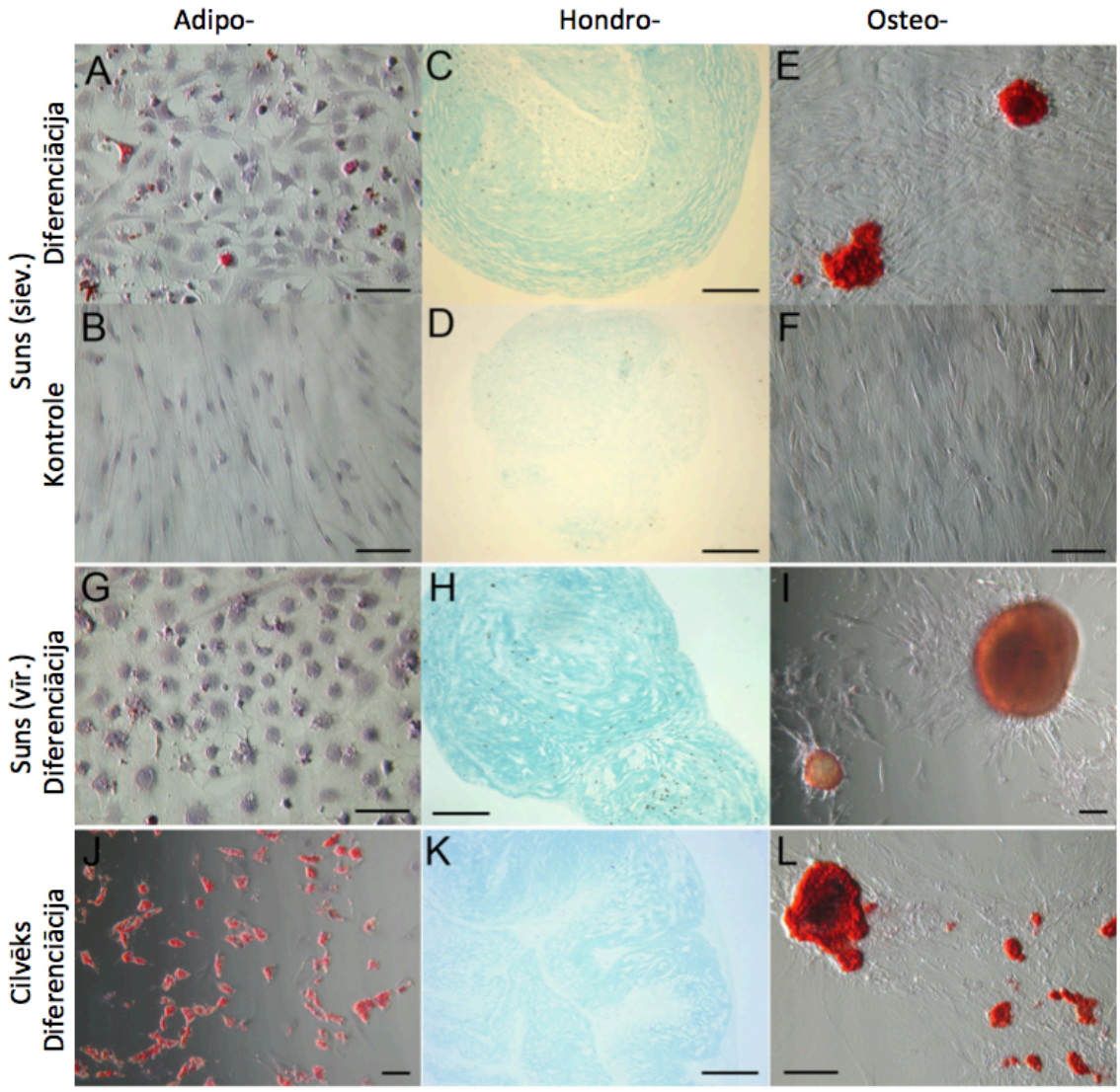

3. attēls. No suņa un cilvēka taukaudiem izdalītu 6. pasāžas cilmes šūnu *in vitro* diferenciācija adipogēnajā, hondrogēnajā un osteogēnajā virzienā. (A, G, J un B) Diferencēto un kontroles šūnu Oil Red O krāsojums. Šūnas papildus krāsotas ar hematoksilīnu. (C, H, K un D) Diferencēto un kontroles šūnu Alcian Blue krāsojums. (E, F, L un I) Diferencēto un kontroles šūnu Alizarin Red S krāsojums. Mēroga skala100 µm.

3.1.4. ASC imunosupresīvās īpašības

Lai noteiktu hASC inhibitoro efektu uz T šūnu proliferāciju, tika izmantotas hASC (donora kods CS-5) no P3, P6 un P9. Šis efekts tika izvērtēts, audzējot kopā hASC un PBMNC, kuras stimulētas ar fitohemaglutinīnu (PHA), dažādās attiecībās. Ar PHA stimulētas PBMNC tika pielietotas kā pozitīvā kontrole, bet vienas pašas PBMNC - kā negatīvā kontrole. Ievērojama hASC spēja izraisīt PBMNC proliferāciju netika novērota, un PHA stimulācijai nebija proliferāciju izraisoša efekta uz hASC (4. A attēls). ASC un ar PHA stimulētu autologu PBMNC blasttransformācijas reakcijā tika detektēts no devas atkarīgs visu triju pasāžu hASC imunosupresīvais efekts, kas sasniedza savu maksimumu pie hASC:PBMNC attiecības 1:1 (4. B attēls). Būtisks PBMNC proliferācijas samazinājums tika novērots arī pie hASC:PBMNC attiecības 1:10, izmantojot hASC no P3. Tas liek domāt, ka agrāku pasāžu hASC var uzrādīt izteiktāku imunosupresīvo efektu nekā vēlāku pasāžu šūnas. Dažādu MSC populāciju imunosupresīvās īpašības, ilgstoši kultivējot, nav plaši pētītas. Tikai daži pētījumi par šo tēmu ir publicēti, un tie parāda, ka hASC imunosupresīvais efekts neatšķiras starp P2 un P5 (Cui at al.,

2007) un MSC nezaudē savu imunosupresīvo aktivitāti līdz P6 vai P7 (Samuelsson at al., 2009), bet tā samazinās pēc P7, salīdzinot ar agrākām pasāžām (Auletta at al., 2001).

P6 cASC imunosupresīvais efekts tika pārbaudīts tādā pašā veidā. cASC demonstrēja statistiski nozīmīgu PBMNC proliferācijas samazinājumu, kad cASC:PBMNC attiecība sasniedza 1:40 vai mazāk (5. A attēls) (rezultāti ar vīriešu kārtas cASC ir parādīti šeit kā piemērs). Tāpat kā hASC eksperimentā, novērotais cASC imunosupresīvais efekts bija atkarīgs no devas, sasniedzot savu maksimumu pie cASC:PBMNC attiecības 1:1, un cASC un hASC imunosupresīvo spēju regresijas analīze apstiprina šo līdzību (5. B attēls).

Dati no ASC un autologu PBMNC blasttransformācijas reakcijas parādīja, ka ASC, kuras audzētas barotnē ar AS un pie 5% skābekļa koncentrācijas, nomāc PBMNC proliferāciju no devas atkarīgā veidā tāpat kā hASC (Cui at al., 2007, Yañez at al., 2006) vai cASC (*Kang et al., 2008; Russell et al., 2016*), kuras kultivētas standarta barotnē ar FBS. Šādai ASC imunosupresīvajai spējai var būt nozīmīgs terapeitiskais potenciāls neskaitāmu imunoloģisko saslimšanu ārstēšanā gan cilvēkiem, gan suņiem.

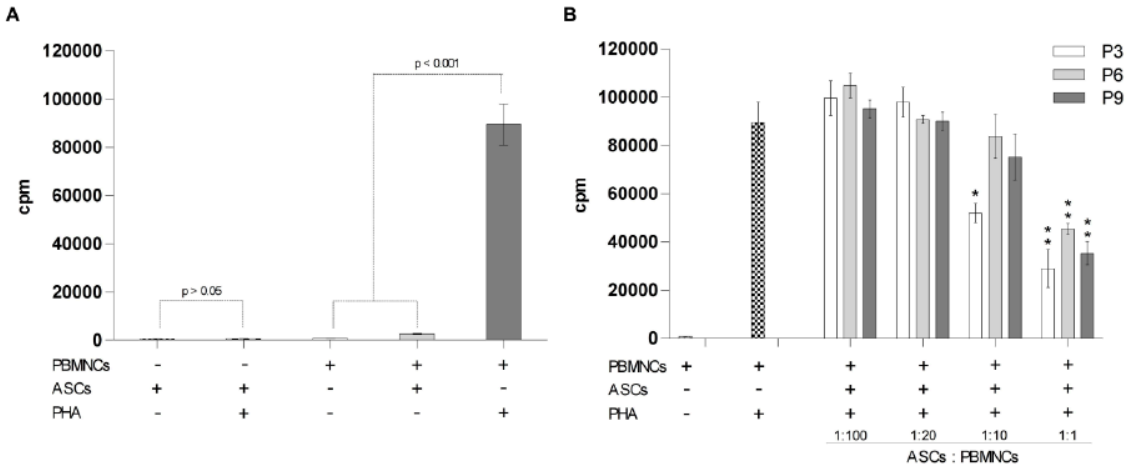

4. attēls. No cilvēka taukaudiem izdalītu cilmes šūnu (hASC) un autologu perifēro asiņu mononukleāro šūnu (PBMNC) blasttransformācijas reakcija. (A) Negatīvās un pozitīvās kontroles. (B) Dažādu pasāžu hASC nomācošais efekts uz PHA stimulētu PBMNC proliferāciju *in vitro*. Rezultāti ir izteikti kā skaitījumi minūtē (cpm). Dati parāda vidējo ± SD no trīs atkārtojumiem. Zvaigznītes norāda uz statistiski nozīmīgu atšķirību, salīdzinot ar PHA stimulētām PBMNC; *p < 0,05, **p < 0,01. P – pasāža; PHA – fitohemaglutinīns.

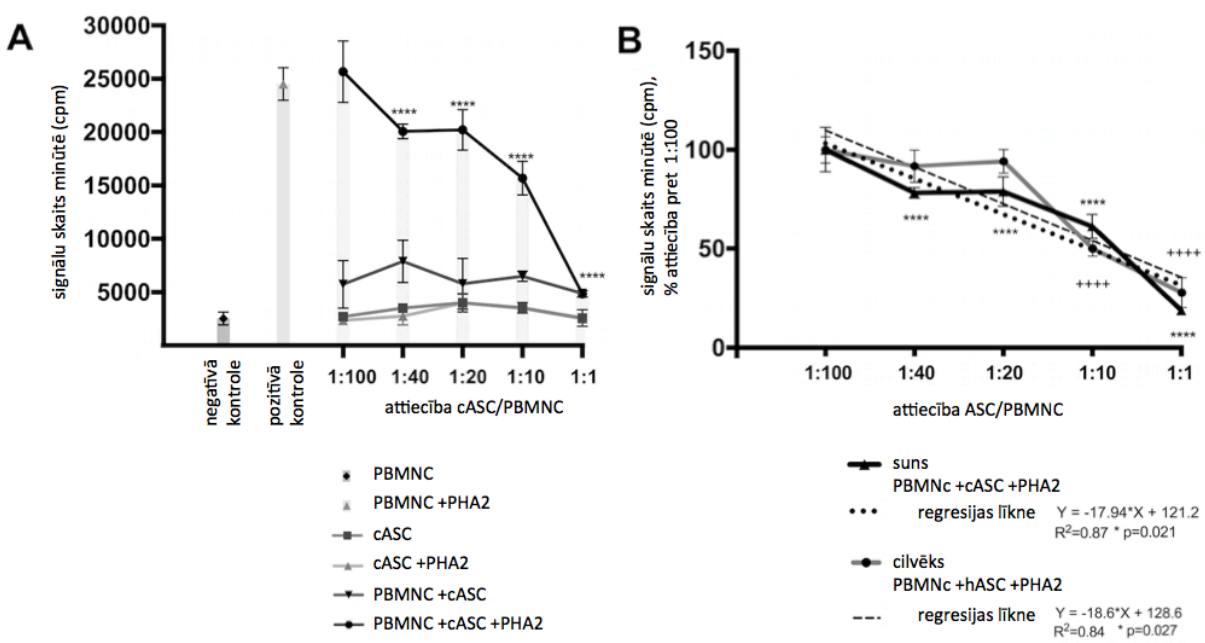

5. attēls. No taukaudiem izdalītu cilmes šūnu (ASC) un autologu perifēro asiņu mononukleāro šūnu (PBMNC) blasttransformācijas reakcija. (A) 6. pasāžas suņa ASC (cASC) nomācošais efekts uz PHA stimulētu PBMNC proliferāciju *in vitro*. Rezultāti ir izteikti kā skaitījumi minūtē. (B) cASC un cilvēka ASC (hASC) imunosupresīvo spēju salīdzinājums. Dati parāda vidējo ± SD no trīs atkārtojumiem. Zvaigznītes norāda uz statistiski nozīmīgu atšķirību, salīdzinot ar PHA stimulētām PBMNC; ****p < 0,0001 (cASC); ++++p < 0,0001 (hASC). PHA2 – fitohemaglutinīns beigu koncentrācijā 2 µg/ml.

3.2. hASC *in vitro* senescence

ASC *in vitro* drošība tiek raksturota ar šo šūnu morfofunkcionālo stāvokli senescences procesa laikā. Lai noteiktu *in vitro* pavairotu ASC drošumu, ir nepieciešams pārbaudīt to bioloģisko novecošanos šūnu kultivēšanas laikā.

3.2.1. hASC augšanas kinētika, morfoloģija un klonogenitāte

Lai novērtētu hASC senescenci, astoņu donoru cilmes šūnu kultūras (1. tabula) tika pakļautas ilgstošai *in vitro* kultivēšanai. Individuālās hASC kultūras sasniedza proliferācijas arestu ievērojami dažādā laikā, kā to parāda atšķirības attiecīgajās kumulatīvajās PD vērtībās (6. A attēls). Trīs šūnu kultūras pārstāja dalīties jau pēc trijām (CS-4) vai četrām (CS-5, CS-7) pasāžām (kumulatīvās PD bija attiecīgi 8,02, 8,30 un 10,19) un tika izslēgtas no turpmākā senescences novērtējuma kā nesekmīgi pavairotas. Atlikušajās hASC kultūrās kumulatīvais PD skaits bija robežās no 14,69 (CS-6) līdz 28,97 (CS-8) (1. tabula).

1. tabula. Pētījumā izmantoto no cilvēka taukaudiem izdalītu mezenhimālo cilmes šūnu kultūru pārskats.

Kultūras kods	Kriouzgla-bāšanas ilgums, gados	Donora vecums, gados	Donora dzimums	Sākuma pasāža	Beigu pasāža	Kumulatīvais PD
CS-1	3	61	vīr.	P3	P11	20.46
CS-2	2.5	*57*	siev.	P3	P9	17.46
CS-3	2	63	vīr	P3	P13	23.28
CS-4	2	43	vīr	P3	P5	8.03
CS-5	1.5	47	vīr	P4	P7	8.29
CS-6	3	38	siev.	P3	P8	14.69
CS-7	2.5	38	vīr	P3	P6	10.19
CS-8	3.5	27	siev.	P3	P14	28.97

P - pasāža; PD - populācijas dubultošanās.

Visu šūnu kultūru proliferācijas ātrums pavairošanas laikā samazinājās nevienmērīgi (6. B attēls), lai gan tika uzturēta pastāvīga sadalīšanas attiecība, pārsējot vienlīdz blīvas monoslāņa šūnu kultūras. Viens (CS-1, CS-3, CS-6, CS-8) vai divi (CS-2) izteikti paaugstināta PDT pīķi tika novēroti kultivēšanas vidusdaļā, kam sekoja proliferācijas reaktivācija sekojošajās pasāžās. Visu hASC kultūru proliferācijas spēja tika zaudēta ļoti strauji pēdējā pasāžā, ko pierāda PDT pieaugums 3,7 līdz vairāk nekā 10 reizes, salīdzinot ar priekšpēdējo pasāžu. Arī nelielais kumulatīvais PD skaita pieaugums pēdējā pasāžā norādīja uz proliferācijas arestu (6. A attēls). Ir ziņots, ka MSC proliferācijas potenciāls samazinās gan ar pieaugošu kultivēšanas laiku, gan ar donora vecumu (Izadpanah et al., 2006). Mēs atklājām pozitīvu regresiju starp pasāžu skaitu un PDT ($p < 0,05$) CS-1 un CS-3 paraugos, taču CS-6 un CS-8 gadījumos p vērtība bija tuva būtiskuma robežai. Šāda saistība nebija novērojama CS-2 paraugā augšanas līknes īpatnību dēļ. Pēc nesekmīgi pavairoto hASC kultūru izslēgšanas no analīzes, pārējos paraugus varēja iedalīt divās atšķirīgās vecuma kategorijās: virs 50 (CS-1, CS-2, CS-3) un zem 40 gadiem (CS-6, CS-8). Būtiskas atšķirības augšanas kinētika starp šīm grupām netika novērotas, lai gan nelielais paraugkopas lielums varētu samazināt šī novērojuma ticamību.

Morfoloģiski visas hASC kultūras uzrādīja tipisku vārpstveida izskatu agrās pasāžās. Ilgtermiņa kultivēšanas laikā tika novērotas visbiežāk aprakstītās izmaiņas, kas saistītas ar šūnu novecošanos: vidējā šūnu izmēra un heterogenitātes pieaugums, šūnu saplacināšanās, neregulāra šūnu forma un granulāru ieslēgumu uzkrāšanās citoplazmā. Tāpat vēlākās pasāžās šūnām vairāk bija tendence augt zvaigžņveida sakopojumos, nevis veidot monoslāni (6. C attēls). Taču līdzīgi svārstībām hASC augšanas ātrumā kultivēšanas laikā, arī morfoloģiskās izmaiņas neuzkrājās vienmērīgi. Atkārtota vārpstveida šūnu parādīšanās tika novērota CS-1 parauga P8. Šīs šūnas dominēja arī P9 un P10, un tām piemita paaugstinātas proliferatīvās spējas, ko apliecina PDT samazinājums par 37,5% un 54,2% attiecīgi P9 un P10, salīdzinot ar P7 (6. B attēls). Līdzīgi novērojumi tika detektēti arī citās hASC kultūrās.

Agrās pasāžās starp donoriem netika novērotas būtiskas atšķirības šūnu morfoloģijā. Tomēr ilgtermiņa kultivēšanas laikā kļuva redzamas donoru specifiskas īpašības šūnu izskatā (dati nav parādīti), norādot uz atšķirīgām novecošanas norisēm individuālās hASC kultūrās. Taču neskatoties uz to, visas šūnu kultūras sasniedza galējo senescenci tipiski novecojušu šūnu izskatā un nespēja dalīties tālāk.

Izmaiņas hASC klonogenitātē tika noteiktas, pielietojot CFU pārbaudi. Pētījumos ir ziņots, ka koloniju veidošanas spēja negatīvi korelē ar PDT, donora vecumu un pasāžu skaitu (Digirolamo at al., 1999). Mūsu rezultāti parādīja negatīvu korelāciju starp CFU testa vērtību un PDT, bet tā nebija būtiska ($p > 0,05$). Taču pastāvēja statistiski nozīmīga negatīva saistība starp CFU testa vērtību un pasāžu skaitu ($p < 0,05$). Tāpat kā iepriekš, tika novērotas donoru atšķirības (6. D attēls).

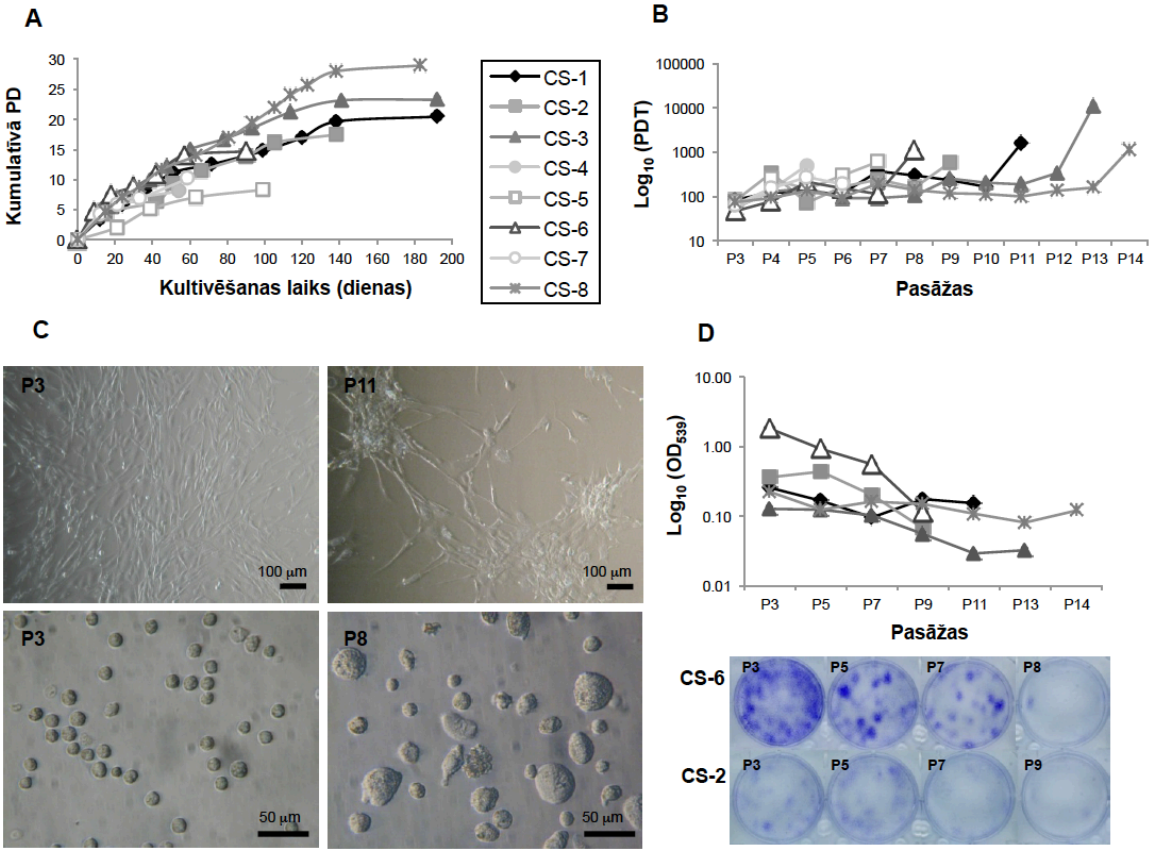

6. attēls. No cilvēka taukaudiem izdalītu dažādu donoru (CS-1–CS-8) cilmes šūnu (hASC) proliferācijas spēja, morfoloģija un klonogenitāte ilgtermiņa *in vitro* kultivēšanas laikā. (A) Kumulatīvās populācijas dubultošanās (PD). (B) hASC proliferācijas līknes, kas parāda populācijas dubultošanās laiku (PDT) katrā pasāžā. (C) hASC morfoloģija ilgtermiņa kultivēšanas laikā. Monoslāņa šūnas agrā (augšējais kreisais) un vēlā (augšējais labais) pasāžā, un suspendētas šūnas agrā (apakšējais kreisais) un vēlā (apakšējais labais) pasāžā. (D) hASC klonogenitātes potenciāls. Augšējais attēls – relatīvās CFU testa vērtības; apakšējais attēls – CFU testa plate, kas parāda donoru atšķirības. OD - optiskais blīvums.

3.2.2. hASC diferenciācija

Tika analizētas atšķirības adipogēnās un osteogēnās diferenciācijas potenciālā starp hASC no agras (P3) un vēlas (P9) pasāžas. Diferenciācija par adipocītiem tika pārbaudīta, krāsojot iekššūnas lipīdu granulas ar Oil Red O krāsvielu pēc 16 dienu kultivēšanas diferenciācijas barotnē. Osteoģenēze tika pārbaudīta ar sārmainās fosfatāzes aktivitātes noteikšanu un kalcija nogulšņu krāsošanu ar Alizarin Red S pēc 30 dienu diferenciācijas. Rezultāti apstiprināja hASC spēju diferencēties šajās divu veidu šūnu līnijās, bet ar dažādu efektivitāti starp donoriem (7. attēls). Gan lipīdu ieslēgumu uzkrāšanās, gan ekstracelulārais kalcijs bija būtiski samazināts P9, salīdzinot ar P3 (7. A, B attēls), taču sārmainās fosfatāzes aktivitātes līmenis palika nemainīgs abās pasāžās (7. C attēls).

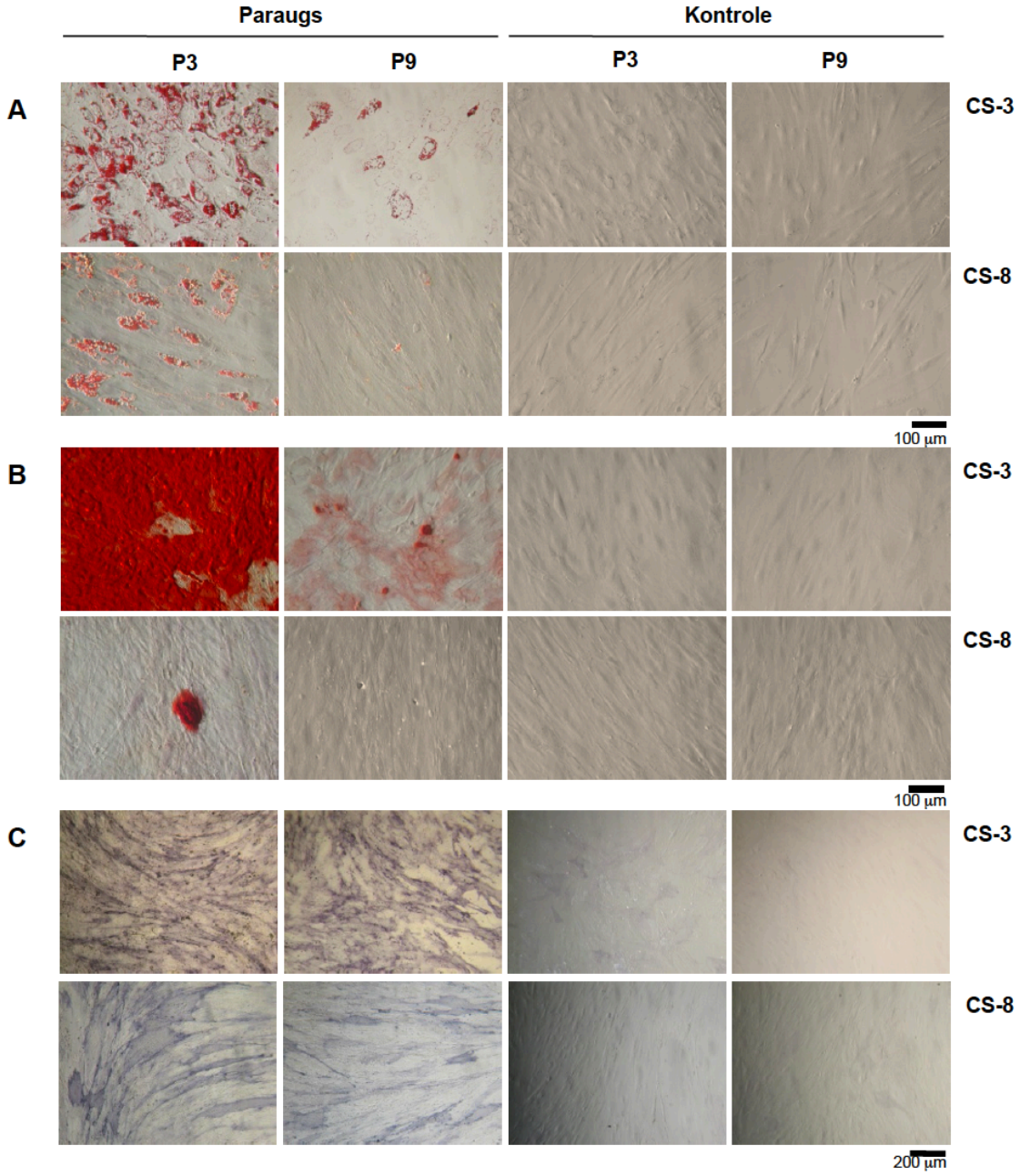

7. attēls. No cilvēka taukaudiem izdalītu cilmes šūnu (hASC) diferenciācijas potenciāls divās šūnu līnijās. Ir parādīts salīdzinājums starp diviem zīmīgiem hASC paraugiem (donori CS-3 un CS-8) no agras (P3) un vēlas (P9) pasāžas, kas ataino donoru specifiskas atšķirības. (A) Diferenciācija par adipocītiem, ko pierāda lipīdu ieslēgumu krāsojums ar Oil Red O. (B, C) Diferenciācija par osteocītiem, kas noteikta pēc ekstracelulārā kalcija Alizarin Red S krāsojuma (B) un sārmainās fosfatāzes aktivitātes (C).

3.2.3. Ar senescenci saistītās β-galaktozidāzes ekspresija

SA-β-gal ir vispārpieņemts šūnu senescences rādītājs, un tās ekspresija tika noteikta katrā otrajā hASC pasāžā ilgtermiņa kultivēšanas laikā. Kā gaidīts, neliela vai nekāda SA-β-gal ekspresija tika atklāta agrās pasāžās, un tā turpināja pieaugt turpmākās šūnu kultivēšanas gaitā (8. attēls). Šis rezultāts tika apstiprināts ar regresijas analīzi, kas atklāja pozitīvu saistību starp SA-β-gal ekspresijas vērtību un pasāžu skaitu. Tomēr SA-β-gal ekspresijas līmeņa svārstību dēļ CS-1, CS-3 un CS-8 paraugos (dati nav parādīti) tā nebija būtiska ($p > 0,05$). Interesanti, ka šīs

svārstības sakrita ar tām, kas tika novērotas šūnu augšanas analīzē, un to apstiprināja arī statistiski nozīmīga pozitīva korelācija ($p < 0,05$) starp SA-β-gal ekspresijas līmeni un PDT.

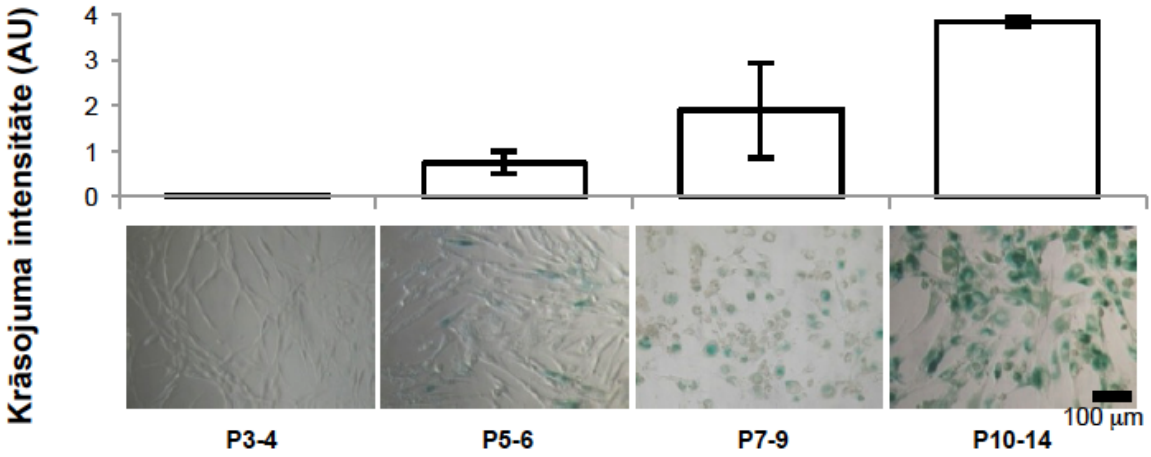

8. attēls. Ar senescenci saistītās β-galaktozidāzes (SA-β-gal) ekspresija no cilvēka taukaudiem izdalītās cilmes šūnās (hASC) ilgtermiņa kultivēšanas laikā. Paaugstināta SA-β-gal ekspresija hASC ilgtermiņa kultivēšanas laikā (apakšējie attēli) ar attiecīgajiem vizuālā novērtējuma datiem (augšējais grafiks). AU - arbitrārās vienības; P - pasāža. Kļūdu stabiņi parāda standartnovirzi.

3.2.4. Relatīvais telomēru garums (RTL) un hASC subpopulāciju noteikšana

Lai pārbaudītu, vai hASC senescences fenotips ir saistīts ar izmaiņām telomēru garumā, tika pielietota fluorescences *in situ* hibridizācijas metode priekš plūsmas citometrijas (Flow FISH), izmantojot ar FITC konjugētas telomērām specifiskas peptīdu nukleīnskābju zondes. Specifiskā fluorescence tika aprēķināta, atņemot to šūnu autofluorescenci, kurām zonde netika pievienota. Katram paraugam tika pievienotas Jurkat šūnas attiecībā 1:1, lai normalizētu atšķirības starp eksperimentiem. Rezultāti parādīja, ka RTL būtiski samazinājās CS-3 un CS-8 paraugos, salīdzinot savā starpā pirmo un pēdējo pasāžu (attiecīgi 52,3% un 35,8%, $p < 0,05$) (9. A attēls). Taču tāpat kā iepriekšējos testos, pasāžu laikā bija novērojamas RTL svārstības, norādot uz senescences procesa sarežģīto dabu.

Lai noteiktu, vai telomēru garuma pieaugums, kas tika novērots dažās pasāžās, varētu būt noticis telomēru pseidopagarināšanās rezultātā, ko izraisa dažādu šūnu subpopulāciju klātbūtne, tika analizēts uz priekšu vērstās gaismas izkliedes signāls pret telomēru specifisko FITC fluorescenci. Pārsteidzošā kārtā, visos paraugos un visās pasāžās tika atklātas divas labi atšķiramas hASC subpopulācijas, bet ar dažādām kvantitatīvajām attiecībām starp donoriem (9. B attēls). Šis rezultāts bija specifisks hASC, jo tāds novērojums netika atklāts vienlaicīgi testētajām Jurkat šūnām (9. B attēls, apakšējā diagramma). Interesants ir fakts, ka atklātajās subpopulācijās būtiski atšķīrās RTL un šūnu izmērs ($p < 0,05$, 9. C, D attēls), tāpēc tās tika nodēvētas par populācijām S ("mazās" šūnas) un L ("lielās" šūnas). S populācijas vidējais RTL bija 0,95 līdz 1,75 reizes īsāks nekā L populācijai, un atšķirība šūnu izmērā bija divkārša līdz trīskārša, atkarībā no parauga.

Pakāpenisks RTL samazinājums pa pasāžām tika novērots abās CS-3 un CS-8 paraugu populācijās, bet CS-1 gadījumā - tikai L populācijā ($p < 0,05$). Tāpat RTL saīsināšanās CS-1, CS-3 un CS-8 paraugos notika daudz straujāk L populācijā, salīdzinot ar S populāciju, bet pēdējā pasāžā RTL atšķirība starp abām populācijām kļuva nebūtiska. Tā kā pēdējā pasāžā šūnas zaudēja savas proliferatīvās spējas ļoti ātri (6. A, B attēls), tad tas var norādīt uz kritisko telomēru garumu, kas bloķē tālāku proliferāciju. CS-2 un CS-6 paraugi sekoja citam modelim. CS-6 gadījumā nevienā no populācijām netika novērotas būtiskas RTL izmaiņas pa pasāžām (p

>0,05), bet CS-2 gadījumā izmaiņas tika detektētas tikai S populācijā, bet tās nebija būtiski saistītas ar pasāžu skaitu (p>0,05). Tādējādi šo hASC kultūru senescenci var būt izraisījuši citi faktori, nevis kritiski īsas telomēras.

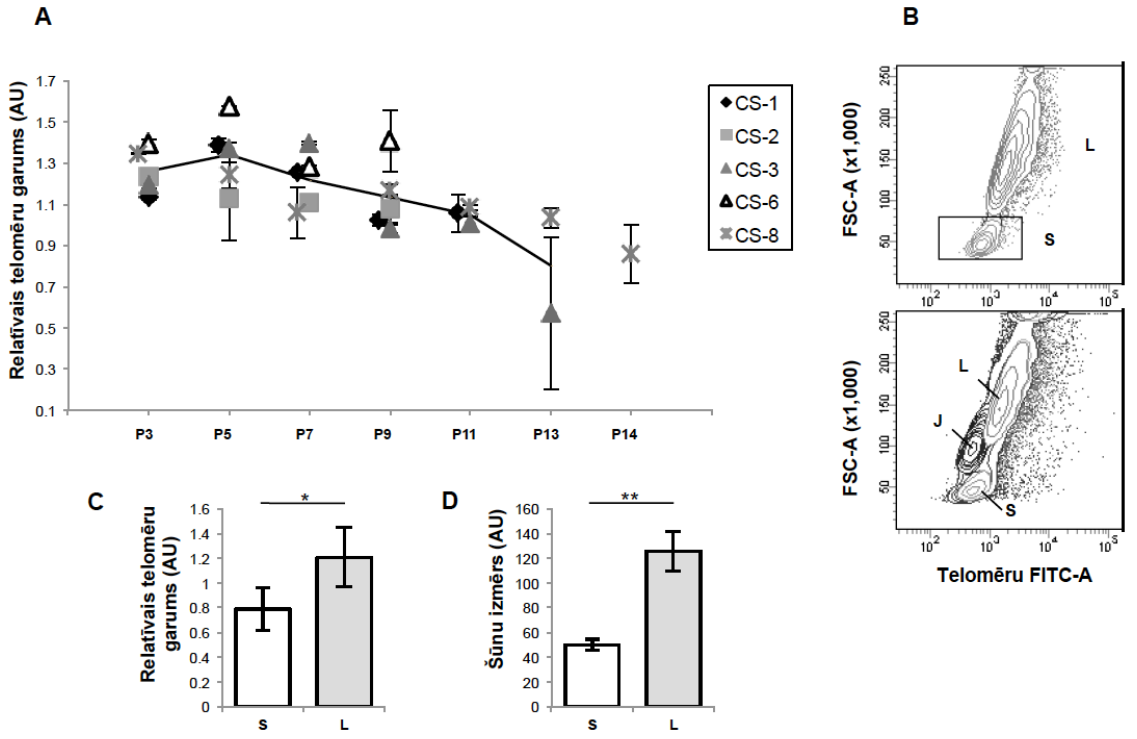

9. attēls. *In vitro* pavairotu no cilvēka taukaudiem izdalītu dažādu donoru (CS-1–CS-8) cilmes šūnu (hASC) relatīvais telomēru garums (RTL) un hASC subpopulāciju noteikšana. (A) RTL dinamikas Flow FISH analīze ilgtermiņa kultivēšanas laikā. Katrs datu punkts ir izteikts kā vidējais ± SD no dubultiem mērījumiem. Nepārtrauktā līnija ataino piecu (P3-9), trīs (P11) un divu (P13) paraugu vidējo RTL. (B) RTL mērījumu laikā tika atklātas divas hASC subpopulācijas (S un L) (augšējā diagramma). Taču kontroles Jurkat šūnās bija tikai viena populācija (apakšējā diagramma, J). S un L populācijas atšķiras pēc to RTL (C) un šūnu izmēra (D) (dati izteikti kā piecu paraugu CS-1,2,3,6,8 visu analizēto pasāžu vidējais ± SD; *p < 0,05, **p = 0,001). AU - arbitrārās vienības; P - pasāža.

Ilgtermiņa kultivēšanas laikā tika novērotas izmaiņas abu subpopulāciju kvantitatīvajās attiecībās donoriem specifiskā veidā. Salīdzinot S populācijas lieluma dinamiku ar proliferācijas palēlināšanās pīķiem (6. B attēls), tika atklāts, ka šie pīķi atbilst vai nu S populācijas šūnu augstākajam procentuālajam daudzumam (CS-1 gadījumā S šūnu daudzums bija 2,6% P3 un 10,9% P7; CS-8 gadījumā – 3,0% P3 un 32,6% P7) vai nozīmīgam RTL samazinājumam S populācijā (CS-3 gadījumā RTL samazinājās par 35% P9, salīdzinot ar P7; CS-2 gadījumā – par 49% P7, salīdzinot ar P5).

Tiek uzskatīts, ka MSC kultūras ir heterogēnas un tās veido šūnu subpopulācijas ar dažāda veida iezīmēm, ieskaitot potenciālu diferencēties vairākās šūnu līnijās, augšanas īpatnības un klonogenitāti (Lee at al., 2010; Rada at al., 2011). Šūnu subpopulācijas, kam piemīt specifiskas īpašības, pavairošanas laikā ir iespējams atlasīt (Cholewa at al., 2011). Tomēr paliek jautājums, vai S un L populāciju atklājums ataino "īstās" hASC subpopulācijas. Lai sagatavotu šūnas RTL mērījumam, tās tiek pakļautas tādiem skarbiem apstākļiem kā denaturācijai augstā temperatūrā haotropiska līdzekļa (formamīda) klātbūtnē, kas ir parādījis kaitīgu ietekmi uz hromosomu morfoloģiju (Winkler at al., 2003). Turklāt ir ziņots, ka karstums un formamīda apstrāde izmaina cilvēka leikocītu apakšgrupu gaismas izkliedes īpašības, salīdzinot ar neapstrādātu kontroli (Baerlocher at al., 2002). Šajā pētījumā tika pamanīta arī šūnu piebriešana

pēc ilgākas noturēšanas hibridizācijas maisījumā, un tā bija atkarīga no bufera sastāva, kas izmantots šūnu suspendēšanai. Tādējādi S un L populāciju uz priekšu vērstās gaismas izkliedes signāli obligāti nenorāda šo šūnu patieso izmēru, bet tie būtu vairāk jāuztver kā pārbaudīto hASC iezīme, kuras rezultātā veidojas divas atšķirīgas atbildes reakcijas uz šūnu apstrādes apstākļiem un ir nosakāmas ar Flow FISH metodi. Neskatoties uz to, šo divu populāciju RTL atšķirība ir skaidri redzama. Turklāt, lai gan kontroles Jurkat šūnas tika pakļautas tādai pašai apstrādei, tās saglabāja savu optisko homogenitāti un netika sadalītas atsevišķās subpopulācijās, liekot domāt, ka šis fenomens nav vienkārši artefakts.

Lai arī ir aprakstīti vairāki senescences mehānismi, telomēru garuma saīsināšanās ir pētīta visvairāk. Citas pētījumu grupas ziņo par dažādiem rezultātiem saistībā ar telomēru garuma lomu senescences izraisīšanā (Noh at al., 2010; Samsonraj at al., 2013). Iegūti rezultāti ļāva secināt, ka pētītajās hASC kultūrās var novērot gan no telomērām atkarīgus, gan neatkarīgus novecošanās mehānismus. Balstoties uz telomēru saīsināšanās veidu, kas tika novērots S un L populācijās, mēs domājam, ka trīs hASC kultūras (CS-1, CS-3, CS-8) sasniedza replikatīvo senescenci (L populācijas telomēru garums sasniedza S populācijas telomēru garumu kultivēšanas beigās), bet pārējās divas (CS-2, CS-6) – priekšlaicīgo senescenci (L populācijas telomēru garums būtiski nemainījās). Trīs paraugi, kas tika izslēgti no pētījuma (CS-4, CS-5, CS-7), visticamāk, var tikt pievienoti priekšlaicīgās senescences grupai. Ir ziņots, ka MSC pārstāj dalīšanos, kad to telomēras sasniedz aptuveni 10 kb garumu (Baxter at al., 2004). Taču tāpat ir zināms, ka kritiskais telomēru garums var būt tik zems kā 4.5 kb (Bodnar at al., 1998). Ņemot vērā vidējo ziņoto Jurkat šūnu telomēru garumu (11.5 kb) (Treff at al., 2011), kuras kalpoja kā RTL analīzes kontrole, mūsu gadījumā ekstrapolētais L subpopulācijas telomēru garums pēdējā pasāžā CS-1, CS-3 un CS-8 paraugos bija attiecīgi 9,89, 6,78 un 8,28 kb, kas ir saskaņā ar zinātnisko literatūru un replikatīvās senescences jēdzienu. No otras puses, tie paši mērījumi atklāja, ka CS-2 paraugā telomēru garums bija 13.57 kb un CS-6 paraugā - 17.82 kb, papildus apstiprinot pieņēmumu par priekšlaicīgo senescenci šajos paraugos. Turklāt šo paraugu kopējais PD skaits bija zemāks nekā CS-1, CS-3 un CS-8 paraugos (1. tabula), un tāds pats rezultāts tika novērots SA-β-gal testā, kur vidējā enzīma ekspresija CS-2 un CS-6 paraugu pēdējā pasāžā bija 1,88 reizes zemāka nekā citu paraugu pēdējās pasāžās (dati nav parādīti).

Spriežot pēc mūsu rezultātiem, priekšroka vienai no abām senescneces formām – replikatīvajai vai priekšlaicīgajai – šūnās tiek dota donoram specifiskā veidā. Visas hASC kultūras tika sākotnējie iegūtas vienādā veidā, pakļautas stresam, izmainot kultivēšanas apstākļus, un pavairotas vienlaicīgi vienos un tajos pašos apstākļos. Tomēr viens no galvenajiem novērojumiem šī pētījuma laikā ir augstais atšķirību līmenis, kas redzams individuālu donoru hASC kultūrās. Jau iepriekš MSC, kuras iegūtas no dažādiem donoriem, ir novērotas atšķirīgas augšanas īpašības un funkcionalitāte (Digirolamo at al.,1999), un tas, visticamāk, ir izskaidrojams ar katra donora atšķirīgo ģenētisko fonu, slimības vēsturi un dzīvesveidu.

3.3. cASC *in vivo* drošums

ASC *in vivo* drošums tika pārbaudīts, izmantojot tikko atkausētas cASC no P5, kuras audzētas hipoksiskos apstākļos AS klātbūtnē un pakļautas diviem sasaldēšanas un atkausēšanas cikliem. Šīs šūnas tika intravenozi ievadītas diviem bīglu šķirnes suņiem. Sākotnēji tikai šķīdums ar 10% DMSO, kas ir atrodams šūnu iesaldēšanas barotnē, tika injicēts intravenozi, lai pārbaudītu tā iespējamos blakusefektus. Tam sekoja cASC terapeitiskās devas ievadīšana un piecas reizes lielākas devas ievadīšana mēnesi vēlāk. Pirmajā stadijā tika pārbaudīts plaušu "barjeras" efekts, novērtējot asins un urīna testu rezultātus, elektrokardiogrammu, ehokardiogrammu un uzvedību, lai izslēgtu plaušu trombembolisma risku. Otrajā stadijā tika veikta dzīvnieku nekropsija un tai sekojoša histomorfoloģiskā analīze, lai noteiktu vēlīnas izmaiņas audos un izslēgtu atipisku audu vai audzēju veidošanās risku.

3.3.1. Dzīvnieku uzvedība

Dzīvnieku uzvedība tika vērtēta pirms un pēc intravenozas cASC un 10% DMSO šķīduma ievadīšanas. Sabiedriskuma tests parādīja, ka abi suņi saglabāja mieru un relaksētu ķermeņa stāju. Viņi apostīja un izpētīja pārbaudes un procedūru telpas, kā arī veidoja acu kontaktu un mierīgu sociālo kontaktu ar cilvēkiem. Abi suņi ļāvās zobu pārbaudei 5 sec bez pretošanās. Tāpat viņi neizvairījās no glaudīšanas un dažādu ķermeņa daļu aiztikšanas, ieskaitot asti un ausis, vismaz 5 sec. Visu procedūru gaitā dzīvnieki bija mierīgi, un cASC vai DMSO ievadīšana neizraisīja nekādas izmaiņas augstāk minētajā dzīvnieku uzvedībā.

3.3.2. Asins un urīna testi

Pēc 10% DMSO injekcijas nozīmīgas izmaiņas asins un urīna testu rezultātos netika novērotas.

Tāpat asins testi bija normāli pēc terapeitiskās cASC devas (2x106 dzīvas šūnas/kg) ievadīšanas, izņemot kopējo bilirubīna līmeni asinīs sieviešu kārtas sunim, kas bija 25 µmol/l (normālās vērtības ir 0–10,20 µmol/l) 24 h pēc cASC ievadīšanas un 11 µmol/l 3 dienas pēc šūnu ievadīšanas procedūras (10. attēls). Urīna testi parādīja, ka bilirubīna un urobilinogēna līmeņi urīnā sieviešu kārtas sunim bija paaugstināti 24 h pēc cASC ievadīšanas, kad bilirubīns tika novērtēts kā ++ (norma ir +) un urobilinoēns bija 140 µmol/l (norma ir 3,5 µmol/l). Bilirubīna līmenis asinīs palika nedaudz palielināts arī 3 un 7 dienas pēc cASC ievadīšanas. Vīriešu kārtas sunim bilirubīna līmenis asinīs un urīnā bija normāls visu laiku.

Pēc otrās cASC ievadīšanas mēnesi vēlāk, izmantojot piecas reizes lielāku šūnu devu (1x107 dzīvas šūnas/kg), asins un urīna testi bija normāli, izņemot bilirubīna līmeni urīnā sieviešu kārtas sunim, kas bija paaugstināts 24 h un 3 dienas pēc šūnu ievadīšanas procedūras.

Tā kā primārie aknu parametri bija normas robežās (ALAT, ASAT, LDH, sārmainā fosfatāze, kopējais olbaltums un albumīns) un kopējā asins aina bija normāla, tad novērotā bilirubinēmija, bilirubinūrija un urobilinogenūrija var būt saistīta ar DMSO metabolismu, kura laikā DMSO pārvēršas par dimetilsulfīdu (DMS), ietekmējot žultsvadu sistēmu, vai individuālām atšķirībām žultsvadu izvades sistēmā. Pēc intravenozas ievadīšanas DMSO pussabrukšanas periods ir 9 h, un tas kā DMS tiek izvadīts caur nierēm, elpošanas orgānu sistēmu un žultsvadu sistēmu (Blythe et al., 1986). Tāpat iespējams, ka šie paaugstinātie rādītāji bija vieglas hemolīzes rezultāts pēc cASC injekcijas. Taču hepatocītu bojājumi var tikt izslēgti normālas aknu bioķīmijas dēļ.

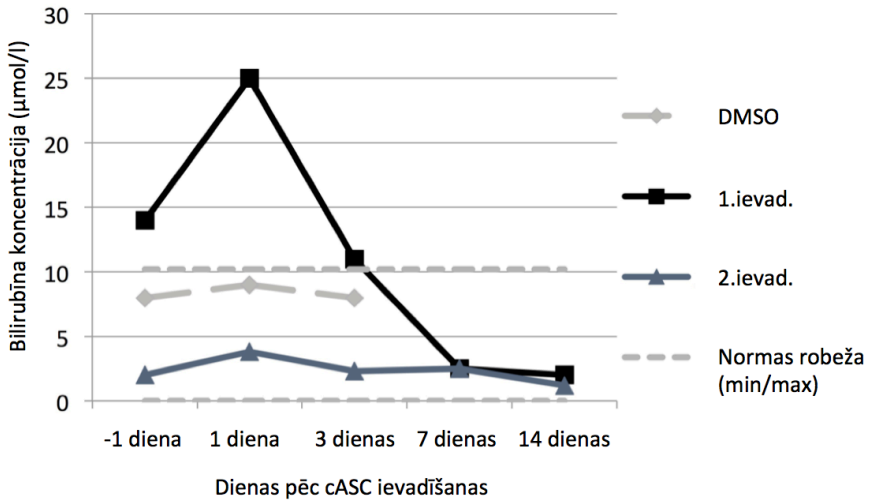

10. attēls. Kopējais bilirubīna līmenis asinīs pēc intravenozas 10% dimetilsulfoksīda (DMSO), no suņa taukaudiem izdalītu cilmes šūnu (cASC) terapeitiskās devas ($2x10^6$ dzīvas šūnas/kg) (1. ievad.) un piecas reizes lielākas devas (2. ievad.) ievadīšanas sieviešu kārtas sunim.

3.3.3. Elektrokardiogrāfija un ehokardiogrāfija

Elektrokardiogrāfijas un ehokardiogrāfijas rezultāti neuzrādīja nekādas novirzes no normas ne pirms, ne pēc abām cASC ievadīšanām. Procedūras laikā tika reģistrētas pārejošas sinusa tahikardijas epizodes, ko, visticamāk, izraisīja stress un kuras galvenokārt tika detektētas manipulācijas un dzīvnieka fiksēšanas laikā. Holtera monitorings neparādīja nekādus sirdsdarbības traucējumus, kas varētu liecināt par miokarda bojājumiem.

Papildus tam, pārbaudītie asins koagulācijas faktori arī nebija izmainīti. Kopumā netika novērota neviena akūta reakcija, piemēram, tromboze, ko varētu sagaidīt pēc cASC ievadīšanas. Tādējādi plaušu "barjeras" efekta pārbaude pēc intravenozas cASC ievadīšanas ļāva izslēgt plaušu trombembolisma risku un parādīja pirmās stadijas cASC drošumu.

3.3.4. Histomorfoloģiskie atklājumi

Dzīvnieku audu un orgānu histomorfoloģiskā analīze vairāk nekā divus gadus pēc šūnu ievadīšanas procedūras atklāja tikai nelielas un relatīvi nespecifiskas izmaiņas, kas var nebūt saistītas ar cASC ievadīšanu. Visbūtiskākās izmaiņas bija subkapsulāri un subpleirāli iekaisuma perēkļi, kas tika atrasti plaušās un nierēs. Nierēs (sieviešu kārtas sunim) un plaušās (abiem suņiem) tika novērotas nelielas granulomas ar eozinofīlajiem leikocītiem, tāpēc nevar izslēgt to iespējamo parazītisko izcelsmi (ieskaitot *Dirofilaria repens*), lai gan suņi regulāri tika attārpoti. Vienā gadījumā īslaicīga *Dirofilaria repens* mikrofloras klātbūtne suņos tika novērota, bet pēc ārstēšanas tā pazuda.

Pastiprināta limfoīdo audu hiperplāzija ar vieglu zarnu iekaisumu tika atrasta vīriešu kārtas suņa zarnu traktā. Šim dzīvniekam bieži tika klīniski novēroti mīksti vai šķidri izkārnījumi, taču laboratoriskie izmeklējumi neuzrādīja ne parazītiskus, ne bakteriālus patogēnus, un tā, visticamāk, jāuzskata par individuālā suņa īpatnību. Tāpat nevar izslēgt jutību pret kādu no barības sastāvdaļām.

Vīriešu kārtas suņa nierēs tika atrasta fokāla segmentāla fibroze, bet urīnpūslī, prostatā, urīnizvadkanālā, nierēs un nieres bļodiņā - hronisks iekaisums. Šīs izmaiņas var norādīt uz pārejošu bakteriālu infekciju, kas parasti notiek nejauši. Tāpat arī aknu mikrogranulomas, sklerotiski asinsvadu kamoliņi nierēs (abiem suņiem), minimāls zarnu iekaisums un limfoīdo audu hiperplāzija (sieviešu kārtas sunim) var tikt uzskatīti par nejaušiem atradumiem, kas ir bieži sastopami suņu sekcijās (Sato et al., 2012).

Atrastās izmaiņas aizkrūtes dziedzerī var būt radušās tīmusa hiperplāzijas vai tā nepilnīgas samazināšanās dēļ, kas bieži ir novērojama laboratorijas bīglu šķirnes suņiem (Sato et al., 2012). Šādas izmaiņas salīdzinoši bieži var detektēt arī parastiem suņiem, kuri nav paredzēti eksperimentiem. Tomēr iespēja, ka aizkrūtes dziedzera hiperplāzija ir saistīta ar cASC ievadīšanu, nevar tikt pilnībā izslēgta.

Kopumā netika atrastas nekādas būtiskas blakusparādības, nevēlami notikumi vai audzēju veidošanās pazīmes, parādot arī otrās stadijas cASC drošumu. Tika identificēta virkne hronisku izmaiņu, un ir teorētiski iespējams, ka dažās no tām var būt saistītas ar intravenozu cASC ievadīšanu. Taču daļa no šīm izmaiņām var tikt attiecinātas uz sporādiskām izmaiņām laboratorijas bīglu šķirnes suņos, kuri tiek izmantoti toksikoloģijas pētījumiem (Sato et al., 2012).

Tā kā gan cilvēkiem, gan suņiem piemīt līdzīgas autoimūnas saslimšanas, piemēram, reimatoīdais atrīts, 1. tipa diabēts un dermatomiozīds, kuras varētu ārstēt ar ASC palīdzību, tad ētiski apstiprināti un dabiski slimi suņi varētu kalpot kā ideāli piemēroti mājdzīvnieki slimību modeļiem nākotnes pētījumos. Tas ļautu izmeklēt ASC terapeitisko efektivitāti bez nepieciešamības izraisīt šīs slimības mākslīgi. Tāpat ASC varētu tikt izmantotas ar šādām autoimūnām slimībām sirgstošu suņu eksperimentālai ārstēšanai. Rezultāti, kas tiktu iegūti suņu modeļos, nodrošinātu būtisku informāciju, kas nepieciešama priekš ASC terapijas plānošanas cilvēkiem.

3.4. ASC sagatavošanas metodoloģijas specifika

Saskaņā ar Regulas (EK) Nr. 1394/2007 28. pantu par ATMP (Regulation, 2007), HE gadījumos ATMP (piemēram, ASC) tiek sagatavotas ārpus rutīnas apstākļiem, balstoties uz katra ražotāja specifisko metodoloģiju. Šajā gadījumā "ārpus rutīnas apstākļiem" tiek saprasts kā šī procesa uzlabošana reālajā laikā ar mērķi attīstīt personalizētu un riskam piemērotu ārstēšanas pieeju. Šī pētījuma laikā mēs esam izstrādājuši specifisku ASC sagatavošanas procesa metodoloģiju ārpus rutīnas apstākļiem, kas tika izmantota gan priekš hASC, gan cASC, un pārbaudījuši pēc šīs metodoloģijas sagatavotu cASC drošumu pēc to intravenozas ievadīšanas. Mūsu metodoloģijas galveno specifiku veido: a) AS izmantošana ASC pavairošanas, kas tiek veikta hipoksiskos apstākļos (5% skābeklis), un iesaldēšanas laikā; b) ASC pakļaušana diviem sasaldēšanas un atkausēšanas cikliem pirms intravenozas ievadīšanas; c) tikko atkausētu ASC izmantošana *in vivo* ievadīšanai; d) kultivēto ASC autologs pielietojums. Mūsu ASC sagatavošanas metodoloģijas pārskats ir parādīts 11. attēlā.

Šī metodoloģija ir veidota tā, lai iegūtu pēc iespējas mazāk apstrādātas un izmainītas ASC, jo tās tiek iesaldētas pēc P1 un uzglabātas personalizētai reģeneratīvajai terapijai nākotnē. Saglabājot ASC turpmākam pielietojumam, ir ļoti svarīgi tās iesaldēt visagrākajā iespējamajā pasāžā. Pieprasījums pēc jaunu, veselu, nenovecojušu cilmes šūnu uzglabāšanas kļūst arvien lielāks, un straujā šūnu apstrādes tehnoloģiju attīstība un uzlabošana padara iespējamu neliela daudzuma apstrādātu šūnu saglabāšanu. Tāpēc mēs esam izvēlējušies saglabāt šūnas iesaldētā stāvoklī jau pēc P1.

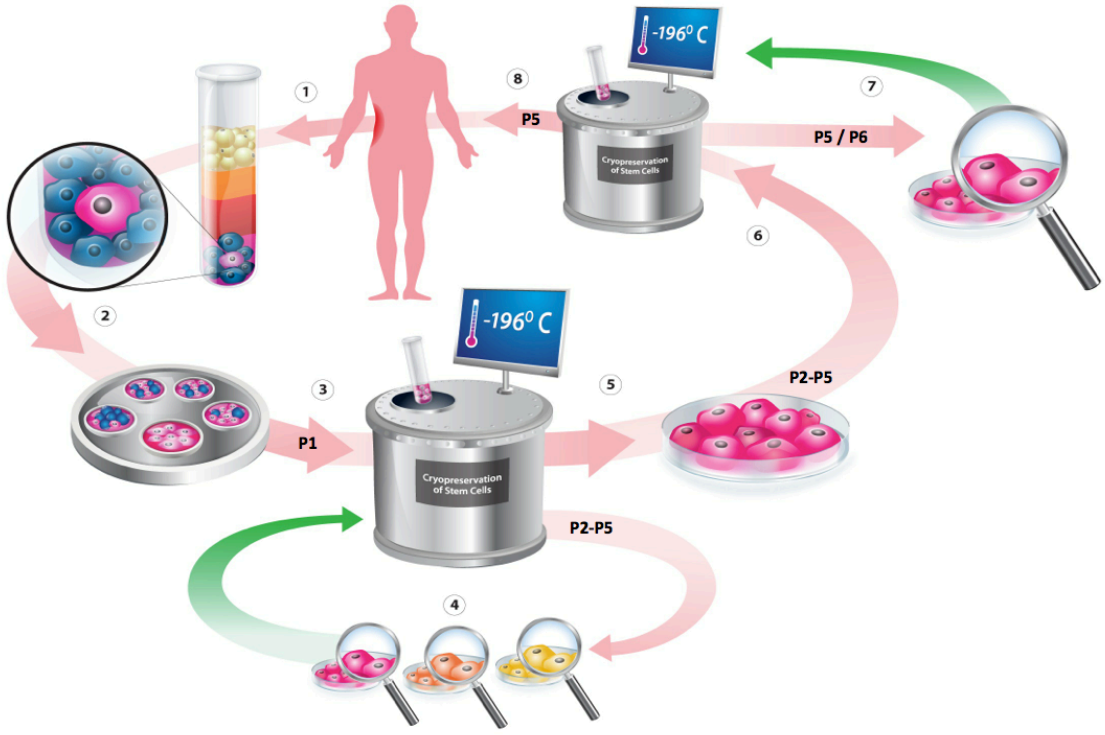

11. attēls. No taukaudiem izdalītu donoram specifisku cilmes šūnu (ASC) ražošanas process. 1. Pacienta uzņemšana. 2. Taukaudu paņemšana un ASC iegūšana. 3. ASC iesaldēšana pēc pirmās pasāžas (P1) un šo šūnu ilgtermiņa uzglabāšana. 4. ASC analīze un šūnu kultivēšanas apstākļu personalizēta optimizācija. 5. Iesaldēto ASC atkausēšana un pacientam specifiska ASC pavairošana, balstoties uz individuāli optimizēto protokolu. 6. Terapijai sagatavoto ASC otrā iesaldēšana. 7. Pavairotās ASC partijas papildus analīze. 8. Personalizētu ASC ievadīšana pacientam.

Ņemot vērā šī pētījuma laikā atklātās atšķirības starp donoriem un cilmes šūnu subpopulāciju heterogenitāti, kas izraisa donoriem specifisku šūnu augšanu, ir ļoti svarīgi pielietot personalizētu un individuāli pielāgotu protokolu ASC sagatavošanai. Mēs izstrādājām jaunu pieeju dažādu pacientu cilmes šūnu pavairošanai un pārbaudei ārpus rutīnas apstākļiem. Mēs izmantojam ASC no P2 līdz P5, lai veiktu personalizētu šūnu kultivēšanas apstākļu un barotnes sastāva optimizāciju, un tas tiek darīts laika posmā starp pirmo un otro šūnu iesaldēšanu. Šāda pieeja ļauj noteikt katram indivīdam vispiemērotāko protokolu, tādējādi uzlabojot šūnu produkta efektivitāti un drošumu. Tā rezultātā nākamajā ražošanas solī var tikt izmantots individuāli optimizēts šūnu kultivēšanas protokols, lai sagatavotu terapeitisko ASC devu. Šajā pētījumā tika novērtēta standarta metode ASC kultivēšanai, kas iekļāva AS un hipoksisku apstākļu izmantošanu, un nākotnē tā kalpos kā kontroles metode, lai būtu ar ko salīdzināt optimizētos šūnu audzēšanas apstākļus.

Kad katram indivīdam ir atrasti optimālie ASC kultivēšanas apstākļi, iesaldētās šūnas var tikt atkausētas un efektīvi pavairotas, ja pacientam rodas tāda klīniskā nepieciešamība. Pēc personalizētas ASC pavairošanas šūnas tiek iesaldētas otro reizi sekojošu iemeslu dēļ: a) ir nepieciešams papildus laiks, lai pārbaudītu konkrēto šūnu partiju pirms ievadīšanas; b) pacienta iespējas saņemt terapiju var nesakrist ar ASC gatavības laiku; c) plānotais ASC terapijas laiks var tikt aizkavēts; d) ASC pavairošana var tikt veikta attālināti, ja medicīnas iestādē nav pieejama specializēta šūnu laboratorija. Šāda personalizēta ASC sagatavošanas metodoloģija piedāvā iespēju ārstēt parastajai terapijai rezistentas slimības, kā arī uzlabot dzīves kvalitāti vecumdienās, izmantojot tikko atkausētas ASC kā personalizētu terapiju, piemēram, miokarda infarkta vai insulta gadījumos (Honmou et al., 2011; McIntosh et al., 2013). Mūsu jaunā pieeja ASC sagatavošanas procesa uzlabošanai reālajā laikā iet tālāk par standarta ražošanas procesu un piedāvā personalizētu un riskam piemērotu ārstēšanu saskaņā ar labas ražošanas praksi.

4. Secinājumi

1. AS var kalpot kā vērtīgs FBS aizstājējs šūnu kultivēšanas barotnē. Gan hASC, gan cASC, kuras audzētas barotnē ar AS un pie 5% skābekļa koncentrācijas, saglabā savu raksturīgo vārpstveida morfoloģiju, virsmas marķieru ekspresiju, diferenciācijas spēju un imunosupresīvo efektu. Šīs īpašības neietekmē arī divkārša šūnu sasaldēšana un atkausēšana.
2. hASC un cASC populācijas ir fenotipiski homogēnas. hASC vienlaicīgi ekspresē tādus virsmas marķierus kā CD29, CD44, CD73, CD90 un CD105, bet cASC – CD44, CD73 un CD90. Abu veidu ASC ir negatīvas pēc CD14, CD34, CD45 un HLA-DR, un hASC papildus neuzrāda CD19 ekspresiju. Pozitīvo virsmas marķieru proteīnu ekspresija hASC populācijā pieaug pa pasāžām.
3. Gan hASC, gan cASC spēj diferencēties par adipocītiem, osteocītiem un hondrocītiem, tomēr cASC diferenciācija adipogēnajā virzienā ir vāja. hASC adipogēnās un osteogēnās diferenciācijas potenciāls atšķiras starp donoriem.
4. Gan hASC, gan cASC būtiski samazina T šūnu proliferāciju, un šī imunosupresīvā spēja ir atkarīga no šūnu devas. Abu veidu ASC sasniedz savu maksimālo efektu pie ASC:PBMNC attiecības 1:1.
5. hASC un cASC ir līdzīgas pēc šūnu morfoloģijas, virsmas marķieru ekspresijas, diferenciācijas potenciāla un imunomodulatīvajām spējām, un tās atbilst minimālajiem MSC definēšanas kritērijiem.
6. hASC *in vitro* pavairošana izraisa šūnu novecošanos, ko pierāda izmaiņas šūnu morfoloģijā, PDT un SA-β-gal ekspresijas pieaugums, kā arī klonogenitātes un diferenciācijas potenciāla samazināšanās vēlākās pasāžās. Trīs no pārbaudītajām hASC kultūrām sasniedza replikatīvo senescenci, bet pārējās piecas – priekšlaicīgo senescenci.
7. Visu darbā pārbaudīto donoru hASC kultūras satur divas labi nodalāmas šūnu subpopulācijas, kurām atšķiras RTL un šūnu lielums. Ilgtermiņa šūnu kultivēšanas laikā abu subpopulāciju kvantitatīvās attiecības mainās, un tas notiek katram donoram atšķirīgā veidā.
8. hASC *in vitro* senescences process ir nevienmērīgs un katram šūnu donoram specifisks.
9. Pētījumā izmantotajiem suņiem novērojama atšķirīga organisma reakcija uz DMSO.
10. Terapeitiskās cASC devas un piecas reizes lielākas šūnu devas intravenoza ievadīšana suņiem nerada būtiskas blaknes vai nevēlamus notikumus un neizraisa ļaundabīgu audzēju veidošanos.
11. Darba gaitā izstrādāto metodoloģiju var pielietot personalizēta ASC produkta sagatavošanā ārpus rutīnas apstākļiem, ko iespējams izmantot kā ATMP klīnisko izņēmumu gadījumos.

5. Aizstāvamās tēzes

1. Katra donora ASC piemīt individuālas un būtiskas atšķirības šūnu augšanā, novecošanā un funkcionalitātē, kas pamato nepieciešamību pēc personalizētas pieejas jaunieviesto terapijas zāļu izstrādē.
2. ASC, kuras sagatavotas pēc darba gaitā izstrādātās metodoloģijas, 5. pasāžā parāda morfoloģiski neizmainītu un fenotipiski homogēnu šūnu populāciju ar optimālu MSC virsmas marķieru proteīnu ekspresiju, kam piemīt multilīniju diferenciācijas spēja un būtisks imunosupresīvs potenciāls. Ņemot vērā iespēju sagatavot terapijai nepieciešamo šūnu devu līdz 5. pasāžas beigām, šī ASC pasāža ir atbilstošākā potenciālam klīniskajam pielietojumam.
3. Atkārtota 5. pasāžas autologu cASC ievadīšana suņiem neizraisa būtiskas blaknes. Akūtas reakcijas nav novērojamas, un vēlīnas izmaiņas audos un orgānos arī nav detektējamas, parādot šo šūnu drošumu suņa modelī un sniedzot būtisku informāciju ASC terapijas izmantošanai cilvēkiem.

6. Pateicības

Es novērtēju vērtīgos padomus un palīdzību no Tatjanas Kozlovskas, Prof. Paula Pumpēna, Prof. Aijas Žilevičas, Ances Bogdanovas-Jātnieces, Diānas Legzdiņas, Sergeja Ņikuļšina, Ilzes Matises-VanHoutanas, Ilzes Pētersones, Ilmāra Dūrīša, Anetes Romanauskas, Daces Skrastiņas, Rafaela Joffes, Mārtiņa Kāļa, Šimona Svirska, Prof. Alberta Auzāna, Agneses Ezertas, Zitas Muižnieces, Māras Vasiļevskas, Jūlijas Spelas, Annas Veidemanes, Agņa Zvaigznes, Gulšenas Eivazovas, Rūtas Brūveres, Liānas Pliss, Renātes Rankas, Daces Pjanovas, Kaspara Tāra, Zinaīdas Šomšteines un Elmāra Grēna visa pētījuma laikā.

Literatūras saraksts

Abdi, R., Fiorina, P., Adra, C. N., Atkinson, M., & Sayegh, M. H. (2008). Immunomodulation by Mesenchymal Stem Cells : A Potential Therapeutic Strategy for Type 1 Diabetes. Diabetes, 57(7), 1759–1767.

Abumaree, M., Al Jumah, M., Pace, R.A., Kalionis, B. (2012). Immunosuppressive properties of mesenchymal stem cells. Stem Cell Rev., 8:375–392.

Aggarwal, S., Pittenger, M.F. (2005). Human mesenchymal stem cells modulate allogeneic immune cell responses. Blood, 105:1815-1822.

Anjos-Afonso, F., Siapati, E.K., Bonnet, D. (2004) *In vivo* contribution of murine mesenchymal stem cells into multiple cell-types under minimal damage conditions. Journal of cell science, 117, 5655-5664.

Astori, G., Vignati, F., Bardelli, S., Tubio, M., Gola, M., Albertini, V., … Moccetti, T. (2007). "*In vitro*" and multicolor phenotypic characterization of cell subpopulations identified in fresh human adipose tissue stromal vascular fraction and in the derived mesenchymal stem cells. Journal of Translational Medicine, 5, 55.

Auletta, J.J., Zale, E.A., Welter, J.F., Solchaga, L.A. (2001). Fibroblast growth factor-2 enhances expansion of human bone marrow-derived mesenchymal stromal cells without diminishing their immunosuppressive potential. Stem Cells Int, 235176.

Baer, P.C., Kuçi, S., Krause, M., Kuçi, Z., Zielen, S., Geiger, H., ... Schubert. R. (2013). Comprehensive phenotypic characterization of human adipose-derived stromal/stem cells and their subsets by a high throughput technology. Stem Cells Dev, 22:330-239.

Baerlocher, G.M., Mak, J., Tien, T., Lansdorp, P.M. (2002) Telomere length measurement by fluorescence *in situ* hybridization and flow cytometry: tips and pitfalls. Cytometry, 47:89-99.

Baker, D..J., Sedivy, J.M. (2013). Probing the depths of cellular senescence. Journal Cell Biol., 202(1):11-13.

Bartholomew, A., Sturgeon, C., Siatskas, M., Ferrer, K., McIntosh, K., Patil, S., ... Hoffman, R. (2002). Mesenchymal stem cells suppress lymphocyte proliferation *in vitro* and prolong skin graft survival *in vivo*. Exp Hematol, 30:42-48.

Basciano, L., Nemos, C., Foliguet, B., de Isla, N., de Carvalho, M., Tran, N., Dalloul, A. (2011) Long term culture of mesenchymal stem cells in hypoxia promotes a genetic program maintaining their undifferentiated and multipotent status. BMC cell biology, 12, 12.

Baxter, M.A., Wynn, R.F., Jowitt, S.N., Wraith, J.E., Fairbairn, L.J., Bellantuono, I. (2004). Study of telomere length reveals rapid aging of human marrow stromal cells following *in vitro* expansion. Stem Cells, 22:675-682.

Bentzon, J.F., Stenderup, K., Hansen, F.D., Schroder, H.D., Abdallah, B.M., Jensen, T.G., Kassem, M. (2005). Tissue distribution and engraftment of human mesenchymal stem cells immortalized by human telomerase reverse transcriptase gene. Biochemical and biophysical research communications, 330, 633-640.

Beyth, S., Borovsky, Z., Mevorach, D., Liebergall, M., Gazit, Z., Aslan, H., ... Rachmilewitz, J. (2005). Human mesenchymal stem cells alter antigen-presenting cell maturation and induce T-cell unresponsiveness. Blood, 105:2214-2219.

Blythe, L.L., Craig, A.M., Christensen, J.M., Appell, L.H., Slizeski, M.L. (1986). Pharmacokinetic disposition of dimethyl sulfoxide administered intravenously to horses. American journal of veterinary research, 47, 1739-1743.

Bodnar, A.G., Ouellette, M., Frolkis, M., Holt, S.E., Chiu, C.P., Morin, G.B., ... Wright, W.E. (1998). Extension of life-span by introduction of telomerase into normal human cells. Science, 279:349-352.

Bogdanova, A., Berzins, U., Nikulshin, S., Skrastina, D., Ezerta, A., Legzdina, D., Kozlovska, T. (2014). Characterization of human adipose-derived stem cells cultured in

autologous serum after subsequent passaging and long term cryopreservation. Journal of stem cells, 9, 135-148.
Bogdanova, A., Bērziņš, U., Brūvere, R., Eivazova, G., Kozlovska, T. (2010). Adipose-derived stem cells cultured in autologous serum maintain the characteristics of mesenchymal stem cells. Proc Latv Acad Sci, Sect B, Nat Exact Appl Sci, 64:106-113.
Bonab, M.M., Alimoghaddam, K., Talebian, F., Ghaffari, S.H., Ghavamzadeh, A., Nikbin, B. (2006). Aging of mesenchymal stem cell *in vitro*. BMC Cell Biol. 7:14.
Capra, E., Beretta, R., Parazzi, V., Viganò, M., Lazzari, L., Baldi, A., Giordano, R. (2012). Changes in the proteomic profile of adipose tissue-derived mesenchymal stem cells during passages. Proteome Sci, 10:46.
Chabannes, D., Hill, M., Merieau, E., Rossignol, J., Brion, R., Soulillou, P., Cuturi, M. C. (2007). A role for heme oxygenase-1 in the immunosuppressive effect of adult rat and human mesenchymal stem cells. Blood, 110:3691-3694.
Chamberlain, G., Fox, J., Ashton, B., Middleton, J. (2007). Concise review: mesenchymal stem cells: their phenotype, differentiation capacity, immunological features, and potential for homing. Stem Cells, 25:2739-2749.
Cholewa, D., Stiehl, T., Schellenberg, A., Bokermann, G., Joussen, S., Koch, C., ... Wagner, W. (2011). Expansion of adipose mesenchymal stromal cells is affected by human platelet lysate and plating density. Cell Transplant, 20:1409-1422.
Corcione, A., Benvenuto, F., Ferretti, E., Giunti, D., Cappiello, V., Cazzanti, F., ... Uccelli, A. (2006). Human mesenchymal stem cells modulate B-cell functions. Blood, 107, 367-372.
Cristofalo, V.J., Pignolo, R.J. (1993). Replicative senescence of human fibroblast-like cells in culture. Physiol Rev. 73(3):617-638.
Cui, L., Yin, S., Liu, W., Li, N., Zhang, W., Cao, Y. (2007), Expanded adipose-derived stem cells suppress mixed lymphocyte reaction by secretion of prostaglandin E2. Tissue Eng, 13:1185-1195.
Cyranoski, D. (2010). Korean deaths spark inquiry. Nature, 468, 485.
Dahl, JA., Duggal, S., Coulston, N., Millar, D., Melki, J., Shahdadfar, A., ... Collas, P. (2008). Genetic and epigenetic instability of human bone marrow mesenchymal stem cells expanded in autologous serum or fetal bovine serum. Int J Dev Biol, 52:1033-1042.
De Jesus, M.M., Santiago, J.S., Trinidad, C.V., See, M.E., Semon, K.R., Fernandez, M.O. Jr., Chung, F.S. (2016). Autologous Adipose-Derived Mesenchymal Stromal Cells for the Treatment of Psoriasis Vulgaris and Psoriatic Arthritis: A Case Report. Cell transplantation, 25, 2063-2069.
De Miguel, M.P., Fuentes-Julián, S., Blázquez-Martínez, A., Pascual, CY., Aller, MA., Arias, J., Arnalich-Montiel, F. (2012). Immunosuppressive properties of mesenchymal stem cells: advances and applications. Curr Mol Med, 12:574-591.
De Rosa, A., De Francesco, F., Tirino, V., Ferraro, G.A., Desiderio, V., ... Papaccio, G. (2009). A new method for cryopreserving adipose-derived stem cells: an attractive and suitable large-scale and long-term cell banking technology. Tissue Eng Part C Methods, 15:659–667.
Desiderio, V., De Francesco, F., Schiraldi, C., De Rosa, A., La Gatta, A., Paino, F., ... Papaccio, G. (2013). Human Ng2+ adipose stem cells loaded *in vivo* on a new crosslinked hyaluronic acid-Lys scaffold fabricate a skeletal muscle tissue. Journal of cellular physiology, 228, 1762-1773.
Di Nicola, M., Carlo-Stella, C., Magni, M., Milanesi, M., Longoni, P.D., Matteucci, P., Grisanti, S., Gianni, A.M. (2002). Human bone marrow stromal cells suppress T-lymphocyte proliferation induced by cellular or nonspecific mitogenic stimuli. Blood, 99, 3838-3843.
Digirolamo, C.M., Stokes, D., Colter, D., Phinney, D.G., Class, R., Prockop, D.J. (1999). Propagation and senescence of human marrow stromal cells in culture: a simple colony-forming assay identifies samples with the greatest potential to propagate and differentiate. Br J Haematol, 107:275-281.

Dimri G.P., Lee X., Basile G., Acosta M., Scott G., Roskelley C., ... Pereira-Smith O. (1995). A biomarker that identifies senescent human cells in culture and in aging skin *in vivo*. Proc Natl Acad Sci USA. 92(20):9363-9367.
Djouad, F., Plence, P., Bony, C., Tropel, P., Apparailly, F., Sany, J., ... Jorgensen, C. (2003). Immunosuppressive effect of mesenchymal stem cells favors tumor growth in allogeneic animals. Blood, 102:3837-3844.
Dominici, M., Le Blanc, K., Mueller, I., Slaper-Cortenbach, I., Marini, F., Krause, D., ... Horwitz, E. (2006). Minimal criteria for defining multipotent mesenchymal stromal cells. The International Society for Cellular Therapy position statement. Cytotherapy, 8, 315-317.
Dulic, V. (2013). Senescence regulation by mTOR. Methods Mol Biol. 965:15-35.
Eggenhofer, E., Benseler, V., Kroemer, A., Popp, F.C., Geissler, E.K., Schlitt, H.J., ... Hoogduijn, M.J. (2012). Mesenchymal stem cells are short-lived and do not migrate beyond the lungs after intravenous infusion. Frontiers in immunology, 3, 297.
Eggenhofer, E., Luk, F., Dahlke, M.H., Hoogduijn, M.J. (2014). The life and fate of mesenchymal stem cells. Frontiers in immunology, 5, 148.
Estrada JC., Torres Y., Benguría A., Dopazo A., Roche E., Carrera-Quintanar L., ... Bernad A. (2013). Human mesenchymal stem cell-replicative senescence and oxidative stress are closely linked to aneuploidy. Cell Death Dis. 4:e691.
European Commission (2014). Report from the commission to the European Parliament and the Council in accordance with article 25 of regulation (EC) no 1394/2007 of the European Parliament and of the Council on advanced therapy medicinal products and amending directive 2001/83/EC and regulation (EC) no 726/2004.
Evans-Galea, M.V., Wielgosz, M.M., Hanawa, H., Srivastava, D.K., Nienhuis, A.W. (2007). Suppression of clonal dominance in cultured human lymphoid cells by addition of the cHS4 insulator to a lentiviral vector. Mol Ther, 15:801-809.
Fang, B., Li, N., Song, Y., Li, J., Zhao, R.C., Ma, Y. (2009). Cotransplantation of haploidentical mesenchymal stem cells to enhance engraftment of hematopoietic stem cells and to reduce the risk of graft failure in two children with severe aplastic anemia. Pediatric transplantation, 13, 499-502.
Fang, B., Song, Y., Liao, L., Zhang, Y., Zhao, R.C. (2007). Favorable response to human adipose tissue-derived mesenchymal stem cells in steroid-refractory acute graft-versus-host disease. Transplantation proceedings, 39, 3358-3362.
Fischer, U.M., Harting, M.T., Jimenez, F., Monzon-Posadas, W.O., Xue, H., Savitz, S.I., ... Cox, C.S., Jr. (2009). Pulmonary passage is a major obstacle for intravenous stem cell delivery: the pulmonary first-pass effect. Stem cells and development, 18, 683-692.
Furlani, D., Ugurlucan, M., Ong, L., Bieback, K., Pittermann, E., Westien, I., ... Ma, N. (2009). Is the intravascular administration of mesenchymal stem cells safe? Mesenchymal stem cells and intravital microscopy. Microvascular research, 77, 370-376.
Geisler S., Textor M., Kuhnisch J., Konnig D., Klein O., Ode A., ... Duda G.N. (2012). Functional comparison of chronological and *in vitro* aging: differential role of the cytoskeleton and mitochondriain mesenchymal stromal cells. PLoS One. 7(12):e52700.
General Secretariat of the Council to Delegations; Document number 15054/15: Personalised medicine for patients – Council conclusions (7 December 2015): http://data.consilium.europa.eu/doc/document/ST-15054-2015-INIT/en/pdf.
Ghannam, S., Bouffi, C., Djouad, F., Jorgensen, C., Noel, D. (2010). Immunosuppression by mesenchymal stem cells: mechanisms and clinical applications. Stem cell research & therapy, 1, 2.
Goh, B. C., Thirumala, S., Kilroy, G., Devireddy, R. V., Gimble, J. M. (2007). Cryopreservation characteristics of adipose-derived stem cells: maintenance of differentiation potential and viability. J Tissue Eng Regen Med, 1: 322–324.
González-Cruz, R.D., Darling, E.M. (2013). Adipose-derived stem cell fate is predicted by cellular mechanical properties. Adipocyte, 2:87-91.

Gronthos, S., Franklin, D.M., Leddy, H.A., Robey, P.G., Storms, R.W., Gimble, J.M. (2001). Surface protein characterization of human adipose tissue-derived stromal cells. J Cell Physiol, 189:54-63.
Gruber, H.E., Somayaji, S., Riley, F., Hoelscher, G.L., Norton, H.J., Ingram, J., Hanley, E.N. Jr. (2012). Human adipose-derived mesenchymal stem cells: serial passaging, doubling time and cell senescence. Biotech Histochem, 87:303-11.
Hall, M.N., Rosenkrantz, W.S., Hong, J.H., Griffin, C.E., Mendelsohn, C.M. (2010). Evaluation of the potential use of adipose-derived mesenchymal stromal cells in the treatment of canine atopic dermatitis: a pilot study. Veterinary therapeutics : research in applied veterinary medicine, 11, E1-14.
Han, S.M., Kim, H.T., Kim, K.W., Jeon, K.O., Seo, K.W., Choi, E.W., Youn, H.Y. (2015). CTLA4 overexpressing adipose tissue-derived mesenchymal stem cell therapy in a dog with steroid-refractory pemphigus foliaceus. BMC veterinary research, 11, 49.
Harley C.B., Futcher A.B., Greider C.W. (1990). Telomeres shorten during ageing of human fibroblasts. Nature. 345(6274):458-460.
Hemann M.T., Strong M.A., Hao L.Y., Greider C.W. (2001). The shortest telomere, not average telomere length, is critical for cell viability and chromosome stability. Cell. 107(1):67-77.
Honmou, O., Houkin, K., Matsunaga, T., Niitsu, Y., Ishiai, S., Onodera, R., ... Kocsis, J.D. (2011). Intravenous administration of auto serum-expanded autologous mesenchymal stem cells in stroke. Brain, 134, 1790-1807.
Hu, X., Yu, S.P., Fraser, J.L., Lu, Z., Ogle, M.E., Wang, J.A., Wei, L. (2008). Transplantation of hypoxia-preconditioned mesenchymal stem cells improves infarcted heart function via enhanced survival of implanted cells and angiogenesis. The Journal of thoracic and cardiovascular surgery, 135, 799-808.
Hung, S.C., Pochampally, R.R., Hsu, S.C., Sanchez, C., Chen, S.C., Spees, J., Prockop, D.J. (2007). Short-term exposure of multipotent stromal cells to low oxygen increases their expression of CX3CR1 and CXCR4 and their engraftment *in vivo*. PloS one, 2, e416.
Im, W., Chung, J., Kim, S.H., Kim, M. (2011). Efficacy of autologous serum in human adipose-derived stem cells; cell markers, growth factors and differentiation. Cell Mol Biol (Noisy-le-grand), 57. Suppl:OL1470-5.
Ivanovic, Z. (2009). Hypoxia or *in situ* normoxia: The stem cell paradigm. Journal of cellular physiology, 219, 271-275.
Izadpanah R., Trygg C., Patel B., Kriedt C., Dufour J., Gimble J.M., Bunnell B.A. (2006). Biologic properties of mesenchymal stem cells derived from bone marrow and adipose tissue. J Cell Biochem. 99(5):1285-1297.
Jung, J.W., Kwon, M., Choi, J.C., Shin, J.W., Park, I.W., Choi, B.W., Kim, J.Y. (2013). Familial occurrence of pulmonary embolism after intravenous, adipose tissue-derived stem cell therapy. Yonsei medical journal, 54, 1293-1296.
Kaji, H. (2016). Adipose Tissue-Derived Plasminogen Activator Inhibitor-1 Function and Regulation. Comprehensive Physiology. 6:1873–1896.
Kang, M.H., Park, H.M. (2014). Evaluation of adverse reactions in dogs following intravenous mesenchymal stem cell transplantation. Acta veterinaria scandinavica, 56, 16.
Karagiannis, K., Proklou, A., Tsitoura, E., Lasithiotaki, I. (2017). Impaired mRNA Expression of the Migration Related Chemokine Receptor CXCR4 in Mesenchymal Stem Cells of COPD Patients. Int. J. Inflam., 2017, 6089425.
Katz, A.J., Tholpady, A., Tholpady, S.S., Shang, H., Ogle, R.C. (2005). Cell surface and transcriptional characterization of human adipose-derived adherent stromal (hADAS) cells. Stem Cells, 23:412-423.
Kim, M., Kim, D.I., Kim, E.K., Kim, C.W. (2017). CXCR4 Overexpression in Human Adipose Tissue-Derived Stem Cells Improves Homing and Engraftment in an Animal Limb Ischemia Model. Cell transplantation, 26, 191-204.
Kisiel, A.H., McDuffee, L.A., Masaoud, E., Bailey, T.R., Esparza Gonzalez, B.P., Nino-Fong, R. (2012). Isolation, characterization, and *in vitro* proliferation of canine

mesenchymal stem cells derived from bone marrow, adipose tissue, muscle, and periosteum. American journal of veterinary research, 73, 1305-1317.
Kraitchman, D.L., Tatsumi, M., Gilson, W.D., Ishimori, T., Kedziorek, D., Walczak, P., ... Bulte, J.W. (2005). Dynamic imaging of allogeneic mesenchymal stem cells trafficking to myocardial infarction. Circulation, 112, 1451-1461.
Kuilman, T., Michaloglou, C., Mooi, W.J., Peeper, D.S. (2010). The essence of senescence. Genes Dev. 24(22):2463-2479.
Lansdorp, P.M., Verwoerd, N.P., van de Rijke, F.M., Dragowska, V., Little, M.T., Dirks, R.W., ... Tanke H.J. (1996). Heterogeneity in telomere length of human chromosomes. Hum Mol Genet. 5(5):685-691.
Le Blanc, K., Tammik, L., Sundberg, B., Haynesworth, S.E., Ringden, O. (2003). Mesenchymal stem cells inhibit and stimulate mixed lymphocyte cultures and mitogenic responses independently of the major histocompatibility complex. Scandinavian journal of immunology, 57, 11-20.
Lee, B.Y., Han, J.A., Im, J.S., Morrone, A., Johung, K., Goodwin, E.C., ... Hwang E.S. (2006). Senescence-associated beta-galactosidase is lysosomal beta-galactosidase. Aging Cell. 5(2):187-195.
Lee, C.C., Christensen, J.E., Yoder, M.C., Tarantal, A.F. (2010). Clonal analysis and hierarchy of human bone marrow mesenchymal stem and progenitor cells. Exp Hematol, 38:46-54.
Lee, E.Y., Xia, Y., Kim, W.S., Kim, M.H., Kim, T.H., Kim, K.J., ... Sung, J.H. (2009). Hypoxia-enhanced wound-healing function of adipose-derived stem cells: increase in stem cell proliferation and up-regulation of VEGF and bFGF. Wound repair and regeneration : official publication of the Wound Healing Society [and] the European Tissue Repair Society, 17, 540-547.
Legzdina, D., Romanauska, A., Nikulshin, S., Kozlovska, T., Berzins, U. (2016). Characterization of Senescence of Culture-expanded Human Adipose-derived Mesenchymal Stem Cells. International journal of stem cells, 9, 124-136.
Leroux, L., Descamps, B., Tojais, N.F., Seguy, B., Oses, P., Moreau, C., ... Duplaa, C. (2010). Hypoxia preconditioned mesenchymal stem cells improve vascular and skeletal muscle fiber regeneration after ischemia through a Wnt4-dependent pathway. Molecular therapy : the journal of the American Society of Gene Therapy, 18, 1545-1552.
Li, Q., Zhang, A., Tao, C., Li, X., Jin, P. (2013). The role of SDF-1-CXCR4/CXCR7 axis in biological behaviors of adipose tissue-derived mesenchymal stem cells *in vitro*. Biochemical and biophysical research communications, 441, 675-680.
Lim, J.Y., Ra, J.C., Shin, I.S., Jang, Y.H., An, H.Y., Choi, J.S., ... Kim, Y.M. (2013). Systemic transplantation of human adipose tissue-derived mesenchymal stem cells for the regeneration of irradiation-induced salivary gland damage. PloS one, 8, e71167.
Lin, K., Matsubara, Y., Masuda, Y., Togashi, K., Ohno, T., Tamura, T., ... Douglas, A. (2008). Characterization of adipose tissuederived cells isolated with the Celution system. Cytotherapy, 10:417-426.
Liu, G., Zhou, H., Li, Y., Li, G., Cui, L., Liu, W., Cao, Y. (2008). Evaluation of the viability and osteogenic differentiation of cryopreserved human adiposederived stemcells. Cryobiology, 57(1):18-24.
Liu, H., Liu, S., Li, Y., Wang, X., Xue, W., Ge, G., Luo, X. (2012). The role of SDF-1-CXCR4/CXCR7 axis in the therapeutic effects of hypoxia-preconditioned mesenchymal stem cells for renal ischemia/reperfusion injury. PloS one, 7, e34608.
Lo Sicco, C., Reverberi, D., Balbi, C., Ulivi, V., Principi, E., Pascucci, L., ... Tasso, R. (2017). Mesenchymal Stem Cell-Derived Extracellular Vesicles as Mediators of Anti-Inflammatory Effects: Endorsement of Macrophage Polarization. Stem cells translational medicine, 6, 1018-1028.
Lysaght, T., Lipworth, W., Hendl, T., Kerridge, I., Lee, T.L., Munsie, M., ... Stewart, C. (2017) The deadly business of an unregulated global stem cell industry. J Med Ethics. Nov;43(11):744-746.

Martinello, T., Bronzini, I., Maccatrozzo, L., Mollo, A., Sampaolesi, M., Mascarello, F., ... Patruno, M. (2011). Canine adipose-derived-mesenchymal stem cells do not lose stem features after a long-term cryopreservation. Res Vet Sci., 91(1):18-24.
Martins, A.A., Paiva, A., Morgado, J.M., Gomes, A., Pais, M.L. (2009). Quantification and immunophenotypic characterization of bone marrow and umbilical cord blood mesenchymal stem cells by multicolor flow cytometry. Transplant Proc, 41:943-6.
Mauney, J.R., Kaplan, D.L., Volloch, V. (2004). Matrix-mediated retention of osteogenic differentiation potential by human adult bone marrow stromal cells during ex vivo expansion. Biomaterials. 25(16):3233-3243.
McIntosh, K.R., Frazier, T., Rowan, B.G., Gimble, J.M. (2013). Evolution and future prospects of adipose-derived immunomodulatory cell therapeutics. Expert review of clinical immunology, 9, 175-184.
Meisel, R., Zibert, A., Laryea, M., Göbel, U., Däubener, W., Dilloo D. (2004). Human bone marrow stromal cells inhibit allogeneic T-cell responses by indoleamine 2,3-dioxygenase-mediated tryptophan degradation. Blood, 103:4619-4621.
Mitchell, J.B., McIntosh, K., Zvonic, S., Garrett, S., Floyd, Z.E., Kloster, A., ... Gimble, J.M. (2006). Immunophenotype of human adipose-derived cells: temporal change in stromalassociated and stem cell–associated markers. Stem Cells, 24:376-85.
Mizuno, N., Shiba, H., Ozeki, Y., Mouri, Y., Niitani, M., Inui, T., ... Kurihara, H. (2006). Human autologous serum obtained using a completely closed bag system as a substitute for foetal calf serum in human mesenchymal stem cell cultures. Cell Biol Int, 30:521-524.
Moll, G., Le Blanc, K. (2015). Engineering more efficient multipotent mesenchymal stromal (stem) cells for systemic delivery as cellular therapy. ISBT Science Series, 10, 357-365.
Muzes, G., Sipos, F. (2016). Heterogeneity of Stem Cells: A Brief Overview. Methods in molecular biology (Clifton, N.J.), 1516, 1-12.
Naylor, R.M., Baker, D.J., van Deursen, J.M. (2013). Senescent cells: a novel therapeutic target for aging and age-related diseases. Clin Pharmacol Ther. 93(1):105-116.
Neupane, M., Chang, C.C., Kiupel, M., Yuzbasiyan-Gurkan, V. (2008). Isolation and characterization of canine adipose-derived mesenchymal stem cells. Tissue engineering. Part A, 14, 1007-1015.
Nimura, A., Muneta, T., Koga, H., Mochizuki, T., Suzuki, K., Makino, H., ... Sekiya, I. (2008). Increased proliferation of human synovial mesenchymal stem cells with autologous human serum. Comparisons with bone marrow mesenchymal stem cells and with fetal bovine serum. Arthritis Rheum, 58:501–510.
Noh, H.B., Ahn, H.J., Lee, W.J., Kwack, K.B., Kwon, Y.D. (2010). The molecular signature of *in vitro* senescence in human mesenchymal stem cells. Genes Genomics, 32:87-93.
O'Kell, A.L., Wasserfall, C., Catchpole, B., Davison, L.J., Hess, R.S., Kushner, J.A., Atkinson, M.A. (2017). Comparative Pathogenesis of Autoimmune Diabetes in Humans, NOD Mice, and Canines: Has a Valuable Animal Model of Type 1 Diabetes Been Overlooked? Diabetes, 66, 1443-1452.
Ohki, R., Tsurimoto, T., Ishikawa, F. (2001). *In vitro* reconstitution of the end replication problem. Mol Cell Biol. 21(17):5753-5766.
Park, E., Patel, A.N. (2010). Changes in the expression pattern of mesenchymal and pluripotent markers in human adipose-derived stem cells. Cell Biol Int, 34:979- 984.
Prologo, J.D., Hawkins, M., Gilliland, C., Chinnadurai, R., Harkey, P., Chadid, T., ... Brewster, L. (2016). Interventional stem cell therapy. Clinical radiology, 71, 307-311.
Ra, J.C., Kang, S.K., Shin, I.S., Park, H.G., Joo, S.A., Kim, J.G., ... Kurtz, A. (2011a). Stem cell treatment for patients with autoimmune disease by systemic infusion of culture-expanded autologous adipose tissue derived mesenchymal stem cells. Journal of translational medicine, 9, 181.
Ra, J.C., Shin, I.S., Kim, S.H., Kang, S.K., Kang, B.C., Lee, H.Y., ... Kwon, E. (2011b). Safety of intravenous infusion of human adipose tissue-derived mesenchymal stem cells in animals and humans. Stem cells and development, 20, 1297-1308.

Rada, T., Reis, R.L. (2011). Gomes ME. Distinct stem cells subpopulations isolated from human adipose tissue exhibit different chondrogenic and osteogenic differentiation potential. Stem Cell Rev 2011;7:64-76.
Raggi, C., Berardi, A.C. (2012). Mesenchymal stem cells, aging and regenerative medicine. Muscles Ligaments Tendons J. 2(3):239-242.
Regulation, E.C. (2007) No. 1394/2007 of the European Parliament and of the Council of 13 November 2007 on advanced therapy medicinal products and amending directive 2001/83/EC and regulation (EC) no 726/2004. J Eur Union, 324, 121-137.
Reich, C.M., Raabe, O., Wenisch, S., Bridger, P.S., Kramer, M., Arnhold, S. (2012). Isolation, culture and chondrogenic differentiation of canine adipose tissue- and bone marrow-derived mesenchymal stem cells--a comparative study. Veterinary research communications, 36, 139-148.
Rodriguez, A.M., Elabd, C., Amri, E.Z., Ailhaud, G., Dani, C. (2005). The human adipose tissue is a source of multipotent stem cells. Biochimie, 87(1): 125-128.
Rosova, I., Dao, M., Capoccia, B., Link, D., Nolta, J.A. (2008). Hypoxic preconditioning results in increased motility and improved therapeutic potential of human mesenchymal stem cells. Stem cells (Dayton, Ohio), 26, 2173-2182.
Samsonraj, R.M., Raghunath, M., Hui, J.H., Ling, L., Nurcombe, V., Cool, S.M. (2013). Telomere length analysis of human mesenchymal stem cells by quantitative PCR. Gene, 519:348-355.
Samuelsson, H., Ringdén, O., Lönnies, H., Le Blanc, K. (2009). Optimizing *in vitro* conditions for immunomodulation and expansion of mesenchymal stromal cells. Cytotherapy, 11:129-136.
Sato, J., Doi, T., Wako, Y., Hamamura, M., Kanno, T., Tsuchitani, M., Narama, I. (2012). Histopathology of incidental findings in beagles used in toxicity studies. Journal of toxicologic pathology, 25, 103-134.
Sato, K; Ozaki, K; Oh, I; Meguro, A; Hatanaka, K; Nagai, T; ... Ozawa, K. (2007). Nitric oxide plays a critical role in suppression of T-cell proliferation by mesenchymal stem cells. Blood, 109:228-234.
Schellenberg, A., Hemeda, H., Wagner, W. (2013). Tracking of replicative senescence in mesenchymal stem cells by colony-forming unit frequency. Methods Mol Biol. 976:143-154.
Sethe S., Scutt A., Stolzing A. (2006). Aging of mesenchymal stem cells. Ageing Res Rev. 5(1):91-116.
Shahdadfar, A., Frønsdal, K., Haug, T., Reinholt, F.P., Brinchmann, J.E. (2005). *In vitro* expansion of human mesenchymal stem cells: choice of serum is a determinant of cell proliferation, differentiation, gene expression, and transcriptome stability. Stem Cells, 23:1357-1366.
Shapiro, H.M., Shapiro, H.M. (2003). Practical flow cytometry. 4th Edition, Wiley-Liss, 736 pp.
Shay J.W., Wright W.E. (2000). Hayflick, his limit, and cellular ageing. Nat Rev Mol Cell Biol. 1(1):72–76.
Sparrow, R.L., Tippett, E. (2005). Discrimination of live and early apoptotic mononuclear cells by the fluorescent SYTO 16 vital dye. Journal of immunological methods, 305, 173-187.
Spees, J.L., Gregory, C.A., Singh, H., Tucker, H.A., Peister, A., Lynch, P.J. ... Prockop, D.J. (2004). Internalized antigens must be removed to prepare hypoimmunogenic mesenchymal stem cells for cell and gene therapy. Molecular therapy : the journal of the American Society of Gene Therapy, 9, 747-756.
Stepien, A., Dabrowska, N.L., Maciagowska, M., Macoch, R.P. (2016). Clinical Application of Autologous Adipose Stem Cells in Patients with Multiple Sclerosis: Preliminary Results, Mediators of Inflammation, 5302120.
Takemitsu, H., Zhao, D., Yamamoto, I., Harada, Y., Michishita, M., Arai, T. (2012). Comparison of bone marrow and adipose tissue-derived canine mesenchymal stem cells. BMC veterinary research, 8, 150.

Tatsumi, K., Ohashi, K., Matsubara, Y., Kohori, A., Ohno, T., Kakidachi, H., ... Okano, T. (2013). Tissue factor triggers procoagulation in transplanted mesenchymal stem cells leading to thromboembolism. Biochemical and biophysical research communications, 431, 203-209.
Treff, N.R., Su, J., Taylor, D., Scott, R.T. Jr. (2011). Telomere DNA deficiency is associated with development of human embryonic aneuploidy. PLoS Genet 2011;7:e1002161.
Tsai, C.C., Chen, Y.J., Yew, T.L., Chen, L.L., Wang, J.Y., Chiu, C.H., Hung, S.C. (2011). Hypoxia inhibits senescence and maintains mesenchymal stem cell properties through down-regulation of E2A-p21 by HIF-TWIST. Blood, 117, 459-469.
Tse, W.T., Pendleton, J.D., Beyer, W.M., Egalka, M.C., Giunan, E.C. (2003). Suppression of allogeneic T-cell proliferation by human marrow stromal cells: implications in transplantation. Transplantation, 2003, 75:389-397.
Tsuji, W., Rubin, J.P., Marra, K.G. (2014). Adipose-derived stem cells: Implications in tissue regeneration. World journal of stem cells, 6, 312-321.
Tu, Z., Li, Q., Bu, H., Lin, F. (2010). Mesenchymal Stem Cells Inhibit Complement Activation by Secreting Factor H. Stem Cells and Development, 19(11):1803-1809.
Tyndall, A., Uccelli, A. (2009). Multipotent mesenchymal stromal cells for autoimmune diseases: teaching new dogs old tricks. Bone marrow transplantation, 43, 821-828.
Varma, M.J., Breuls, RG., Schouten, T.E., Jurgens, W.J., Bontkes, H.J., Schuurhuis, G.J., ... van Milligen, F.J. (2007). Phenotypical and functional characterization of freshly isolated adipose tissue-derived stem cells. Stem Cells Dev, 16:91-104.
Veriter, S., Andre, W., Aouassar, N., Poirel, H.A., Lafosse, A., Docquier, P.L., Dufrane, D. (2015). Human Adipose-Derived Mesenchymal Stem Cells in Cell Therapy: Safety and Feasibility in Different "Hospital Exemption" Clinical Applications. PloS one, 10, e0139566.
Vieira, N.M., Brandalise, V., Zucconi, E., Secco, M., Strauss, B.E., Zatz, M. (2010). Isolation, characterization, and differentiation potential of canine adipose-derived stem cells. Cell transplantation, 19, 279-289.
Vives, J., Carmona, G. (2015). Guide to Cell Therapy GxP: Quality Standards in the Development of Cell-Based Medicines in Non-pharmaceutical Environments. Academic Press. 266 pp.
von Zglinicki T., Saretzki G., Ladhoff J., d'Adda di Fagagna F., Jackson S.P. (2005). Human cell senescence as a DNA damage response. Mech Ageing Dev. 126(1):111-117.
Wagner, W., Horn, P., Castoldi, M., Diehlmann, A., Bork, S., Saffrich, R., ... Ho, A.D. (2008). Replicative senescence of mesenchymal stem cells: a continuous and organized process. PLoS One. 3(5):e2213.
Wall, M.E., Bernacki, S.H., Loboa, E.G. (2007). Effects of serial passaging on the adipogenic and osteogenic differentiation potential of adipose-derived human potential of adipose-derived human mesenchymal ste cells. Tissue Eng, 13:1291-1298.
Winkler, R., Perner, B., Rapp, A., Durm, M., Cremer, C., Greulich, K.O., Hausmann, M. (2003). Labelling quality and chromosome morphology after low temperature FISH analysed by scanning far-field and near-field optical microscopy. J Microsc, 209:23-33.
Yañez, R., Lamana, M.L., García-Castro, J., Colmenero, I., Ramírez, M., Bueren, J.A. (2006). Adipose tissue-derived mesenchymal stem cells have *in vivo* immunosuppressive properties applicable for the control of the graft-versus-host disease. Stem Cells, 24:2582-2591.
Yang, X.F., He, X., He, J., Zhang, L.H., Su, X.J., Dong, Z.Y., ... Li, Y.L. (2011). High efficient isolation and systematic identification of human adipose-derived mesenchymal stem cells. J Biomed Sci, 18:59.
Zhao, H., Darzynkiewicz, Z. (2013). Biomarkers of cell senescence assessed by imaging cytometry. Methods Mol Biol. 965:83-92.
Zhu, Y., Liu, T., Song, K., Fan, X., Ma, X., Cui, Z. (2008). Adipose-derived stem cell: a better stem cell than BMSC. Cell Biochem Funct, 26:664-675.

Zuk, P.A., Zhu, M., Ashjian, P., De Ugarte, D.A., Huang, J.I., Mizuno, H., ... Hedrick, M.H. (2002). Human adipose tissue is a source of multipotent stem cells. Mol Biol Cell., 13(12), 4279-4295.
Zuk, P.A., Zhu, M., Mizuno, H., Huang, J., Futrell, J.W., Katz, A.J., ... Hedrick, M.H. (2001). Multilineage cells from human adipose tissue: implications for cell-based therapies. Tissue engineering, 7, 211-228.
Zvonic, S., Lefevre, M., Kilroy, G., Floyd, Z.E., DeLany, J.P., Kheterpal, I., ... Gimble, J.M. (2007). Secretome of primary cultures of human adipose-derived stem cells: modulation of serpins by adipogenesis, Mol. Cell. Proteom. 6 (1):18–28.

PIELIKUMS - publikācijas

PROCEEDINGS OF THE LATVIAN ACADEMY OF SCIENCES. Section B
DOI: 10.1515/prolas-2018-0004

CHARACTERISATION AND *IN VIVO* SAFETY OF CANINE ADIPOSE-DERIVED STEM CELLS*

Uldis Bērziņš[1,3,#], Ilze Matise-VanHoutana[2], Ilze Pētersone[2], Ilmārs Dūrītis[2], Sergejs Ņikuļšiņs[4], Ance Bogdanova-Jātniece[1], Mārtiņš Kālis[5], Šimons Svirskis[5], Dace Skrastiņa[1], Agnese Ezerta[1], and Tatjana Kozlovska[1]

[1] Latvian Biomedical Research and Study Centre, 1 Rātsupītes Str., Rīga, LV-1067, LATVIA

[2] Faculty of Veterinary Medicine, Latvia University of Agriculture, 2 Lielā Str., Jelgava, LV-3001, LATVIA

[3] Stem Cells Technologies Ltd., Rīga, LATVIA

[4] Children's Clinical University Hospital, 45 Vienības gatve, Rīga, LV-1004, LATVIA

[5] Augusts Kirhenšteins Institute of Microbiology and Virology, Rīga Stradiņš University, 5 Rātsupītes Str., Rīga, LV-1067, LATVIA

[#] Corresponding author, uldis@cst.lv

Communicated by Tatjana Kozlovska

The study characterises canine adipose-derived stem cells (cASCs) in comparison to human ASCs (hASCs) and tests their safety in a canine model after intravenous administration. cASCs from two dogs were cultured under hypoxic conditions in a medium supplemented with autologous serum. They were plastic adherent, spindle-shaped cells that expressed CD73, CD90, and CD44 but lacked CD45, CD14, HLA-DR, and CD34. cASCs differentiated toward adipogenic, osteogenic, and chondrogenic lineages, although adipogenic differentiation capacity was low. Blast transformation reaction demonstrated that these cells significantly suppress T-cell proliferation, and this ability is dose-dependent. Intravenous administration of a cell freezing medium, therapeutic dose of cASCs (2×10^6 live cells/kg), and five times higher dose of cASCs showed no significant side effects in two dogs. Microscopic tissue lesions were limited to only mild, non-specific changes. There were no signs of malignancy. The results of the study indicate that cASCs are similar to hASCs and are safe for therapeutic applications in a canine model. The proposed methodology for ASC preparation on a non-routine basis, which includes individually optimised cell culture conditions and offers risk-adapted treatment, could be used for future personalised off-the-shelf therapies, for example, in myocardial infarction or stroke.

Key words: *autologous adipose-derived stem cells, stem cell safety, pulmonary first-pass effect, advanced therapy medicinal products, hospital exemption.*

INTRODUCTION

Regenerative medicine is a rapidly advancing field of research that offers broad possibilities for treating severe diseases resistant to conventional therapies. It is expected that the significance of regenerative medicine will continue to increase in future; it may become one of the main branches of personalised medicine, which offers tailoring of treatments to specific needs, characteristics, and preferences of each patient during every stage of medical care (www.fda.gov). Personalisation of regenerative medicine has already facilitated the emergence of such innovative therapies as advanced therapy medicinal products (ATMPs) that encompass gene and cell therapy as well as tissue engineering (Anonymous, 2014; General, 2015; Vives and Carmona, 2015).

The use of mesenchymal stem cells (MSCs) as ATMP is a promising aspect of regenerative medicine. Since it was demonstrated that MSCs can be readily obtained from adipose tissue (Zuk *et al*., 2001), fat has become a valuable source of MSCs. These cells are ideally suited for the development of effective cell-based therapies due to their multilineage differentiation ability (Zuk *et al*., 2002; Desiderio *et al*., 2013), capacity to migrate to the site of injury (Liu *et al*., 2012; Li *et al*., 2013; Karagiannis *et al*., 2017; Kim *et al*., 2017) and regenerate damaged tissues (Lim *et al*., 2013; Tsuji *et al*., 2014), as well as due to their immunomodulatory potential (Tyndall and Uccelli, 2009; Ghannam *et al*., 2010; Lo Sicco *et al*., 2017). Research has shown that adipose-derived stem cells (ASCs) can be used to treat immune disorders, including graft-versus-host disease (Fang *et al*.,

* Supplementary data associated with this article can be found in the online version.

2007; Fang *et al*., 2009), psoriasis (De Jesus *et al*., 2016), and multiple sclerosis (Stepien *et al*., 2016).

ASCs as ATMP can be applied for human therapy in cases of so-called hospital exemptions (HEs), employing personally prepared autologous stem cells. One of the first steps in the applications of such ATMP is to verify the process and to gain experience using animal models. Companion animals, including dogs, naturally develop chronic autoimmune diseases such as atopic dermatitis (Hall *et al*., 2010), pemphigus (Han *et al*., 2015), and diabetes mellitus (Abdi *et al*., 2008; Kim *et al*., 2017; O'Kell *et al*., 2017) that are similar to human disorders (Carrade and Borjesson, 2013; de Bakker *et al*., 2013; Hoffman and Dow, 2016) and could be treated using ASCs. However, before undertaking such treatments, safety tests using laboratory dogs should be performed. The results and knowledge of ASC therapy in dogs can be further used for human treatments.

The International Society for Cellular Therapy has proposed basic criteria that allow identifying MSCs (Dominici *et al*., 2006), and based on those we have previously characterised human ASCs (hASCs) (Bogdanova *et al*., 2014; Legzdina *et al*., 2016). In this study, the same criteria were used to assess canine ASCs (cASCs) in addition to establishing their safety after two intravenous administrations in a canine model. Here, the term 'safety' implies the evaluation of the risk-benefit ratio (Veriter *et al*., 2015), which was analysed in two stages. In the first stage, a pulmonary first-pass effect was assessed by evaluating blood and urine test results, electrocardiogram, echocardiogram and behaviour to rule out the risk of pulmonary thromboembolism. It is known that after intravenous administration of MSCs, they are initially trapped in the lungs (Fischer *et al*., 2009; Eggenhofer *et al*., 2012; Prologo *et al*., 2016). Intravenous infusion of ASCs is safe (Ra *et al*., 2011a; Ra *et al*., 2011b; Kang and Park, 2014), but cryopreserved or freshly thawed cells may cause a potential risk of pulmonary embolism, oedema, and even death (Furlani *et al*., 2009; Cyranoski, 2010; Jung *et al*., 2013; Tatsumi *et al*., 2013; Lysaght *et al*., 2017). It could be provoked by the aggregate formation in blood vessels as well as the response of the complement and immune system to infused ASCs (Eggenhofer *et al*., 2014; Moll and Le Blanc, 2015). In the second stage, necropsy of animals and subsequent histomorphological analysis were performed to detect late changes in tissues and exclude the risk of atypical tissue or tumour formation. After a pulmonary first-pass effect, ASCs tend to migrate to the sites of injury/inflammation (Anjos-Afonso *et al*., 2004; Bentzon *et al*., 2005; Kraitchman *et al*., 2005). However, there is not enough evidence showing that after homing to injured tissues ASCs do not show signs of malignisation or form uncharacteristic tissues at the homing site.

The aim of this study was to develop a specific ASC preparation methodology as well as characterise cASCs that were prepared using this methodology and to test their safety in a canine model after intravenous administration. Our methodology included several aspects: a) use of autologous serum (AS) during ASC expansion under hypoxic conditions (5% oxygen) and cryopreservation; b) exposure of ASCs to two freeze-thaw cycles before intravenous infusion; c) use of freshly thawed ASCs for *in vivo* administration; and d) autologous application of cultured ASCs.

MATERIALS AND METHODS

Legal permits for use of animals and cells in research. Animal experiments were done in accordance to standards outlined for ethical use of animals in research approved by the Food and Veterinary Service of the Ministry of Agriculture of the Republic of Latvia (permit No. 23). The dogs were kept and experiments were carried out at the Clinical Institute of the Latvian University of Agriculture, Jelgava, Latvia, by trained veterinary medical professionals. hASCs were isolated from human subcutaneous adipose tissue after consent was obtained from the donor in accordance with permit No. 12 issued by the Latvian Central Medical Ethics Committee. Processing of human and canine adipose tissue, ASC expansion, freezing, and storing took place at Stem Cell Technologies Ltd., Rīga, Latvia. Characterisation of ASCs was performed at the Latvian Biomedical Research and Study Centre, Rīga, Latvia.

Characterisation of experimental animals. Two Beagle dogs were studied, one female and one male. Neither of the animals had been sterilised/castrated. Both animals were obtained from a certified laboratory animal facility CEDS (France). The animals were 2.5 years old at the time of cASC administration and 5 years old at the time of euthanasia. The body weight at the time of cASC administration was 14.5 kg (female) and 18.5 kg (male). After euthanasia, the body weight was 17 kg (female) and 18.4 kg (male), the body condition was good (3.5 points for a female and 3 points for a male on a 5 point scale).

Animal care and nutrition during the experiments. The animals were kept in heated, insulated 2 × 1.5 m box rooms with ventilation. The animal facility had separate rooms for food preparation (kitchen), staff changing, shower, and toilet. All rooms were easy to disinfect and had a separate drainage system. Dry Complex Technical Feed was given twice daily, and fresh water was available continuously. Walking was provided three times daily. Physiological parameters (rectal temperature, respiratory rate, and heart rate) were controlled twice daily; mucous and subcutaneous lymph node examinations were done once daily.

Autologous serum (AS) preparation. Blood was collected as described in the section "Pulmonary first-pass effect" and allowed to clot for 1 h at room temperature. The serum was collected, centrifuged at 2000 rpm for 30 min, filtered through a 0.2 μm mesh, aliquoted, and stored at –20 ^{o}C.

ASC isolation, expansion, and characterisation. Collection of canine adipose tissue. The animals were premedicated by subcutaneous atropine sulphate injection (0.05 mg/kg) to reduce the anaesthetic side effects and intramuscular sedative injection (0.02 mg/kg acepromazine maleate).

Intravenous injection of ketamine hydrochloride (6 mg/kg) and diazepam (0.6 mg/kg) was administered for a temporary anaesthesia.

To prepare the skin for surgery, a 15 × 15 cm area of hair from the right caudoventral quadrant of abdominal wall was shaved, followed by washing with soap, disinfection with 70% alcohol three times and disinfection with iodine alcohol solution three times.

An incision 5 cm in length, parallel to the body's longitudinal axis (medial plane) 5–7 cm laterally from the white line was made in the skin layer. Subcutaneous fat was obtained by cutting an about 5 ml piece of tissue with scissors. After that sutures were placed in the subcutis (Safil, Aesculap, USA) and the skin (Supramid, S. Jackson, Inc., Unites States). Post-operative care of the animals consisted of continuous monitoring of the physiological parameters during the surgery and 2 h after the end of the anaesthetic effect as well as daily maintenance of the surgical wound until complete healing.

ASC extraction and expansion. The method of ASC isolation has been described previously for hASCs (Bogdanova *et al*., 2014; Legzdina *et al*., 2016). Briefly, 5 ml of the collected adipose tissue was scissored and treated with 0.3% pronase (EMD Millipore, USA) for 1 h at +37 ^{o}C and centrifuged for 7 min at 1000 rpm. The obtained cell pellet was suspended, filtered through a 40 μm mesh membrane, and centrifuged again for 5 minutes. Erythrocytes were lysed for 3 min at +37 ^{o}C using erythrocyte lysis buffer Hybri-Max (Sigma-Aldrich, Germany). The cell pellet was suspended in a fresh cell culture medium DMEM/F12 (Life Technologies, United Kingdom) containing 10% AS, 2 mM L-glutamine (Life Technologies, United Kingdom), 20 ng/ml basic fibroblast growth factor (BD, USA), and 100 U/ml: 100 g/ml penicillin–streptomycin (Life Technologies, United Kingdom) and seeded onto a 75 cm^2 tissue culture flask (regarded as passage 0 (P0)). At all steps, ASCs were cultured at +37 ^{o}C, 5% CO_2, and 5% O_2 in a hypoxic workstation (Xvivo System, Biospherix, USA).

Non-adherent cells were removed on the day after seeding by extensive washing with phosphate-buffered saline (PBS) (Life Technologies, United Kingdom). The remaining cells were cultured in a medium containing 10% AS for the first ten days and 5% AS thereafter. At the end of P1, the cells were frozen in DMEM/F12 supplemented with 10% dimethyl sulfoxide (DMSO) (Sigma-Aldrich, Germany) and 20% AS and stored in liquid nitrogen. After at least three months of storage, ASCs were thawed and cultured as previously through P2 to P5, freezing the propagated ASCs at the end of P5 for the second time. After at least three months of storage, ASCs from P5 were thawed and used for the subsequent characterisation.

Multicolour flow cytometry. Flow cytometry analysis of cASCs was performed using freshly thawed cells from P5 according to a conventional protocol (Shapiro and Shapiro, 2003). Briefly, the thawed cells were washed with PBS and resuspended at a concentration of 5×10^6 cells/ml. The cells were tested for viability using a 0.5 μM cell-permeant fluorescent Syto16 nucleic acid stain (Life Technologies, UK), separating live (positive) cells from apoptotic cell population on the FITC channel (Sparrow and Tippett, 2005). cASCs were further tested for aneuploidy and mitotic activity, using a PI-based Cycletest Plus DNA kit and the ModFit software (Becton-Dickinson, USA).

Two paired samples where used for phenotyping. The first sample was stained with antibodies to CD90 (APC, eBioscience, USA, clone YKIX337.217), CD44 (PerC-Cy5.5, Exbio, Czech Republic, clone IM7), CD73 (Pe-Cy7, eBioscience, USA, clone AD2), and CD34 (PE, Exbio, Czech Republic, clone 1H6) and an antibody cocktail to CD45 (FITC, eBioscience, USA, clone YKIX716.13), CD14 (FITC, eBioscience, USA, clone 61D3), and HLA-DR (FITC, eBioscience, USA, clone L243). The second sample was stained with corresponding isotypic control antibodies. The cells were incubated in the dark for 30 min, washed, resuspended in PBS, and analysed within two hours. The analysis was performed using a BD FacsCanto II flow cytometer (Becton Dickinson, USA) with standard 3-laser configuration; at least 10 000 events were acquired in each sample. The Infinicyt software (Cytognos S.L., Spain) was used for data analysis and image generation.

Trilineage differentiation of ASCs. Methods for *in vitro* adipo-, osteo- (Legzdina *et al*., 2016), and chondrogenic (Bogdanova *et al*., 2014) differentiation of ASCs using human ASCs have been described previously. In this study, we employed the same methods for cASCs, using hASCs as a control. Differentiation of ASCs was performed at P6 (after thawing the cells from P5 and seeding them).

Co-culture of cASCs and autologous PBMNCs (blast transformation). The method for blast transformation has been described previously (Bogdanova *et al*., 2014). Briefly, autologous peripheral blood mononuclear cells (PBMNCs) were obtained from freshly isolated peripheral blood samples using a Ficoll-Paque Premium density gradient (GE Healthcare, Uppsala, Sweden). PBMNCs were cultured in RPMI-1640 medium (Life Technologies, United Kingdom) supplemented with 10% AS, 2 mM L-glutamine and 100 U/ml : 100 g/ml penicillin–streptomycin in the presence of cASCs (P6) at different ratios (cASCs:PBMNCs — $5 \times 10^4 : 5 \times 10^4$ (1 : 1), $5 \times 10^3 : 5 \times 10^4$ (1 : 10), $2.5 \times 10^3 : 5 \times 10^4$ (1 : 20), $1.25 \times 10^3 : 5 \times 10^4$ (1 : 40), $5 \times 10^2 : 5 \times 10^4$ (1 : 100)) and phytohemagglutinin (Sigma-Aldrich, Germany) at a final concentration of 2 μg/ml for 96 h at +37 ^{o}C, 5% CO_2. Then 1 μCi of [3H]-deoxythymidine (GE, United Kingdom) was added to each well for the last 18 hours. Analysis of radioactive thymidine incorporation was done using a liquid scintilation beta counter (Beckman Coulter, USA).

Autologous cASC administration. Prior to cephalic vein catheterisation, premedication with an intramuscular injection of acepromazine maleate (0.5 mg/kg) for sedation of the animal was administered. The puncture area was pre-

pared as follows: a 5 × 5 cm area of the cephalic groove was shaved, and the skin was disinfected with 70% alcohol (3×) and iodine alcohol solution (1×). An aseptic puncture of the external cephalic vein with a G18 needle was performed, and a catheter was attached using leucoplast tape and a bandage.

First, to evaluate the potential side-effects of a DMSO (control medium) and to describe its excretion, 100 ml of physiological saline containing 10% DMSO was injected intravenously. Second, a therapeutic dose of 2×10^6 live, freshly thawed, non-washed autologous cASCs (P5) per kg of body weight in a total volume of 100 ml (adjusted with a physiological saline) was administered to the experimental dogs. Third, a five times higher dose of cASCs (1×10^7 live cells/kg) was intravenously injected one month later.

Pulmonary first-pass effect. Assessment of dogs' behaviour. In order to evaluate the dogs' behaviour, partial behavioural assessment tests were performed before and after intravenous administration of DMSO medium and cASCs. A sociability test was used to determine dog's behaviour in a room by evaluating body postures, sniffing, exploring, eye contact, and social contact with humans. A teeth exam was employed to test dog's response to teeth and mouth inspection for five seconds. A handling test was used to evaluate dog's response to touching and stroking of various body parts for five seconds, including the tail and the ears.

Blood and urine sample collection. To collect blood samples, the premedication and preparation of the puncture area were performed as described in section 2.6. A G16 needle was used and 50 ml (but no more than 0.5% of body weight) of blood was collected.

Urine and blood samples were collected 24 h before and 12, 24, and 72 h after the infusion of DMSO medium as well as 24 h before and 24 h, 72 h, 7 days, and 14 days after the administration of cASCs. Blood samples were collected from *v. jugularis* or *v. saphena* into vacutainers with serum stabiliser (for biochemical tests), EDTA (for hematological and morphological characterisation) or sodium citrate (for determination of coagulation factors) (Becton Dickinson, USA). Morning urine mid-stream samples were collected, stored at +4 ^{o}C and examined up to 3 h after collection.

Determination of haematological, biochemical, and coagulation factors. Biochemical tests were performed with an Ortho Vitros DT60/DTEII/DTSC analyser (Ortho Clinical Diagnostics, USA) using a disposable slide colorimetric assay. Biochemical blood tests were also performed at the certified (accreditation certificate No. LATAK-M-43400-2011) company's "Centrālā laboratorija" Ltd. laboratory (Reg. No. 215/L 430-C) by standard laboratory protocols in compliance with LVS NE ISO 15189:2008 standard.

Blood haematological examinations were run automatically using a Nihon Kohden MEK 6318 K analyser (Nihon Kohden, Japan) and morphological examinations were performed by evaluating blood smears on a binocular microscope Omax at magnification of 40–2000× (Omax, South Korea).

Coagulation factors were determined one day before and one day after a single infusion of 10% DMSO as well as before both administrations of cASCs. Blood samples for coagulation factor determination were collected in tubes with 3.8% sodium citrate; plasma was centrifuged, frozen at –20 °C, and sent to the IDEXX Vet Med Laboratory (IDDEXX GmbH, Germany) for analyses. The following coagulation factors were tested: prothrombin time (PT), activated partial thromboplastin time (aPTT) and fibrinogen. Their normal values were: aPTT < 13.5 s; fibrinogen 1.2–2.9 g/l; prothrombin time seconds.

Urine samples were analysed by Combi-Screen Vet 11 Plus test strips (Analyticon, Germany), recording the result 60 s after application. Urine density was determined using a refractometer. Urine samples were centrifuged at 3500 rpm for 10 min, and urine sediments were examined for leukocytes, erythrocytes, epithelial cells, bacteria (number/HPF), crystals and cylinders (number/LPF) using a binocular microscope Omax at magnification of 40–2000×.

Cardiac monitoring. Electrocardiographic examination was performed 24 h before and 3, 7, and 14 days after both cASC infusions. Echocardiography was performed 24 h before and three days after the administrations of cASCs. Additionally, continuous Holter monitoring was performed 24 h prior to the administrations of cASCs as well as during the first 24 h after both cASC infusions.

Electrocardiographic examinations were performed with a BTL-08 apparatus (BTL Industries, Inc., USA) while the animals were sleeping on the right lateral side. Six leads (I, II, III, aVR, aVL, aVF) were obtained. Data were saved and processed using the BTL software (BTL Industries, Inc., USA). The electrocardiogram was used to analyse the heart rhythm: primary rhythm transmitter specified (sinoatrial node, sinus rhythm) and heart rate. The II-lead was used for P-QRS-T analysis.

Echocardiographic examinations were performed with an ultrasound scanner Philips HD-11 (Philips, the Netherlands) while the animals were sleeping on the right lateral side to obtain right-side parasternal proximal and transverse projections of the heart and on the left lateral side to obtain left-side parasternal apical projections. Standard measurements of the left ventricle in systole and diastole (M mode), visual assessment of the right ventricle and the atrium, left atrial and aortic measurements (in 2D mode), and dopplerographic examination with the determination of transmitral and transtricuspid blood flow (PW dopplerography) and aortic and pulmonary arterial blood flow (CW dopplerography) were performed.

For Holter monitoring, we used a Televet 100 system (Telvet, Germany), attaching electrodes to the animal's chest. Standard leads I, II, and III were obtained. The obtained data were analysed using Televet 100 software. The cardiac

rhythm was analysed from the electrocardiogram. The primary rhythm pacemaker (sinoatrial node), the average heart rate at each monitoring hour, and the maximum and minimum heart rates were determined.

Euthanasia, necropsy, and histological examination. The animals were sacrificed using euthanasia solution T-61 (0.3 ml/kg), which contained 200 mg embutramide, 50 mg mebezoniumiodide, and 5 mg tetracaine hydrochloride in 1 ml of the solution. The euthanasia solution was administered intravenously after intramuscular sedative injection (0.02 mg/kg acepromazine maleate) and intravenous injection of anaesthetic agents ketaminum (4 mg/kg) and diazepam (0.4 mg/kg).

Necropsy was done 30 min after euthanasia; bodies of dogs subjected to necropsies were in excellent post-mortem condition. No muscle stiffness or autolysis were observed. Hair, skin, and nails were clean. In the female dog, outer body orifices were clean and without excretions. In the male dog, anus was open, stained with dry feces; the rest of the outer orifices were clean and without excretions. The female dog had minor hypostasis on the right side.

Representative samples of animal tissues and organs were collected and fixed in 10% formalin (Sigma-Aldrich, Germany) for at least 24 h. Smaller sections were trimmed for embedding in paraffin. After tissue dehydration with ascending grades of ethanol, samples were embedded in paraffin and sectioned in 4 μm thickness. Obtained tissue sections were stained with haematoxylin and eosin and analysed using a microscope Nicon or Olympus BX51.

Statistical analysis. Comparison of means between different groups was performed using One-Way Analysis of Variance (ANOVA). Brown-Forsythe and Bartlett's tests were applied to study whether the collected data were normally distributed. Between-subjects and intra-subjects differences among groups were assessed with ordinary two-way ANOVA followed by a post-hoc test. In all cases, two-stage step-up method of Benjamin, Krieger, and Yekutieli was used as the post-hoc analysis. p values less than 0.05 were considered as statistically significant. Graphs, calculations, and statistical analyses of blast transformation data were obtained using GraphPad Prism software version 7.0 for Mac (GraphPad Software, USA). Results were represented as the mean ± SD.

RESULTS

***In vitro* characterization of cASCs.** Morphology of cASCs. Similarly to hASCs, isolated cASCs were plastic-adherent and exhibited typical spindle-shaped morphology. These characteristics of MSCs were affected neither by the use of a cell culture medium that contained AS instead of foetal bovine serum, nor cell culturing under 5% oxygen. cASCs preserved their fibroblast-like morphology until P6 and after two freeze-thaw cycles (Fig. 1).

Characterisation of cASC surface markers. Multicolour flow cytometry (Fig. 2) of both cell cultures demonstrated a phenotypically homogenous cASC population that was strongly positive for MSC markers CD44 and CD73, intermediately positive for CD90 and negative for hematopoietic stem cell marker CD34 and a cocktail of leukocyte lineage

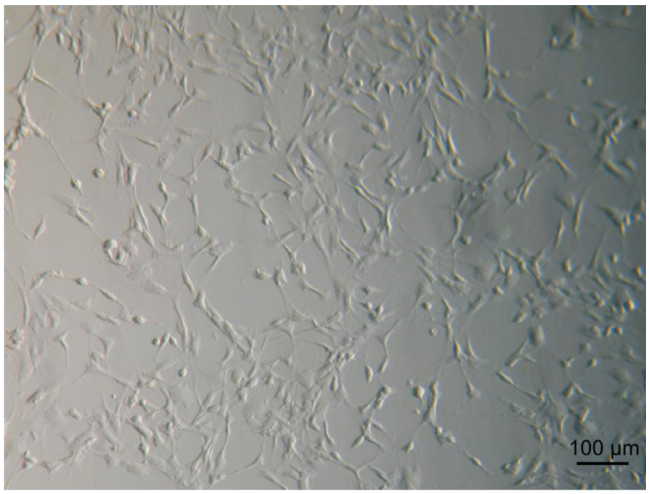

Fig. 1. Morphology of canine adipose-derived stem cells at passage 6. Scale bar 100 μm.

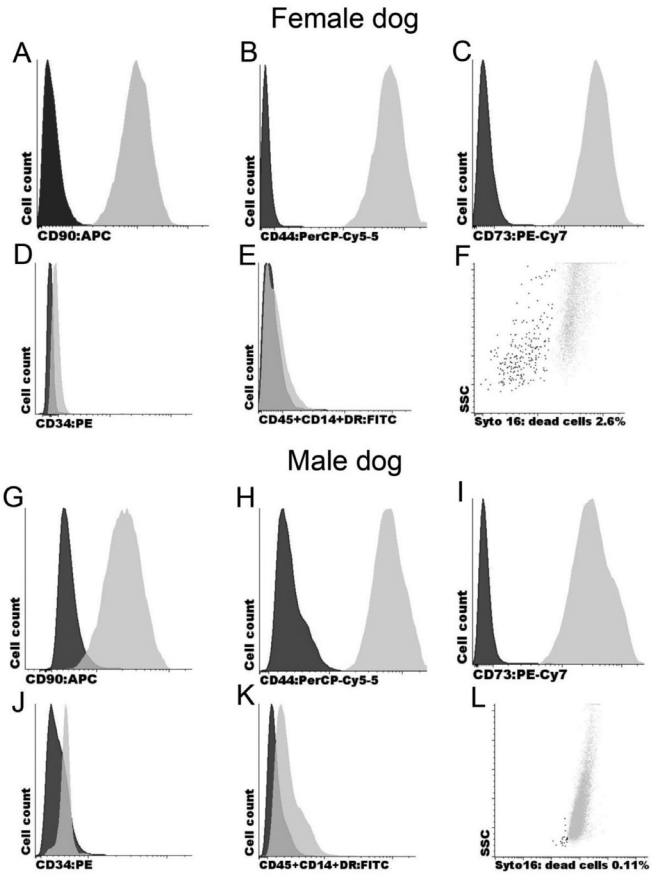

Fig. 2. Phenotypic analysis of freshly thawed canine adipose-derived stem cells at passage 5 using multicolour flow cytometry. (A–E, G–K) Expression of cell surface markers CD90, CD44, CD73, CD34, CD45, CD14, and HLA-DR (dark peak – isotype control, light peak – specific staining). (F, L) Syto 16 cell viability stain (dark dots – apoptotic cells, light dots – live cells).

antigens CD45, CD14, and HLA-DR, thus complying to MSC criteria (Dominici *et al*., 2006).

Syto16 staining showed that the proportion of apoptotic cells was below 5% in both samples (Fig. 2 F, L), indicating good cell viability. DNA staining detected no aneuploidy; the PI-defined proliferating fraction (S + G2) was 2.97% in the male dog and 6.91% in the female dog.

Trilineage differentiation of the ASCs. To assess *in vitro* differentiation potential of cASCs, the cells from P6 were differentiated toward adipogenic, chondrogenic, and osteogenic lineages. In parallel, hASCs, also from P6, were subjected to the same differentiation protocols serving as a positive control. The obtained results showed that both cASCs and hASCs possess similar chondrogenic and osteogenic differentiation potential. Alcian Blue staining of chondrogenic differentiation (Fig. 3 C, H, K) confirmed the presence of sulfated glycosaminoglycans, characteristic to the extracellular matrix of chondrocytes, and cartilage-like lacunae structures. Calcium deposits within mineralised extracellular matrix produced by differentiated osteoblasts were detected by Alizarin Red S staining of osteogenic differentiation (Fig. 3 E, I, L). Adipogenesis was assessed using the Oil Red O stain of adipogenic differentiation (Fig. 3 A, G, J). Although cASCs demonstrated the potential to differentiate into adipocytes, it was highly reduced compared to hASCs. Only a few cASCs showed accumulation of intracellular lipid droplets, despite their altered morphology. Both cASCs and hASCs exhibited no signs of adipogenic or osteogenic differentiation in control media, except for a faint blue staining observed in the chondrogenic control medium. As an example, only the results of cASCs in the control medium from the female dog are shown here (Fig. 3 B, D, F).

Immunosuppressive properties of cASCs. To test the effect of cASCs on PBMNC proliferation, cASCs were co-cultured with autologous, phytohemagglutinin (PHA)-stimulated PBMNCs. Non-stimulated PBMNCs served as a negative control, and PHA-stimulated PBMNCs were used as a positive control. cASCs demonstrated a statistically

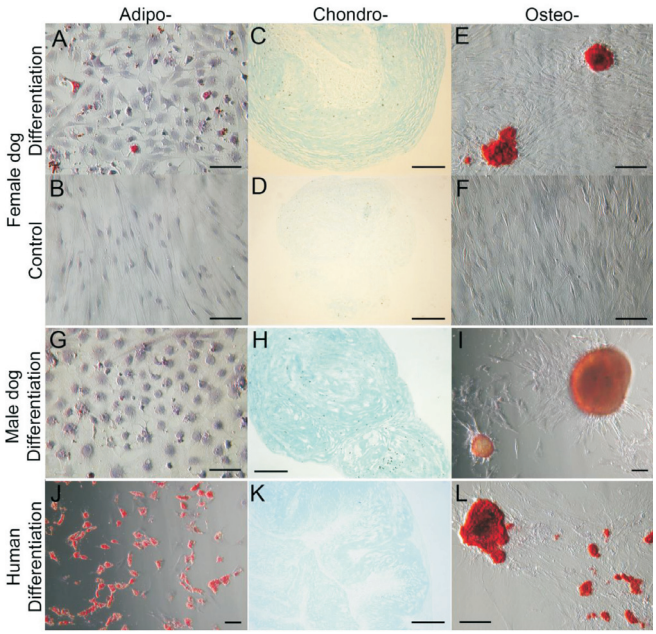

Fig. 3. In vitro differentiation of canine and human adipose-derived stem cells toward adipogenic, chondrogenic, and osteogenic lineages. (A, G, J, and B) Oil Red O staining of differentiated and control cells. The cells were counterstained with haematoxylin. (C, H, K, and D) Alcian Blue staining of differentiated and control cells. (E, F, L, and I) Alizarin Red S staining of differentiated and control cells. Scale bar 100 μm.

significant reduction of PBMNC proliferation when the cASC:PBMNC ratio reached 1 : 40 or less (Fig. 4 A). The observed immunosuppressive effect of cASCs was dose dependent, reaching its peak at cASC : PBMNC ratio 1 : 1. We found the same tendency in tests using hASCs (Bogdanova *et al*., 2014), and the regression analysis of cASC and hASC immunosuppressive ability confirmed their similarity (Fig. 4 B).

Evaluation of a pulmonary first-pass effect. Animal behaviour**.** Before and after intravenous administrations of cASCs as well as 10% DMSO solution, animal behaviour was evaluated to assess the pulmonary first-pass effect. The sociability test showed that both dogs remained calm with

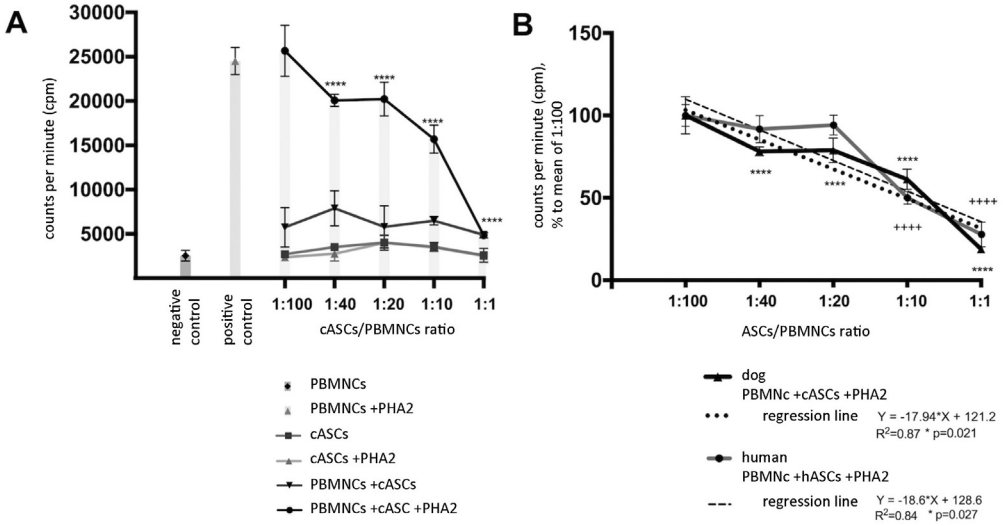

Fig. 4. Co-culture of adipose-derived stem cells (ASCs) and autologous peripheral blood mononuclear cells (PBMNCs). (A) The suppressive effect of canine ASCs (cASCs) from passage 6 on the proliferation of PHA-stimulated PBMNCs *in vitro*. The results are expressed as counts per minute. (B) Comparison of immunosuppressive ability of cASCs and human ASCs (hASCs). Data represent mean ± SD of triplicates. Asterisk indicates statistically significant difference when compared to the PHA-stimulated PBMNCs; ****$p < 0.0001$ (cASCs); ++++$p < 0.0001$ (hASCs); PHA2 – phytohemagglutinin at a final concentration of 2 μg/ml.

relaxed body postures. They sniffed and explored examination and procedure rooms and made an eye contact as well as calm social contact with humans. Both dogs allowed teeth examination for five seconds without struggle. Similarly, they did not avoid stroking and touching of various body parts, including the tail and the ears, for at least five seconds. Throughout the procedures, the animals remained calm, and the administrations of cASCs or DMSO did not provoke any changes in the above-mentioned animal behaviour.

Blood and urine tests. No significant alterations in the blood and urine test results were observed after 10% DMSO infusion.

Similarly, blood tests were normal after the administration of a therapeutic cASC dose (2×10^6 live cells/kg), except for total blood bilirubin level in the female dog which was 25 μmol/l (normal range is 0–10.20 μmol/l) 24 h after the cASC administration and 11 μmol/l three days after the cell infusion (Fig. 5). Urine tests showed that urine bilirubin and urobilinogen levels were elevated, bilirubin being rated as ++ (norm: +) and urobilinogen 140 μmol/l (norm: 3.5 μmol/l) 24 h after the cASC infusion in the female dog. The urine bilirubin levels remained slightly elevated also three and seven days after the cASC administration. The blood and urine bilirubin levels were normal at all time points in the male dog.

After the second administration of a five times higher cASC dose (1×10^7 live cells/kg) one month later, the blood and urine test results were normal, except for urine bilirubin levels which were elevated 24 h and three days after the cASC administration in the female dog.

Electrocardiography and echocardiography. Electrocardiographic and echocardiographic parameters did not show any deviations from the norm either before or after both cASC administrations. During the procedure, episodes of transient, supposedly stress-induced, sinus tachycardia were observed, which were detected mainly during the manipulation and animal fixation. In Holter monitoring (Fig. 6), we did not detect ectopic rhythm disturbances that could indicate myocardial damage.

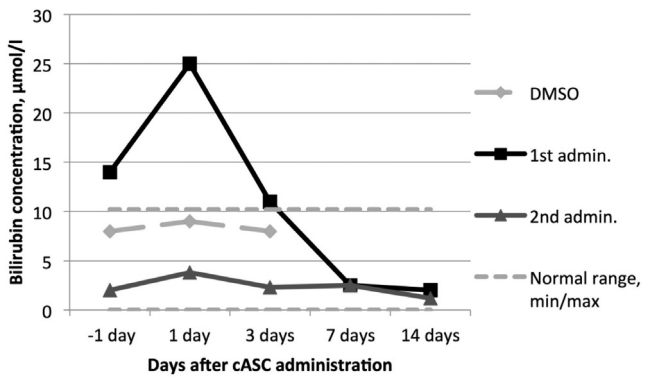

Fig. 5. Blood total bilirubin levels after intravenous administration of 10% dimethyl sulfoxide (DMSO), the therapeutic dose (2×10^6 live cells/kg) of canine adipose-derived stem cells (cASCs) (1st admin.), and the five times higher dose (2nd admin.) in the female dog.

Histomorphological findings. Histomorphological analysis of the animal organs and tissues more than two years after the cASC administration is described in detail and illustrated in Supplement (Appendix A). Briefly, only minor and relatively non-specific alterations were found in the tissues, and they might be unrelated to cASC administration. No significant side effects, undesirable events or signs of malignancy were detected.

DISCUSSION

Specifics of the ASC preparation methodology. In accordance with Article 28 of Regulation (EC) 1394/2007 on ATMPs (Anonymous, 2007), in cases of HEs, ATMPs (e.g., ASCs) are prepared on a non-routine basis and according to each manufacturer's specific methodology. In this case, "non-routine" is understood as an enhancement of ASC preparation process in real time and a target for personalised and risk-adapted treatment. An overview of our ASC preparation protocol is shown in Figure 7. Our methodology is designed to obtain ASCs that are processed and altered as little as possible, since they are cryopreserved after P1 and stored for personalised regenerative therapy in the future. When storing ASCs for future applications, it is crucial to freeze them at the earliest passage possible. Demand for the storage of young, healthy, non-aged stem cells is becoming more widespread, and the rapid development and improvement of cell processing technologies makes it possible to

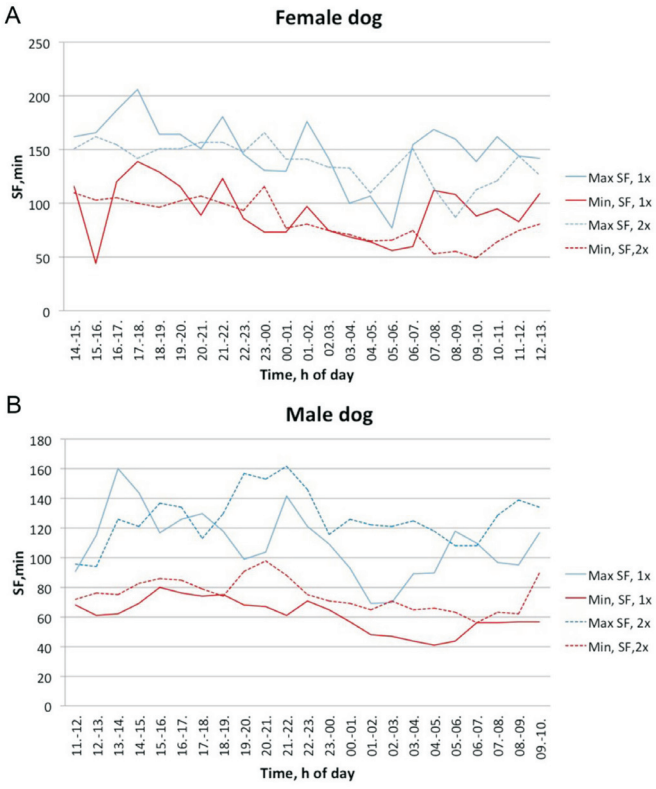

Fig. 6. Heart rate analysis during 24 h Holter monitoring after intravenous administration of the therapeutic dose (2×10^6 live cells/kg) of canine adipose-derived stem cells (1×) and the five times higher dose (2×). SF – systolic frame.

Fig. 7. Manufacturing process of donor-specific adipose-derived stem cells (ASCs). 1. Patient recruitment. 2. Acquisition of adipose tissue and isolation of ASCs. 3. Cryopreservation of ASCs after the first cell passage and their long-term storage. 4. Analysis of ASCs and personalized optimisation of cell culture conditions. 5. Thawing of cryopreserved ASCs and patient-specific ASC propagation based on individually optimised protocol. 6. The second freezing of ASCs prepared for therapy. 7. Additional analysis of propagated ASC batch. 8. Personalized ASC administration to the patient.

store small amounts of processed cells. Therefore, we have chosen to cryopreserve ASCs already after the P1.

Taking into account differences between donors and heterogeneity of stem cell subpopulations (Legzdina *et al*., 2016; Muzes and Sipos, 2016), resulting in donor-specific cell growth, it is highly important to employ a personalised and individually adapted protocol for ASC preparation. We introduce a novel approach for the propagation and examination of stem cells from different patients on a non-routine basis. We used ASCs from P2 to P5 for a personalised optimisation of cell culture conditions and media composition, which are tested between the first and the second freezing. This allows to identify the most suitable protocol for each individual, thus improving efficiency and safety of the cell product. Therefore, an individually optimised cell culturing protocol can be used for the preparation of a therapeutic ASC dose at the next step of production. In this study, we evaluated the standard method for ASC culturing, which included the use of autologous serum and hypoxic conditions (5% oxygen), and it will serve as a control method in the future for comparison to optimised cell culture conditions.

When optimal ASC culture conditions have been found for each individual, the cryopreserved cells can be thawed and effectively expanded if a clinical need for the patient emerges. After personalised ASC propagation, the cells are frozen again for the following reasons: a) additional time is needed to test the particular cell lot before administration; b) the planned time of the ASC therapy may be delayed; c) ASC expansion can be performed remotely if a specialised cell laboratory is not available at a medical institution. Such personalised methodology for ASC preparation offers a prospect for the treatment of conventional therapy-resistant diseases as well as improvement of quality of life at older age by using freshly thawed ASCs as a personalised off-the-shelf therapy, for example, in cases of myocardial infarction or stroke (Honmou *et al*., 2011; McIntosh *et al*., 2013). Our novel approach to enhance the preparation process of ASCs in real time goes beyond the standard manufacturing process and offers a personalised and risk-adapted treatment in compliance with good manufacturing practices.

Characteristics of cASCs. In this study we demonstrated that MSCs can be readily obtained from canine adipose tissue, and their characteristics are similar to hASCs. The results confirmed that cASCs exhibit characteristic spindle-shaped morphology, which has been observed previously (Neupane *et al*., 2008; Vieira *et al*., 2010; Martinello *et al*., 2011), and can be easily propagated *in vitro* using autologous serum in a cell growth medium. After five cell passages, they represented a phenotypically homogenous ASC population that was positive for typical MSC markers such as CD90, CD44 and CD73 but lacked the expression of CD34, CD45, CD14, and HLA class II. Comparable surface marker expression patterns of cASCs have been described previously (Vieira *et al*., 2010; Kisiel *et al*., 2012; Martinello *et al*., 2011; Reich *et al*., 2012; Russell *et al*., 2016; Takemitsu *et al*., 2012). Most of the previous studies have detected consistent expression of CD90 and CD44 in addition to other positive surface markers, but the expression of CD73 varies across the studies. While some reports have shown moderate CD73 expression (Russell *et al*., 2016), others have failed to detect it (Vieira *et al*., 2010; Takemitsu *et al*., 2012). Similarly, the majority of studies have found no expression of CD45 in cASCs, but mild expression of CD14 and CD34 has been detected (Vieira *et al*., 2010; Russell *et al*., 2016). This discrepancy could be explained by different harvest sites of adipose tissue (Sullivan *et al*., 2016) or variation in antibodies used for the analysis.

Similarly to hASCs, cASCs can differentiate toward chondrogenic, osteogenic, and adipogenic lineages, although their ability to differentiate into adipocytes was very low. The same tendency has been reported before (Vieira *et al*., 2010), but the optimisation of the induction protocol has improved adipogenic differentiation (Neupane *et al*., 2008). We have also tried to revise our differentiation protocol accordingly, but it failed to promote cASC differentiation into adipocytes (data not shown). Since cASC multilineage differentiation was performed at P6, this could also explain the weak adipogenic differentiation. Our previous studies using hASCs have shown a similar tendency. We have observed a decline in adipogenic and osteogenic differentiation potential in later hASC passages, and this characteristic was donor-specific (Bogdanova *et al*., 2014; Legzdina *et al*., 2016). It is possible that the same applies to cASCs.

Clinical interest in MSCs has been facilitated by their immunomodulatory abilities and inhibitory effect on T cell as well as B cell proliferation (Di Nicola *et al*., 2002; Le Blanc *et al*., 2003; Corcione *et al*., 2006). Our data from co-culture of cASCs and autologous PBMNCs demonstrated that cASCs suppress proliferation of PBMNCs in a dose-dependent manner, reaching the most effective reduc-

tion of PBMNC proliferation at a ratio 1 : 1, similarly to hASCs. Other studies have also shown immunosuppressive ability of cASCs (Kang *et al*., 2008; Russell *et al*., 2016), and this immunomodulatory effect is partially mediated by soluble factors (Kang *et al*., 2008). This immunosuppressive ability of ASCs may have a significant therapeutic potential in treating numerous immunological disorders both in humans and dogs.

Overall characteristics of cASCs verified their conformance to MSC criteria (Dominici *et al*., 2006) and showed their resemblance to hASCs.

***In vivo* safety of cASCs**. In order to increase the safety of ASCs, our methodology included the use of autologous serum instead of conventional foetal bovine serum during ASC expansion and cryopreservation. This helped to eliminate the risk of contamination with foreign proteins that could lead to a possible autoimmune reaction against a patient's own stem cells (Spees *et al*., 2004). Additionally, to increase the chances of survival of *in vitro* expanded MSCs after administration, it is important to minimise the differences between conditions in a cell culture and the site of implantation. Since virtually all cell cultures are maintained under atmospheric oxygen concentration (21%), but oxygen concentration in tissues can vary between 4–14% in the well irrigated organs and 0–4% in bone marrow (Ivanovic, 2009), implanted MSCs can encounter a massive hypoxic stress leading to apoptosis. Therefore, our methodology involves ASC expansion under 5% oxygen to provide an environment more similar to *in vivo* conditions and to minimise cell stress. Previous research has shown that MSCs cultured under hypoxic conditions display enhanced ability to repair infarcted myocardium due to the lower cell death and increased angiogenesis (Hu *et al*., 2008) and exhibit more rapid tissue regeneration potential (Leroux *et al*., 2010), enhanced wound-healing function (Rosova *et al*., 2008; Lee *et al*., 2009) as well as increased engraftment in vivo (Hung *et al*., 2007) when compared to the cells cultured under normoxic conditions. It has been demonstrated that culturing at reduced oxygen helps to maintain the multipotent and undifferentiated state of MSCs (Basciano *et al*., 2011) and can prevent proliferative senescence and increase their lifespan (Tsai *et al*., 2011).

In this study, freshly thawed cASCs from P5, cultured under hypoxic conditions in the presence of autologous serum and exposed to two freeze-thaw cycles, were intravenously administered to two Beagle dogs. At first, only a solution containing 10% DMSO, which is found in a cell freezing medium, was intravenously injected to test its potential side-effects followed by a therapeutic dose of cASCs and a five times higher dose of cells one month later. DMSO has a half-life of 9 h after intravenous administration, and it is excreted as dimethylsulphide (DMS) via the kidneys, respiratory system, and bile duct system (Blythe *et al*., 1986). While the primary liver parameters were within normal range (ALAT, ASAT, LDH, alkaline phosphatase, total protein, and albumin) and blood count was normal, bilirubinaemia, bilirubinuria, and urobilinogenuria were found after cASC administration. This may be due to the effect of DMSO metabolism in which DMSO transforms into DMS affecting the bile duct system or individual differences in the bile duct excretion system. Alternatively, it may also be the result of a mild haemolysis after cASC injection. However, damage to hepatocytes can be excluded due to normal liver biochemistry. Blood coagulation factors were not affected and electrocardiogram, echocardiogram, and behavioural monitoring did not show any serious deviations. None of acute reactions expected after cASC administration, such as thrombosis, were detected. Therefore, the assessment of a pulmonary first-pass effect after cASC intravenous injection allowed to eliminate the risk of pulmonary thromboembolism and demonstrated the first stage safety of cASCs.

The second stage of cASC safety was evaluated two years later by histomorphological analysis of organs and tissues to detect late changes in tissues and exclude the possibility of cASC malignisation. The most significant changes were subcapsular and subpleural inflammation foci found in lungs and kidneys. In kidneys (female) and lungs (female and male), small granulomas with eosinophilic leukocytes were observed; therefore, their parasitic origin (including *Dirofilaria repens*) cannot be excluded, although the dogs were regularly dewormed. In one instance, a temporary presence of *Dirofilaria repens* in the microflora was observed in the Beagles, but the microfilariae disappeared after the treatment.

Enhanced hyperplasia of lymphoid tissues with a mild inflammation of intestines was detected in the intestinal tract of the male dog. Soft to liquid faeces were often clinically observed in that animal, but laboratory tests did not show either parasitic or bacterial pathogens, and it is likely to be considered a dog's individual response. Sensitivity to some feed ingredient also could not be excluded.

Focal segmental fibrosis was found in kidneys, and chronic inflammation was detected in urinary bladder, prostate, urethra, kidneys, and renal pelvis of the male dog. These changes may indicate a transient bacterial infection and often occur incidentally. Also, liver microgranulomas, sclerotic glomeruli in the kidneys (both dogs), minimal inflammation in the intestines and lymphoid tissue hyperplasia (female dog) are considered to be incidental finds that are often encountered in dog sections (Sato *et al*., 2012).

Changes in the thymus may be due to incomplete thymic involution, which is often observed in laboratory Beagles (Sato *et al*., 2012), or to hyperplasia of the thymus. Both could be seen rather often in non-experimental dogs. However, the possibility that thymus hyperplasia is associated with cASC injections could not be ruled out.

Overall, the changes in tissues found in both dogs are slight and relatively non-specific. It is difficult to judge whether any of them might be a result of cASC administration. Series of chronic changes were identified, and it is theoretically possible that some of them may be related to the intra-

venous injection of cASCs. However, part of the observed changes may be referred to as sporadic changes in laboratory Beagles used in toxicological studies (Sato *et al*., 2012).

Since humans and dogs share similar autoimmune diseases, e.g., rheumatoid arthritis, type 1 diabetes mellitus and dermatomyositis that could be treated using ASCs, ethically approved and naturally ill dogs could serve as ideal companion animal disease models in the future studies. It would allow to explore the therapeutic efficacy of ASCs without a need to induce the diseases artificially. ASCs could be also used for experimental treatment of dogs with such autoimmune diseases. Results obtained in canine models would provide essential information necessary for planning ASC therapy in humans.

CONCLUSION

This study showed that our specific methodology used for the preparation of ASCs and their subsequent administration protocol in a dog model are safe and do not raise any concerns about undesirable events or side effects. The safety of the methodology was especially evidenced by the ASC pulmonary first-pass effect test. Taking into account a plethora of similarities between dog and human biology, we propose that further applications of our methodology for canine disease treatment experiments might lead to a cure of analogous human diseases.

ACKNOWLEDGEMENTS

We appreciate valuable help and advice from Prof. Pauls Pumpēns, Prof. Aija Žilēviča, Prof. Alberts Auzāns, Diāna Legzdiņa, Rafaels Joffe, Zita Muižniece, Māra Vasiļevska, Jūlija Spela, Anna Veidemane, Agnis Zvaigzne, and Gulšena Eivazova during the study.

This work was supported by the grants No. 10.0014 and No. 09.1283 of the Latvian Council of Science.

CONFLICTS OF INTEREST

There are no conflicts of interest.

REFERENCES

Abdi, R., Fiorina, P., Adra, C. N., Atkinson, M., Sayegh, M. H. (2008). Immunomodulation by mesenchymal stem cells. *Diabetes,* **57**, 1759–1767.

Anjos-Afonso, F., Siapati, E. K., Bonnet, D. (2004). *In vivo* contribution of murine mesenchymal stem cells into multiple cell-types under minimal damage conditions. *J. Cell Sci.,* **117**, 5655–5664.

Anonymous (2007). No. 1394/2007 of the European Parliament and of the Council of 13 November 2007 on advanced therapy medicinal products and amending directive 2001/83/EC and regulation (EC) no 726/2004. *J. Eur. Union*, **324**, 121–137.

Anonymous (2014). Report from the commission to the European Parliament and the Council in accordance with article 25 of regulation (EC) no 1394/2007 of the European Parliament and of the Council on advanced therapy medicinal products and amending directive 2001/83/EC and regulation (EC) no 726/2004. Available from: https://publications.europa.eu/en/publication-detail/-/publication/2dc18b82-b6c8-11e3-86f9-01aa75ed71a1 (accessed 30.01.2018).

Anonymous (2015). General Secretariat of the Council to Delegations; Document number 15054/15: Personalised medicine for patients: Council conclusions. 07.12.2015. Available from: http://data.consilium.europa.eu/doc/document/ST-15054-2015-INIT/en/pdf (accessed 30.01.2018).

Basciano, L., Nemos, C., Foliguet, B., de Isla, N., de Carvalho, M., Tran, N., Dalloul, A. (2011). Long term culture of mesenchymal stem cells in hypoxia promotes a genetic program maintaining their undifferentiated and multipotent status. *BMC Cell Biol.,* **12**, 12.

Bentzon, J. F., Stenderup, K., Hansen, F. D., Schroder, H. D., Abdallah, B. M., Jensen, T. G., Kassem, M. (2005). Tissue distribution and engraftment of human mesenchymal stem cells immortalized by human telomerase reverse transcriptase gene. *Biochem. Biophys. Res. Comm.,* **330**, 633–640.

Blythe, L. L., Craig, A. M., Christensen, J. M., Appell, L. H., Slizeski, M. L. (1986). Pharmacokinetic disposition of dimethyl sulfoxide administered intravenously to horses. *Amer. J. Vet. Res.,* **47**, 1739–1743.

Bogdanova, A., Berzins, U., Nikulshin, S., Skrastina, D., Ezerta, A., Legzdina, D., Kozlovska, T. (2014). Characterization of human adipose-derived stem cells cultured in autologous serum after subsequent passaging and long term cryopreservation. *J. Stem Cells,* **9**, 135–148.

Carrade, D. D., Borjesson, D. L. (2013). Immunomodulation by mesenchymal stem cells in veterinary species. *Compar. Med.,* **63**, 207–217.

Corcione, A., Benvenuto, F., Ferretti, E., Giunti, D., Cappiello, V., Cazzanti, F., Risso, M., Gualandi, F., Mancardi, G. L., Pistoia, V., Uccelli, A. (2006). Human mesenchymal stem cells modulate B-cell functions. *Blood*, **107**, 367–372.

Cyranoski, D. (2010). Korean deaths spark inquiry. *Nature*, **468**, 485.

de Bakker, E., Van Ryssen, B., De Schauwer, C., Meyer, E. (2013). Canine mesenchymal stem cells: State of the art, perspectives as therapy for dogs and as a model for man. *Vet. Quart.*, **33**, 225–233.

De Jesus, M. M., Santiago, J. S., Trinidad, C. V., See, M. E., Semon, K. R., Fernandez, M. O., Jr., Chung, F. S. (2016). Autologous adipose-derived mesenchymal stromal cells for the treatment of *Psoriasis vulgaris* and psoriatic arthritis: A case report. *Cell Transplant.*, **25**, 2063–2069.

Desiderio, V., De Francesco, F., Schiraldi, C., De Rosa, A., La Gatta, A., Paino, F., d'Aquino, R., Ferraro, G. A., Tirino, V., Papaccio, G. (2013). Human Ng2+ adipose stem cells loaded *in vivo* on a new crosslinked hyaluronic acid-Lys scaffold fabricate a skeletal muscle tissue. *J. Cell. Physiol.*, **228**, 1762–1773.

Di Nicola, M., Carlo-Stella, C., Magni, M., Milanesi, M., Longoni, P. D., Matteucci, P., Grisanti, S., Gianni, A. M. (2002). Human bone marrow stromal cells suppress T-lymphocyte proliferation induced by cellular or nonspecific mitogenic stimuli. *Blood*, **99**, 3838–3843.

Dominici, M., Le Blanc, K., Mueller, I., Slaper-Cortenbach, I., Marini, F., Krause, D., Deans, R., Keating, A., Prockop, D., Horwitz, E. (2006). Minimal criteria for defining multipotent mesenchymal stromal cells. The International Society for Cellular Therapy position statement. *Cytotherapy*, **8**, 315-–317.

Eggenhofer, E., Benseler, V., Kroemer, A., Popp, F. C., Geissler, E. K., Schlitt, H. J., Baan, C. C., Dahlke, M. H., Hoogduijn, M. J. (2012). Mesenchymal stem cells are short-lived and do not migrate beyond the lungs after intravenous infusion. *Frontiers Immunol.*, **3**, 297.

Eggenhofer, E., Luk, F., Dahlke, M. H., Hoogduijn, M. J. (2014). The life and fate of mesenchymal stem cells. *Frontiers Immunol.*, **5**, 148.

Fang, B., Li, N., Song, Y., Li, J., Zhao, R. C., Ma, Y. (2009). Cotransplantation of haploidentical mesenchymal stem cells to enhance engraftment of hematopoietic stem cells and to reduce the risk of graft failure in two children with severe aplastic anemia. *Pediatric Transplant.*, **13**, 499–502.

Fang, B., Song, Y., Liao, L., Zhang, Y., Zhao, R. C. (2007). Favorable response to human adipose tissue-derived mesenchymal stem cells in ste-

roid-refractory acute graft-versus-host disease. *Transplant. Proc.*, **39**, 3358–3362.

Fischer, U. M., Harting, M. T., Jimenez, F., Monzon-Posadas, W. O., Xue, H., Savitz, S. I., Laine, G. A., Cox, C. S., Jr. (2009). Pulmonary passage is a major obstacle for intravenous stem cell delivery: The pulmonary first-pass effect. *Stem Cells Devel.*, **18**, 683–692.

Furlani, D., Ugurlucan, M., Ong, L., Bieback, K., Pittermann, E., Westien, I., Wang, W., Yerebakan, C., Li, W., Gaebel, R., Li, R. K., Vollmar, B., Steinhoff, G., Ma, N. (2009). Is the intravascular administration of mesenchymal stem cells safe? Mesenchymal stem cells and intravital microscopy. *Microvasc. Res.*, **77**, 370–376.

Ghannam, S., Bouffi, C., Djouad, F., Jorgensen, C., Noel, D. (2010). Immunosuppression by mesenchymal stem cells: Mechanisms and clinical applications. *Stem Cell Res. Ther.*, **1**, 2.

Hall, M. N., Rosenkrantz, W. S., Hong, J. H., Griffin, C. E., Mendelsohn, C. M. (2010). Evaluation of the potential use of adipose-derived mesenchymal stromal cells in the treatment of canine atopic dermatitis: A pilot study. *Vet. Ther. Res. Appl. Vet. Med.*, **11**, E1–14.

Han, S. M., Kim, H. T., Kim, K. W., Jeon, K. O., Seo, K. W., Choi, E. W., Youn, H. Y. (2015). CTLA4 overexpressing adipose tissue-derived mesenchymal stem cell therapy in a dog with steroid-refractory pemphigus foliaceus. *BMC Vet. Res.*, **11**, 49.

Hoffman, A. M., Dow, S. W. (2016). Concise review: Stem cell trials using companion animal disease models. *Stem Cells* (Dayton, Ohio), **34**, 1709–1729.

Honmou, O., Houkin, K., Matsunaga, T., Niitsu, Y., Ishiai, S., Onodera, R., Waxman, S. G., Kocsis, J. D. (2011). Intravenous administration of auto serum-expanded autologous mesenchymal stem cells in stroke. *Brain*, **134**, 1790–1807.

Hu, X., Yu, S. P., Fraser, J. L., Lu, Z., Ogle, M. E., Wang, J. A., Wei, L. (2008). Transplantation of hypoxia-preconditioned mesenchymal stem cells improves infarcted heart function via enhanced survival of implanted cells and angiogenesis. *J. Thor. Cardiovasc. Surg.*, **135**, 799–808.

Hung, S. C., Pochampally, R. R., Hsu, S. C., Sanchez, C., Chen, S. C., Spees, J., Prockop, D. J. (2007). Short-term exposure of multipotent stromal cells to low oxygen increases their expression of CX3CR1 and CXCR4 and their engraftment *in vivo*. *PloS One*, **2**, e416.

Ivanovic, Z. (2009). Hypoxia or in situ normoxia: The stem cell paradigm. *J. Cell. Physiol.*, **219**, 271–275.

Jung, J. W., Kwon, M., Choi, J. C., Shin, J. W., Park, I. W., Choi, B. W., Kim, J. Y. (2013). Familial occurrence of pulmonary embolism after intravenous, adipose tissue-derived stem cell therapy. *Yonsei Med. J.,* **54**, 1293–1296.

Kang, J. W., Kang, K. S., Koo, H. C., Park, J. R., Choi, E. W., Park Y. H. (2008). Soluble factors-mediated immunomodulatory effects of canine adipose tissue-derived mesenchymal stem cells. *Stem Cells Devel.*, **17**, 681–694.

Kang, M. H., Park, H. M. (2014). Evaluation of adverse reactions in dogs following intravenous mesenchymal stem cell transplantation. *Acta Vet. Scand.*, **56**, 16.

Karagiannis, K., Proklou, A., Tsitoura, E., Lasithiotaki, I. (2017). Impaired mRNA expression of the migration related chemokine receptor CXCR4 in mesenchymal stem cells of COPD patients. *Int. J. Inflam.*, **2017**, 6089425.

Kim, M., Kim, D. I., Kim, E. K., Kim, C. W. (2017). CXCR4 overexpression in human adipose tissue-derived stem cells improves homing and engraftment in an animal limb ischemia model. *Cell Transplant.,* **26**, 191–204.

Kisiel, A. H., McDuffee, L. A., Masaoud, E., Bailey, T. R., Esparza Gonzalez, B. P., Nino-Fong, R. (2012). Isolation, characterization, and in vitro proliferation of canine mesenchymal stem cells derived from bone marrow, adipose tissue, muscle, and periosteum. *Amer. J. Vet. Res.*, **73**, 1305–1317.

Kraitchman, D. L., Tatsumi, M., Gilson, W. D., Ishimori, T., Kedziorek, D., Walczak, P., Segars, W. P., Chen, H. H., Fritzges, D., Izbudak, I., Young, R. G., Marcelino, M., Pittenger, M. F., Solaiyappan, M., Boston, R. C., Tsui, B. M., Wahl, R. L., Bulte, J. W. (2005). Dynamic imaging of allogeneic mesenchymal stem cells trafficking to myocardial infarction. *Circulation*, **112**, 1451–1461.

Le Blanc, K., Tammik, L., Sundberg, B., Haynesworth, S. E., Ringden, O. (2003). Mesenchymal stem cells inhibit and stimulate mixed lymphocyte cultures and mitogenic responses independently of the major histocompatibility complex. *Scand. J. Immunol.*, **57**, 11–20.

Lee, E. Y., Xia, Y., Kim, W. S., Kim, M. H., Kim, T. H., Kim, K. J., Park, B. S., Sung, J. H. (2009). Hypoxia-enhanced wound-healing function of adipose-derived stem cells: Increase in stem cell proliferation and up-regulation of VEGF and bFGF. *Wound Repair Regen.,* **17**, 540–547.

Legzdina, D., Romanauska, A., Nikulshin, S., Kozlovska, T., Berzins, U. (2016). Characterization of senescence of culture-expanded human adipose-derived mesenchymal stem cells. *Int. J. Stem Cells*, **9**, 124–136.

Leroux, L., Descamps, B., Tojais, N. F., Seguy, B., Oses, P., Moreau, C., Daret, D., Ivanovic, Z., Boiron, J. M., Lamaziere, J.M., Dufourcq, P., Couffinhal, T., Duplaa, C. (2010). Hypoxia preconditioned mesenchymal stem cells improve vascular and skeletal muscle fiber regeneration after ischemia through a Wnt4-dependent pathway. *Mol. Ther.,* **18**, 1545–1552.

Li, Q., Zhang, A., Tao, C., Li, X., Jin, P. (2013). The role of SDF-1-CXCR4/CXCR7 axis in biological behaviors of adipose tissue-derived mesenchymal stem cells *in vitro*. *Biochem. Biophys. Res. Comm.*, **441**, 675–680.

Lim, J. Y., Ra, J. C., Shin, I. S., Jang, Y. H., An, H. Y., Choi, J. S., Kim, W. C., Kim, Y. M. (2013). Systemic transplantation of human adipose tissue-derived mesenchymal stem cells for the regeneration of irradiation-induced salivary gland damage. *PloS One*, **8**, e71167.

Liu, H., Liu, S., Li, Y., Wang, X., Xue, W., Ge, G., Luo, X. (2012). The role of SDF-1-CXCR4/CXCR7 axis in the therapeutic effects of hypoxia-preconditioned mesenchymal stem cells for renal ischemia/reperfusion injury. *PloS One*, **7**, e34608.

Lo Sicco, C., Reverberi, D., Balbi, C., Ulivi, V., Principi, E., Pascucci, L., Becherini, P., Bosco, M. C., Varesio, L., Franzin, C., Pozzobon, M., Cancedda, R., Tasso, R. (2017). Mesenchymal stem cell-derived extracellular vesicles as mediators of anti-inflammatory effects: Endorsement of macrophage polarization. *Stem Cells Transl. Med.*, **6**, 1018–1028.

Lysaght, T., Lipworth, W., Hendl, T., Kerridge, I., Lee, T.L., Munsie, M., Waldby, C., Stewart, C. (2017). The deadly business of an unregulated global stem cell industry. *J. Med. Ethics*, **43** (11).

Martinello, T., Bronzini, I., Maccatrozzo, L., Mollo, A., Sampaolesi, M., Mascarello, F., Decaminada, M., Patruno, M. (2011). Canine adipose-derived-mesenchymal stem cells do not lose stem features after a long-term cryopreservation. *Res. Vet. Sci.,* **91**, 18–24.

McIntosh, K. R., Frazier, T., Rowan, B. G., Gimble, J. M. (2013). Evolution and future prospects of adipose-derived immunomodulatory cell therapeutics. *Expert Rev. Clin. Immunol.*, **9**, 175–184.

Moll, G., Le Blanc, K. (2015). Engineering more efficient multipotent mesenchymal stromal (stem) cells for systemic delivery as cellular therapy. *ISBT Science Series*, **10**, 357–365.

Muzes, G., Sipos, F. (2016). Heterogeneity of stem cells: A brief overview. *Meth. Mol. biol.* (Clifton, N.J.), **1516**, 1–12.

Neupane, M., Chang, C.C., Kiupel, M., Yuzbasiyan-Gurkan, V. (2008). Isolation and characterization of canine adipose-derived mesenchymal stem cells. *Tissue Eng. Part A*, **14**, 1007–1015.

O'Kell, A. L., Wasserfall, C., Catchpole, B., Davison, L. J., Hess, R. S., Kushner, J. A., Atkinson, M. A. (2017). Comparative pathogenesis of autoimmune diabetes in humans, NOD mice, and canines: Has a valuable animal model of Type 1 Diabetes been overlooked? *Diabetes*, **66**, 1443–1452.

Prologo, J. D., Hawkins, M., Gilliland, C., Chinnadurai, R., Harkey, P., Chadid, T., Lee, Z., Brewster, L. (2016). Interventional stem cell therapy. *Clin. Radiol.*, **71**, 307–311.

Ra, J. C., Kang, S. K., Shin, I. S., Park, H. G., Joo, S. A., Kim, J. G., Kang, B.-C., Lee, Y. S., Nakama, K., Piao, M. (2011a). Stem cell treatment for patients with autoimmune disease by systemic infusion of culture-expanded

autologous adipose tissue derived mesenchymal stem cells. *J. Translat. Med.*, **9**, 181.

Ra, J. C., Shin, I. S., Kim, S. H., Kang, S. K., Kang, B. C., Lee, H. Y., Kim, Y. J., Jo, J. Y., Yoon, E. J., Choi, H. J. (2011b). Safety of intravenous infusion of human adipose tissue-derived mesenchymal stem cells in animals and humans. *Stem Cells Devel.*, **20**, 1297–1308.

Reich, C. M., Raabe, O., Wenisch, S., Bridger, P. S., Kramer, M., Arnhold, S. (2012). Isolation, culture and chondrogenic differentiation of canine adipose tissue- and bone marrow-derived mesenchymal stem cells—a comparative study. *Vet. Res. Comm.*, **36**, 139–148.

Rosova, I., Dao, M., Capoccia, B., Link, D., Nolta, J. A. (2008) Hypoxic preconditioning results in increased motility and improved therapeutic potential of human mesenchymal stem cells. *Stem Cells* (Dayton, Ohio), **26**, 2173–2182.

Russell, K. A., Chow, N. H. C., Dukoff, D., Gibson, T. W. G., LaMarre, J., Betts, D. H., Koch, T. G. (2016). Characterization and immunomodulatory effects of canine adipose tissue- and bone marrow-derived mesenchymal stromal cells. *PLoS One*, **11**, e0167442.

Sato, J., Doi, T., Wako, Y., Hamamura, M., Kanno, T., Tsuchitani, M., Narama, I. (2012). Histopathology of incidental findings in beagles used in toxicity studies. *J. Toxicol. Pathol.*, **25**, 103–134.

Shapiro, H. M., Shapiro, H. M. (2003). *Practical Flow Cytometry*. *4th edn.* Wiley-Liss. 736 pp.

Sparrow, R. L., Tippett, E. (2005). Discrimination of live and early apoptotic mononuclear cells by the fluorescent SYTO 16 vital dye. *J. Immunol. Meth.*, **305**, 173–187.

Spees, J. L., Gregory, C. A., Singh, H., Tucker, H. A., Peister, A., Lynch, P. J., Hsu, S. C., Smith, J., Prockop, D. J. (2004). Internalized antigens must be removed to prepare hypoimmunogenic mesenchymal stem cells for cell and gene therapy. *Mol. Ther.,* **9**, 747–756.

Stepien, A., Dabrowska, N. L., Maciagowska, M., Macoch, R. P. (2016). Clinical application of autologous adipose stem cells in patients with multiple sclerosis: Preliminary results, *Mediators Inflamm.*, **2016**, 5302120.

Sullivan, M. O., Gordon-Evans, W. J., Fredericks, L. P., Kiefer, K., Conzemius, M. G., Griffon, D. J. (2016). Comparison of mesenchymal stem cell surface markers from bone marrow aspirates and adipose stromal vascular fraction sites. *Frontiers Vet. Sci*., **2**, **82**.

Takemitsu, H., Zhao, D., Yamamoto, I., Harada, Y., Michishita, M., Arai, T. (2012). Comparison of bone marrow and adipose tissue-derived canine mesenchymal stem cells. *BMC Vet. Res.*, **8**, 150.

Tatsumi, K., Ohashi, K., Matsubara, Y., Kohori, A., Ohno, T., Kakidachi, H., Horii, A., Kanegae, K., Utoh, R., Iwata, T., Okano, T. (2013). Tissue factor triggers procoagulation in transplanted mesenchymal stem cells leading to thromboembolism. *Biochem. Biophys. Res. Comm.*, **431**, 203–209.

Tsai, C. C., Chen, Y. J., Yew, T. L., Chen, L. L., Wang, J. Y., Chiu, C. H., Hung, S. C. (2011). Hypoxia inhibits senescence and maintains mesenchymal stem cell properties through down-regulation of E2A-p21 by HIF-TWIST. *Blood*, **117**, 459–469.

Tsuji, W., Rubin, J. P., Marra, K. G. (2014). Adipose-derived stem cells: Implications in tissue regeneration. *World J. Stem Cells*, **6**, 312–321.

Tyndall, A., Uccelli, A. (2009). Multipotent mesenchymal stromal cells for autoimmune diseases: Teaching new dogs old tricks. *Bone Marrow Transplantation*, **43**, 821–828.

Veriter, S., Andre, W., Aouassar, N., Poirel, H. A., Lafosse, A., Docquier, P. L., Dufrane, D. (2015). Human adipose-derived mesenchymal stem cells in Cell therapy: Safety and feasibility in different "Hospital Exemption" clinical applications. *PloS One*, **10**, e0139566.

Vieira, N. M., Brandalise, V., Zucconi, E., Secco, M., Strauss, B. E., Zatz, M. (2010). Isolation, characterization, and differentiation potential of canine adipose-derived stem cells. *Cell Transplant.*, **19**, 279–289.

Vives, J., Carmona, G. (2015). *Guide to Cell Therapy GxP: Quality Standards in the Development of Cell-Based Medicines in Non-pharmaceutical Environments*. Academic Press. 266 pp.

Zuk, P. A., Zhu, M., Ashjian, P., De Ugarte, D. A., Huang, J. I., Mizuno, H., Alfonso, Z. C., Fraser, J. K., Benhaim, P., Hedrick, M. H. (2002). Human adipose tissue is a source of multipotent stem cells. *Mol. Biol. Cell*, **13**, 4279–4295.

Zuk, P. A., Zhu, M., Mizuno, H., Huang, J., Futrell, J. W., Katz, A. J., Benhaim, P., Lorenz, H. P., Hedrick, M. H. (2001). Multilineage cells from human adipose tissue: implications for cell-based therapies. *Tissue Eng.*, **7**, 211–228.

Received 25 September 2017
Accepted in the final form 10 November 2017

NO SUŅU TAUKAUDIEM IZDALĪTO CILMES ŠŪNU RAKSTUROJUMS UN *IN VIVO* DROŠĪBA

Šis pētījums raksturo no suņa taukaudiem izdalītas cilmes šūnas (cASC) salīdzinājumā ar cilvēka ASCs (hASC) un pārbauda to drošumu pēc intravenozas ievadīšanas suņa modelī. cASC tika iegūtas no diviem suņiem un audzētas hipoksiskos apstākļos barotnē, kas saturēja autologo serumu. Tās bija vārpstveida šūnas, kas spēja piestiprināties pie plastmasas un ekspresēja tādus virsmas marķierus kā CD73, CD90 un CD44, bet neuzrādīja CD45, CD14, HLA-DR un CD34 ekspresiju. Šīs cASC diferencējās adipogēnajā, osteogēnajā un hondrogēnajā virzienā, taču to diferenciācija par adipocītiem bija vāja. Blasttransformācijas reakcija parādīja, ka cASC būtiski samazina T šūnu proliferāciju un šī spēja ir atkarīga no šūnu devas. Intravenoza šūnu iesaldēšanas barotnes, terapeitiskās cASC devas ($2x10^6$ dzīvas šūnas/kg) un piecas reizes lielākas cASC devas ievadīšana suņiem neradīja būtiskas blaknes. Audu histomorfoloģiskā analīze atklāja tikai nelielas un relatīvi nespecifiskas izmaiņas, un nekādas malignizācijas pazīmes netika novērotas. Iegūtie rezultāti liecina, ka cASC ir līdzīgas hASC un drošas terapeitiskam pielietojumam. Mūsu ieviestā metodoloģija ASC sagatavošanai ārpus rutīnas apstākļiem, kas iekļauj individuāli optimizētus šūnu audzēšanas apstākļus un piedāvā riskam piemērotu ārstēšanu, var tikt izmantota personalizētai, nekavējoties pieejamai terapijai nākotnē, piemēram, miokarda infarkta vai insulta gadījumā.

SUPPLEMENT

to the paper

CHARACTERISATION AND *IN VIVO* SAFETY OF CANINE ADIPOSE-DERIVED STEM CELLS

Uldis Bērziņš, Ilze Matise-VanHoutana, Ilze Pētersone, Ilmārs Dūrītis, Sergejs Ņikuļšins, Ance Bogdanova-Jātniece, Mārtins Kālis, Šimons Svirskis, Dace Skrastiņa, Agnese Ezerta, and Tatjana Kozlovska

doi: 10.2478/prolas-2018-0004

APPENDIX A. Results of histomorphological analysis

1. Gross and histomorphological examination of the female dog (Case 1)

1.1. Circulatory system

Gross description

Heart mass was 138.4 g, right ventricular wall – 0.4 cm, left ventricular wall – 1.3 cm, thickness of interventricular septum – 1.2 cm. Heart size was within the normal range. A small, smooth, nodular thickening was found on the edge of the left atrioventricular valve (minimal endocardiosis) (Figure 1.1 A).

Microscopic lesions

Mild histiocyte infiltrates were located focally between muscle fibers (Figure 1.1 B). No changes in the myocardial fibers were observed.

Diagnoses: Chronic minimal endocardiosis in the left atrioventricular valve; focal minimal interstitial histiocyte infiltration in the heart.

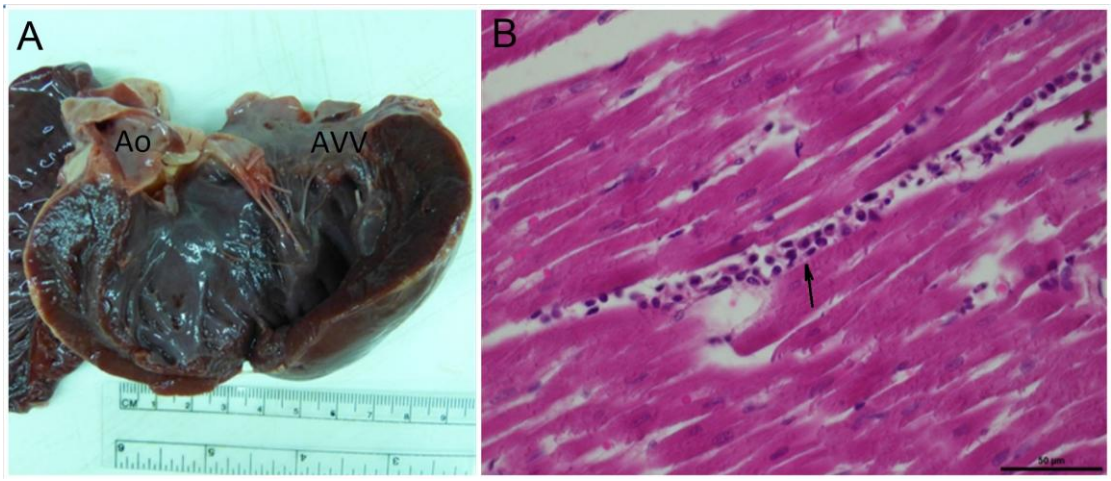

Figure 1.1. A – left ventricle of the heart (Ao – aorta; AVV – atrioventricular valve); B – myocardium of the left ventricle of the heart (HE staining, 400x), focal histiocyte infiltration (arrow) in the myocardium.

1.2. Respiratory system

Gross description

Larynx and trachea were within normal limits. Lungs were red, their caudal lobes were darker red (Figure 1.2 A). A large amount of foamy fluid (pulmonary edema) oozed from the cut surface. There were several small lymph nodes (3×0.4×0.3 cm and 2×0.5×0.5 cm) at the site of tracheal bifurcation (Figure 1.2 C).

Microscopic lesions

1.2.1. Lungs

A small number of mononuclear cells (including histiocytes) were located around multifocal medium sized blood vessels (veins). A similar focal, small cluster was observed also in the alveolar interstitial tissues. Alveoli were diffusely filled with eosinophilic edema fluid. Subpleurally, perivascular small mononuclear cell infiltration and focal pleural fibrosis were detected (Figure 1.2 B). Among the mononuclear cells there were lymphocytes, histiocytes and round cells with granular cytoplasm (Figure 1.2 D).

1.2.2. Tracheobronchial lymph node

The lymph node contained medium-sized lymphoid follicles, which were also present into the medulla. The medulla contained plasma cells, histiocytes, and lymphocytes. Macrophages with antracoid pigment were observed focally.

Diagnoses: Agonal edema in the lungs; perivascular, interstitial and subpleural minimal mononuclear cell infiltration in the lungs; mild chronic multifocal fibrosis in the pleura; mild hyperplasia with a mild anthracosis in the tracheobronchial lymph node.

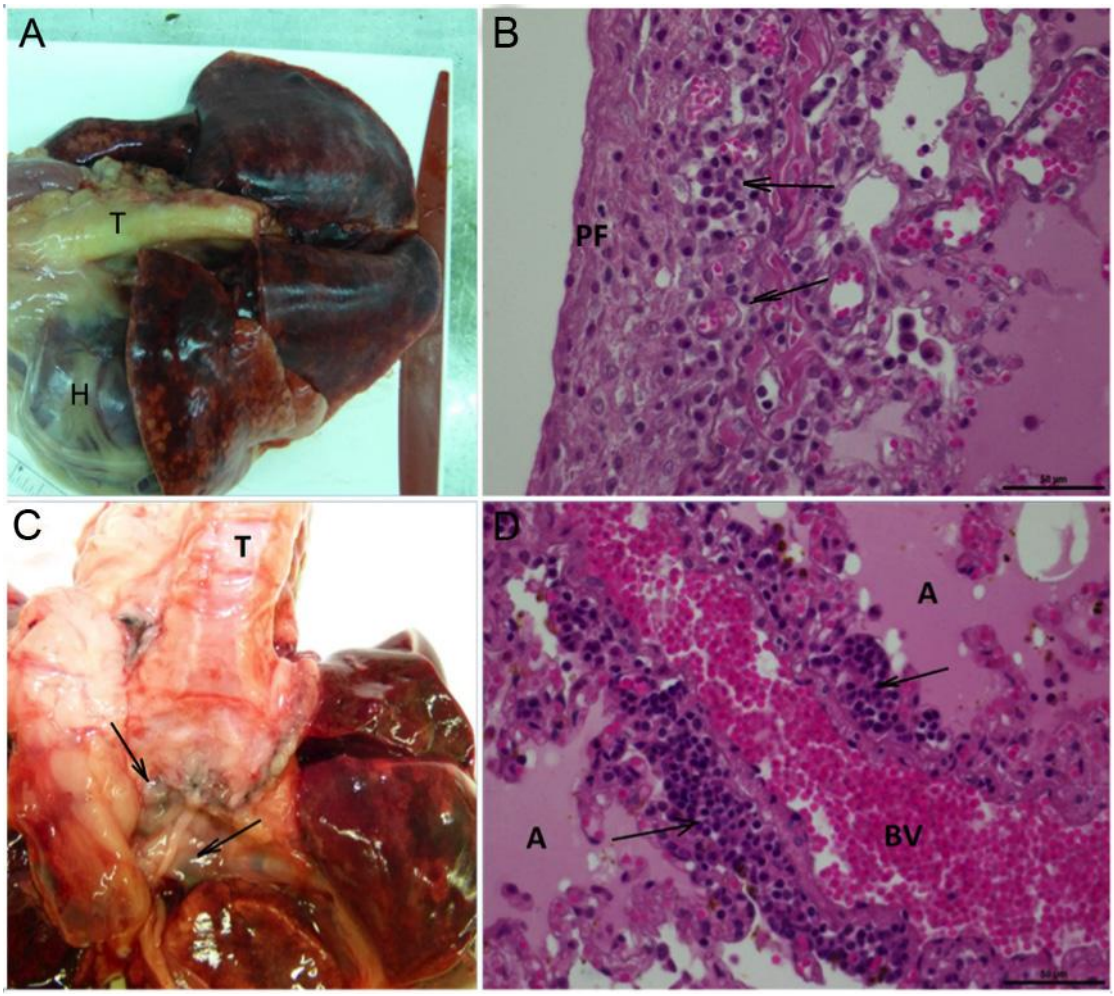

Figure 1.2. A – Lungs – congestion and pulmonary edema (T – trachea; H – heart); B – lungs (HE staining, 400×) – pleural fibrosis (PF) and subpleural mononuclear cell (arrows) infiltrates; C – lymph nodes (arrows) at the tracheal bifurcation site (T – trachea); D – lungs (HE staining, 400×) – perivascular mononuclear cell (arrows) infiltrate and alveolar edema (BV – blood vessel; A – alveoli filled with edema fluid).

1.3. Lymphatic system

Gross description

Spleen weight was 70.2 g. Nodular thickenings were found at the hilus of the spleen (Figure 1.3 A). On the parietal surface, two irregular scars (1 cm in diameter and 2×0.7 cm) were detected (Figure 1.3 B). Thymic tissue (7×3×0.7 cm, 12.2 g) was located near the heart. Bone marrow was lipid-rich, gray (femur).

Micropscopic lesions

1.3.1. Spleen

Minimal extramedullary hematopoiesis (megakaryocytes, granulocytes) was observed. Splenic capsule was focally thickened due to fibrosis and contained clusters of lymphoid cells (Figure 1.3 C).

1.3.2. Thymus

There were small remnants of thymic tissue surrounded by adipose tissue. Thymic tissues were composed of moderately cellular cortex and a less cellular medulla (Figure 1.3 D), in which a small number of thymic epithelial cells were observed (Figure 1.3 E).

1.3.3. Mediastinal lymph node

Subcapsular sinuses and the medulla of the lymph node contained medium to high numbers of siderophages admixed with small number of eosinophilic leukocytes. There were no lesions in the cortex; secondary lymphoid follicles were not apparent.

1.3.4. Bone marrow

Bone marrow was hypocellular (10–15%). M:E cell ratio was 3 : 1 (within the normal range). Megakaryocytes were not observed, which may be due to relative hypocellularity of the bone marrow.

Diagnoses: Minimal extramedullary hematopoiesis and focal capsular fibrosis in the spleen; mild thymic hyperplasia; mild eosinophilic lymphadenitis with hemosiderosis in the mediastinal lymph node.

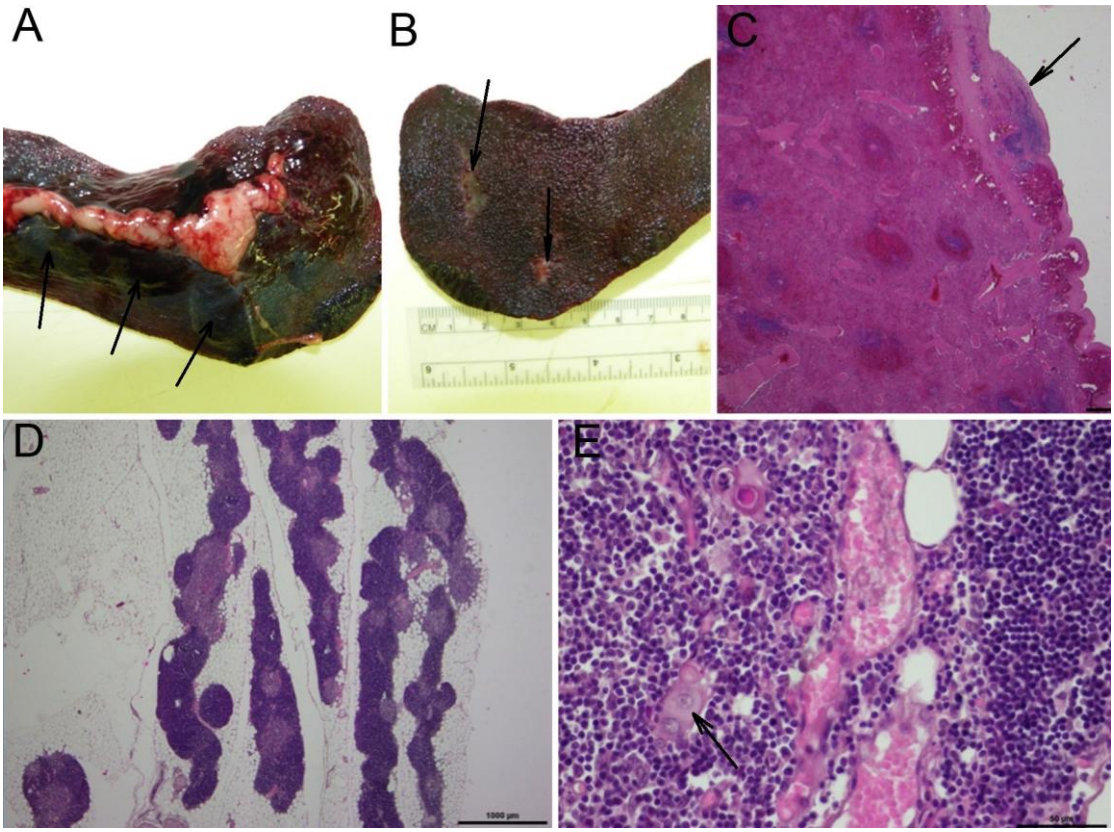

Figure 1.3. A – spleen – nodular thickenings (arrows) in the area of the hilus of spleen; B – spleen – multifocal areas of fibrosis (arrows) on the parietal surface; C –spleen (HE staining, 20×) – focal fibrosis (arrow) of the splenic capsule; D – thymus (HE staining, 20×) – tissue is composed of distinct cortex and medulla; E – thymus (HE staining, 400×) – thymic epithelial cells (arrow) are visible between the lymphocytes in the medulla.

1.4. Digestive system

Gross description

Gray plaques (dental calculus) were observed on the premolar and molar teeth. Gingival margin was mildly thickened (hyperplasia) (Figure 1.4 A). Stomach was filled with kibble (Figure 1.4 B). The fundic part of the gastric mucosa was purple–pink, the pyloric part – pink–gray. Contents of the small intestine were green, semiliquid and mucous; mucosa – light pink, covered with mucus (Figure 1.4 C). Contents of the colon were green, semiliquid; mucosa – pale pink (Figure 1.4 D). Liver weight was 896 g. Parietal surface of the right lateral lobe was slightly uneven and discolored, cut surface was denser than in other liver lobes (Figure 1.4 E, F).

Gallbladder was semi-filled with light yellow–greenish bile. Pancreas weight was 50.5 g. Peripancreatic lymph nodes were slightly enlarged (1×1.5×1 and 1.5×1×0.7 cm) and slightly edematous.

Microscopic lesions

1.4.1. Gastric mucosa of the fundus

There were several small infiltrates of lymphocytes and plasma cells in the basal aspect of the mucosa.

1.4.2. Gastric mucosa of the pyloric

There were several small lymphocyte infiltrates in the basal layer of the mucosa admixed with a eosinophils (Figure 1.4 G). Spiral bacteria were detected in the lumia of some.

1.4.3. Small intestine

In the basal layer of the mucosa, there were small numbers of lymphocytes and eosinophils and moderate numbers of plasma cells scattered below the crypts (Figure 1.4 H). A focal lymphoid nodule (gut-associated lymphoid tissue, GALT) was located in the *ileum* part of the intestinal mucosa.

1.4.4. Pancreas

Significant microscopic changes were not observed.

1.4.5. Peripancreatic lymph node

Lymphoid follicles were hyperplastic with prominent germinal centers (Figure 1.4 I). Large numbers of plasma cells and histiocytes were found in the medulla, with evidence of erythrophagocytosis.

1.4.6. Colon

Small numbers of plasma cells, lymphocytes, and eosinophils were scattered in the basal layer of the mucosa.

1.4.7. Liver

The capsular surface of the right lateral lobe was thickened with fibrous tissue, containing small biliary ductules and small numbers of lymphocytes and histiocytes as well as rare eosinophils (Figure 1.4 J). Lymphocytes and histiocytes were scattered in parenchyma, including centrilobular zones and portal areas (Figure 1.4 K). Multifocal dilatation in lymph vessels was observed adjacent to several central veins and portal areas. There was a moderate amount of glycogen in hepatocytse, and some of them contained a yellow pigment (lipofuscin). Less than 1% of hepatocytes contained intranuclear acidophilic inclusions. Fibrosis was not observed on the capsular surface of other lobes, but remaining lesions were similar, including clusters of mononuclear cells which formed small microgranulomas (Figure 1.4 L).

Diagnoses: Moderately severe, chronic dental calculus with gingival hyperplasia; minimal chronic lymphoplasmacytic and eosinophilic enteritis; capsular fibrosis and centrilobular and periportal lymph vessel dilatation in the right lateral lobe of the liver; multifocal, minimal microgranulomas and mild lymph vessel dilatation in all lobes of the liver; follicular, moderately severe peripancreatic lymph node hyperplasia.

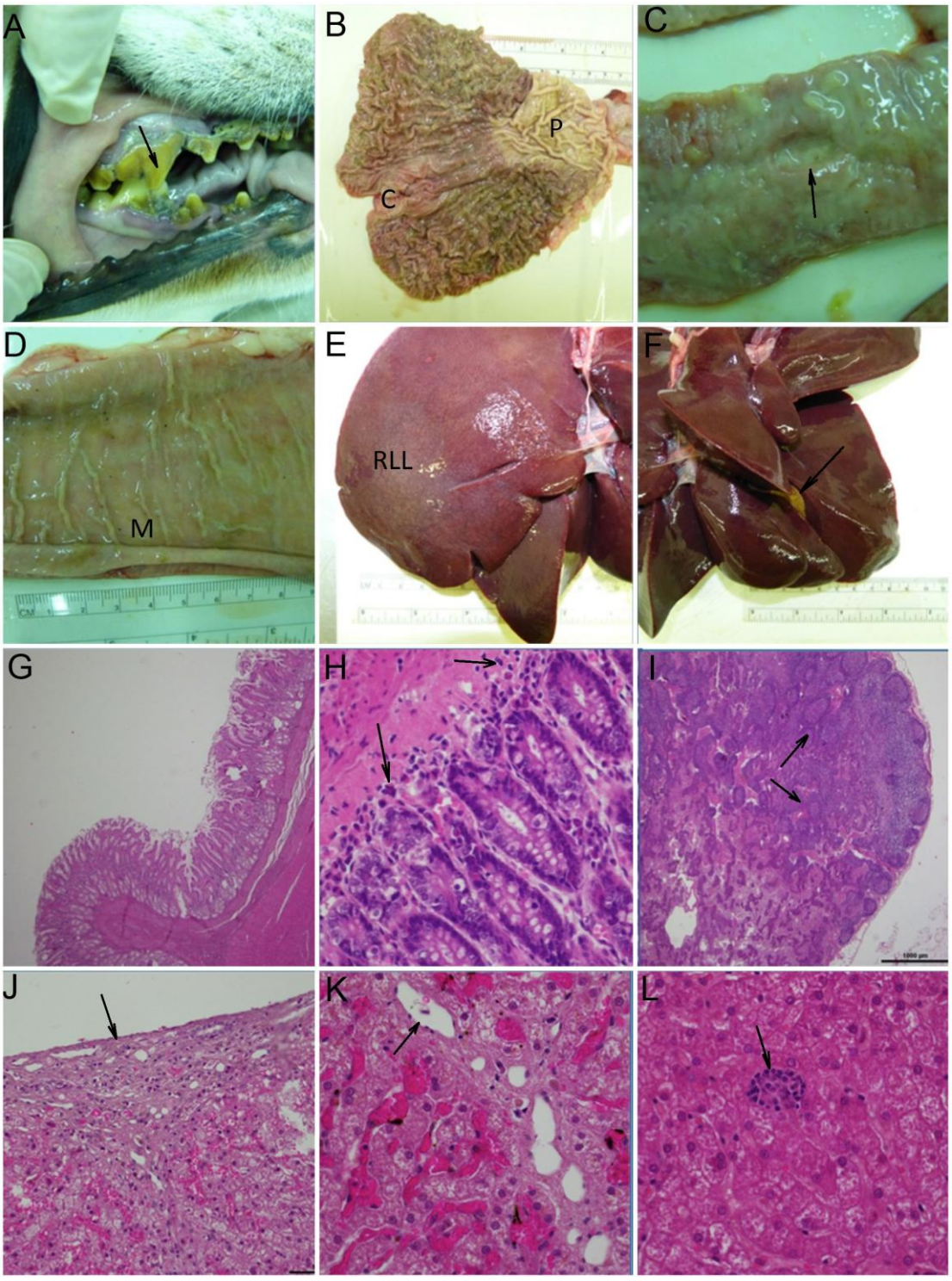

Figure 1.4. A – gums and teeth – dental calculus on the molar teeth (arrow); B – stomach (C – cardia; P – pylorus); C – small intestine with gut-associated lymphoid tissue (GALT, arrow); D – colon (M – mucosa); E – liver – right lateral lobe (RLL); F – liver – visceral surface (arrow – gall bladder); G – stomach, pyloric glands (HE staining, 20×); H - small intestine, *ileum* (HE staining, 400×) – small number of lymphocytes and plasma cells in the basal layer of the mucous membrane below crypts (arrows); I – peripancreatic lymph node (HE staining, 20×) – follicular hyperplasia (arrows); J – liver (HE staining, 200×) – capsular fibrosis (arrow); K – liver (HE staining, 400×) – central vein (arrow, near the capsular fibrosis area); L – liver (HE staining, 400×) – focal mononuclear cell cluster (microgranuloma, arrow).

1.5. Urinary system

Gross description

Right kidney weight – 53.8 g, left kidney – 55.8 g (Figure 1.5 A, B). On the capsular surface of the kidneys there were multiple (about 20) 1–2 mm, white foci extending into the subcapsular surface of the kidneys. The right kidney was more affected than the left one. Urinary bladder was filled with clear urine.

Microscopic lesions

1.5.1. Kidneys

Focal, subcapsular, medium-sized inflammation was observed (Figure 1.5 C), containing histiocytes, plasma cells, lymphocytes, and eosinophils (Figure 1.5 D, E). Approximately 1–5% of glomeruli had mild sclerotic changes – thickened Bowman's capsule, reduced glomerular tufts, thickened mesangium (Figure 1.5 G). Individual glomeruli also had increase in mesangial cells (Figure 1.5 H).

1.5.2. Urinary bladder

Significant microscopic changes were not observed.

Diagnoses: Interstitial multifocal granulomatous and eosinophilic chronic moderate nephritis; multifocal, minimal mezangioproliferative glomerulonephritis.

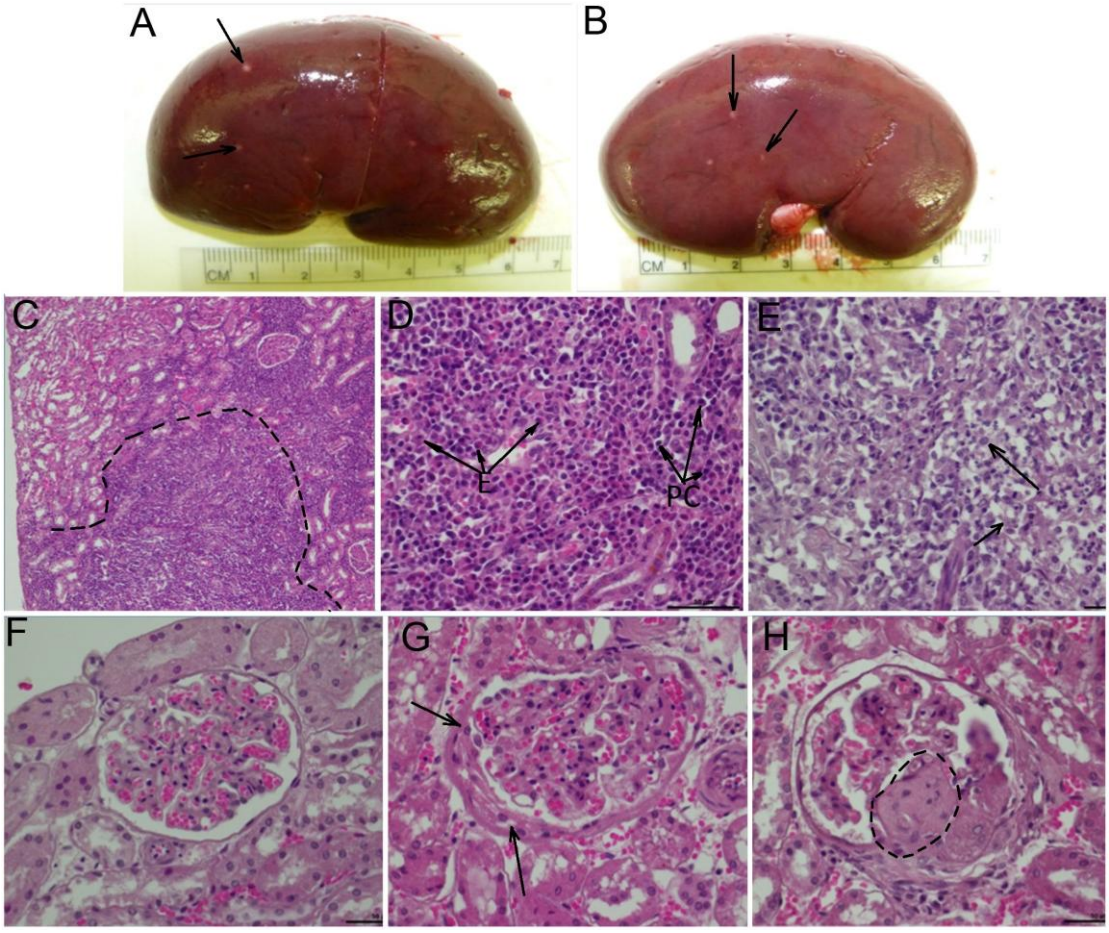

Figure 1.5. A, B – kidneys with small, pinpoint foci (arrows) on the capsule surface; C – kidney (HE staining, 100×) – subcapsular inflammation (dotted line); D – kidney (HE staining, 400×) – inflammation containing a large number of plasma cells (PC) and eosinophils (E); E – kidney (HE staining, 400×) – vacuolated macrophages (arrows) are observed within inflammation; F – kidney (HE staining, 400×) – normal glomerulus; G – kidney (HE staining, 400×) – glomerulus with a thickened Bowman's capsule (arrows); H – kidney (HE staining, 400×) – glomerulus with an expanded mesangium (dotted line).

1.6. Reproductive system

Gross description

Female genital organs were without significant changes.

Microscopic lesions

1.6.1. Ovaries

The ovaries contained several corpora lutea. In the cortex there were follicles at various stages of development. Ovarian structure was within normal limits.

1.6.2. Uterus

No significant microscopic lesions were observed. Smooth muscle layers were thin, compact; muscle fibers were of small diameter.

1.7. Endocrine system

Gross description

Adrenal glands. Right – 1.9 g, left –- 2.3 g, no significant changes.

Thyroid glands. Right – 0.5 g, left – 0.7 g.

Microscopic lesions

No significant microscopic lesions were observed in the adrenal cortex, thyroid gland, and parathyroid gland.

1.8. Nervous system

Gross description

Brain weight was 89.7 g. Mild thickening (fibrosis) was observed in the soft tissues of the meninges.

Microscopic lesions

Significant microscopic lesions were not observed.

1.9. Musculoskeletal system

No significant macroscopic or microscopic lesions were observed.

2. Gross and histomorphological examination of the male dog (Case 2)

2.1. Circulatory system

Gross description

Heart weight was 153.8 g, right ventricular wall – 0.6 cm, left ventricular wall – 1.4 cm, interventricular septum thickness – 1.2 cm. Heart shape was normal. Lumen of the left ventricle was slightly dilated (Figure 2.1).

Microscopic lesions

No significant microscopic changes were observed.

Diagnosis: Moderate left ventricular dilation of the heart.

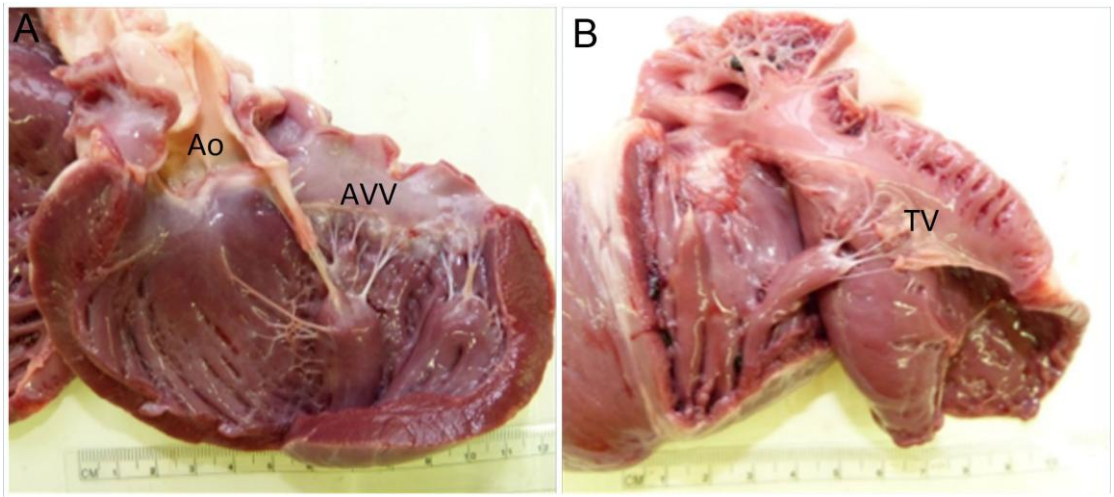

Figure 2.1. A – heart, lumen of the left ventricle is moderately enlarged (dilatation) (Ao – aorta; AVV – atrioventricular valve); B – the right ventricle of the heart (TV – tricuspid valve).

2.2. Respiratory system

Gross lesions

Larynx and trachea were within the normal limits. Lungs were purple–pink. There was focal atelectasis (0.5×5 cm) on the ventral surface of the right medial lobe (Figure 2.2 A, B). In the right caudal lobe, there were 4–5 small, dense nodules (0.3–0.5 cm in diameter). There were similar small nodules: one in the accessory lobe (0.3 cm in diameter) and three in the left caudal lobe (0.3–0.5 cm in diameter). In the left cranial lobe there was a small (0.2 cm in diameter) calcification focus. At the site of tracheal bifurcation there were bronchial lymph nodes (2×1×0.7 cm, on both sides) with a green–gray section edge surface.

Microscopic lesions

2.2.1. Lungs

In the lungs there was multifocal, in some areas extensive inflammation characterized by multifocal aggregates of histiocytes with areas of necrosis in the center (Figure 2.2 C, D, E). There were deposits of fibrin in the alveolar lumina. Fibrin deposits were partially organized, infiltrated with inflammatory cells – moderate numbers of plasma cells and eosinophils (Figure 2.2 F). There were perivascular infiltrates of lymphocytes and plasma cells both in the inflammatory foci and in other parts of the lung parenchyma (Figure 2.2 G). There were foci of atelectasis and small peribronchial anthracosis (Figure 2.2 H) observed multifocally (Figure 2.2 H).

2.2.2. Tracheobronchial lymph node

The lymph node was hyperplastic containing secondary lymphoid follicles extending into the medulla. Paracortical areas were expanded (Figure 2.2 I). There were histiocytes in subcapsular sinuses. Histiocytes and plasma cells were also detected in the medulla. Small foci of erythrophagocytosis were observed.

Diagnoses: Multifocal histiocytic and eosinophilic pneumonia with fibrin deposits in the lungs; moderate follicular and paracortical hyperplasia with erythrophagocytosis in the tracheobronchial lymph node.

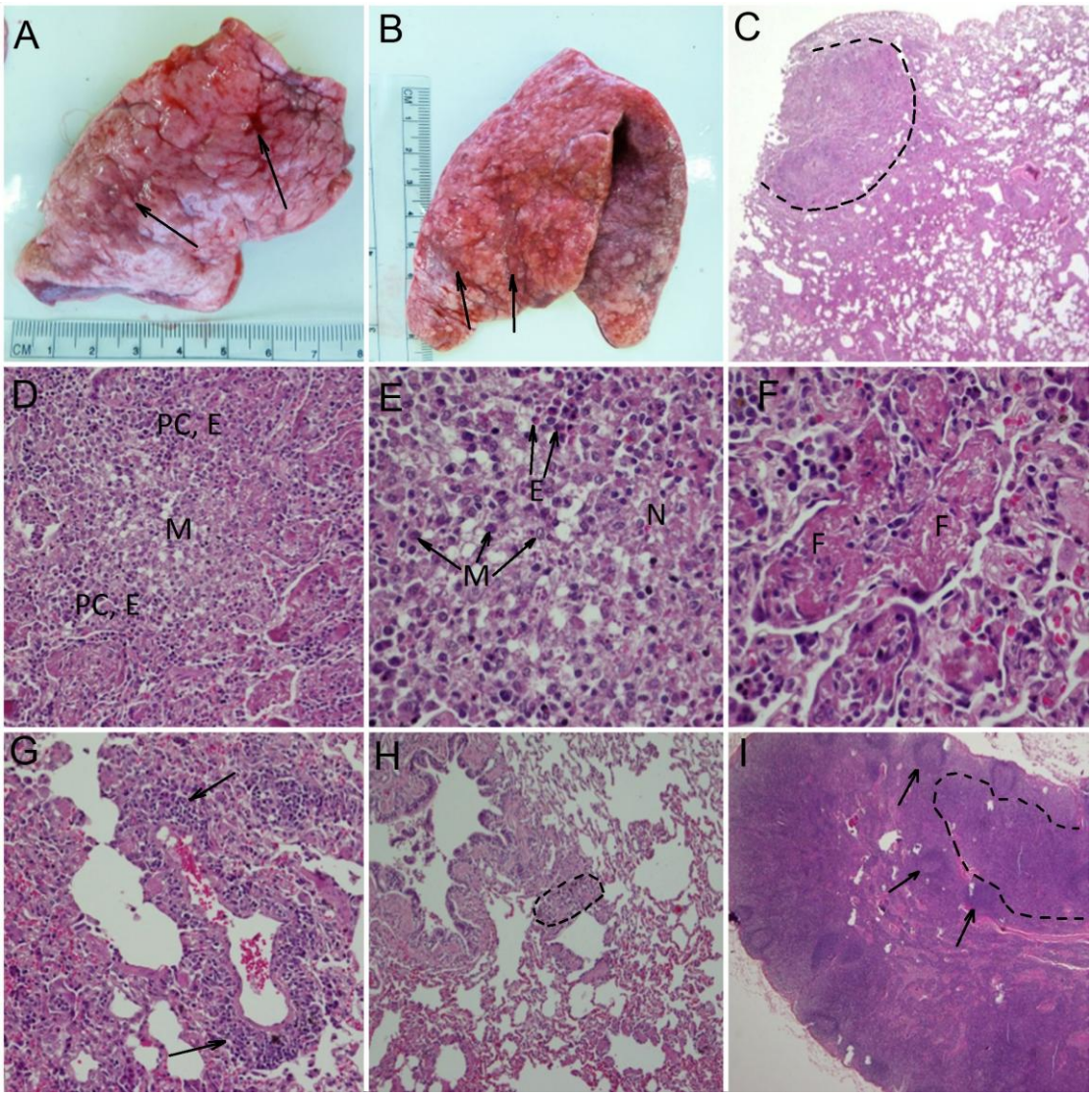

Figure 2.2. A – lungs with small foci of atelectasis (arrows); B – lungs with multifocal, small areas of atelectasis (arrows); C – lungs (HE staining, 20×) – focal subpleural inflammation (dotted line); D – lungs (HE staining, 200×) – subpleural inflammation with macrophages (M) in the center and plasma cells (PC) and eosinophils (E) at the periphery; E – lungs (HE staining, 400×) – an inflammation focus with macrophages (M) and necrosis (N) (E – eosinofils); F – lungs (HE staining, 400×) – deposits of intra-alveolar fibrin (F) (partially organized); G – lungs (HE staining, 200×) – perivascular mononuclear cell infiltrates (arrows); H – lungs (HE staining, 100×) – peribronchiolar anthracosis (dotted line); I – tracheobronchial lymph node (HE staining, 20×) – follicular (F – follicles) and paracortical (dotted line) hyperplasia.

2.3. Lymphatic system

Gross description

Spleen mass was 81.2 g. Cut surface of the spleen did not bulge; a small amount of blood oozed from the cut surface. Thymic tissue was found at the base of the heart (6×4×0.5 cm, weight × 13.9 g). Cervical lymph nodes were enlarged: right – 3×1.5×0.5 cm, left – 4.5×1.8×1 cm.

Microscopic lesions

2.3.1. Spleen

Minimal extramedullary hematopoiesis (megakaryocytes, metarubricytes) was observed (Figure 2.3 A).

2.3.2. Bone marrow

Bone marrow was normocellular (30%) (Figure 2.3 B). All hematopoietic cell lines were represented. M : E cell ratio was 2 : 1 (within the normal range). Small numbers (1–3%) of plasma cells were seen.

2.3.3. Thymus

Thymic lobules were moderately sized, surrounded by adipose tissues (Figure 2.3 C). Thymic lobules were composed of densely cellular cortex and less cellular medulla (Figure 2.3 D).

2.3.4. Cervical lymph node

The lymph node was hyperplastic and contained secondary lymphoid follicles which extended into the medulla (Figure 2.3 E). Paracortical areas were also expanded.

Diagnoses: Minimal extramedullary hematopoiesis in the spleen; moderate thymic hyperplasia; moderate follicular and paracortical hyperplasia in the cervical lymph nodes.

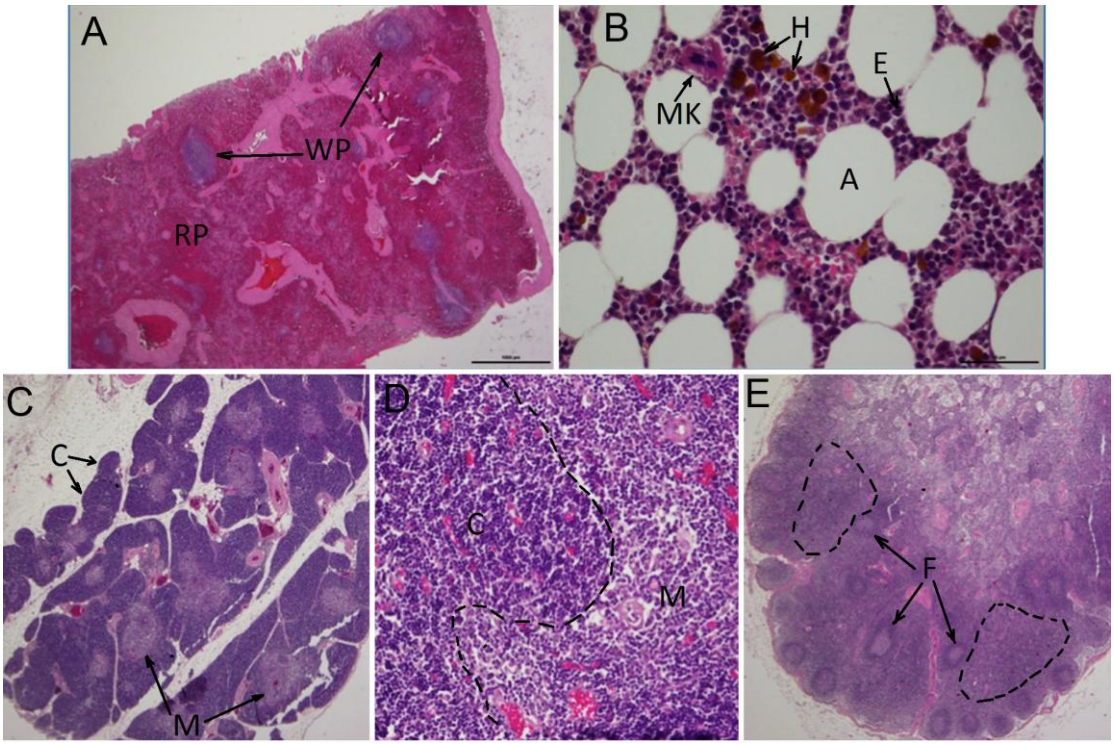

Figure 2.3. A – spleen (WP – white pulp; RP – red pulp) (HE staining, 20×); B – bone marrow (HE staining, 400×) – the photographed area is dominated by erythroid cell precursors (E) and hemosiderin deposits (H) (A – adipocytes; MK – megakariocyte); C – thymus (C – cortex; M – medulla) (HE staining, 20×); D – thymus (HE staining, 200×) – densely cellular cortex (C) and less cellular medulla (M); E – cervical lymph node (HE staining, 20×) – follicular (F – follicles) and paracortical (dotted line) hyperplasia.

2.4. Digestive system

Gross description

Gray plaques (dental calculus) were found on the premolar and, to a larger extent, molar teeth. Gingiva was mildly thickened (hyperplasia) (Figure 2.4 A, B). Tongue was cyanotic. Stomach was filled with kibble and grass stalks. The mucosa of fundus was purple–pink, the mucosa of pyloris – pink–gray; mucosal folds were slightly thickened (Figure 2.4 C). The proximal part of the small intestine contained small amount of yellow mucus (Figure 2.4. D), which turned into greenish, liquid contents in the proximal part of the *jejunum* and became thicker in the distal part of the

jejunum. Mucosa was slightly reddened, with thickened folds and adherent mucus. Throughout the small intestine, there were submucosal lymphoid tissue foci also apparent from serosal surface (Figure 2.4 E, F, G). These were well delineated, oval, gray–pink plaques (*jejunum* – 3–4 pcs., *ileum* – 2 pcs.: 7×1 cm and 5×1 cm). The colon was filled with large amount of liquid to paste-like, green contents. The distal part of the colon was very dilated. Mucosa was pale pink, with small mucosal folds (Figure 2.4 H). *Cecum* was filled with moderate amount, of green, paste-like contents; mucosa was gray–pink, with small folds. Numerous dense clusters of lymphoid tissue forming were seen in the colon (Figure 2.4 I). Liver weight was 1082 g. The parietal surface of the right lateral lobe was irregular and thickened with fibrous connective tissue. The cut surface whad increased density. Mucosa of the gallbladder was slightly uneven. Pancreas weight was 80 g. There were multiple small nodules (<10 pcs, 1 mm in diameter)scattered within parenchyma.

Microscopic lesions

2.4.1. Gastric mucosa of the fundus

There were several small infiltrates of lymphocytes in the basal aspect of the mucosa.

2.4.2. Gastric mucosa of the pyloris

There were several small lymphocyte infiltrates in the basal layer of the mucosa. Long, spiral-shaped bacteria were detected in the lumens of occasional gland.

2.4.3. Small intestine

In the ileum there were small to medium numbers of lymphocytes admixed with eosinophils scattered below the crypts (Figure 2.4 N). There is a small number of plasma cells scattered between crypts in the basal aspect of the mucosa (Figure 2.4 O). There were extensive lymphoid follicles (GALT) located in the submucosa of the *ileum*.

2.4.4. Colon

A small number of plasma cells were scattered in the basal aspect of the mucosa between the crypts. There are a small number of lymphocytes admixed with eosinophils scattered in the mucosa below the crypts. Occasionally, small GALT were found in submucosa. A small number of plasma cells were found in *cecum*, the basal aspect of the mucosa. Several expansile lymphoid tissue clusters (GALT) were located in submucosa (Figure 2.4 P, Q, R).

2.4.5. Liver

Capsular surface of the liver was thickened with fibrous tissue, containing profiles of small biliary ductules and small numbers of lymphocytes, histiocytes, and rare eosinophils (Figure 2.4 S). There are rare, small clusters of lymphocytes and histiocytes scattered randomly in in the liver, including centrilobularly and in portal zones (Figure 2.4 V). There was dilatation of lymph vessels around a few central veins and in a few portal zones (Figure 2.4 T). There was a moderate amount of glycogen in the hepatocytes, and some of them contained a yellow pigment (lipofuscin). There were intranuclear acidophilic inclusions in less than 1% of hepatocytes.

2.4.6. Gall bladder

Multifocal, medium-sized lympho-follicular infiltrates were observed in hyperplastic mucosa (Figure 2.4 W, X). Occasionally, there are mucus-filled cysts in the mucosa.

2.4.7. Pancreas

Significant microscopic changes were not observed.

2.4.8. Mesenteric lymph node

The lymph node was enlarged but with a normal structure (Figure 2.4 Y). The cortex contained lymphoid follicles, including secondary follicles with germinal centers.

There were plasma cells and histiocytes in medullary sinuses and foci of erythrophagocytosis.

Diagnoses: Moderately severe, chronic dental calculus with gingival hyperplasia; minimal, chronic, lymphocytic, and eosinophilic enteritis with GALT hyperplasia; minimal lymphoplasmacytic colitis with severe GALT hyperplasia; capsular fibrosis and centrilobular and periportal dilatation of lymphatics in the right lateral lobe of the liver; multifocal, minimal microgranulomas in all lobes of the liver; cystic hyperplasia and mild, chronic lymphoplasmacytic inflammation in the gall bladder; moderately severe hyperplasia in the mesenteric lymph node.

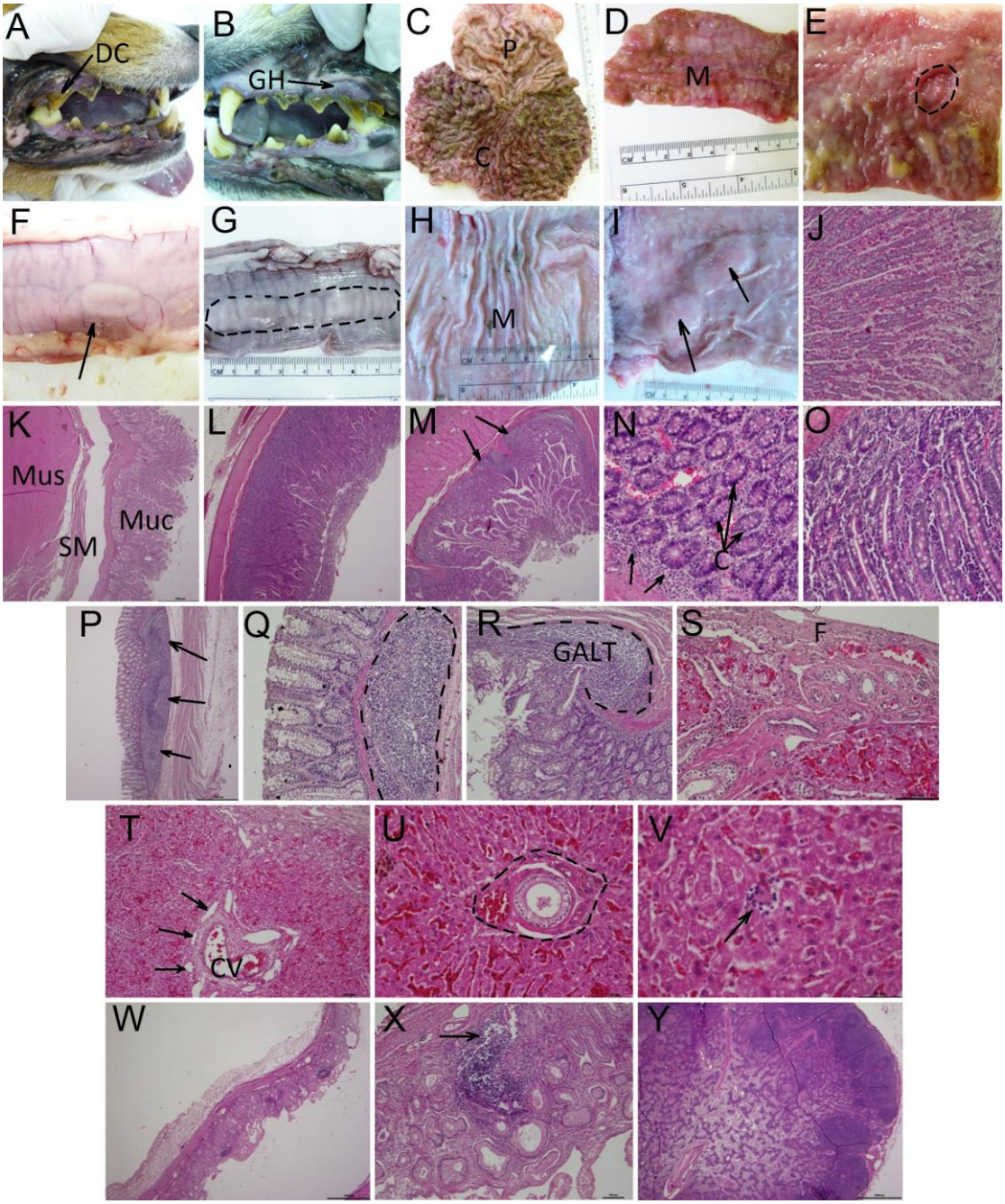

Figure 2.4. A, B – oral cavity, teeth, gums, dental calculus (DC) and gum hyperplasia (GH); C – stomach (mucosal surface) (P – pylorus; C – cardia); D – small intestine (M – mucosal surface); E – small intestine, mucosal surface with GALT (dotted line); F, G – small intestine (serosa; S – serosal surface) with a lymphoid tissue cluster (dotted line – GALT); H – colon (M – mucosal surface); I – colon (mucosal surface) with GALT (arrows); J – stomach, fundal gland mucosa (HE staining, 100×);

K – stomach, pyloric gland mucosa (Muc) (SM – submucosa; Mus – muscular layer) (HE staining, 20×); L - small intestine (HE staining, 20x); M – small intestine (HE staining, 20×) – multifocal lymphoid tissue (GALT – arrows) in the mucosa; N – small intestine (HE staining, 200×) – moderate numbers of lymphocytes and eosinophils (arrows) scattered below the crypts (C); O – small intestine (HE staining, 200×) – plasma cells are scattered in the lamina propria of mucosa; P – colon (HE staining, 20×) – there are prominent GALT clusters (arrows) in the submucosa; Q,R – colon (HE staining, 100×) – there are prominent GALT clusters (dotted line) in the submucosa; S – liver (HE staining, 200×) – subcapsular fibrosis (F), proliferation of small biliary ductules and inflammatory cell infiltrates; T – liver (HE staining, 100×) – dilated lymphatics (arrows) around the central vein (CV); U – liver (HE color, 200×) – portal triad (dotted line); V – liver (HE staining, 400×) – minimal mononuclear cell infiltrate (arrow); W – gall bladder (HE staining, 20×) – multifocal lymphofollicular aggregates scattered in the hyperplastic mucosa; X – gall bladder (HE staining, 100×) – multifocal lymphofollicular aggregates (arrow) scattered in the hyperplastic mucosa; Y – mesenteric lymph node (HE staining, 20×) – follicular and parafollicular hyperplasia.

2.5. Urinary system

Gross description

Right kidney weight – 80.2 g, left kidney – 84.6 g. There were multiple (eight on the right, six on the left) small, 1–2 mm, white pin-point foci extending into the subcapsular cortex of both kidneys (Figure 2.5 A, B). There was a focal depression d on the capsular surface of the right kidney; it was 2 mm wide, with gray tissue extending 1 cm into the cortex. Urinary bladder was moderately filled with clear urine.

Microscopic lesions

2.5.1. Kidneys

There were multifocal subcapsular medium-sized inflammatory foci composed of histiocytes, plasma cells, lymphocytes and eosinophils (Figure 2.5 C). In the center of inflammatory foci there were macrophages (Figure 2.5 D). Sclerotic changes were observed in 1–5% of glomeruli, especially around the inflammatory foci and near the corticomedullar junction. There were also small plasma and lymphocytic infiltrates around the arteries (Figure 2.5 E).

In the renal cortex of right kidney there was segmental fibrosis with loss of tubules, scattered lymphocytes, and infiltrates of plasma cells (Figure 2.5 F,G). Glomeruli had thickened capillary loops (Figure 2.5 J) and an increased numbers of mesangial cells (early sclerotic changes). An increase in the mesangial matrix in capillary loops was observed in a rare glomerulus (Figure 2.5 I). Moderately severe and rather extensive lymphoplasmic inflammation infiltrate was identified in submucosa of the renal pelvis (Figure 2.5 K,L).

2.5.2. Urinary bladder

There was lymphoplasmacytic inflammation in the mucosa of urinary bladder with occasional formation of lympho-follicular structures (Figure 2.5 M, N).

Diagnoses: Interstitial multifocal granulomatous and eosinophilic chronic, moderate nephritis with segmented fibrosis, loss of tubules and glomerular sclerosis; chronic moderately severe lymphoplasmacytic pyelitis; multifocal minimal mesangioproliferative glomerulonephritis; mild, chronic, lymphoplasmacitic cystitis.

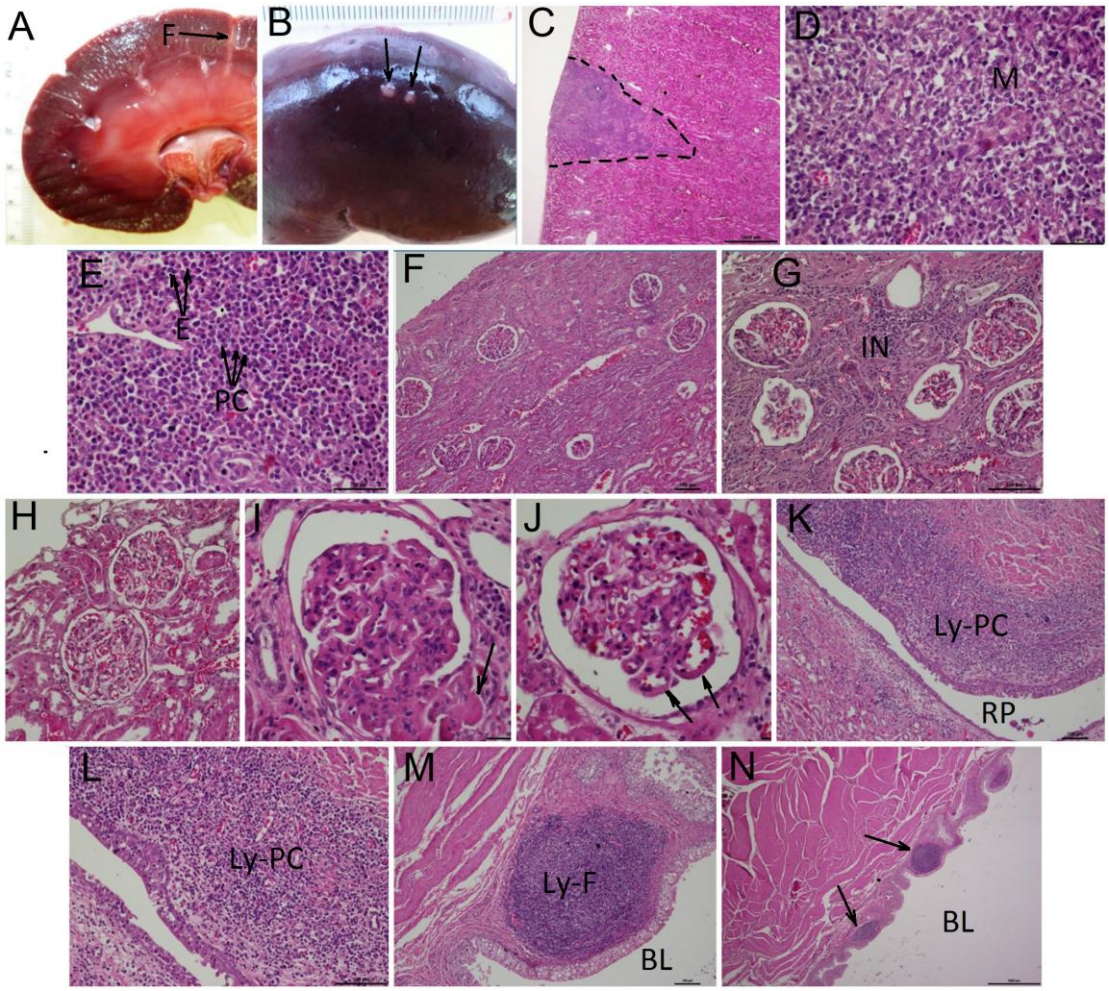

Figure 2.5. A – kidney, subcapsular nodule and focal segmental fibrosis (F); B – kidney, subcapsular nodules (arrows); C – kidney (HE staining, 20×) – subcapsular inflammation (dotted line); D – kidney (HE staining, 400×) – macrophages (M) in the center of the inflammation; E – kidney (HE staining, 400×) – plasma cells (PC) and eosinophils (E) in the periphery of the inflammation; F – kidney (HE staining, 100×) – segmental fibrosis; G –- kidney (HE staining, 200×) – chronic interstitial nephritis (IN) in the area of segmental fibrosis; H – kidney (HE staining, 400×) – glomeruli (within normal limits); I – kidney (HE staining, 400×) – an increased amount of mesangial matrix in the glomerulus (arrow); J – kidney (HE staining, 400×) – glomeruli (arrows) with thickened capillary loops; K – kidney (HE staining, 100×) – moderately severe lymphocyte and plasma cell infiltration (Ly-PC) in the renal pelvis (RP); L – kidney (HE staining, 200×) – moderately severe lymphocyte and plasma cell infiltration (Ly-PC) in the renal pelvis (RP); M – urinary bladder (HE staining, 200×) – lymphofollicular mononuclear cell cluster (Ly-F) in mucosa (BL – bladder lumen); N – urinary bladder (HE staining, 20×) – multifocal lymphofollicular mononuclear cell clusters (arrows) in the lamina propria of mucosa (BL – bladder lumen).

2.6. Reproductive system

Gross description

Male genital organs were without significant changes. Right testicle – 15.6 g, left testicle – 17.4 g.

Microscopic lesions

2.6.1. Prostate

In the prostate there were variably sized areas of multifocal lymphoplasmacytic inflammation surrounding prostatic tubules and acini partially effacing them (Figure 2.6 A, B). Some tubules were partially necrotic and there were neutrophils in their

lumina. Prostatic urethral inflammation was similar to that observed in the renal pelvis (Figure 2.6 C, D).

2.6.2. Testicles

There was spermiostasis with agglutinated spermatozoa and necrotic cells present in the lumen of several efferent ductules (Figure 2.6 E). There were low numbers of multinucleated cells and mild degeneration of Sertoli cells.

Diagnoses: Moderately severe chronic multifocal lymphoplasmacytic prostatitis; mild, chronic lymphoplasmacytic urethritis; mild, focal spermiostasis in the testicles.

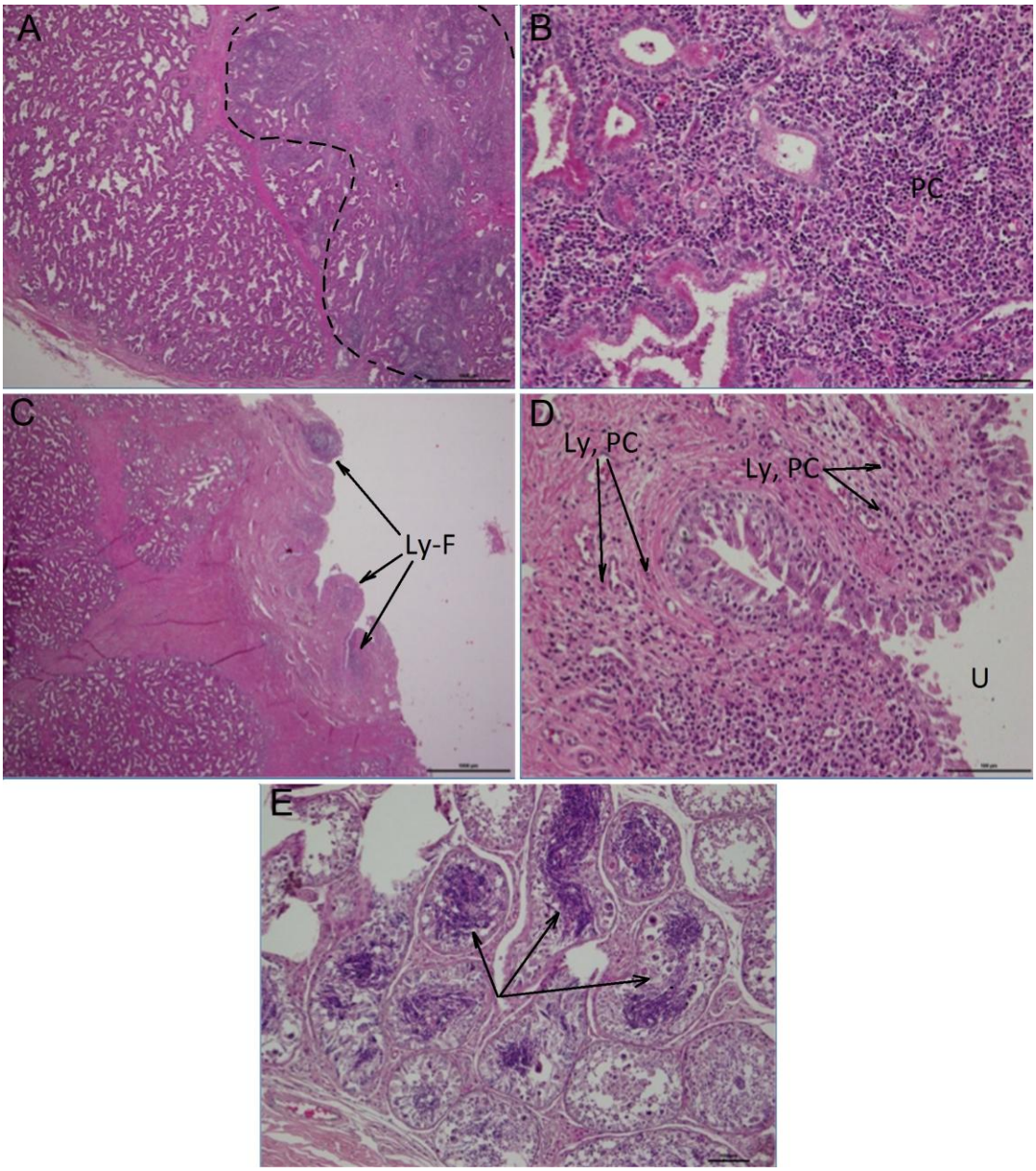

Figure 2.6. A – prostate (HE staining, 20x) – lymphoplasmacytic focally spreadind inflammation (dotted line); B – prostate (HE staining, 200×) – lymphoplasmacytic inflammation (PC – plasma cells); C – prostatic urethra (HE staining, 20×) – inflammation similar to the urinary bladder and renal pelvis (Ly-F – lymphofollicular inflammation); D – prostatic urethra (U) (HE staining, 200×) – inflammation similar to the urinary bladder and renal pelvis (Ly, PC – lymphocytes and plasma cells); E – testicle (HE staining, 100×) – spermiostasis in multifocal seminiferous tubules (arrows).

2.7. Endocrine system

Gross description

Adrenal gland. Right adrenal gland – 0.9 g, left – 1.2 g, without significant changes.
Thyroid gland. Right thyroid gland – 0.6 g, left – 0.6 g.

Microscopic lesions

2.7.1. Adrenal gland

There were no significant microscopic lesions. Thyroid gland. Moderate variability in follicular size was observed – multifocal follicles were reduced in diameter (Figure 2.7. A, B).

Diagnosis: Mild, multifocal follicular atrophy in the thyroid gland.

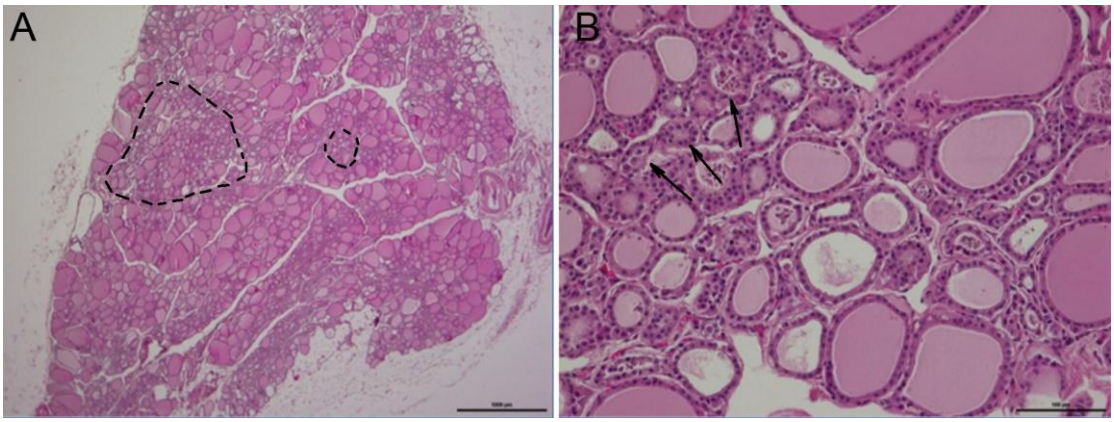

Figure 2.7. A – thyroid gland (HE staining, 20×) – multifocal follicles (dotted line) are reduced in size; B – thyroid gland (HE staining, 200×) – multifocal follicles (arrows) are reduced in size.

2.8. Nervous system

Gross description

Brain weight was 88.6 g. Mild thickening (fibrosis) was observed in the soft tissues of the meninges.

Microscopic lesions

Significant microscopic lesions were not observed.

2.9. Musculoskeletal system

Significant gross or microscopic lesions were not observed.

International Journal of Stem Cells Vol. 9, No. 1, 2016 http://dx.doi.org/10.15283/ijsc.2016.9.1.124

ORIGINAL ARTICLE

Characterization of Senescence of Culture-expanded Human Adipose-derived Mesenchymal Stem Cells

Diana Legzdina[1,*], Anete Romanauska[1,*], Sergey Nikulshin[2], Tatjana Kozlovska[1], Uldis Berzins[1]

[1]*Latvian Biomedical Research and Study Centre, Riga, Latvia,*
[2]*Children's Clinical University Hospital, Clinical Laboratory, Riga, Latvia*

Background and Objectives: Adipose-derived mesenchymal stem cells (ADSCs) are promising candidates in regenerative medicine. The need for *in vitro* propagation to obtain therapeutic quantities of the cells imposes a risk of impaired functionality due to cellular senescence. The aim of the study was to analyze *in vitro* senescence of previously cryopreserved human ADSCs subjected to serial passages in cell culture.
Methods and Results: ADSC cultures from 8 donors were cultivated until proliferation arrest was reached. A gradual decline of ADSC fitness was observed by altered cell morphology, loss of proliferative, clonogenic and differentiation abilities and increased β-galactosidase expression all of which occurred in a donor-specific manner. Relative telomere length (RTL) analysis revealed that only three tested cultures encountered replicative senescence. The presence of two ADSC subsets with significantly different RTL and cell size was discovered. The heterogeneity of ADSC cultures was supported by the intermittent nature of aging seen in tested samples.
Conclusions: We conclude that the onset of *in vitro* senescence of ADSCs is a strongly donor-specific process which is complicated by the intricate dynamics of cell subsets present in ADSC population. This complexity needs to be carefully considered when elaborating protocols for personalized cellular therapy.

Keywords: Human adipose-derived mesenchymal stem cells, Serial passage, Cell aging, Relative telomere length, Subpopulations, Heterogeneity

Introduction

Multipotent stem cells (MSCs) were isolated from adipose tissue for the first time by Zuk and colleagues in 2001 (1). Although MSCs can be found in a variety of tissues fat holds several advantages over others. The frequency of stem cells in fat is 500-fold higher compared to bone marrow (BM), a "golden standard" of adult stem cells (2). Evidence suggests superior proliferative activity of ADSCs over BM stem cells (3). In addition, the procedure of fat collection is relatively easy to perform and less burdensome for donor.

Senescence is metabolically active and stable state of cells both *in vitro* and *in vivo* characterized by irreversible cell proliferation arrest and dramatic changes in cell morphology, metabolism, gene expression and secretory phenotype (4).

In 1961, it was discovered that human fibroblasts possessed a limited proliferative capacity in culture, a phenomenon known as replicative senescence (5). DNA of telomeres, terminal structures of chromosomes, shortens during each S phase of cell cycle due to inability of DNA polymerase to complete the replication of lagging DNA

Accepted for publication November 6, 2015, Published online May 30, 2016
Correspondence to **Diana Legzdina**
Latvian Biomedical Research and Study Centre, Ratsupites Str.1 k-1, Riga, LV-1067, Latvia
Tel: +371 67808200, Fax: +371 67442407
E-mail: dianal@biomed.lu.lv
*These authors contributed equally to this work.

strand. Hence, telomere shortening acts as a mitotic clock which determines replicative senescence (6).

Premature senescence, on the other hand, is caused by factors other than critically short telomeres. Among them are the lack of nutrients and cell-to-cell contacts (7), UV radiation (8), reactive oxygen species (9), chemotherapy (10), altered chromatin structure (11), and oncogenes (12).

A variety of biomarkers is studied to characterize MSC senescence. Among them, the most popular ones are associated with morphological and proliferative changes (13), increased expression of senescence-associated β-galactosidase (SA-β-gal) (14), the loss of MSC trilineage differentiation potential (15), cell cycle arrest (16), epigenetic modifications (17), oxidative stress (18), telomere shortening and DNA damage (19), activation of tumor suppressors p53, RB1 and $p16^{INK4}$ (17, 20, 21). In addition, formation of senescence-associated heterochromatic foci (22) and promyelocytic leukemia protein bodies (23), as well as altered microRNA expression profile (24) have been observed.

A plenitude of clinical data gathered both from animal and human studies suggest broad clinical applicability of MSCs (25, 26). However, a single treatment protocol may require as many as 10～400 million cells to attain clinical significance. Therefore, pre-transplantation cultivation of MSCs is a prerequisite. For this reason, it is essential to study MSC *in vitro* senescence especially given the lack of standardised MSC expansion protocols among laboratories.

The aim of this work was to analyze *in vitro* senescence of human culture-expanded ADSCs. Previously frozen and long-term cryopreserved ADSC cultures from 8 donors were cultivated until proliferation arrest was reached. Cell senescence was characterized with respect to cell morphology, proliferative abilities, potential of adipo- and osteogenesis, SA-β-gal expression, metabolic activity, accumulation of intracellular peroxide, transcriptional activity (monitoring of 25 gene expression by reverse transcription polymerase chain reaction (RT-PCR)), as well as relative telomere length.

Materials and Methods

Cell source

ADSC cultures from eight donors were used in the study (Table 1). All cell cultures were retrieved from a cell bank where they were stored at passage 2 (P2) (except for cells from donor CS-5 which were stored at P3). ADSCs were isolated from human subcutaneous adipose tissue in accordance with The Latvian Central Medical Ethics Committee (permit No.12) after informed consent. Primary ADSCs cultures were cultivated in 5% autologous serum in hypoxic conditions (5% O_2) and prepared for storage (5×10^6 cells per ml) as described elsewhere (27).

Cell culture

After thawing, cells were counted in Bürker chamber and seeded on 75 cm^2 tissue culture flasks (～2×10^5 cells per flask) in DMEM/F12 medium containing 10% fetal bovine serum (FBS), 20 ng/ml basic fibroblast growth factor (bFGF), 2 mM L-glutamine and 100 μ/ml:100 μg/ml penicillin-streptomycin (all reagents were obtained from Life Technologies, Paisley, UK, except for bFGF – BD, Franklin Lakes, New Jersey, USA) and cultured in a humidified atmosphere at +37°C, 5% CO_2. Medium was replaced every third day. When ～80～90% confluency was reached cells were detached using cell dissociation reagent (TrypLE Express Enzyme, Life Technologies). A portion of cells were split at a ratio 1:5 for further subculturing. Remaining cells were frozen in DMEM/F12 medium containing 10% DMSO (Gaylord Chemical, Slidell, Louisiana, USA) and 20% FBS and stored in liquid nitrogen for later analysis. Passaging was continued maintaining the 1:5 split ratio until confluency could not be reached within

Table 1. Summary of adipose-derived mesenchymal stem cell cultures used in the study

Culture code	Donor age	Donor sex	Length of cryo-preservation, years	Initial passage	Last passage	Cumulative PDs
CS-1	61	Male	3	P3	P11	20.46
CS-2	57	Female	2.5	P3	P9	17.46
CS-3	63	Male	2	P3	P13	23.28
CS-4	43	Male	2	P3	P5	8.03
CS-5	47	Male	1.5	P4	P7	8.29
CS-6	38	Female	3	P3	P8	14.69
CS-7	38	Male	2.5	P3	P6	10.19
CS-8	27	Female	3.5	P3	P14	28.97

P: passage; PDs: population doublings.

four weeks.

Proliferation kinetics

Cells were counted using Bürker chamber at the end of each passage. Population doubling time (PDT) and the number of population doublings (PD) were calculated according to formulas $PDT=\ln 2*T/\ln(N_T/N_0)$, and $PD=T/PDT$, respectively, where T – culture time, N_T–cell number at the end of a passage, N_0–cell number at the beginning of a passage.

Colony forming unit (CFU) assay

Two replicates of 10^3 cells were seeded in a six-well culture dish using the same medium as that for cell culture and cultivated for 2 weeks in a humidified atmosphere at +37°C and 5% CO_2. Medium was changed every fourth day. Dishes were placed on ice and washed twice with cold phosphate-buffered saline (PBS) (Life Technologies). Cells were fixed with ice-cold methanol for 10 min, removed to room temperature and stained with 0.5% crystal violet dye (Sigma-Aldrich, Steinheim, Germany) solution in methanol. The stain was dissolved with 0.5% sodium dodecyl sulphate and absorbance was measured at 539 nm wave length.

Adipo- and osteogenic differentiation

For adipogenesis, ADSCs were cultivated in 12-well culture dishes until 90% confluent. Regular culture medium was replaced with adipogenesis induction medium containing DMEM with high glucose content (Life Technologies), 10% FBS (Life Technologies), 2 mM L-glutamine (Life Technologies), 10 μg/ml human insulin (Life Technologies), 1 μM dexamethasone (Sigma-Aldrich), 100 μM indomethacin (Sigma-Aldrich), 0.5 mM 3-isobutyl-1-methylxanthine (Sigma-Aldrich), 5 μg/ml gentamicin (Life Technologies). Cells in control wells were cultivated in DMEM (high glucose) supplemented with 10% FBS. Cells were cultured in a humidified atmosphere at +37°C and 5% CO_2 and medium was replaced every third day. Lipid droplets were detected after 16 days by Oil Red O (Sigma-Aldrich) staining.

For osteogenesis, ADSCs seeded on 12-well plates were allowed to reach 70% confluency. Osteogenic differentiation was induced by adding medium containing DMEM with low glucose content (Life Technologies), 10% FBS (Life Technologies), 2 mM L-glutamine (Life Technologies), 10 mM glycerol-2-phosphate (Sigma-Aldrich), 50 μM L-ascorbic acid (Sigma-Aldrich), 0.1 μM dexamethasone (Sigma-Aldrich), 5 μg/ml gentamicin (Life Technologies). Control cells were cultivated in DMEM (low glucose) with 10% FBS. Cells were cultured in a humidified atmosphere at +37°C and 5% CO_2 and medium was replaced every third day. After 30 days, extracellular calcium accumulation was detected by Alizarin Red S (Sigma-Aldrich) staining and alkaline phosphatase activity was determined using BCIP/NBT (Sigma-Aldrich) as a substrate.

SA-β-galactosidase assay

2.5×10^4 cells were seeded in a 96-well plate in triplicates. After 48 hours, β-gal expression was detected using Senescence Cells Histochemical Staining Kit (Sigma-Aldrich) according to manufacturer's instructions. To obtain a quantifiable result, images of stained cells were acquired with PowerShot S80 digital camera (Canon, Melville, New York, USA) and evaluated by two independent observers according to two parameters – color intensity and percentage of stained cells per field of view. For color measurement, a 5-point intensity scale was developed where 0 equaled 'no staining' and 5 – 'very dark color'.

MTT assay

2.5×10^4 cells were seeded in a 96-well plate in triplicates. After 48 hours, MTT assay was performed using Vybrant® MTT Cell Proliferation Assay Kit (Life Technologies) according to manufacturer's instructions. Absorbance was measured at 539 nm after overnight dissolution of formazan.

Quantitative peroxide assay

100 μl of ADSCs (1×10^6 cells per ml) were lysed by repeated freezing in liquid nitrogen and thawing at 42°C. Peroxide level in cell lysates was determined using Pierce™ Quantitative Peroxide Assay Kit (Thermo Scientific, Rockford, Illinois, USA) according to manufacturer's instructions on lipid-compatible procedure. Absorbance was measured at 620 nm.

Reverse transcriptase polymerase chain reaction

RNA was isolated from ADSCs with TRI reagent (Sigma-Aldrich) according to manufacturer's instructions except that RNA was precipitated in isopropanol overnight at −20°C in the presence of 120 ng of glycogen (Thermo Scientific). RNA quality and quantity was determined by NanoDrop® ND-1000 spectrophotometer (Thermo Scientific). 500 ng of DNase-treated RNA was subjected to complementary DNA synthesis using RevertAid™ First Strand cDNA Synthesis Kit (Thermo Scientific). The reaction was carried out with oligo(dT) primer according to manufacturer's instructions. 1 μl of cDNA was added to a PCR reaction mixture containing 2X PCR Master Mix (Thermo Scientific) and 0.4 μM pri-

mers (Metabion, Planegg, Germany) to amplify a set of genes (Table S1). Reaction conditions were as follows: initial denaturation at 94°C for 3 min followed by 30 cycles of 94°C for 30 s, 60°C for 30 s and 72°C for 45 s, finished with a 5 min extension at 72°C. Amplification products were visualized by ethidium bromide staining in agarose gel electrophoresis. Densitometric analysis of acquired images was carried out using ImageJ software (version 1.48).

Telomere Flow FISH

Relative telomere length of cultured ADSCs was assessed with Telomere PNA Kit/FITC for Flow Cytometry (Dako, Glostrup, Denmark) according to manufacturer's instructions using BD FACSCanto™ flow cytometer with BD FACSDiva™ Software (version 7.0). Jurkat cell line (ATCC/LGC Standards, Boras, Sweden) served as inner control. Each sample was assayed twice. 20 000 events were counted per measurement. Flow cytometer calibration was performed using BD Cytometer Setup and Tracking Beads. Results were analyzed using Infinicyt™ software (version 1.5.0) (Cytognos, Salamanca, Spain).

DNA index

DNA index of ADSC and Jurkat cells was measured with CycleTEST™ PLUS DNA Reagent Kit (BD) using BD FACSCanto™ flow cytometer and ModFit LT v3.3 software (version 3.3) (BD). The procedure was carried out on freshly thawed cells according to manufacturer's instructions.

Statistical analysis

Statistical analysis was performed in R software (version 3.0.2). Comparison of two data sets was done by t-test or Wilcoxon's test based on homogeneity of dispersions which was determined by F-test. Relation between results obtained by two different tests was assessed by correlation or regression analysis. For correlation analysis, Shapiro-Wilk test for normality was used to determine whether data were normally distributed. Depending on normality, Pearson or Spearman correlation was used. Regression analysis was performed using *lm*() function. Regression assumptions were tested by graphic analysis. The influence of each data point on regression model was estimated with Cook's distance. Significance level for all tests were $\alpha = 0.05$.

Results

Proliferation capacity and morphology of ADSCs during *in vitro* long-term cultivation

Growth kinetics: To assess cellular senescence in ADSCs, cell cultures from eight donors were subjected to long-term *in vitro* cultivation. For most donors, cells had been cryopreserved at P2 before beginning of the study (Table 1). After reaching confluency, a portion of cells was frozen for later analysis while the rest were reseeded to start the next passage. Subculturing was terminated if more than 4 weeks were necessary for cells to become confluent. Individual ADSC cultures reached the state of proliferation arrest after a considerably different time as were seen by differences in their respective cumulative PD values (Fig. 1A). Three cultures (CS-4, CS-5 and CS-7) stopped proliferating as early as after three (CS-4) or four (CS-5, CS-7) passages (cumulative PDs were 8.02, 8.30 and 10.19, respectively) and were excluded from further senescence evaluation as unsuccessfully expanded. In the remaining cultures, the number of cumulative PD varied from 14.69 (CS-6) to 28.97 (CS-8) (Table 1).

The proliferation rates of all cultures decreased unevenly during expansion (Fig. 1B) despite maintaining consistent split ratio of equally dense monolayer cultures. One (CS-1, CS-3, CS-6, CS-8) or two (CS-2) pronounced peaks of increased PDT were observed in the middle part of cultivation followed by reactivation of proliferation in subsequent passages. Proliferative ability of all cultures was lost very rapidly at the last passage indicated by 3.7 to more than 10-fold increase of PDT comparing to penultimate passage. The arrested proliferation was also denoted by the minimal increase of cumulative PDs at the last passage (Fig. 1A). It has been reported that MSC proliferation potential lowers both with increasing time in culture and donor age (13). We found a positive regression between passage number and PDT ($p < 0.05$) in samples CS-1 and CS-3, while in the case of CS-6 and CS-8, p value was close to significance level. Such relation was absent in CS-2 due to specifics of the growth curve. After the exclusion of unsuccessfully expanded cultures the rest of the samples fell into two distinct age categories – above 50 (CS-1, CS-2, CS-3) and under 40 years (CS-6, CS-8). There were no significant differences in growth kinetics between these groups, although the small sample size might compromise the validity of this observation.

Morphology: Morphologically, all cultures showed typical spindle-shaped appearance of MSCs at early passages. During long-term culture, the commonly described senescence-associated changes were observed: the increase of average cell size and heterogeneity, flattening of cells, irregular cell shape, and accumulation of granular inclusions in cytoplasm. Also, cells in late passages had a tendency to grow in star-shaped clusters rather than to form monolayers (Fig. 1C). However, similarly to pre-

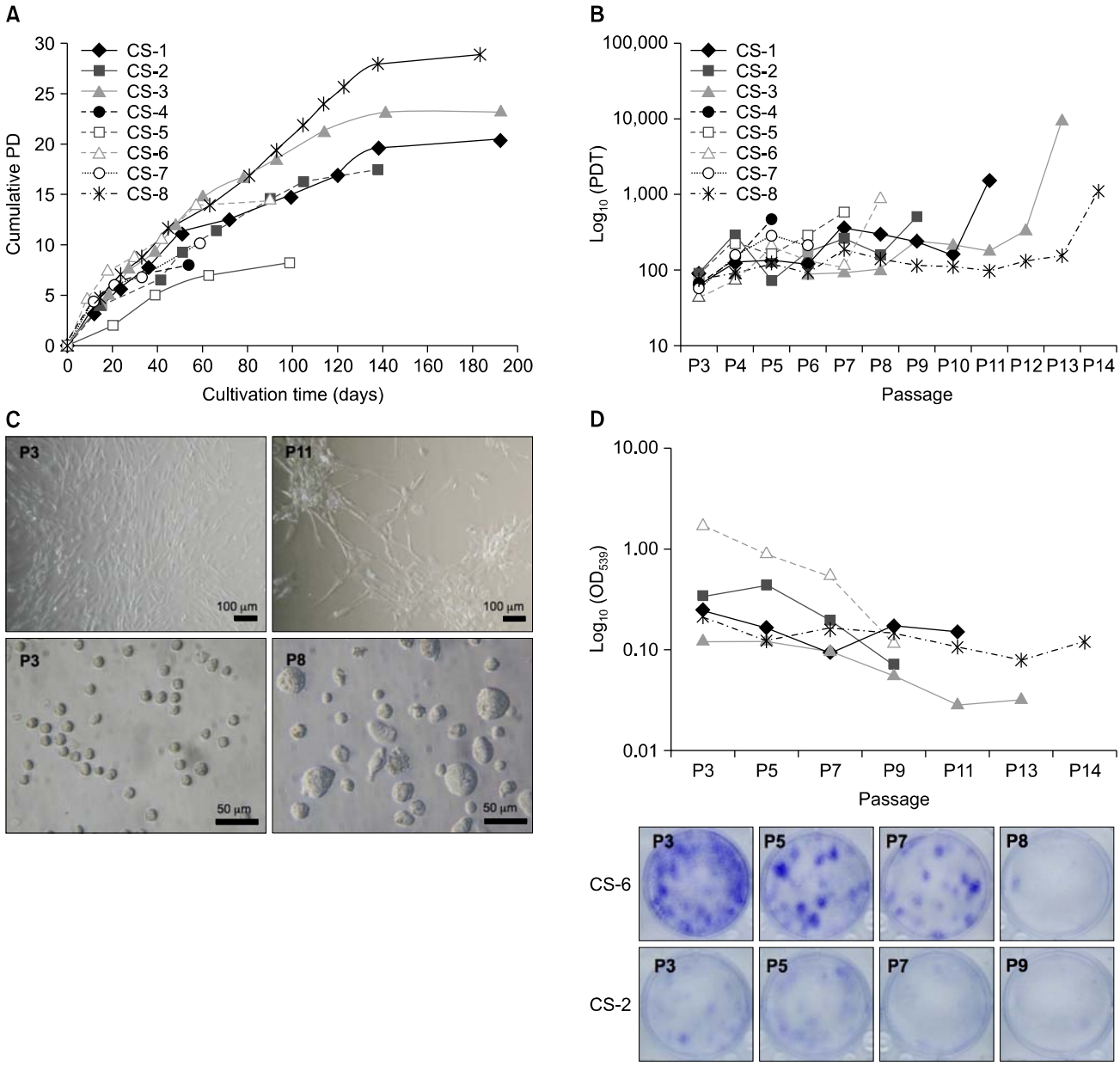

Fig. 1. Proliferation capacity and morphology of ADSCs during *in vitro* long-term cultivation. (A) Cumulative population doublings (PD). (B) ADSC proliferation curves showing population doubling time (PDT) at each passage. (C) ADSC morphology during long-term cultivation. Monolayer cells from early (upper-left) and late (upper-right) passage, and suspended cells from early (lower-left) and late (lower-right) passage are shown. (D) Clonogenicity potential of ADSCs. Upper panel –relative CFU test values; lower panel – an image of CFU test wells reflecting donor variance. OD: optical density.

viously described fluctuations in ADSC growth rates during culture, morphological changes did not accumulate evenly. Reappearance of spindle-shaped cells could be observed at P8 of sample CS-1 (Fig. S1). These cells dominated during P9 and P10 and possessed heightened proliferative abilities as indicated by decrease of PDT by 37.5% and 54.2% at P9 and P10, respectively when comparing to P7 (Fig. 1B). Similar observations were made in other ADSC cultures as well (data not shown).

At early passages, no significant differences in cell morphology were observed among donors. During long-term cultivation, donor-specific characteristics of cell appearance became visible (Fig. S2) indicating different course of aging in individual cultures. Nevertheless, all cultures

reached terminal senescence having a typical look of aged cells and were unable to further divide.

Clonogenicity: Alterations in ADSC clonogenic property was assessed using CFU assay. 10^3 cells were seeded in a six-well plate in two replicates, cultured for 2 weeks and stained with crystal violet. Since we observed a tendency of cells to grow in a more diffused manner rather than form dense colonies the dye was dissolved after staining and quantified spectrophotometrically. Others have shown that colony forming ability negatively correlates with PDT, donor's age and passage number (28). Our results showed a negative correlation between CFU test value and PDT, but it was not significant ($p>0.05$). Nevertheless, statistically significant negative relation between CFU test value and passage number existed ($p<0.05$). Again, the presence of donor variance was observed (Fig. 1D). This was illustrated by CFU test value of sample CS-6 which exceeded that of other cultures 7.47 times on average at P3. However, this difference rapidly declined during culture and reached the level of other samples at the last passage.

Senescence-related alterations of ADSC properties

Differentiation: Differences in adipo- and osteogenic potential between ADSCs from early (P3) and late (P9) passage were analyzed. Adipogenesis was assessed by staining intracellular lipid droplets with Oil Red O after 16 days of cultivation in adipogenesis induction medium. Osteogenesis was demonstrated by alkaline phosphatase activity and Alizarin Red S staining of accumulated calcium deposits after 30 days of differentiation. The results confirmed the ability of ADSCs to differentiate into the two lineages albeit with varying efficiencies among donors (Fig. 2). Accumulation of both lipid inclusions and extracellular calcium reduced dramatically at P9 compared to P3 (Fig. 2A, B). On the other hand, the level of alkaline phosphatase activity remained unchanged between passages (Fig. 2C).

Senescence-associated β-galactosidase expression: As a common indicator for cellular senescence, expression of SA-β-gal was determined by a histochemical staining method. Every other passage of long-term culture-expanded ADSCs was analyzed. Images of non-overlapping fields of view were evaluated by two independent observers to quantify SA-β-gal expression levels. As expected, little or no SA-β-gal expression was detected in early passages with subsequent increase during further cultivation (Fig. 3A). This result was confirmed by regression analysis revealing a positive association between SA-β-gal expression value and passage number. However, this was not significant ($p>0.05$) due to fluctuations of SA-β-gal expression levels in samples CS-1, CS-3 and CS-8 (Fig. S3). Interestingly, these fluctuations were concomitant with those observed in growth analysis confirmed by statistically significant positive correlation ($p>0.05$) between SA-β-gal expression level and PDT.

Metabolic activity: ADSC metabolic activity was assessed by MTT (3-(4,5-dimethylthiazol-2-yl)-2,5-diphenyltetrazolium bromide) assay. Every other passage was tested. MTT test results showed no association with passage number in neither sample ($p>0.05$) indicating that, in our experimental conditions, changes of enzymatic activity in cells were not directly related to time in culture or PDT. However, the overall metabolic activity was higher in early passages, decreased during culture and increased once again towards the end of cultivation (Fig. 3B). This result might be explained by a shift in dominant cellular functions during long-term culture. Accordingly, elevated metabolic activity at early passages is consistent with rapid proliferation which ceases as cells approach senescence. In support of this, the lowest absorption values were detected at passages with proliferation slowdown peaks in growth curves (CS-1-P7, CS-2-P7, CS-3-P9, CS-6-P5) (Fig. 1B). The subsequent increase of metabolic activity at late passages could, on the other hand, be explained by such energy-consuming cellular phenomena as senescence-associated secretory phenotype (SASP), characterized by an active secretion of chemokines, cytokines, and other factors participating in inflammation, growth stimulation, tissue remodeling and matrix degradation, and autophagy, a process of nonspecific degradation of cytoplasmic components, which has been shown to be functionally linked to SASP, at least in certain cases (29). Thus, according to our data, increased MTT test values after a 'fall' might be associated with senescence.

Intracellular peroxide: Fluctuations of intracellular peroxide in ADSCs were measured quantitatively. Standard curve was generated using 2-fold serially diluted H_2O_2 starting with 1 mM standard. For precision, dilutions were prepared twice and each set of standards was measured in duplicate. Since the standard curve was not linear over the entire assay range only low end range was used ($R^2=0.9983$) (Fig. 3C, left panel). The measurements of samples fell in this range.

Intracellular peroxide levels showed no association with neither passage number, nor PDT, nor metabolic activity ($p>0.05$). Peroxide concentrations varied among donors and there were substantial fluctuations even among passages of a single donor (Fig. 3C, right panel). Thus, no direct association between peroxide accumulation and sen-

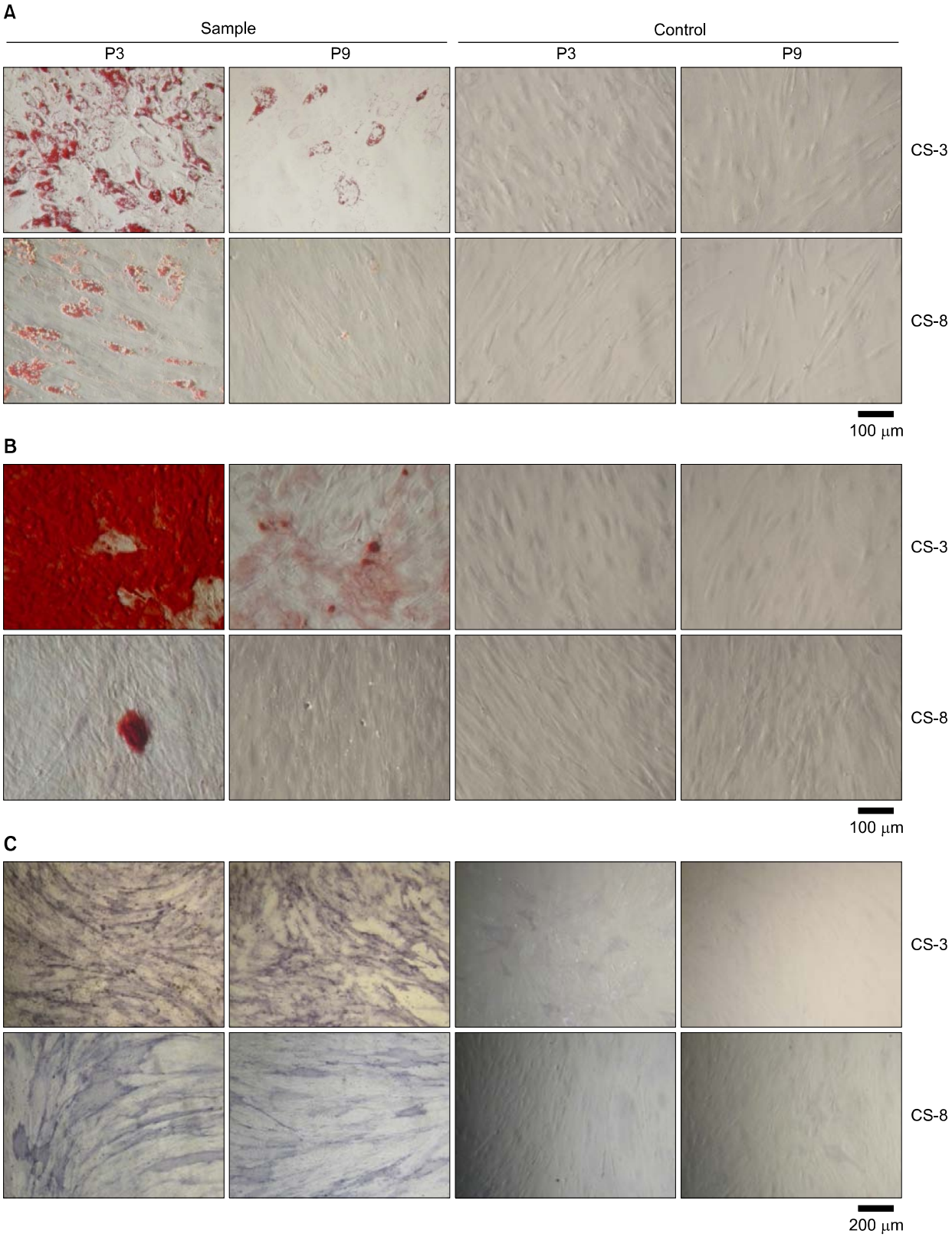

Fig. 2. Bilineage potential of ADSCs. Shown is the comparison of early (P3) and late (P9) passage of two representative samples (CS-3 and CS-8) reflecting donor-specific differences. (A) Adipogenesis detected by Oil Red O staining of lipid inclusions. (B, C) Osteogenesis detected by (B) Alizarin Red S staining of extracellular calcium, and (C) alkaline phosphatase activity.

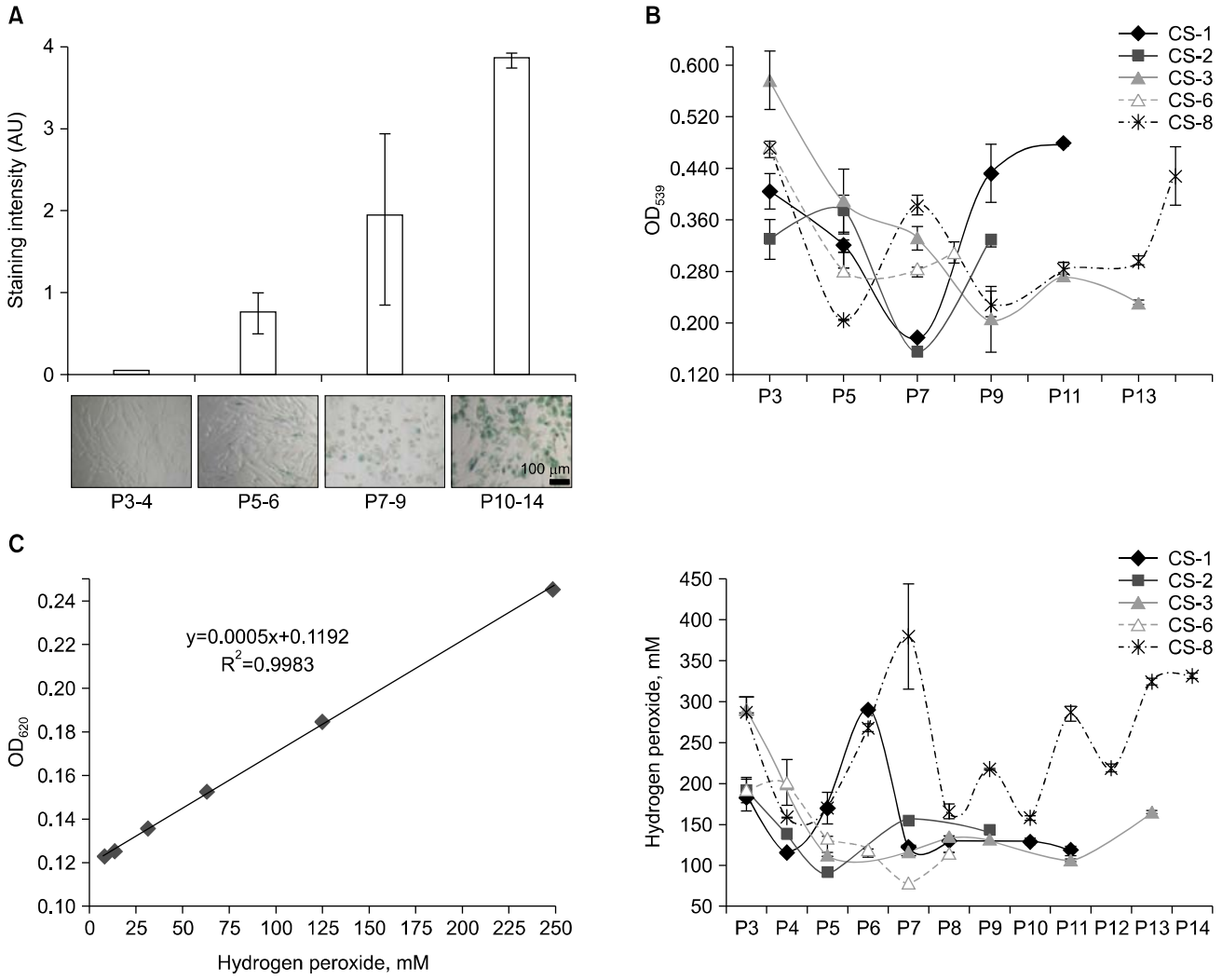

Fig. 3. Senescence-related changes of ADSC phenotype. (A) SA-β-gal expression was tested histochemically. Images were subjected to visual evaluation by two observers with regard to color intensity and percentage of stained cells per field of view. A typical view of increased SA-β-gal expression in ADSCs during long-term culture is shown (lower panel) with the respective visual evaluation data (upper panel) (B) ADSC metabolic activity determined by MTT assay. Optical density (OD) readings are expressed as mean of triplicate measurements. (C) Quantity of hydrogen peroxide in ADSCs. H_2O_2 standard curve is shown (left panel). H_2O_2 measurements of samples are expressed as mean of two replicates (right panel). AU: arbitrary units; P: passage. Error bars indicate standard deviation.

escence was proved in this study.

Gene expression profiles and transcription activities: To screen for alterations in gene expression in ADSCs during long-term culture 25 genes associated with such cellular functions as DNA repair, cell cycle regulation, antioxidation activity, apoptosis and epigenetic regulation were studied. Relative gene expression was determined by reverse transcription PCR and normalized against β-actin expression. The amplified products were visualized by ethidium bromide staining and quantified by densitometry analysis. Out of 25 genes tested, transcripts of three genes (*TERT*, *BIRC5*, *GSTA5*) were not detected in neither culture except CS-8 showing weak expression of *BIRC5* (data not shown). For the rest of the genes, expression profiles were strongly donor-specific (Fig. S4) and rendered it impossible to associate the transcription of any of the genes with the development of senescence.

RTL and detection of ADSC subpopulations: To determine whether ADSC senescence phenotype was associated with alterations in telomere length, fluorescence *in situ* hybridization technique for flow cytometry (Flow FISH) was utilized using FITC-conjugated telomere-specific peptide nucleic acid (PNA) probes. The specific fluorescence was calculated by subtracting autofluorescence of

cells without probe. Jurkat cells were added to each sample at a 1:1 ratio to normalize for inter-experimental variations. Cells in G0/G1 phase were discriminated by propidium iodide staining. Given the pseudodiploid karyotype of Jurkat cells (30) DNA index measurement was made. It was 1.00 for ADSCs (2n) and 1.83 for Jurkat cells (data not shown).

Results indicated that RTL significantly decreased in two samples (CS-3 and CS-8) when comparing the first and last passage (52.3% and 35.8%, respectively, $p<0.05$) (Fig. 4A). However, fluctuations of RTL were seen during passaging as in the previous tests indicating the complex nature of senescence process.

To test whether the increase of telomere length observed in some passages could occur due to pseudo-lengthening of telomeres because of the presence of various cell subpopulations, forward scatter signal versus telomere-specific FITC fluorescence were analyzed. Surprisingly, two well-separated ADSC subpopulations were detected in all samples and passages analyzed albeit at varying quantitative relations among donors (Fig. 4B, Table 2). This result was specific to ADSCs since no such observation was made for simultaneously tested Jurkat cells (Fig. 4B, lower panel). Interestingly, the discovered subpopulations differed significantly in terms of RTL and cell size ($p<0.05$, Fig. 4C, D) and were designated as S population for 'small' cells and L population for 'large' cells. The mean RTL of S population was 0.95 to 1.75 times shorter than that of L population, while the difference of cell size was 2 to 3-fold depending on the sample.

As seen in Table 2, a gradual decrease of RTL during passaging was detected in both populations of CS-3 and CS-8 but for CS-1, only in L population ($p<0.05$). Furthermore, the shortening of RTL occurred more rap-

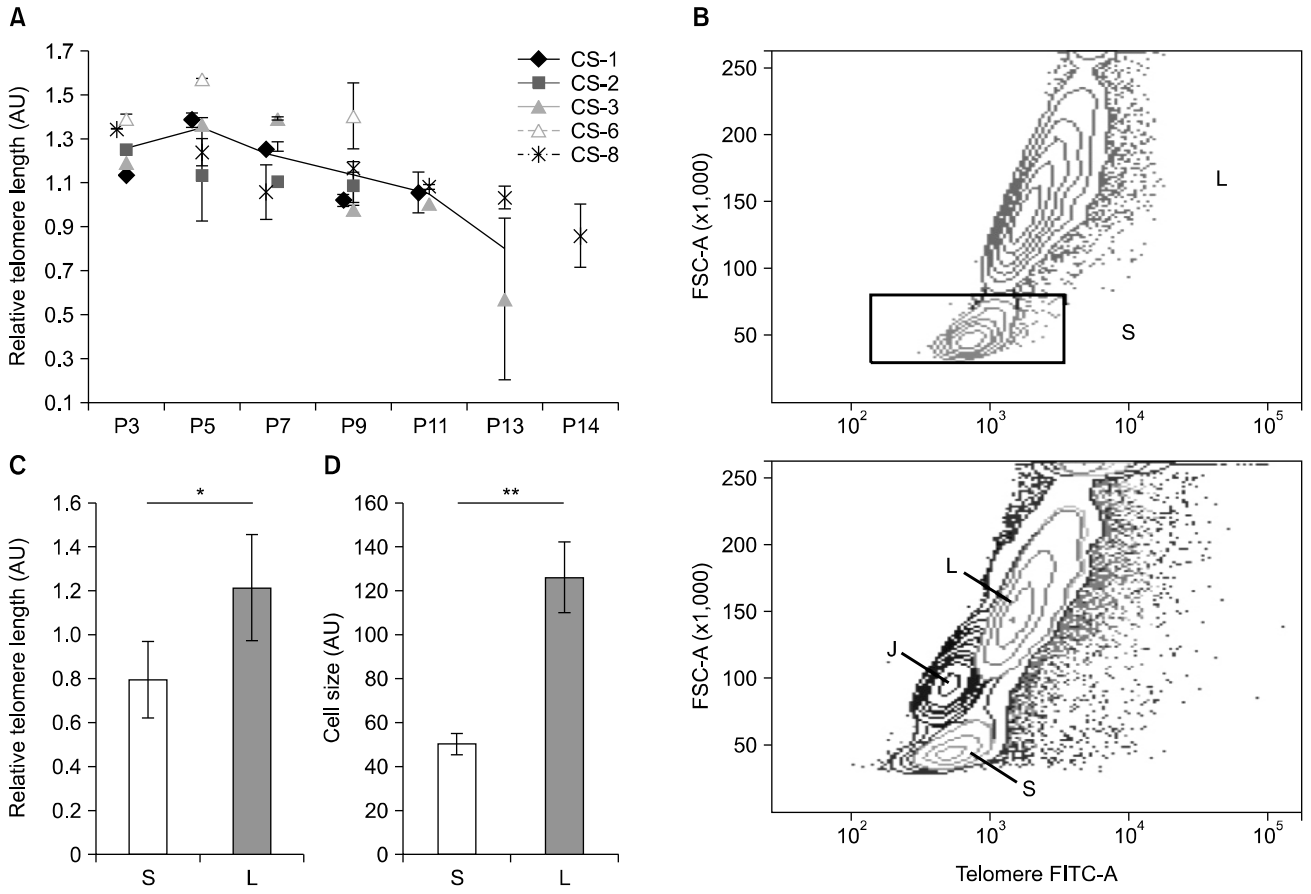

Fig. 4. Relative telomere length (RTL) of culture-expanded ADSCs and identification of cell subpopulations. (A) Flow FISH analysis of RTL dynamics during long-term culture. Each data point is expressed as mean±standard deviation of duplicate measurements. Continuous line represents mean RTL of five (P3-9), three (P11), and two (P13) samples. (B) The presence of two ADSC subpopulations (S and L) during RTL measurement was detected (upper panel). In contrast, only a single population of control Jurkat cells existed (lower panel, J). The S and L populations differed with respect to their RTL (C) and cell size (D) (data expressed as mean of all analyzed passages of five samples CS-1,2,3,6,8±standard deviation; *$p<0.05$, **$p=0.001$). AU: arbitrary units; P: passage.

Table 2. Comparison of relative telomere length (RTL), quantitative ratio and cell size of cell subpopulations S and L as identified by Flow FISH in adipose-derived mesenchymal stem cell cultures

Sample	RTL (AU)		Quantitative ratio (%)		Cell size (AU)	
	S	L	S	L	S	L
CS-1						
P3	0.82±0.01	1.17±0.02	2.6±0.99	97.4±0.99	51.75±1.48	114.95±0.21
P5	0.84±0.03	1.39±0.04	7.0±0.99	93.0±0.03	46.70±0.14	123.90±4.95
P7	0.81±0.00	1.29±0.00	10.9±0.35	89.1±0.35	46.55±0.35	124.55±1.20
P9	0.80±0.03	0.95±0.03	2.0±0.14	98.0±0.14	56.45±0.64	123.70±0.57
P11	0.91±0.12	0.86±0.11	3.0±0.70	97.0±0.70	50.18±1.83	113.03±2.51
CS-2						
P3	0.96±0.02	1.21±0.02	2.1±0.21	97.9±0.21	58.62±0.07	113.55±0.07
P5	0.79±0.18	1.27±0.29	6.3±0.42	93.7±0.42	49.50±0.42	128.4±2.26
P7	0.40±0.00	1.10±0.00	7.3±0.78	92.7±0.78	46.88±0.95	103.07±1.27
P9	0.62±0.03	1.18±0.05	18.3±2.04	81.7±2.04	52.04±0.54	162.35±2.61
CS-3						
P3	0.90±0.02	1.21±0.03	3.9±0.35	96.1±0.35	50.60±2.80	115.26±3.32
P5	0.90±0.03	1.32±0.04	7.0±0.28	93.0±0.28	49.39±0.59	130.28±0.73
P7	0.81±0.01	1.34±0.01	14.7±4.38	85.3±4.38	47.67±0.28	124.92±1.08
P9	0.53±0.01	1.01±0.03	3.7±0.49	96.3±0.49	47.51±0.71	119.38±0.14
P11	0.57±0.03	1.01±0.05	3.0±0.35	97.0±0.35	56.69±0.04	136.50±0.26
P13	0.43±0.27	0.59±0.38	29.4±0.99	70.6±0.99	59.40±0.29	131.33±3.79
CS-6						
P3	0.93±0.02	1.36±0.03	2.7±0.21	97.3±0.21	46.88±0.79	109.16±0.50
P5	1.07±0.00	1.63±0.00	4.3±0.92	95.7±0.92	47.91±0.73	124.96±0.56
P7	1.01±0.01	1.32±0.01	5.5±0.35	94.5±0.35	47.80±0.74	120.36±1.97
P8	0.91±0.13	1.55±0.22	6.0±0.92	94.0±0.92	52.18±1.57	138.02±0.46
CS-8						
P3	0.90±0.00	1.40±0.00	3.0±0.14	97.0±0.14	46.50±1.41	123.25±0.63
P5	0.95±0.07	1.40±0.11	20.5±2.05	79.6±2.05	46.75±0.64	117.8±2.12
P7	0.87±0.04	1.32±0.06	32.6±2.62	67.5±2.62	46.95±1.06	130.85±5.87
P9	0.70±0.02	1.21±0.04	24.8±2.47	75.3±2.47	45.00±0.57	112.50±0.07
P11	0.69±0.01	1.09±0.02	24.0±1.41	76.0±1.41	45.30±0.14	110.40±0.57
P13	0.67±0.04	0.99±0.06	26.9±1.55	73.1±1.55	51.45±0.07	136.40±0.00
P14	0.75±0.20	0.72±0.19	11.5±0.35	88.6±0.35	58.85±1.20	177.25±2.90

Data are expressed as means of duplicate measurements±standard deviation. AU: arbitrary units; P: passage.

idly in L population compared to S in samples CS-1, CS-3 and CS-8, and, at the last passage, RTL difference between populations became insignificant. Since the cells lost their proliferative ability very rapidly at the last passage (Fig. 1A, B), this might indicate the critical telomere length blocking further proliferation. On the other hand, samples CS-2 and CS-6 followed a different pattern. For CS-6, there were no significant RTL changes during passaging in neither population ($p>0.05$), while for CS-2, changes were seen only in S population, but they were not significantly associated with passage number ($p>0.05$, Table 2). Thus, the senescence of these cultures might be caused by factors other than critically short telomeres.

During passaging, changes in quantitative relation between subpopulations were observed in a donor-specific manner (Table 2). When the dynamics of S population quantity and peaks of proliferation slowdown (Fig. 1B) were compared, it was found that peaks corresponded either to the highest percentage of S population cells (for CS-1, the amount of S cells was 2.6% in P3 and 10.9% in P7; for CS-8 – 3.0% in P3 and 32.6% in P7) or to substantial RTL decrease in the S population (for CS-3, RTL decreases by 35% in P9 compared to P7; for CS-2 – by 49% in P7 compared to P5).

Discussion

In this study, we aimed to analyze the development of senescence of eight ADSC cultures previously frozen and stored in liquid nitrogen for 1.5 to 3.5 years.

Originally, all cultures were obtained and cultivated at 5% oxygen in the presence of autologous serum before they were cryopreserved. By contrast, this work employed ambient oxygen and FBS as a serum source which might have impacted the course of senescence. However, such conditions mimic a realistic situation when patient's cells have been cryopreserved in a tiered cell banking system, a recommended practice to minimize microbial contamination and facilitate large-scale cGMP-compliant cell production (31). In this case, cells can be stored in a master bank for an unknown period of time before further manufacturing is required. Due to evolving technological and regulatory requirements long-preserved cell products may become unintentionally exposed to suboptimal culture conditions.

MSC cultures are thought to be heterogeneous, comprised of subpopulations of cells with diverse features including multilineage potential, growth properties and clonogenicity (32, 33) During expansion, cell subsets possessing specific properties can be selected (34). Our data confirm the complex structure of MSC population by interrelated fluctuations of growth rate, morphology and SA-β-gal expression. Furthermore, an interesting observation was made by telomere Flow FISH when two distinct ADSC populations with significantly different cell size and RTL were found. The question remains whether this finding represents 'real' subpopulations of ADSCs. To prepare cells for RTL measurement they are subjected to harsh conditions such as high-temperature denaturation in the presence of a chaotropic agent (formamide) which is shown to have a detrimental effect on chromosomal morphology (35). Furthermore, Baerlocher and colleagues reported that heat and formamide treatment changed light scatter properties of human leukocyte subsets compared to untreated control (36). They also noticed swelling of cells upon prolonged exposure to hybridization mixture which depended on the composition of buffer used to suspend cells. Thus, forward scatter signals of S and L population are not necessarily an indication of the true size of these cells but should rather be perceived as a feature of tested ADSCs resulting in two distinct responses to treatment conditions as measured by Flow FISH. Nevertheless, the RTL difference of these two populations is clearly seen. Furthermore, unlike ADSCs, the control Jurkat cells, though undergoing the same treatment, retained their optical homogeneity and were not separated into distinct subpopulations, thus suggesting that the phenomenon is not a pure artifact.

Although several mechanisms of senescence are described, reduction of telomere length is studied in most detail. Other groups have reported mixed results concerning the role of telomere length in causing senescence (37, 38). The data obtained in this study allow us to conclude that both telomere-dependent and independent mechanisms could be observed in studied ADSC cultures. According to the telomere shortening pattern observed in S and L populations (Table 2) we hypothesize that three cultures (CS-1, CS-3, CS-8) entered replicative senescence (telomere length of L population reached that of S population at the end of cultivation), the other two (CS-2, CS-6) – premature senescence (telomere length of L populations did not change significantly). The three samples excluded from the study (CS-4, CS-5 and CS-7) are likely to be added to premature senescence group. It is reported that MSCs cease to proliferate when their telomeres reach approximately 10 kb in length (15). However, it is also known that critical telomere length can be as low as 4.5 kb (39). In our case, considering the reported average telomere length of Jurkat cells (11.5 kb) (40) that served as a control for RTL analysis, the extrapolated telomere lengths of L subpopulation at the last passage were 9.89, 6.78 and 8.28 kb in samples CS-1, CS-3 and CS-8, respectively which is in agreement with literature and the concept of replicative senescence. On the other hand, the same measurement revealed 13.57 kb in CS-2 and 17.82 kb in CS-6 further supporting the assumption of premature senescence in these samples. Moreover, the total number of PDs of these samples was lower than CS-1, CS-3 and CS-8 (Table 1) and the same result was seen in SA-β-gal test – the mean expression of the enzyme was 1.88 times lower at the last passage of CS-2 and CS-6 compared to the last passage of other samples (Fig. 4S).

According to our results, the preference for the two forms of senescence – replicative and premature – in the cells is dictated in a donor-specific manner. All ADSC cultures were initially obtained by a similar procedure, were all exposed to stress by changing culture conditions and propagated simultaneously under the same conditions. Nevertheless, one of the main observations in this study is the high level of donor variability. Diverse growth properties and functionality of MSCs obtained from different donors were observed previously (28) and are likely explained by different genetic backgrounds, clinical histories and lifestyle of individual donors.

Conclusions

The work presented here demonstrates that human ADSCs are heterogeneous and consist of cell subpopulations which play a major role in the course of *in vitro* senescence

in every individual cell culture. Moreover, the pattern of *in vitro* aging is strongly donor-specific which my have important implications in personalized medicine.

Acknowledgments

We are thankful to Dr. habil.biol Paul Pumpens for scientific support and advice. This work was supported by the project No.10.0014 of the Latvian Council of Science.

Potential conflict of interest

The authors have no conflicting financial interest.

Supplementary Materials

Supplementary data including four figure can be found with this article online at http://pdf.medrang.co.kr/paper/pdf/IJST/IJST-09-s003.pdf.

References

1. Zuk PA, Zhu M, Ashjian P, De Ugarte DA, Huang JI, Mizuno H, Alfonso ZC, Fraser JK, Benhaim P, Hedrick MH. Human adipose tissue is a source of multipotent stem cells. Mol Biol Cell 2002;13:4279-4295
2. Fraser JK, Wulur I, Alfonso Z, Hedrick MH. Fat tissue: an underappreciated source of stem cells for biotechnology. Trends Biotechnol 2006;24:150-154
3. Ikegame Y, Yamashita K, Hayashi S, Mizuno H, Tawada M, You F, Yamada K, Tanaka Y, Egashira Y, Nakashima S, Yoshimura S, Iwama T. Comparison of mesenchymal stem cells from adipose tissue and bone marrow for ischemic stroke therapy. Cytotherapy 2011;13:675-685
4. Dulic V. Senescence regulation by mTOR. Methods Mol Biol 2013;965:15-35
5. Hayflick L, Moorhead PS. The serial cultivation of human diploid cell strains. Exp Cell Res 1961;25:585-621
6. Shay JW, Wright WE. Hayflick, his limit, and cellular ageing. Nat Rev Mol Cell Biol 2000;1:72-76
7. Ramirez RD, Morales CP, Herbert BS, Rohde JM, Passons C, Shay JW, Wright WE. Putative telomere-independent mechanisms of replicative aging reflect inadequate growth conditions. Genes Dev 2001;15:398-403
8. Rochette PJ, Brash DE. Human telomeres are hypersensitive to UV-induced DNA Damage and refractory to repair. PLoS Genet 2010;6:e1000926
9. Yuan H, Kaneko T, Matsuo M. Relevance of oxidative stress to the limited replicative capacity of cultured human diploid cells: the limit of cumulative population doublings increases under low concentrations of oxygen and decreases in response to aminotriazole. Mech Ageing Dev 1995;81: 159-168
10. Roberson RS, Kussick SJ, Vallieres E, Chen SY, Wu DY. Escape from therapy-induced accelerated cellular senescence in p53-null lung cancer cells and in human lung cancers. Cancer Res 2005;65:2795-2803
11. Munro J, Barr NI, Ireland H, Morrison V, Parkinson EK. Histone deacetylase inhibitors induce a senescence-like state in human cells by a p16-dependent mechanism that is independent of a mitotic clock. Exp Cell Res 2004; 295:525-538
12. Serrano M, Lin AW, McCurrach ME, Beach D, Lowe SW. Oncogenic ras provokes premature cell senescence associated with accumulation of p53 and p16INK4a. Cell 1997;88:593-602
13. Izadpanah R, Trygg C, Patel B, Kriedt C, Dufour J, Gimble JM, Bunnell BA. Biologic properties of mesenchymal stem cells derived from bone marrow and adipose tissue. J Cell Biochem 2006;99:1285-1297
14. Dimri GP, Lee X, Basile G, Acosta M, Scott G, Roskelley C, Medrano EE, Linskens M, Rubelj I, Pereira-Smith O, Peacocke M, Campisi J. A biomarker that identifies senescent human cells in culture and in aging skin in vivo. Proc Natl Acad Sci U S A 1995;92:9363-9367
15. Baxter MA, Wynn RF, Jowitt SN, Wraith JE, Fairbairn LJ, Bellantuono I. Study of telomere length reveals rapid aging of human marrow stromal cells following *in vitro* expansion. Stem Cells 2004;22:675-682
16. Mao Z, Ke Z, Gorbunova V, Seluanov A. Replicatively senescent cells are arrested in G1 and G2 phases. Aging (Albany NY) 2012;4:431-435
17. Yu KR, Kang KS. Aging-related genes in mesenchymal stem cells: a mini-review. Gerontology 2013;59:557-563
18. Rufini A, Tucci P, Celardo I, Melino G. Senescence and aging: the critical roles of p53. Oncogene 2013;32:5129-5143
19. von Zglinicki T, Saretzki G, Ladhoff J, d'Adda di Fagagna F, Jackson SP. Human cell senescence as a DNA damage response. Mech Ageing Dev 2005;126:111-117
20. Thomas DM, Yang HS, Alexander K, Hinds PW. Role of the retinoblastoma protein in differentiation and senescence. Cancer Biol Ther 2003;2:124-130
21. Qian Y, Chen X. Senescence regulation by the p53 protein family. Methods Mol Biol 2013;965:37-61
22. Narita M, Nũnez S, Heard E, Narita M, Lin AW, Hearn SA, Spector DL, Hannon GJ, Lowe SW. Rb-mediated heterochromatin formation and silencing of E2F target genes during cellular senescence. Cell 2003;113:703-716
23. Ferbeyre G, de Stanchina E, Querido E, Baptiste N, Prives C, Lowe SW. PML is induced by oncogenic ras and promotes premature senescence. Genes Dev 2000;14:2015-2027
24. Dhahbi JM, Atamna H, Boffelli D, Magis W, Spindler SR, Martin DI. Deep sequencing reveals novel microRNAs and regulation of microRNA expression during cell senescence. PLoS One 2011;6:e20509
25. Banas A, Teratani T, Yamamoto Y, Tokuhara M, Takeshita F, Osaki M, Kawamata M, Kato T, Okochi H, Ochiya T. IFATS collection: in vivo therapeutic potential of human adipose tissue mesenchymal stem cells after transplantation into mice with liver injury. Stem Cells 2008;26:2705-2712
26. Cho YB, Lee WY, Park KJ, Kim M, Yoo HW, Yu CS.

Autologous adipose tissue-derived stem cells for the treatment of Crohn's fistula: a phase I clinical study. Cell Transplant 2013;22:279-285
27. Bogdanova A, Bērziņš U, Brūvere R, Eivazova G, Kozlovska T. Adipose-derived stem cells cultured in autologous serum maintain the characteristics of mesenchymal stem cells. Proc Latv Acad Sci, Sect B, Nat Exact Appl Sci 2010; 64:106-113
28. Digirolamo CM, Stokes D, Colter D, Phinney DG, Class R, Prockop DJ. Propagation and senescence of human marrow stromal cells in culture: a simple colony-forming assay identifies samples with the greatest potential to propagate and differentiate. Br J Haematol 1999;107:275-281
29. Salama R, Sadaie M, Hoare M, Narita M. Cellular senescence and its effector programs. Genes Dev 2014;28: 99-114
30. Evans-Galea MV, Wielgosz MM, Hanawa H, Srivastava DK, Nienhuis AW. Suppression of clonal dominance in cultured human lymphoid cells by addition of the cHS4 insulator to a lentiviral vector. Mol Ther 2007;15:801-809
31. Crook JM, Stacey GN. Setting quality standards for stem cell banking, research and translation: the international stem cell banking initiative. In: Ilic D, editor. Stem cell banking. New York City, NY, USA: Humana Press Inc; 2014. 5-7
32. Lee CC, Christensen JE, Yoder MC, Tarantal AF. Clonal analysis and hierarchy of human bone marrow mesenchymal stem and progenitor cells. Exp Hematol 2010;38: 46-54
33. Rada T, Reis RL, Gomes ME. Distinct stem cells subpopulations isolated from human adipose tissue exhibit different chondrogenic and osteogenic differentiation potential. Stem Cell Rev 2011;7:64-76
34. Cholewa D, Stiehl T, Schellenberg A, Bokermann G, Joussen S, Koch C, Walenda T, Pallua N, Marciniak-Czochra A, Suschek CV, Wagner W. Expansion of adipose mesenchymal stromal cells is affected by human platelet lysate and plating density. Cell Transplant 2011;20:1409-1422
35. Winkler R, Perner B, Rapp A, Durm M, Cremer C, Greulich KO, Hausmann M. Labelling quality and chromosome morphology after low temperature FISH analysed by scanning far-field and near-field optical microscopy. J Microsc 2003;209:23-33
36. Baerlocher GM, Mak J, Tien T, Lansdorp PM. Telomere length measurement by fluorescence in situ hybridization and flow cytometry: tips and pitfalls. Cytometry 2002;47: 89-99
37. Noh HB, Ahn HJ, Lee WJ, Kwack KB, Kwon YD. The molecular signature of *in vitro* senescence in human mesenchymal stem cells. Genes Genomics 2010;32:87-93
38. Samsonraj RM, Raghunath M, Hui JH, Ling L, Nurcombe V, Cool SM. Telomere length analysis of human mesenchymal stem cells by quantitative PCR. Gene 2013;519: 348-355
39. Bodnar AG, Ouellette M, Frolkis M, Holt SE, Chiu CP, Morin GB, Harley CB, Shay JW, Lichtsteiner S, Wright WE. Extension of life-span by introduction of telomerase into normal human cells. Science 1998;279:349-352
40. Treff NR, Su J, Taylor D, Scott RT Jr. Telomere DNA deficiency is associated with development of human embryonic aneuploidy. PLoS Genet 2011;7:e1002161

Table S1. List of primers used in the study

Gene name	Gene reference number		Sequence	Product length (bp)
CELL CYCLE REGULATION				
ATM	NM000051	Forward	5'-TGTTCCAGGACACGAAGGGAGA-3'	138
		Reverse	5'-CAGGGTTCTCAGCACTATGGGA-3'	
ATR	NM001184	Forward	5'-GGAGATTTCCTGAGCATGTTCGG-3'	100
		Reverse	5'-GGCTTCTTTACTCCAGACCAATC-3'	
BRCA1	NM007294	Forward	5'-CTGAAGACTGCTCAGGGCTATC-3'	155
		Reverse	5'-AGGGTAGCTGTTAGAAGGCTGG-3'	
CHEK1	NM001274	Forward	5'-CTCATGGCAGGGGTGGTTTATC-3'	122
		Reverse	5'-ACTGTTGCCAAGCCAAAGTCTG-3'	
E2F4	NM001950	Forward	5'-GGAAGGTATCGGGCTAATCGAG-3'	126
		Reverse	5'-AGCTCCTCGATCTCTGCCTTGA-3'	
NFKB1	NM003998	Forward	5'-GCAGCACTACTTCTTGACCACC-3'	130
		Reverse	5'-TCTGCTCCTGAGCATTGACGTC-3'	
P16	NM012308	Forward	5'-CTCGTGCTGATGCTACTGAGGA-3'	134
		Reverse	5'-GGTCGGCGCAGTTGGGCTCC-3'	
P53	NM000546	Forward	5'-CCTCAGCATCTTATCCGAGTGG-3'	128
		Reverse	5'-TGGATGGTGGTACAGTCAGAGC-3'	
RB1	NM000321	Forward	5'-AGAGCTTGGTTAACTTGGGAGA-3'	120
		Reverse	5'-CTCATCTAGGTCAACTGCTGC-3'	
DNA REPAIR				
APEX1	NM001641	Forward	5'-TCTTACGGCATAGGCGATGA-3'	111
		Reverse	5'-CAGACCTCGGCCTGCATTAG-3'	
TERT	NM198253	Forward	5'-GCTGACGTGGAAGATGAGCG-3'	146
		Reverse	5'-GCTCGACGACGTACACACTC-3'	
XRCC4	NM003401	Forward	5'-TGATGGTCATTCAGCATGGACT-3'	109
		Reverse	5'-TGCTTTTCTCAGTTCACCAACA-3'	
XRCC6	NM001469	Forward	5'-TGCGTGGATTGTCGTCTTCT-3'	111
		Reverse	5'-CTTCTTCATCGCCCTCGGTT-3'	
APOPTOSIS				
BAX	NM138761	Forward	5'-TCAGGATGCGTCCACCAAGAAG-3'	103
		Reverse	5'-TGTGTCCACGGCGGCAATCATC-3'	
BCL2	NM000633	Forward	5'-ATCGCCCTGTGGATGACTGAGT-3'	127
		Reverse	5'-GCCAGGAGAAATCAAACAGAGGC-3'	
BIRC5	NM001012271	Forward	5'-CCACTGAGAACGAGCCAGACTT-3'	115
		Reverse	5'-GTATTACAGGCGTAAGCCACCG-3'	
CASP3	NM004346	Forward	5'-GGAAGCGAATCAATGGACTCTGG-3'	146
		Reverse	5'-GCATCGACATCTGTACCAGACC-3'	
CASP8	NM001228	Forward	5'-AACCTCGGGGATACTGTCTG-3'	297
		Reverse	5'-CCTGTCCATCAGTGCCATAG-3'	
CASP9	NM001229	Forward	5'-GTTTGAGGACCTTCGACCAGCT-3'	129
		Reverse	5'-CAACGTACCAGGAGCCACTCTT-3'	
ANTIOXIDATION				
GSTA5	NM153699	Forward	5'-CCAAGCTCCACTACTCCAATGC-3'	144
		Reverse	5'-GGAACAGCAAACTCCCATCATTTCT-3'	
PRDX2	NM005809	Forward	5'-CCTTCCAGTACACAGACGAGCA-3'	136
		Reverse	5'-CTCACTATCCGTTAGCCAGCCT-3'	
PRDX5	NM012094	Forward	5'-TGATGCCTTTGTGACTGGCGAG-3'	135
		Reverse	5'-CCAAAGATGGACACCAGCGAATC-3'	
SOD1	NM000454	Forward	5'-CTCACTCTCAGGAGACCATTGC-3'	129
		Reverse	5'-CCACAAGCCAAACGACTTCCAG-3'	
TXN	NM003329	Forward	5'-TTGGTGCTTTGGATCCATTTCCAT-3'	107
		Reverse	5'-CAAGGCTTCCTGAAAAGCAGTCT-3'	

Table S1. Continued.

Gene name	Gene reference number		Sequence	Product length (bp)
EPIGENETICS				
DNMT1	NM001379	Forward	5′-ACCGCTTCTACTTCCTCGAGGCCTA-3′	335
		Reverse	5′-GTTGCAGTCCTCTGTGAACACTGTGG-3′	
HOUSEKEEPING				
ACTB	NM001101	Forward	5′-GAGCTACGAGCTGCCTGAC-3′	110
		Reverse	5′-GGATGCCACAGGACTCCATG-3′	

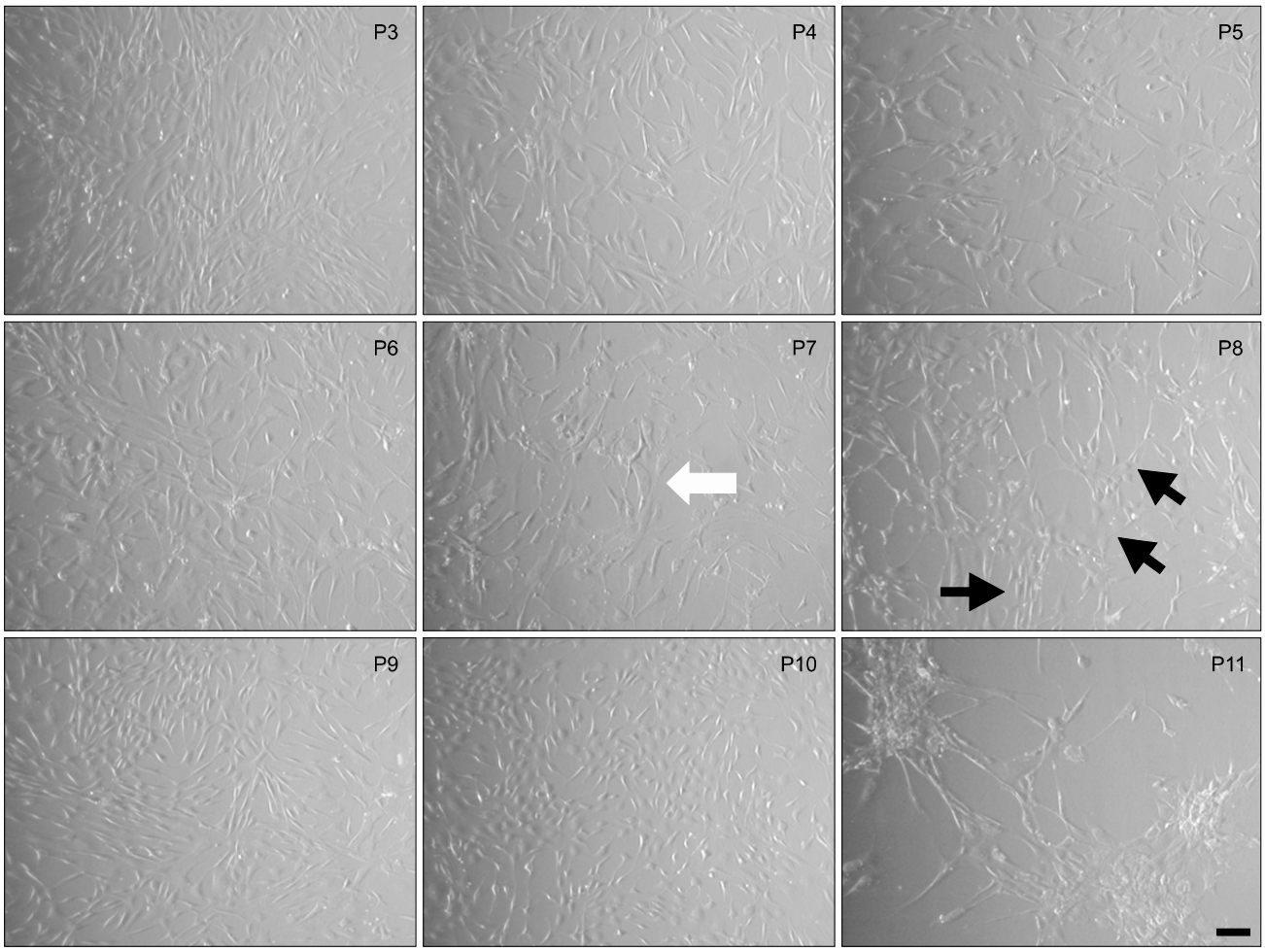

Fig. S1. Changes of adipose-derived mesenchymal stem cell morphology during long-term cultivation. Representative images of sample CS-1 are shown. Note the common senescence-associated enlargement and flattening of cells at passage 7 (P7) (white arrow). The appearance of spindle- and triangular-shaped cells in P8 is depicted by black arrows. These cells dominate during P9 and P10. Scale bar – 100 μm.

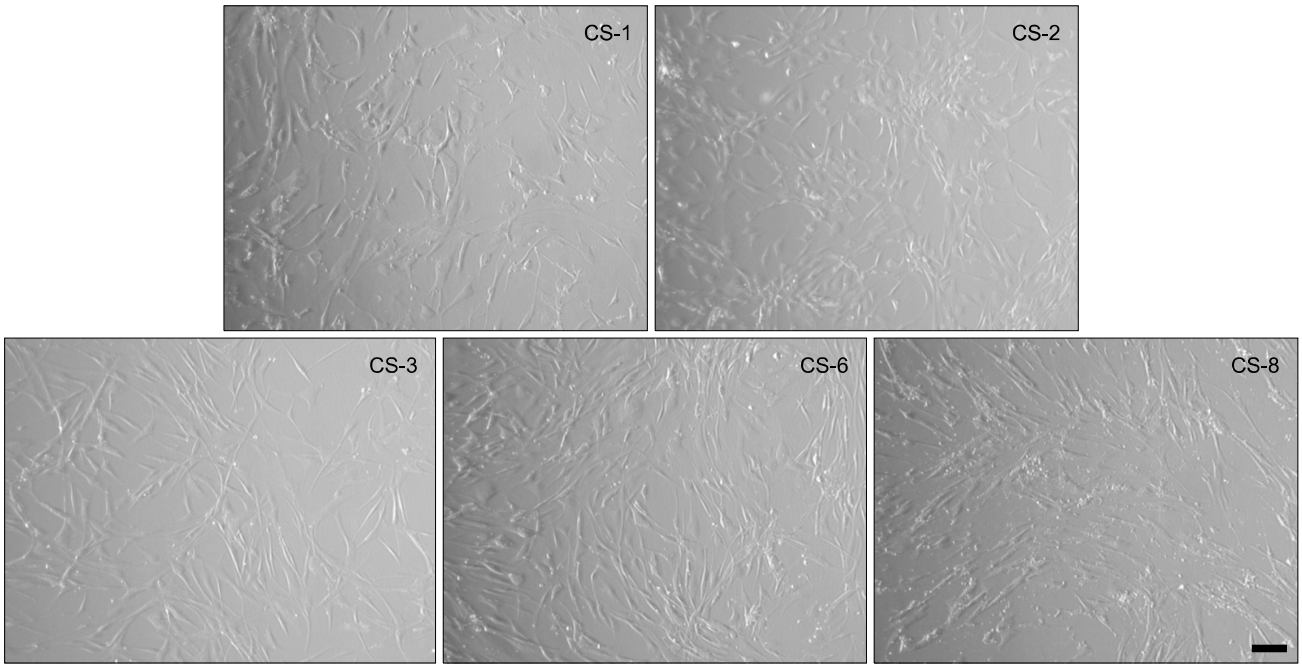

Fig. S2. Morphology of adipose-derived mesenchymal stem cells (ADSCs) obtained from different donors. Comparison of cells at passage 7 (P7) is shown. Cells from donor CS-1 are enlarged and irregular in shape which are typical signs of senescence. For CS-2, small triangular cells clustering in groups are seen. ADSCs of CS-3 appear spindle-shaped with minimal signs of senescence. Image of CS-6 presents a mixed population of cells where large, senescenct cells can be seen among spindle-shaped ones. For CS-8, ADSCs maintain a spindle-shaped appearance and possess a donor-specific pattern to grow in a parallel orientation to each other making the monolayer appear streaky. A lot of cell debris is present. Scale bar = 100 μm.

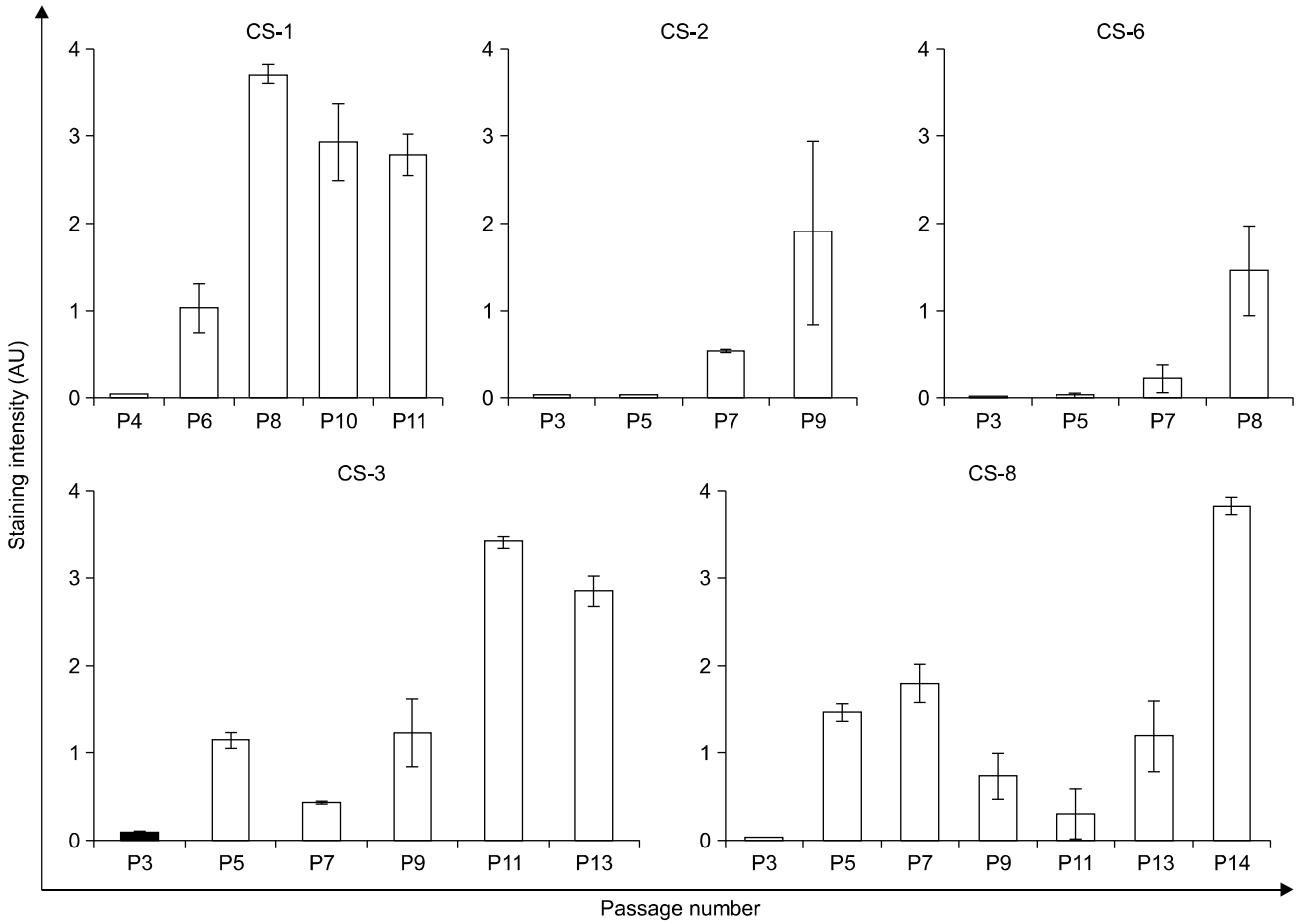

Fig. S3. Quantitative evaluation of senescence-associated β-galactosidase (SA-β-gal) expression. Adipose-derived mesenchymal stem cells from five donors (CS-1,2,3,6,8) were culture-expanded until entering senescence. SA-β-gal expression was tested histochemically. Images were subjected to visual evaluation by two observers with regard to color intensity and percentage of stained cells per field of view. Error bars show standard deviation from two measurements.

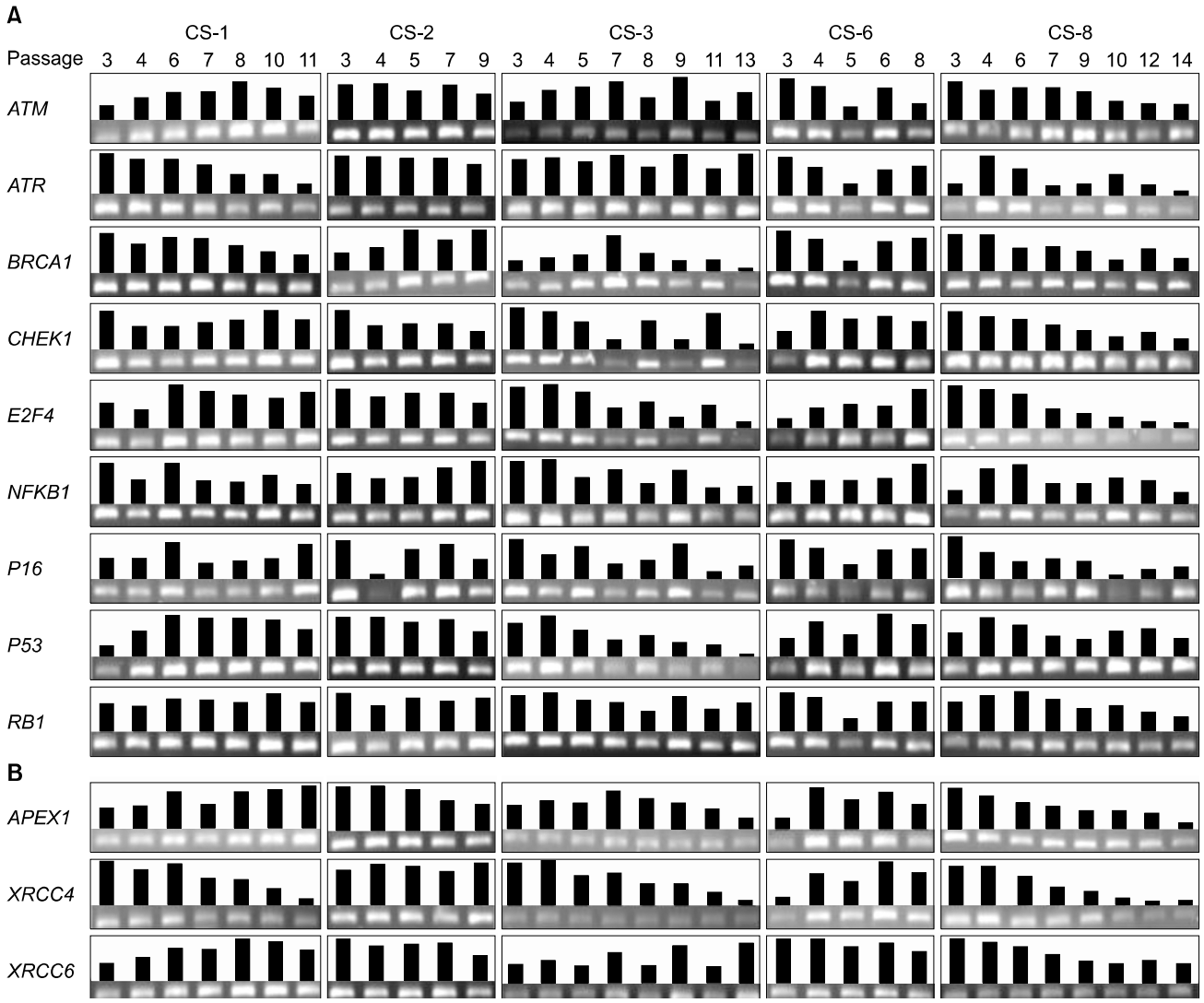

Fig. S4. Gene expression in adipose-derived mesenchymal stem cells (ADSCs) during long-term culture. Messenger RNA was detected in five ADSC cultures (CS-1,2,3,6,8) by reverse-transcriptase polymerase chain reaction. Amplification products were visualized in UV light by ethidium bromide staining. Signal intensity was quantified by pixel density analysis in ImageJ software (version 1.48) and normalized against housekeeping gene signal intensity. Expression of genes involved in (A) cell cycle regulation, (B) DNA repair, (C) apoptosis, (D) antioxidation, and (E) epigenetics was tested. β-actin was used as housekeeping gene (F). Quantification results are expressed in arbitrary intensity units (black bars). The respective gel bands are shown below.

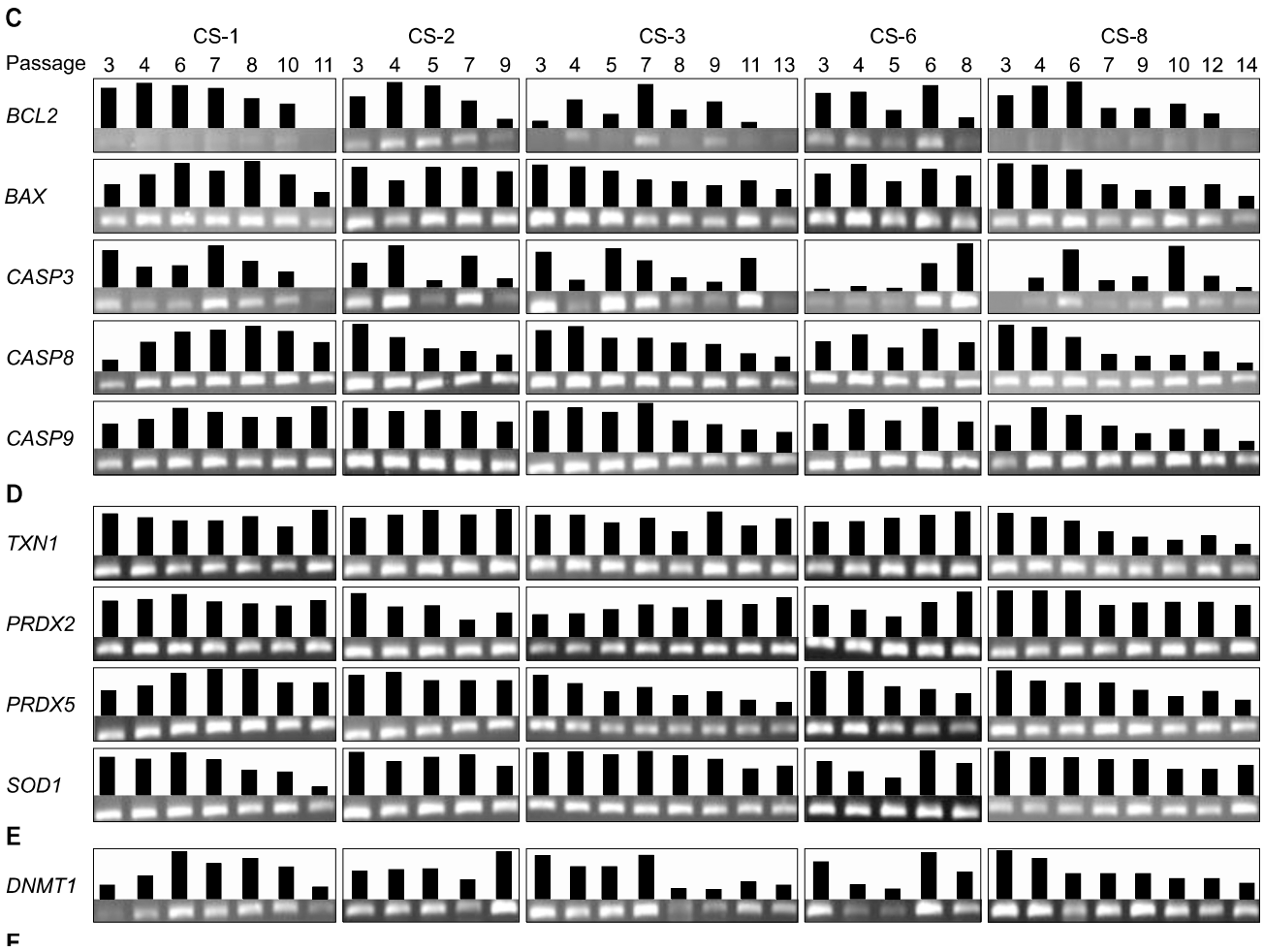

Fig. S4. Continued.

Journal of Stem Cells
Volume 9, Number 3
ISSN: 1556-8539

Characterization of Human Adipose-Derived Stem Cells Cultured in Autologous Serum after Subsequent Passaging and Long Term Cryopreservation

Ance Bogdanova[1#*], Uldis Berzins[1#], Sergey Nikulshin[2], Dace Skrastina[1], Agnese Ezerta[1], Diana Legzdina[1], and Tatjana Kozlovska[1]

[1]Latvian Biomedical Research and Study Centre, Ratsupites Street 1, Riga, LV-1067, Latvia
[2]University Children's Hospital, Clinical Laboratory, Vienibas Gatve 45, Riga, LV-1004, Latvia

Abstract

The aim of this study was to evaluate human adipose-derived stem cells (ASCs) from passage 2 (P2) to P8 cultured in medium containing 5% autologous serum (AS) after a long-term cryopreservation with regards to their surface marker expression, differentiation potential, and immunosuppressive effect in vitro. 8-color flow cytometry and real time PCR were used to determine mesenchymal stem cell (MSC) surface marker expression on ASCs from various passages. In vitro differentiation ability and immunomodulatory properties of ASCs were also tested. Flow cytometry showed that all ASCs express typical MSC markers CD29, CD44, CD73, CD90, CD105 simultaneously, but do not express such markers as HLA-DR, CD34, CD14, CD19, and CD45. Furthermore, median fluorescence intensity of positive cell surface markers increased with each subsequent passage indicating the accumulation of protein expression. The multilineage differentiation demonstrated the ability of ASCs from P6 to efficiently differentiate into adipocytes and chondrocytes, but their potential of osteogenic differentiation was diminished. Data from co-culture of ASCs and autologous peripheral blood mononuclear cells (PBMNCs) indicated that ASCs from P3, P6, and P9 significantly reduce the proliferation of PBMNCs at ASCs:PBMNCs ratio 1:1 and this suppression is dose dependent. This study demonstrated that ASCs from P2 to P8, cultured in the presence of AS, represent a highly homogeneous cell population with a peak accumulation of MSC surface proteins at P5 possessing multilineage differentiation ability and significant immunosuppressive properties after double freezing and more than 4 years of cryopreservation.

Keywords: autologous serum, human adipose-derived stem cells, multi-color flow cytometry, multilineage differentiation, stem cell immunosuppression, stem cell phenotype

# These authors contributed equally to this work
* Corresponding author: Ance Bogdanova, Latvian Biomedical Research and Study Centre, Ratsupites Street 1, Riga, LV-1067, Latvia. E-mail address: ance.bogdanova@biomed.lu.lv

Introduction

Since P. Zuk and her colleagues showed that mesenchymal stem cells (MSCs) can be readily obtained from adipose tissue [1], the potential use of adipose-derived stem cells (ASCs) has experienced a great increase of scientific interest. It has been shown that ASCs bear high proliferative capacity and can undergo multilineage in vitro differentiation into osteocytes, chondrocytes, adipocytes [1,2], smooth muscle cells [3], skeletal muscle cells [4,5], cardiomyocytes [6], neurons [7], endothelial cells [8], hepatocytes [9], and pancreatic cells [10]. Like bone marrow (BM) MSCs, ASCs are spindle-shaped cells with fibroblastoid morphology [1] and normal karyotype that can be easily propagated in vitro and their multi-lineage potential is not altered by freezing/thawing procedure [11]. But in contrast to BM MSCs, ASCs are easier to obtain, display lower donor site morbidity [12] and one milliliter of fat tissue holds 500-fold greater amount of stem cells than the same amount of BM [13].

As the search for the unique MSC marker is still ongoing, a combination of positive and negative markers must be verified to identify MSCs. One of the minimal criteria, set for the identification of MSCs, is the expression of such surface markers as CD105, CD73, CD90 and the lack of expression of CD45, CD34, CD14, CD19, HLA-DR surface molecules [14]. To define ASCs, this list has been extended with CD9, CD10, CD13, CD29, CD44, CD54, CD55, CD59, CD106, CD146, CD166, HLA I as positive and CD31, CD80, CD117, CD133, CD144, c-kit, STRO-1 as negative markers [15]. The availability of elaborate technologies supporting multi-color flow cytometry analysis has allowed scientists to define multiple cellular markers simultaneously, providing immense amount of novel information meanwhile reducing the time spent on data collection [16]. This technological approach can serve as an excellent tool for identification and characterization of MSCs.

Clinical interest has been furthered by the observation that MSC populations display immunomodulatory capacities and their inhibitory effect on T cell proliferation has been studied extensively [17-20]. Although little is known about the molecular mechanisms underlying this phenomena, there is evidence of various factors such as transforming growth factor-β and hepatocyte growth factor [18], prostaglandin E2 [21,22], indoleamine 2,3-deoxygenase [23], heme oxygenase-1 [24], nitric oxide [25], interleukins- 6 and 10, human leukocyte antigen-G5 and matrix metalloproteinases [for reviews, see 26,27] produced by MSCs that could mediate the suppression of T cell proliferation. It has been shown that MSCs can also inhibit the proliferation of T cells by blocking cyclin D2 expression and up-regulating p27Kip1 expression thus arresting cells in the G1 phase of the cell cycle [28]. Other approaches that may be responsible for the ability of MSCs to modulate immune response is induction of CD8+ regulatory T cells [29] or regulatory antigen-presenting cells [30], as well as interference with dendritic cells [21] and inhibition of the formation of cytotoxic T cells [31]. In addition, human MSCs can also inhibit proliferation, differentiation, and chemotaxis of B cells [32]. This immunosuppressive ability of MSCs may have a significant therapeutic potential in the setting of allogeneic transplantation and prevention or treatment of graft-versus-host-disease.

However, to ensure the safety of MSCs intended for the clinical use, all possible threats must be eliminated. The greatest concerns arise about fetal bovine serum (FBS) that is used to supplement most of the cell culture media. The dangers of prion diseases and zoonoses from the FBS are considered to be minimal [33], but it has been shown that 10^8 MSCs grown in the medium supplemented with 20% FBS would carry 7-30 mg of FBS proteins leading to the possible autoimmune reaction against patient's own stem cells [34]. To avoid this risk, the FBS can be substituted with an autologous serum (AS). We have previously shown that ASCs can be effectively cultured and expanded in the presence of AS without the loss of characteristics of MSCs and their differentiation potential [35] and the same applies to BM MSCs [36,37].

This study aimed to test various passages of ASCs, cultured in the medium containing AS, with respect to MSC surface markers, analyzed using 8-color flow cytometry and quantitative real-time PCR, their differentiation potential and immunosuppressive effect in vitro.

Materials and methods

Source of Human Adipose Tissue

Human adipose tissue from abdominal cavity, derived during planned operation, and blood were collected after consent was obtained from the donor (40 years old man, healthy, body mass index – 26.3) in accordance to the permit No.12 by the Latvian Central Medical Ethics Committee. Blood and tissue samples were processed within 3 hours after collection.

Preparation of Autologous Serum

Collected blood was allowed to clot for 1 hour at room temperature (RT). The serum was collected, centrifuged at 2000 rpm for 30 min, filtered through 0.2 μm mesh, aliquoted, and stored at -20^{0}C.

Isolation and Expansion of ASCs

5 ml of adipose tissue were scissored and treated with 0.3% pronase (EMD Millipore, Billerica, Massachusetts, USA) for 1 h at RT with gentle rotation followed by centrifugation for 7 min at 1000 rpm. The pellet was suspended, filtered through 40 μm mesh and centrifuged again for 5 min. Erythrocytes were lysed for 3 min at +37^{0}C using erythrocyte lysis buffer Hybri-Max (Sigma-Aldrich, Steinheim, Germany). Obtained cell pellet was suspended in a fresh cell culture medium (DMEM/F-12 (Life Technologies, Paisley, UK) containing 10% autologous serum, 2 mM L-glutamine (Life Technologies, Paisley, UK), 20 ng/ml basic fibroblast growth factor (BD, Franklin Lakes, New Jersey, USA), 100 U/ml : 100 μg/ml penicillin - streptomycin (Life Technologies, Paisley, UK)) and seeded onto a 75 cm^2 tissue culture flask (regarded as passage 0 (P0)). Cells were cultured at +37^{0}C, 5% CO_2.

Non adherent cells were removed on the next day by extensive washing with phosphate-buffered saline (PBS) (Life Technologies, Paisley, UK). The remaining cells were cultivated in the medium supplemented with 10% AS for first 10 days and 5% AS afterwards. After the second passage, cells were frozen in DMEM/F12 supplemented with 10% dimethyl sulfoxide (Sigma-Aldrich, Steinheim, Germany) and 20% AS and stored in a liquid nitrogen. After thawing ASCs were cultivated as previously through P3 to P8, freezing a fraction of cells before the each subsequent passage. After more than 4 years ASCs from passages 2 to 8 were thawed and used for the following characterization.

Multi-Color Flow Cytometry

Flow cytometry was performed on ASCs P2, P3, P4, P5, and P8. After more than 4 years of cryopreservation, ASCs of each passage were rapidly thawed, resuspended in 2 ml of PBS, centrifuged for 5 min at 600 x g and used for immunostaining. Fluorochrome-labeled anti-human monoclonal antibodies to HLA-DR-V450, CD14/CD19/CD45 cocktail-V500, CD29-PerCP-Cy5.5, CD44-APC-H7 (BD, Franklin Lakes, New Jersey, USA) and CD34-FITC, CD105-PE, CD73-PE-Cy7, CD90-APC (eBioscience, San Diego, California, USA) were used for 8-color flow cytometric analysis. Corresponding isotype controls for gate setting were included in every experiment. In addition, cell viability in every sample was tested using Syto16 fluorescent nucleic acid stain (Life Technologies, Paisley, UK) at FITC channel. Cells were stained as recommended by the manufacturers, washed with PBS, and analysed by 3-laser BD FACSCanto II flow cytometer (BD, Franklin Lakes, New Jersey, USA) using FACSDiva v6.1.3 software. Obtained results were analysed and presented using Infinicyt v1.5.0 (Cytognos, Salamanca, Spain) software.

Flow cytometric cell cycle analysis was performed using the FacsCanto II PE channel, PI-based BD Cycletest Plus kit (BD, Franklin Lakes, New Jersey, USA) and ModFit LT v3.3 software (BD, Franklin Lakes, New Jersey, USA).

In Vitro Differentiation

After the fifth passage ASCs were differentiated into adipocytes, osteoblasts, and chondroblasts (regarded as P6). To induce differentiation, ASCs were cultured in the appropriate induction medium at

+37^{0}C, 5% CO_2. Non-induced cells were maintained in a control medium. Medium was changed every third day. Three replicates for each differentiation were tested.

For adipogenic differentiation, ASCs were cultured in DMEM (high glucose) (Life Technologies, Paisley, UK) supplemented with 10% FBS (Life Technologies, Paisley, UK), 2 mM L-glutamine, 10 µg/ml human insulin (Life Technologies, Paisley, UK), 1 µM dexamethasone (Sigma-Aldrich, Steinheim, Germany), 100 µM indomethacin (Sigma-Aldrich, Steinheim, Germany), 0.5 mM isobutyl-methylxanthine (Sigma-Aldrich, Steinheim, Germany), and 5 µg/ml gentamicin (Life Technologies, Paisley, UK). DMEM (high glucose) supplemented with 10% FBS, 2 mM L-glutamine, and 5 µg/ml gentamicin was used as a control medium. Differentiation was confirmed on day 16 by Oil Red O (Sigma-Aldrich, Steinheim, Germany) staining as previously described [35].

To promote osteogenic differentiation, ASCs were treated with DMEM (low glucose, without L-glutamine and phenol red) (Life Technologies, Paisley, UK) supplemented with 10% FBS, 2 mM L-glutamine, 10 mM glycerol-2-phosphate (Sigma-Aldrich, Steinheim, Germany), 0.1 µM dexamethasone (Sigma-Aldrich, Steinheim, Germany), 50 µM L-ascorbic acid (Sigma-Aldrich, Steinheim, Germany), and 5 µg/ml gentamicin. Control medium consisting of DMEM (low glucose), 10% FBS, 2 mM L-glutamine, and 5 µg/ml gentamicin was used for non-induced cells in osteogenic, as well as chondrogenic differentiation. Osteogenesis was demonstrated on day 28 using Alizarin Red S (Sigma-Aldrich, Steinheim, Germany) staining as previously described [35].

For chondrogenic differentiation, 10 µl of ASCs suspension (concentration $8x10^6$ cells/ml) were allowed to attach to a plastic plate for 30 min at +37^{0}C, 5% CO_2. Then control medium or chondrogenic differentiation medium consisting of DMEM (low glucose, without L-glutamine, and phenol red) supplemented with 10% FBS, 2 mM L-glutamine, 1x insulin-transferrin-selenium-plus (BD, Franklin Lakes, New Jersey, USA), 50 µM L-ascorbic acid, 40µg/ml L-proline (Sigma-Aldrich, Steinheim, Germany), 0.1 µM dexamethasone, 10 ng/ml recombinant human transforming growth factor β3 (Life Technologies, Paisley, UK), and 5 µg/ml gentamicin was added. After 29 days of chondrogenic differentiation, formed cell aggregates were embedded in paraffin, sectioned, and stained with 1% Alcian Blue (Sigma-Aldrich, Steinheim, Germany) in 0.1 N HCl (pH~1) for 30 min followed by washing with 0.1 N HCl.

Total RNA extraction

RNA was extracted from different passages of ASCs immediately after thawing using TRI Reagent (Sigma-Aldrich, Steinheim, Germany) according to the manufacturer's instructions. Quantity and quality of the samples were assessed by measuring the concentration of total RNA and A260/A280 ratio using NanoDrop® ND-1000 spectrophotometer (Thermo Scientific, Wilmington, Delaware, USA).

DNase I treatment and cDNA synthesis

1 µg of total RNA was treated with 1 U RNase-free DNase I (Thermo Scientific, Vilnius, Lithuania) for 30 min at +37^{0}C to remove traces of genomic DNA. After the measurement of concentration of DNase-treated sample with NanoDrop® ND-1000 spectrophotometer, 500 ng of RNA were reverse transcribed into cDNA with oligo$(dT)_{18}$ primers using RevertAid first strand cDNA synthesis kit (Thermo Scientific, Vilnius, Lithuania) in a total volume of 20 µl according to the manufacturer's instructions. Minus reverse transcriptase (RT) sample was also prepared in the same manner by omitting RT from the reaction.

Quantitative Real-Time RT-PCR

Real-time PCR was carried out using MiniOpticon Real-time PCR System (Bio-Rad, Hercules, California, USA). Each reaction was run in triplicate and contained 1 µl of 9-fold diluted cDNA template, primer pairs (synthesized at Metabion, Martinsried, Germany) as listed in Table 1 at a final concentration of 400 nM, 12.5 µl 2x ABsolute Blue QPCR SYBR Green Low ROX Mix (Thermo Scientific, Vilnius, Lithuania) and nuclease-free water

(Thermo Scientific, Vilnius, Lithuania) to 25 µl. PCR cycling conditions included a 95^0C heating step for 15 min to activate DNA polymerase, then 40 cycles of 95^0C for 30 s, 60^0C (CD90 - 58^0C) for 30 s and 72^0C for 30 s. A melting curve was generated at the end of every run to ensure the amplification of a single product. Minus RT controls as well as non-template control were run each time to inspect for possible contamination. PCR efficiencies of each primer pair were obtained from standard curves using 3-fold dilution series of cDNA sample. PCR efficiencies of all primer pairs used in the experiment were in a range from 93% to 99%. For the analysis of relative gene expression $2^{-\Delta C_T}$ method was used.

Table 1. Nucleotide sequences of primers used for real time PCR

Gene	Primer sequence (5' → 3')
β-Actin	Fw: GAGCTACGAGCTGCCTGAC
	Rw: GGATGCCACAGGACTCCATG
CD29	Fw: GAGAAGGATGTTGACGACTGTT
	Rw: CAGTGGGACACTCTGGATTCT
CD44	Fw: CCTCTGCAAGGCTTTCAATA
	Rw: CTTCTATGAACCCATACCTGC
CD73	Fw: CAGCATTCCTGAAGATCCAAG
	Rw: GATTGAGAGGAGCCATCCAG
CD90	Fw: GTCCTCTACTTATCCGCCTTC
	Rw: GACCAGTTTGTCTCTGAGCAC
CD105	Fw: CTCAAGACCAGGAAGTCCATA
	Rw: GATGAGGAAGGCACCAAAG

Co-culture of ASCs and autologous PBMNCs

Autologous peripheral blood mononuclear cells (PBMNCs) were obtained from freshly isolated peripheral blood samples by Ficoll-Paque Premium (GE Healthcare, Uppsala, Sweden) density gradient. $5x10^4$ PBMNCs were cultured in RPMI-1640 (Life Technologies, Paisley, UK) supplemented with 10% AS, 2 mM L-glutamine and 100 U/ml : 100 µg/ml penicillin - streptomycin in the presence of ASCs (P3, P6, P9) at different ratios (ASCs:PBMNCs – $5x10^4$:$5x10^4$ (1:1), $5x10^3$:$5x10^4$ (1:10), $2.5x10^3$:$5x10^4$ (1:20), $5x10^2$:$5x10^4$ (1:100)) and phytohaemagglutinin (Sigma-Aldrich, Steinheim, Germany) at a final concentration 4 µg/ml for 96 h at $+37^0$C, 5% CO_2. 1 µCi of [3H]-deoxythymidine (GE Healthcare, Little Chalfont, UK) was added to each well for the last 18 h. Analysis of radioactive thymidine incorporation was done using liquid scintilation beta counter (Beckman Coulter, Brea, California, USA).

ELISA

Cell culture supernatants either from co-culture of ASCs and autologous PBMNCs or each cell type alone were collected after 48 hours and tested for the presence of TNF and IL10 by ELISA (BD OptEIA, BD, Franklin Lakes, New Jersey, USA) according to the manufacturer's instructions.

Statistical Analysis

Data from real-time PCR and co-culture of ASCs and autologous PBMNCs experiments were presented as mean ± standard deviation (SD) from triplicates.

The statistical analysis was assessed by unpaired Student's t-test and $p < 0.05$ was considered statistically significant.

Results

Morphology of ASCs

Two days after isolation plastic-adherent cells were observed. Approximately half of the obtained cells were spindle-shaped with fibroblast-like morphology, characteristic to MSCs [1], but the rest of the cells were rounded (Figure 1A). Few cell clusters with endothelial appearance, similar to those reported after MSC isolation from umbilical cord [38], were also observed, but after the first passage only cells with MSC phenotype remained. The first ten days ASCs were grown in a medium supplemented with 10% AS but afterwards it was reduced to 5%. After the second passage, cells were frozen and stored in a liquid nitrogen for two months. After thawing, ASCs were seeded onto tissue cultured flasks (regarded as P3) and cultured as previously (Figure 1B). When cells reached 80% confluence, they were trypsinized and subcultured, freezing a part of cells in parallel. During the passaging, cells preserved their fibroblast-like morphology till inspected eighth passage (Figure 1C, D).

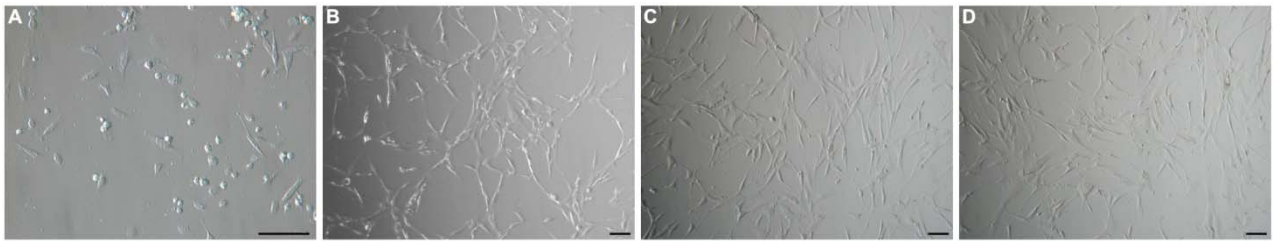

Figure 1. Morphology of ASCs. (A) ASCs on the second day after isolation. (B) ASCs at passage 3. (C) ASCs at passage 6. (D) ASCs at passage 8. Scale bar 100 μm.

Characterization of ASC Surface Markers

Flow cytometric analysis was performed on ASCs cryopreserved after passages 2, 3, 4, 5, 8 and stored for more than 4 years. Cell viability test (Syto 16 staining), which was carried out for each thawed vial, showed that concentration of live cells in all samples was at least 95% (Figure 2). 8-color flow cytometry was used to test 10 different cell surface markers simultaneously on each cell. Obtained results showed that all the cells were positive for MSC markers CD29, CD44, CD73, CD90, CD105 and negative for such markers as HLA-DR, CD34 and a cocktail of CD14/CD19/CD45. While comparing mean fluorescence intensity of individual markers through different passages tested, an increase of marker fluorescence intensity in each subsequent passage was observed, except for a sharp decline in CD44 expression at P5 (Figure 3). Since the ASC population remained phenotypically homogeneous, expressing CD29, CD44, CD73, CD90, and CD105 throughout all passages tested, the increase in fluorescence intensity may indicate the accumulation of protein expression with subsequent passaging. When fluorescence intensity was compared between markers, it can be seen that CD90 was the most abundant marker on the surface of ASCs followed by CD29 and CD73, but CD105 showed the lowest level of expression throughout all passages. Collected data suggest that the peak of protein expression for CD73 and CD44 markers can be observed at P5 and P4 respectively, but in case of CD29, CD90 and CD105 the increase until P8 can be detected.

To complement the flow cytometry data, the expression of positive MSC surface marker genes was analysed with real-time PCR (Figure 4). Obtained results show that the expression of CD29, CD44, CD73, and CD90 genes increased until P4 or P5 and reduced afterwards, but the highest level of CD105 gene expression was detected at P2 followed by decline in subsequent passages.

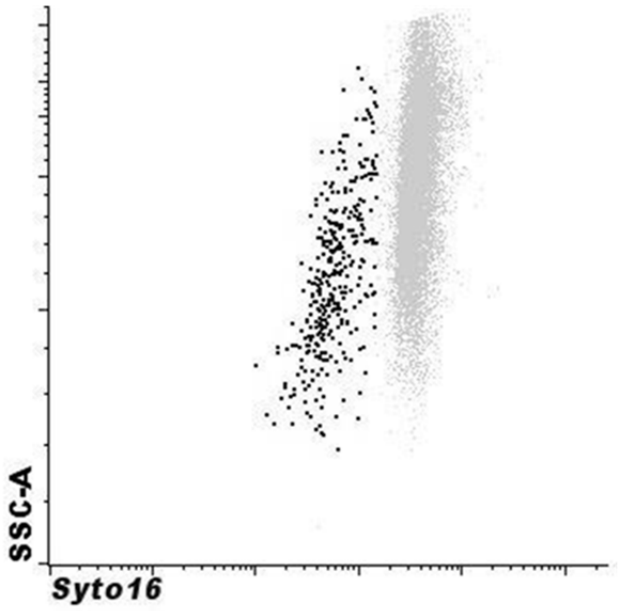

Figure 2. Syto 16 viability stain of ASCs at passage 5 after more than 4 years of cryopreservation. 97% live Syto16 positive cells (grey cluster) are discriminated from Syto16 negative necrotic and apoptotic cells (black dots). Flow cytometry, green fluorescence versus side scatter plot, data analysed by Infinicyt (v1.5.0).

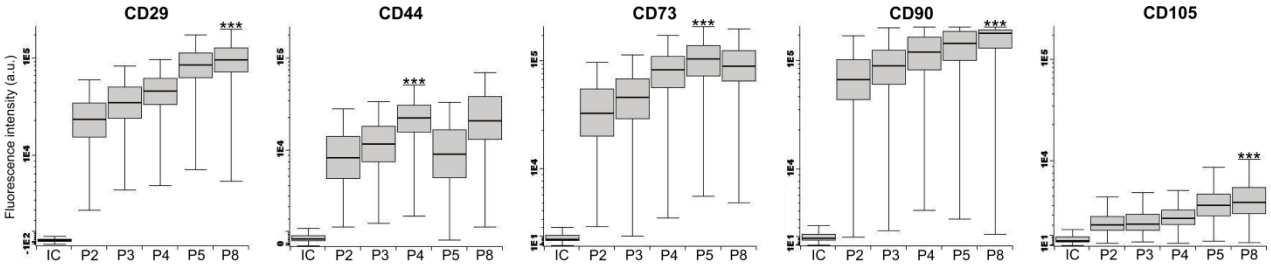

Figure 3. Fluorescence intensity analysis of cell surface marker expression on ASCs of different passages. Results are shown as box plots with median value (line), 25th and 75th percentiles as box and 10th and 90th percentiles as whiskers. Data analysis by Infinicyt software (v1.5.0). Asterisks at passage with the highest fluorescence intensity indicate statistically significant increase when compared to P2. *** $p < 0.001$. IC – isotype control; P – passage; a.u. - arbitrary units.

Additional cell cycle analysis demonstrated that S and G2/M phases comprise a total of approximately 2.8% at P2 and P3, 3.4% at P4 and P5, and 6.6% at P8 (Table 2), showing an increasing cellular activity with following passages. The coefficient of variation of the G1 peak was lower than 4% in every ASC passage tested favouring the quality of cell cycle data. Collectively these results indicate high cell viability after long term cryopreservation and homogeneity of isolated ASCs culture with intensifying positive ASC surface protein expression and cell proliferation in each subsequent passage.

Multilineage differentiation of ASCs

Multilineage differentiation of ASCs cultured in the medium supplemented with AS from P3 has been shown previously [35]. To test whether these cells maintain potential of differentiation in later passages, ASCs from P6 were differentiated into adipocytes, osteocytes, and chondrocytes using the same lineage specific induction factors as before. Adipogenic differentiation and intracellular lipid accumulation was confirmed after 16 days by Oil Red O staining (Figure 5A, D). Osteogenic and chondrogenic induction of ASCs was assessed after 28 days by Alizarin Red S (Figure 5B, E) and Alcian Blue

(Figure 5C, F) staining respectively. Obtained results showed that ASCs from P6 can be effectively differentiated into adipocytes and chondrocytes, but formation of calcified extracellular matrix that would confirm osteogenic differentiation is very poor.

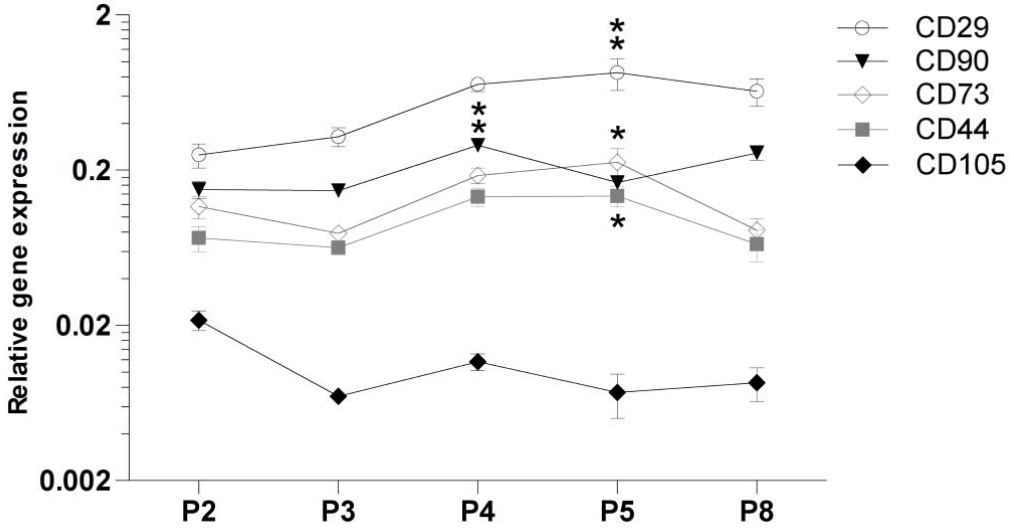

Figure 4. Comparison of relative expression level of positive MSC surface marker genes CD29, CD44, CD73, CD90, and CD105 in ASCs of different passages by real-time PCR (data normalized to β-Actin). Data represent the mean ± SD of triplicates. An asterisk at passage with the highest expression indicates statistically significant increase when compared to P2; *p < 0.05, **p < 0.01. P – passage.

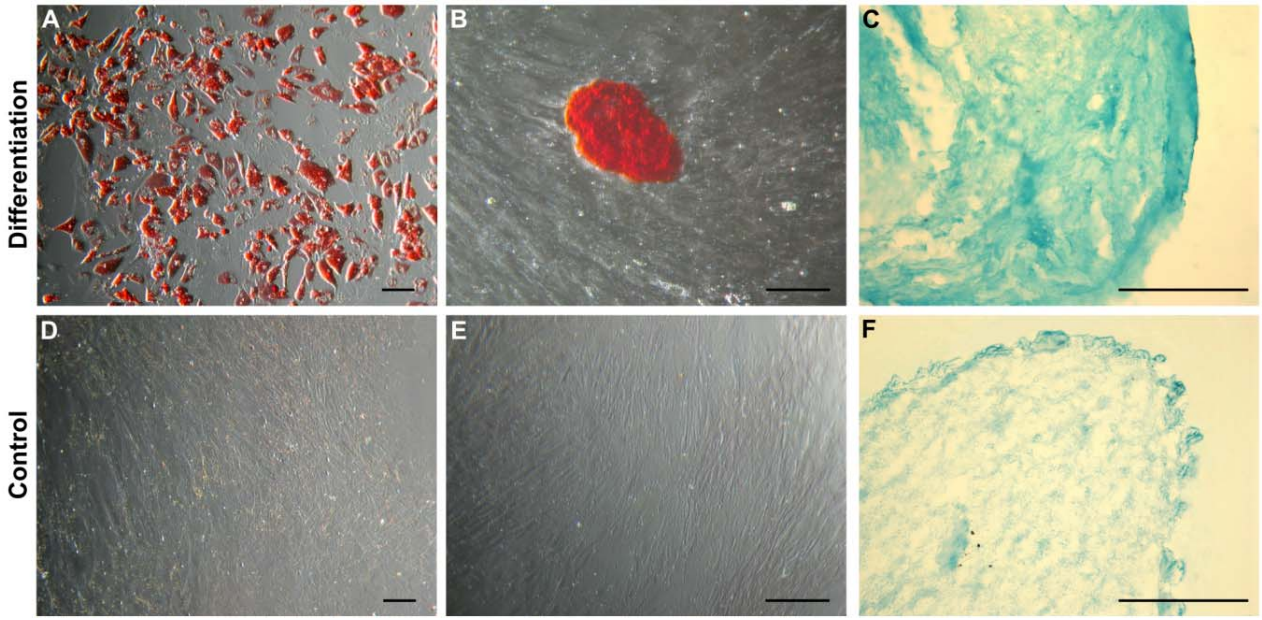

Figure 5. ASCs from P6 differentiated towards adipogenic, osteogenic, and chondrogenic lineages. (A, D) Oil Red O staining of differentiated and control cells. (B, E) Alizarin Red S staining of differentiated and control cells. (C, F) Alcian Blue staining of differentiated and control cells. Scale bar 100 μm.

Table 2. Percentage of ASCs of different passages in S and G2/M phases determined by propidium iodide staining

Passage	S phase %	G2/M phase %	Total %
P2	0.58	2.2	2.78
P3	1.04	1.83	2.87
P4	0.39	3.0	3.39
P5	0.83	2.6	3.43
P8	2.49	4.13	6.62

P – passage.

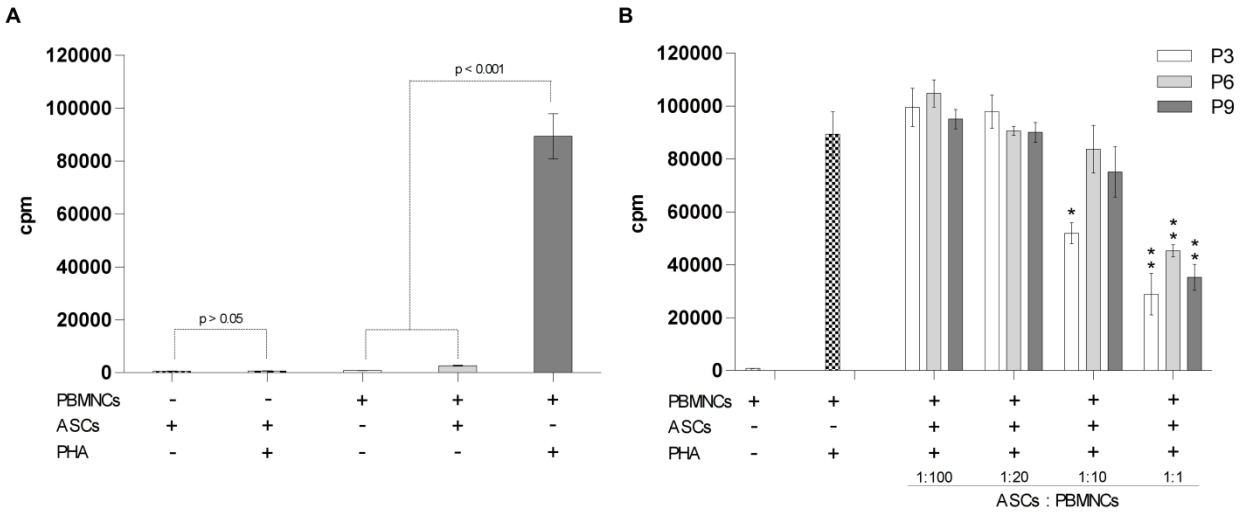

Figure 6. Co-culture of ASCs and autologous PBMNCs. (A) Negative and positive controls. (B) The suppressive effect of ASCs of different passages on the proliferation of PHA-stimulated PBMNCs *in vitro*. The results are expressed as counts per minute (cpm). Data represent the mean ± SD of triplicate wells. An asterisk indicates statistically significant difference when compared to the PHA-stimulated PBMNCs; *p < 0.05, **p < 0.01. P – passage; PHA – phytohemagglutinin.

Immunosuppressive Properties of ASCs

The effect of ASCs from P3, P6, and P9 on autologous PBMNC proliferation was evaluated by co-culture of ASCs and phytohemagglutinin (PHA) stimulated PBMNCs in various proportions. PBMNCs subjected to PHA stimulation was used as a positive control and PBMNCs alone as a negative control. Notable ASCs ability to induce proliferation of PBMNCs was not found and PHA stimulation did not have a proliferative effect on ASCs (Figure 6A). When co-culturing ASCs and PHA-stimulated autologous PBMNCs, a dose dependent immunosuppressive effect of ASCs of all three passages were observed, with a peak at ASCs:PBMNCs ratio 1:1 (Figure 6B). Significant reduction in PBMNC proliferation was also detected at ASCs:PBMNCs ratio 1:10 with ASCs from P3. If the proportion of ASCs:PBMNCs exceeded 1:10, the PHA activated PBMNC proliferation was not affected.

In addition, cell culture supernatants either from co-culture of ASCs and autologous PBMNCs at ratio 1:1 or each cell type alone were collected after 48 hours and tested for the presence of TNF-α and IL-10 by ELISA (data not shown). Obtained results showed significant decline of TNF-α level in a co-culture with ASCs from P6 and P9, when compared to stimulated PBMNCs. When ASCs from P3 were tested, only slight decrease in cytokine production was observed.

No considerable changes for IL-10 level in the co-culture were discovered in any of three passages tested.

Discussion

In a past decade a lot of studies have been devoted to extensively characterizing ASCs according to their phenotypical and functional characteristics starting from cells in stromal vascular fraction (SVF) through late passages [39-46]. Comprehensive analysis of cultured ASCs phenotype has been published recently [47] and properties of new scientific tools such as multi-color flow cytometry have been embraced to characterize different populations of MSCs [42,47-49]. Since ASCs hold several suitable characteristics for therapeutic use, including differentiation potential and immune-modulatory capacities, their safety must be assured before clinical applications. Hence increasing popularity of possible stem cell therapies has led researchers and manufacturers to develop cell culture media devoid of animal components that could cause the possible autoimmune reaction against patient's own stem cells. In our studies for the expansion of autologous stem cells with a potential therapeutic value we use autologous serum instead of FBS for cell culture media as this approach does not influence the characteristics of ASCs [35]. It has been shown that MSCs of various origin proliferate faster [37,50-52] and maintain higher unmethylated state in a long-term culture [53] when cultured in a medium containing AS, but not FBS. In the current study, different passages of ASCs, cultured in the presence of AS, was used to test their surface marker expression, ability to differentiate into adipocytes, osteocytes, chondrocytes, and immunosuppressive properties in vitro.

In our study we have tested ASCs starting from P2. We have chosen this passage because from the 5 ml of fat tissue as an initial material we can harvest around 10^7 cells at the end of P2 that are frozen for a long term storage until the clinical necessity for the patient arises. Fraction of the cryopreserved cells can be thawed, propagated and used for various assays based on patient's needs at any moment. Here we used 5% AS for a growth medium because it is sufficient for effective proliferation of ASCs and more less disruptive to the patient, since the amount of blood needed for the acquirement of AS is lower than it would be if the 10% AS would be applied. We have determined that 5 ml of fat tissue yield approximately 10^9 ASCs at the end of P5 at these culture conditions. It is sufficient for 3-4 repeated injections of ASCs for a 90-100 kg patient using therapeutic dose of $3x10^6$ cells per kg of body weight.

When clinical need for the patient emerges, ASCs from P2 are thawed, expanded till P5 and frozen again. It is important because a) cellular properties must be tested again before injection at the given time point; b) the ability of patient to receive the therapy may not coincide with the time of readiness of ASCs; c) the planned time of injection may be delayed; d) preparation of ASC material can be performed remotely from a medical institution. Therefore, in this study we used flow cytometry analysis to determine the changes in cell surface marker expression at different passages of ASCs after more than 4 years of cryopreservation and double freezing immediately after thawing as it would be just before stem cell injection therapy.

8-color flow cytometry analysis allowed us to detect 10 cell surface markers simultaneously on each cell. We showed that all ASCs, cultured in the medium containing AS, express typical MSC markers CD29, CD44, CD73, CD90, and CD105 concurrently irrespective of passage, demonstrating a very homogeneous cell population as of P2. However median fluorescence intensity of positive cell surface markers increased with each subsequent passage. Negative markers such as HLA-DR, CD34, CD14, CD19, and CD45 were not detected. Other reports have demonstrated the incrementation of expression pattern of positive MSC surface markers with passages [41, 43, 45], while others have not detected the difference from P3 to P12 [46]. The greatest disagreements exist over the expression of CD34 in ASCs. Few studies failed to detect CD34 [4,44], but others reported high levels of CD34 expression [39,54]. It has been recently shown that cells in the SVF and early passages of ASCs express CD34, but the level of expression diminishes with further cell culturing [41-43], although contrary data have also been published showing not only increase of CD34 in later passages, but also accumulation of

haematopoietic marker CD45 in ASCs [45]. As possible reasons to these discrepancies researchers suggest factors secreted by adjacent cells in the early passages [55], different cell culture conditions, donor-specific variability, choice in antibody labeling [47], and individual gating strategies used for flow cytometry [42]. Since we have not tested the expression of the above mentioned surface markers at P0 or P1, we cannot speculate of whether ASCs, cultured in the presence of AS, express CD34 or CD45 at very early passages. But starting from P2, the cultured cells were homogenously CD29, CD44, CD73, CD90, and CD105 positive.

ASC ability to differentiate into other cell types of mesodermal origin is a keystone of verifying their identity. Our results show capacity of ASCs to efficiently differentiate into adipogenic and chondrogenic lineages not only at P3, as we have determined previously [35], but also at P6. However ASCs differentiation into osteocytes was weak at P3 and obtained data suggest that it may have decreased even more at P6. Comparison of the differentiation samples from P3 and P6 was done by visual assessment, and the aim of in vitro differentiation was to evaluate the potency of ASCs from various passages to differentiate into other cell types of mesodermal origin as such not to directly compare the extent of each differentiation between P3 and P6. In the case of osteogenic differentiation the weak formation of calcified extracellular matrix was observed in all triplicates at P3, but Alizarin Red S staining was detected only in one triplicate at P6. As this most likely represents a characteristic of the ASC donor, since the same protocol of differentiation has yielded reliable results with ASCs from different donors (unpublished observations, A.Bogdanova), it is impossible to state that the ability of ASCs, cultured in AS, to differentiate into osteogenic lineage diminishes in later passages. Others show that differential capacity of ASCs, when cultured in the standard media, is preserved through 10 to 13 passages [56,57], but decreases at P25 [44].

To determine the inhibitory effect of ASCs on T cell proliferation, we used ASCs from P3, P6 and P9 as a representation for cryopreserved ASCs from P2, P5 and P8 after thawing and seeding. Data from co-culture of ASCs and autologous PBMNCs showed that ASCs, when grown in the medium supplemented with AS, suppress the proliferation of PBMNCs in a dose dependent manner likewise ASCs cultured in a standard medium with FBS [22,58]. Our results demonstrated that ASCs from P3, P6 and P9 show significant reduction in PBMNC proliferation at ASCs: PBMNCs ratio 1:1, but only ASCs from P3 suppress proliferation of PBMNCs at ASCs:PBMNCs ratio 1:10, suggesting that ASCs from early passages may exhibit more pronounced immunosuppressive effect than those of later passages. The immunosuppressive properties of different MSC populations in prolonged culture have not been widely studied. Only few studies have been published regarding this subject, showing that immunosuppressive effect of ASCs does not differ between P2 and P5 [22] and BM MSCs do not lose immunosuppressive activity through 6 or 7 passages [59], but it decreases after P7 in comparison to earlier passages [60].

It has been shown that the time of ASC culturing can affect their immunophenotypic [45], differential [44], and proteome profile [61] as well as mechanical properties [62]. However clinical applications require extensive expansion of cells to meet the sufficient amount of cells for a patient.

The data presented here demonstrated that ASCs, cultured in the medium supplemented with 5% AS, can be effectively propagated through 8 passages without the loss of fibroblast-like morphology, MSC surface marker expression, differentiation and immunomodulatory potential even after double freezing and more than 4 years of cryopreservation. Our results suggest that ASCs from P5, when cultured in such conditions, represent a highly homogeneous cell population with a peak accumulation of MSC surface protein expression bearing multilineage differentiation ability and significant immunosuppressive properties that can be used for therapeutic purposes.

Disclosure of interests

The authors declare no conflicts of interest.

Acknowledgments

This work was financially supported by the European Regional Development Fund grant 2010/0230/2DP/2.1.1.1.0/10/APIA/VIAA/075. We thank Dr.habil.med. R. Bruvere for performing light microscopy, Dr.habil.biol. P. Pumpens for scientific advice, and "GenMedica" Ltd.

References

[1] Zuk, PA; Zhu, M; Mizuno, H; Huang, J; Futrell, JW; Katz, AJ; et al. Multilineage cells from human adipose tissue: implications for cell-based therapies. *Tissue Eng*, 2001, 7:211-26.

[2] Kern, S; Eichler, H; Stoeve, J; Klüter, H; Bieback, K. Comparative analysis of mesenchymal stem cells from bone marrow, umbilical cord, or adipose tissue. *Stem Cells*, 2006, 24:1294-1301.

[3] Jeon, ES; Moon, HJ; Lee, MJ; Song, HY; Kim, YM; Bae, YC; et al. Sphingosylphosphorylcholine induces differentiation of human mesenchymal stem cells into smooth-muscle-like cells through a TGF-β-dependent mechanism. *J Cell Sci*, 2006, 119:4994–5005.

[4] Zuk, PA; Zhu, M; Ashjian, P; De Ugarte, DA; Huang, JI; Mizuno, H; et al. Human adipose tissue is a source of multipotent stem cells. *Mol Biol Cell,* 2002, 13:4279-95.

[5] Lee, JH; Kemp, DM. Human adipose-derived stem cells display myogenic potential and perturbed function in hypoxic conditions. *Biochem Biophys Res Commun*, 2006, 341:882-88.

[6] Planat-Bénard, V; Menard, C; André, M; Puceat, M; Perez, A; Garcia-Verdugo, JM; et al. Spontaneous cardiomyocyte differentiation from adipose tissue stroma cells. *Circ Res,* 2004, 94:223-29.

[7] Jang, S; Cho, HH; Cho, YB; Park, JS; Jeong, HS. Functional neural differentiation of human adipose tissue-derived stem cells using bFGF and forskolin. *BMC Cell Biol*, 2010, 11:25. doi:10.1186/1471-2121-11-25.

[8] Cao, Y; Sun, Z; Liao, L; Meng, Y; Han, Q; Zhao, RC. Human adipose tissue-derived stem cells differentiate into endothelial cells in vitro and improve postnatal neovascularization in vivo. *Biochem Biophys Res Commun,* 2005, 332:370-79.

[9] Taléns-Visconti, R; Bonora, A; Jover, R; Mirabet, V; Carbonell, F; Castell, JV; et al. Hepatogenic differentiation of human mesenchymal stem cells from adipose tissue in comparison with bone marrow mesenchymal stem cells. *World J Gastroenterol*, 2006, 12:5834-45.

[10] Chandra, V; Swetha, G; Muthyala, S; Jaiswal, AK; Bellare, JR; Nair, PD; et al. Islet-like cell aggregates generated from human adipose tissue derived stem cells ameliorate experimental diabetes in mice. *PloS ONE*, 2011, 6(6):e20615. doi:10.1371/journal.pone.0020615.

[11] Rodriguez, AM; Elabd, C; Amri, EZ; Ailhaud, G; Dani, C. The human adipose tissue is a source of multipotent stem cells. *Biochimie,* 2005, 87:125-28.

[12] Kakudo, N; Shimotsuma, A; Kusumoto, K. Fibroblast growth factor-2 stimulates adipogenic differentiation of human adipose-derived stem cells. *Biochem Biophys Res Commun*, 2007, 359:239-44.

[13] Fraser, JK; Wulur, I; Alfonso, Z; Hedrick, MH. Fat tissue: an underappreciated source of stem cells for biotechnology. *Trends Biotechnol*, 2006, 24:150-54.

[14] Dominici, M; Le Blanc, K; Mueller, I; Slaper-Cortenbach, I; Marini, FC; Krause, DS; et al. Minimal criteria for defining multipotent mesenchymal stromal cells. The International Society for Cellular Therapy position statement. *Cytotherapy,* 2006, 8:315-17.

[15] Schäffler, A; Büchler, C. Concise review: adipose tissue-derived stromal cells – basic and clinical implications for novel cell-based therapies. *Stem Cells*, 2007, 25:818-27.

[16] De Rosa, SC; Brenchley, JM; Roederer, M. Beyond six colors: a new era in flow cytometry. *Nat Med*, 2003, 9:112-17.

[17] Bartholomew, A; Sturgeon, C; Siatskas, M; Ferrer, K; McIntosh, K; Patil, S; et al. Mesenchymal stem cells suppress lymphocyte proliferation in vitro and prolong skin graft survival in vivo. *Exp Hematol,* 2002, 30:42-48.

[18] Di Nicola, M; Carlo-Stella, C; Magni, M; Milanesi, M; Longoni, PD; Matteucci, P; et al. Human bone marrow stromal cells suppress T-lymphocyte proliferation induced by cellular or nonspecific mitogenic stimuli. *Blood,* 2002, 99:3838-43.

[19] Le Blanc, K; Tammik, L; Sundberg, B; Haynesworth, SE; Ringdén, O. Mesenchymal stem cells inhibit and stimulate mixed lymphocyte cultures and mitogenic responses independently of the major histocompatibility complex. *Scand J Immunol*, 2003, 57:11-20.

[20] Tse, WT; Pendleton, JD; Beyer, WM; Egalka, MC; Giunan, EC. Suppression of allogeneic T-cell proliferation by human marrow stromal cells: implications in transplantation. *Transplantation,* 2003, 75:389-97.

[21] Aggarwal, S; Pittenger, MF. Human mesenchymal stem cells modulate allogeneic immune cell responses. *Blood*, 2005, 105:1815-22.

[22] Cui, L; Yin, S; Liu, W; Li, N; Zhang, W; Cao, Y. Expanded adipose-derived stem cells suppress mixed lymphocyte reaction by secretion of prostaglandin E2. *Tissue Eng,* 2007, 13:1185-95.

[23] Meisel, R; Zibert, A; Laryea, M; Göbel, U; Däubener, W; Dilloo D. Human bone marrow stromal cells inhibit allogeneic T-cell responses by indoleamine 2,3-

dioxygenase-mediated tryptophan degradation. *Blood*, 2004, 103:4619-21.

[24] Chabannes, D; Hill, M; Merieau, E; Rossignol, J; Brion, R; Soulillou, P; et al. A role for heme oxygenase-1 in the immunosuppressive effect of adult rat and human mesenchymal stem cells. *Blood,* 2007, 110:3691-94.

[25] Sato, K; Ozaki, K; Oh, I; Meguro, A; Hatanaka, K; Nagai, T; et al. Nitric oxide plays a critical role in suppression of T-cell proliferation by mesenchymal stem cells. *Blood*, 2007, 109:228-34.

[26] Abumaree, M; Al Jumah, M; Pace, RA; Kalionis, B. Immunosuppressive properties of mesenchymal stem cells. *Stem Cell Rev*, 2012, 8:375-92.

[27] De Miguel, MP; Fuentes-Julián, S; Blázquez-Martínez, A; Pascual, CY; Aller, MA; Arias, J; et al. Immunosuppressive properties of mesenchymal stem cells: advances and applications. *Curr Mol Med*, 2012, 12:574-91.

[28] Glennie, S; Soeiro, I; Dyson, PJ; Lam, E; Dazzi, F. Bone marrow mesenchymal stem cells induce division arrest anergy of activated T cells. *Blood,* 2005, 105:2821-27.

[29] Djouad, F; Plence, P; Bony, C; Tropel, P; Apparailly, F; Sany, J; et al. Immunosuppressive effect of mesenchymal stem cells favors tumor growth in allogeneic animals. *Blood,* 2003, 102:3837-44.

[30] Beyth, S; Borovsky, Z; Mevorach, D; Liebergall, M; Gazit, Z; Aslan, H; et al. Human mesenchymal stem cells alter antigen-presenting cell maturation and induce T-cell unresponsiveness. *Blood*, 2005, 105:2214-19.

[31] Rasmusson, I; Ringdén, O; Sundberg, B; Le Blanc, K. Mesenchymal stem cells inhibit the formation of cytotoxic T lymphocytes, but not activated cytotoxic T lymphocytes or natural killer cells. *Transplantation,* 2003, 76:1208-13.

[32] Corcione, A; Benvenuto, F; Ferretti, E; Giunti, D; Cappiello, V; Cazzanti, F; et al. Human mesenchymal stem cells modulate B-cell functions. *Blood,* 2006, 107:367-72.

[33] Doerr, HW; Cinatl, J; Stürmer, M; Rabenau, HF. Prions and orthopedic surgery. *Infection*, 2003, 31:163-71.

[34] Spees, JL; Gregory, CA; Singh, H; Tucker, HA; Peister, A; Lynch, PJ; et al. Internalized antigens must be removed to prepare hypoimmunogenic mesenchymal stem cells for cell and gene therapy. *Mol Ther*, 2004, 9:747-56.

[35] Bogdanova, A; Berzins, U; Bruvere, R; Kozlovska, T. Adipose-derived stem cells cultured in autologous serum maintain the characteristics of mesenchymal stem cells. *Proc Latv Acad Sci., Sect B*, *Nat Exact Appl Sci*, 2010, 64:106-13.

[36] Stute, N; Holtz, K; Bubenheim, M; Lange, C; Blake, F; Zander, AR. Autologous serum for isolation and expansion of human mesenchymal stem cells for clinical use. *Exp Hematol*, 2004, 32:1212-25.

[37] Shahdadfar, A; Frønsdal, K; Haug, T; Reinholt, FP; Brinchmann, JE. In vitro expansion of human mesenchymal stem cells: choice of serum is a determinant of cell proliferation, differentiation, gene expression, and transcriptome stability. *Stem Cells*, 2005, 23:1357-66.

[38] Secco, M; Zucconi, E; Vieira, NM; Fogaça, LLQ; Cerqueira, A; Carvalho, MDF; et al. Multipotent stem cells from umbilical cord: cord is richer than blood! *Stem Cells*, 2008, 26:146-50.

[39] Gronthos, S; Franklin, DM; Leddy, HA; Robey, PG; Storms, RW; Gimble, JM. Surface protein characterization of human adipose tissue-derived stromal cells. *J Cell Physiol*, 2001, 189:54-63.

[40] Katz, AJ; Tholpady, A; Tholpady, SS; Shang, H; Ogle, RC. Cell surface and transcriptional characterization of human adipose-derived adherent stromal (hADAS) cells. *Stem Cells*, 2005, 23:412-23.

[41] Mitchell, JB; McIntosh, K; Zvonic, S; Garrett, S; Floyd, ZE; Kloster, A; et al. Immunophenotype of human adipose-derived cells: temporal change in stromal-associated and stem cell–associated markers. *Stem Cells,* 2006, 24:376-85.

[42] Astori, G; Vignati, F; Bardelli, S; Tubio, M; Gola, M; Albertini, V; et al. "In vitro" and multicolor phenotypic characterization of cell subpopulations identified in fresh human adipose tissue stromal vascular fraction and in the derived mesenchymal stem cells. *J Transl Med,* 2007, 5:55.

[43] Varma, MJO; Breuls, RGM; Schouten, TE; Jurgens, WJFM; Bontkes, HJ; Schuurhuis, GJ; et al. Phenotypical and functional characterization of freshly isolated adipose tissue-derived stem cells. *Stem Cells Dev,* 2007, 16:91-104.

[44] Zhu, Y; Liu, T; Song, K; Fan, X; Ma, X; Cui, Z. Adipose-derived stem cell: a better stem cell than BMSC. *Cell Biochem Funct*, 2008, 26:664-75.

[45] Park, E; Patel, AN. Changes in the expression pattern of mesenchymal and pluripotent markers in human adipose-derived stem cells. *Cell Biol Int*, 2010, 34:979-84.

[46] Yang, XF; He, X; He, J; Zhang, LH; Su, XJ; Dong, ZY; et al. High efficient isolation and systematic identification of human adipose-derived mesenchymal stem cells. *J Biomed Sci,* 2011, 18:59. doi:10.1186/1423-0127-18-59.

[47] Baer, PC; Kuçi, S; Krause, M; Kuçi, Z; Zielen, S; Geiger, H; et al. Comprehensive phenotypic characterization of human adipose-derived stromal/stem cells and their subsets by a high throughput technology. *Stem Cells Dev*, 2013, 22:330-39.

[48] Lin, K; Matsubara, Y; Masuda, Y; Togashi, K; Ohno, T; Tamura, T; et al. Characterization of adipose tissue-derived cells isolated with the Celution system. *Cytotherapy,* 2008, 10:417-26.

[49] Martins, AA; Paiva, A; Morgado, JM; Gomes, A; Pais, ML. Quantification and immunophenotypic characterization of bone marrow and umbilical cord blood mesenchymal stem cells by multicolor flow cytometry. *Transplant Proc,* 2009, 41:943-46.

[50] Mizuno, N; Shiba, H; Ozeki, Y; Mouri, Y; Niitani, M; Inui, T; et al. Human autologous serum obtained using a completely closed bag system as a substitute for foetal calf serum in human mesenchymal stem cell cultures. *Cell Biol Int,* 2006, 30:521-24.

[51] Nimura, A; Muneta, T; Koga, H; Mochizuki, T; Suzuki, K; Makino, H; et al. Increased proliferation of human synovial mesenchymal stem cells with autologous human serum. Comparisons with bone marrow mesenchymal stem cells and with fetal bovine serum. *Arthritis Rheum*, 2008, 58:501–10.

[52] Im, W; Chung, J; Kim, SH; Kim, M. Efficacy of autologous serum in human adipose-derived stem cells; cell markers, growth factors and differentiation. *Cell Mol Biol* (Noisy-le-grand), 2011, 57. Suppl:OL1470-5.

[53] Dahl, JA; Duggal, S; Coulston, N; Millar, D; Melki, J; Shahdadfar, A; et al. Genetic and epigenetic instability of human bone marrow mesenchymal stem cells expanded in autologous serum or fetal bovine serum. *Int J Dev Biol,* 2008, 52:1033-42.

[54] Festy, F; Hoareau, L; Bes-Houtmann, S; Péquin, AM; Gonthier, MP; Munstun, A; et al. Surface protein expression between human adipose tissue-derived stromal cells and mature adipocytes. *Histochem Cell Biol*, 2005, 124:113-21.

[55] Chamberlain, G; Fox, J; Ashton, B; Middleton, J. Concise review: mesenchymal stem cells: their phenotype, differentiation capacity, immunological features, and potential for homing. *Stem Cells*, 2007, 25:2739-49.

[56] Wall, ME; Bernacki, SH; Loboa, EG. Effects of serial passaging on the adipogenic and osteogenic differentiation potential of adipose-derived human mesenchymal ste cells*. Tissue Eng*, 2007, 13:1291-98.

[57] Gruber, HE; Somayaji, S; Riley, F; Hoelscher, GL; Norton, HJ; Ingram, J; et al. Human adipose-derived mesenchymal stem cells: serial passaging, doubling time and cell senescence. *Biotech Histochem*, 2012, 87:303-11.

[58] Yañez, R; Lamana, ML; García-Castro, J; Colmenero, I; Ramírez, M; Bueren, JA. Adipose tissue-derived mesenchymal stem cells have in vivo immunosuppressive properties applicable for the control of the graft-versus-host disease. *Stem Cells*, 2006, 24:2582-91.

[59] Samuelsson, H; Ringdén, O; Lönnies, H; Le Blanc, K. Optimizing in vitro conditions for immunomodulation and expansion of mesenchymal stromal cells. *Cytotherapy*, 2009, 11:129-36.

[60] Auletta, JJ; Zale, EA; Welter, JF; Solchaga, LA. Fibroblast growth factor-2 enhances expansion of human bone marrow-derived mesenchymal stromal cells without diminishing their immunosuppressive potential. *Stem Cells Int*, 2001, 235176. doi:10.4061/2011/235176.

[61] Capra, E; Beretta, R; Parazzi, V; Viganò, M; Lazzari, L; Baldi, A; et al. Changes in the proteomic profile of adipose tissue-derived mesenchymal stem cells during passages. *Proteome Sci*, 2012, 10:46. doi:10.1186/1477-5956-10-46.

[62] González-Cruz, RD; Darling, EM. Adipose-derived stem cell fate is predicted by cellular mechanical properties. *Adipocyte,* 2013, 2:87-91.